Technical Report

TR-02-20

The Buffer and Backfill Handbook

Part 1: Definitions, basic relationships, and laboratory methods

Roland Pusch
Geodevelopment AB

April 2002

Svensk Kärnbränslehantering AB
Swedish Nuclear Fuel
and Waste Management Co
Box 5864
SE-102 40 Stockholm Sweden
Tel 08-459 84 00
+46 8 459 84 00
Fax 08-661 57 19
+46 8 661 57 19

The Buffer and Backfill Handbook

Part 1: Definitions, basic relationships, and laboratory methods

Roland Pusch
Geodevelopment AB

April 2002

Foreword

Part 1 of this Handbook is focused on description of fundamental issues of soil physical and chemical arts and on soil mechanical definitions and relationships. Part 2 comprises a material data basis including also preparation and field testing methods. Part 3 provides a collection of physical and mathematical models and examples of how they can and should be applied.

The present document, which has been prepared by Geodevelopment AB in co-operation with Scandia Consult AB and Clay Technology AB, Sweden, and with TVO, Finland, makes up Part 1. Most of the data and information emanate from the work that Geodevelopment AB and Clay Technology AB have performed for SKB but a number of results from experiments made in and for other organizations have been included as well. A significant number of experimental procedures and ways of characterizing buffers and backfills are included.

The experience from the comprehensive international Stripa Project, concerning both systematic material investigations in the laboratory and the full-scale field experiments, has contributed significantly to this report. However, similar and additional information gained from later work in SKB's Äspö Hard Rock Laboratory and from NAGRA and also from other waste-isolation projects have helped to make this document of assumed international interest.

Contents

1 Symbols and definitions[1]

a_c	=	activity
a_z	=	swelling index
A	=	cross section, creep parameter, weight percentage
A_s	=	contact area
b	=	soil structure coefficient, load factor
B	=	creep parameter
B_s	=	solid phase modulus
B_w	=	bulk modulus
c, c'	=	cohesion
C	=	heat capacity, concentration
C_c	=	compression index, gradation coefficient
C_u	=	uniformity coefficient
d	=	diameter, distance, sample thickness
d_{10}, d_{60}	=	grain diameters
D_a	=	apparent diff. coefficient
D_e	=	effective diff. coefficient
D_p	=	pore diffusivity
D_s	=	surface diffusion coefficient
e	=	void ratio
E	=	modulus of elasticity
F	=	force
g	=	gravity
g_o	=	organic content
g_1, g_c	=	ignition loss
G	=	shear modulus
h	=	settling distance
i	=	hydraulic gradient, activity
I_P	=	plasticity index
I_C	=	consistency index
I_L	=	liquidity index
k	=	(hydraulic) permeability, colorimeter reading
K	=	hydraulic conductivity, compression modulus
K_d	=	sorption factor
l	=	sample length (height)
l_c	=	content of particles with an equivalent stoke diameter smaller than 2 μm
L_S	=	linear shrinkage
m	=	mass, modulus number
m_j	=	modulus number (ref.)
m_s	=	mass of solid matter
m_w	=	mass of water
M	=	oedometer modulus
M^I, M^{II}, M^{III}	=	metal cations
n	=	porosity
p	=	normal stress
p_S	=	swelling pressure
P	=	vapor pressure
q	=	deviator stress
R	=	molar gas constant, roundness
R_S	=	shrinkage ratio
s	=	salt content of pore fluid, scale factor
S	=	expansion ("rebounce"), sphericity
S_r	=	degree of water saturation, vol %
S_t	=	sensitivity
t	=	time
T	=	temperature
u	=	porewater press.
ν	=	Poisson's ratio
V	=	bulk volume
V_d	=	volume of dry soil sample
V_p	=	pore volume
V_s	=	volume of solid matter
V_S	=	volumetric shrinkage
V_w	=	volume of water
V_g	=	volume of gas
w	=	water content (ratio)
w_L	=	liquid limit
w_P	=	plastic limit
w_S	=	shrinkage limit
x	=	variable
y	=	variable

[1] Only major ones are listed

α	=	heat expansion coefficient	ρ_w	=	density of water
α_s	=	swelling index	σ	=	pressure
β	=	stress exponent	σ^1	=	effective press.
ε	=	strain	σ_c^1	=	preconsolidation pressure
γ	=	shear strain	σ_j	=	reference stress
ξ	=	constitutional parameter	τ	=	shear stress
η	=	viscosity	τ_{fu}	=	undrained shear strength
λ	=	heat conductivity	τ_r	=	remoulded shear strength
ν	=	Poisson's ratio	ϕ	=	electrical potential
ρ	=	bulk density	ϕ, ϕ'	=	friction angle
ρ_d	=	dry density	Δl	=	shortening of sample with length (height) l
ρ_s	=	density of solid particles			
ρ_{sat}	=	density of fluid-saturated soil			

Note 1 on "Grain size"
In literature the grain size distribution is expressed as "Percentage finer than", "percent finer by weight", "weight percent passing" etc. They appear in various diagrams quoted from literature sources.

Note 2 on "Symbols"
Some additional symbols that appear in the Handbook are not included here as they are self-explanatory or defined in the text.

1.2 Definitions

1.2.1 General

The basic definitions used here concern mass relationships, consistency, strength parameters and transport properties /1/. They are identical with those proposed for the international ISO/DIS standards Geotechnics in Civil Engineering and Classification of Soil.

1.2.2 Mass relationships

Mass, m [kg]

Mass is the term for the content of materia of a body, and it is usually determined by weighing. The word weight is therefore a common synonym of mass but it is avoided here if the meaning becomes unclear.

Bulk volume, V [m^3]

Bulk volume refers to the soil volume including isolated as well as continuous voids.

Volume of solid matter, V_s [m^3]

The volume of the solid mass or specific volume refers to the total volume minus the void volume.

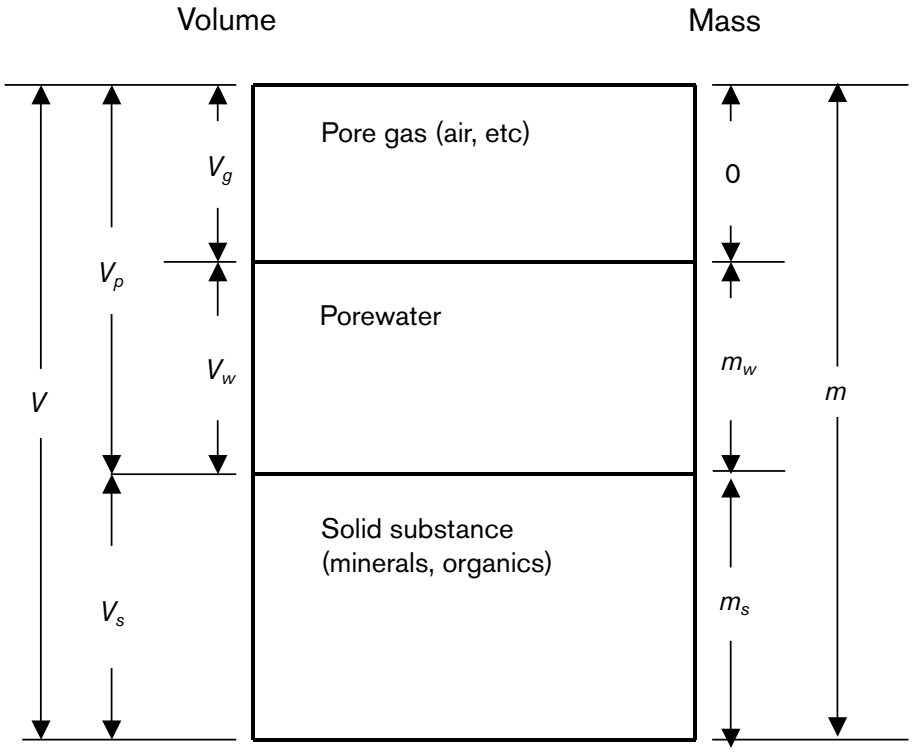

***Figure 1-1**. Schematic picture of the soil constituents.*

For ordinary laboratory work the following symbols and definitions are recommended (cf Figure 1-1).

Bulk density, ρ [kg/m³]

The bulk density is the ratio of the mass to the bulk volume of a given amount of soil:

$$\rho = \frac{m_s + m_w}{V} \tag{1-1}$$

Dry density, ρ_d [kg/m³]

The dry density is the ratio of the solid mass to the bulk volume of a given amount of soil:

$$\rho_d = \frac{m_s}{V} \tag{1-2}$$

Density of solid particles, ρ_s [kg/m³]

The density of solid particles is defined as the ratio of the mass to the true volume of the solid matter in a given amount of soil:

$$\rho_s = \frac{m_s}{V_s} \tag{1-3}$$

Density of pore fluid, ρ_w [kg/m^3]

The density of the fluid in the voids is the ratio of the mass of fluid with its content of dissolved matter to its volume. The pore fluid is conventionally termed porewater, which we will use throughout the document.

Void ratio, e [dimensionless]

$$e = \frac{V_p}{V_s} \tag{1-4}$$

The void ratio is the ratio between pore volume and the volume of solids.

Porosity, n [dimensionless]

$$n = \frac{V_p}{V} \tag{1-5}$$

Porosity is the ratio between the pore volume and the bulk volume of the soil. It is usually expressed in percent units.

The void ratio e and porosity n are interrelated as $n=e/(1+e)$.

Water content, w [%]

The water content gives the ratio between the mass of the porewater and the mass of the solid substance. It is expressed in percent units:

$$w = \frac{m_w}{m_s} \cdot 100 \tag{1-6}$$

Degree of water saturation, S_r [%]

The degree of water saturation is the ratio between the volume of the porewater and the pore volume. It is expressed in percent units:

$$S_r = \frac{V_w}{V_p} \cdot 100 \tag{1-7}$$

Clay content, l_c [%]

The clay content is the ratio between the mass of particles finer than 2 micrometers (μm) and the mass of all soil particles finer than 0.06 mm. It is expressed in percent units.

Ignition loss, g, g_c [%]

The ignition loss is the ratio between the loss of solid mass by heating dry soil and the mass of the dry soil before the heating. g_c denotes the ignition loss of the mineral constituents (primarily clay minerals), while g means the total ignition loss. Both are usually expressed in percent units.

Organic content, g_o [%]

Organic content is the ratio between the mass of the organic substance and the mass of the dry soil. For carbonate-free soil it is the difference between the total ignition loss and a term that contains the clay content.

Salt content of pore fluid, s [% or ppm]

The salt content is the ratio between the mass of dissolved matter (salt) and the mass of water. It is often expressed in percent, but for individual elements, like Na, K, Cl etc, the concentration is usually given in parts per million (ppm).

Gas content, V_g [%]

The content of gas in gaseous form is defined in terms of the fraction in percent of the total volume that the gas occupies at normal temperature and pressure.

pH (acidity)

Negative logarithm for the concentration of free hydrogen ions in the porewater.

1.2.3 Consistency parameters

The term 'consistency' refers in this context primarily to the degree of stiffness and plasticity of a soil in a remoulded state. Physico-chemically, the consistency of the soil depends on the internal bonds between the soil particles, the cohesion. A characteristic of the cohesive soils is that, within certain water content limits, they have a *plastic consistency* in the remoulded state. At lower water content they have a *solid consistency* and at higher water content a *liquid consistency*. As an intermediate state between the solid and the plastic consistency a *semi-solid consistency* is distinguished /1/.

A soil sample having a solid consistency is non-plastic; a brittle rupture occurs at a small deformation.

A soil sample having a plastic consistency is mouldable and maintains its shape after deformation.

A soil sample having a liquid consistency flows out due to its own weight.

Plastic limit, w_P [%]

The plastic limit is the water content at which the soil begins to crumble when rolled out to a 3 mm thread.

Liquid limit, w_L [%]

The liquid limit w_L can be determined according to the percussion method (percussion liquid limit) or the fall-cone method (fall-cone liquid limit) /1/.

The *percussion liquid limit*, determined by Casagrande's liquid limit device, is defined as the water content at which a remoulded soil sample, placed in the cupo of the device and divided into halves by a V-shaped groove, has such a consistency that the two

sample halves flow together 13 mm (½") along the bottom of the groove when the cup is dropped 10 mm 25 times.

The *fall-cone liquid limit* (earlier called the fineness number), determined by the fall-cone method, is defined as the water content at which a remoulded soil sample has such a consistency that the penetration of a 60 g/60° fall-cone is 10 mm (shear strength 1.7 kPa)[2]. The fall-cone liquid limit generally agrees with the percussion liquid limit.

The *sticky limit* was defined by Atterberg as the lowest water content at which the soil sticks to the blade of a metal spatula when the spatula is drawn against the surface of the remoulded soil sample /1/.

For high-plastic clays, the sticky limit is lower than the liquid limit. For low-plastic clays, on the other hand, as well as for organic soils, the sticky limit is higher than the liquid limit.

Shrinkage limit, w_S [%]

The shrinkage limit w_S is defined as the water content at which a saturated soil sample ceases to shrink when dried. At further dessication, air starts to penetrate the pores. At the same time the colour of the sample becomes lighter.

The shrinkage limit can be determined for remoulded samples as well as for undisturbed samples.

Plasticity index, I_P [%]

The plasticity index I_P is defined as the difference between the liquid limit and the plastic limit:

$$I_P = w_L - w_P \tag{1-8}$$

The plasticity index can be regarded as a measure of the plasticity of the soil. For non-plastic soils I_P = 0.

With regard to plasticity, clays are classified either on the basis of the liquid limit w_L or the plasticity index I_P, in four groups (Table 1-1), /1/.

Table 1-1. Classification of clays with respect to their consistency.

Designation	Plasticity index, I_P %	Liquid limit, w_L %
Low plasticity	< 10	< 30
Medium plasticity	10–25	30–50
High plasticity	> 25	> 50–80
Very high plasticity	> 50	> 80

[2] According to British Standard, the (cone) liquid limit is defined as the water content at 20 mm penetration with an 80 g/30° cone, which corresponds to 10 mm penetration with the Swedish 60 g/60° cone, thus giving equal shear strengths.

For very high-plastic soils the undrained shear strength τ_{fu}, determined by the fall cone method is reduced with regard to the value of the liquid limit or the plasticity index.

Liquidity index, I_L [dimensionless]

The liquidity index I_L is defined as:

$$I_L = \frac{w - w_P}{I_P} \tag{1-9}$$

where w = the natural water content of the soil.

The liquidity index is a measure of the consistency of the soil in the remoulded state at the natural water content (Table 1-2) and is also used as an indication of the sensitivity to mechanical disturbance of the soil /1/.

Consistency index, I_C [dimensionless]

The consistency index is defined as:

$$I_C = \frac{w_L - w}{I_P} \tag{1-10}$$

The consistency index is, like the liquidity index, a measure of the consistency of the soil in the remoulded state at the natural water content (Table 1-3). The following relation exists between the consistency index and the liquidity index /1/:

$$I_C = 1 - I_L \tag{1-11}$$

Table 1-2. Liquidity index in relation to consistency limits.

Water content in relation to w_P and w_L	Liquidity index I_L	Consistency of remoulded sample
$w < w_P$	$I_L < 0$	Solid – semi-solid
$w = w_P$	$I_L = 0$	
$w_P < w < w_L$	$0 < I_L < 1$	Plastic
$w = w_L$	$I_L = 1$	
$w > w_L$	$I_L > 1$	Semi-liquid – liquid

Table 1-3. Consistency index in relation to consistency limits.

Water content in relation to w_P and w_L	Consistency index I_L	Consistency of remoulded sample
$w < w_P$	$I_C > 1$	Solid – semi-solid
$w = w_P$	$I_C = 1$	
$w_P < w < w_L$	$1 < I_C < 0$	Plastic
$w = w_L$	$I_C = 0$	
$w > w_L$	$I_C < 0$	Semi-liquid – liquid

Activity, a_c [dimensionless]

The activity a_c is defined as the ratio between the plasticity index and the clay content of the soil, in percentage of material < 0.4 mm:

$$a_c = \frac{I_P}{\%\ \text{clay fraction}} \tag{1-12}$$

The activity is an indication of the colloidal properties of a clay, and is principally dependent on the content and the kind of clay minerals and organic colloids as well as on the electrolyte content of the pore water /2/.

Shrinkage ratio, R_S [dimensionless]

The shrinkage ratio R_S is defined as the ratio between a given volume change, expressed as a percentage of the dry volume, and the corresponding change in water content above the shrinkage limit of a soil mass.

The shrinkage ratio is calculated from data obtained in the shrinkage-limit determination by means of the following formula:

$$R_S = \frac{m_s}{V_D \cdot \rho_w} \tag{1-13}$$

where

V_D = volume of dry sample

Knowing the shrinkage ratio R_S, shrinkage limit w_s and original water content w, the shrinkage of a soil mass when the water content is reduced to, the shrinkage limit or less than that, can be calculated.

Volumetric shrinkage, V_S [%]

The volumetric shrinkage V_S, expressed in per cent of the volume of the soil mass at the shrinkage limit, is obtained by means of the following formula:

$$V_S = \left(w - w_S\right) \cdot R_S \cdot 100 \tag{1-14}$$

Linear shrinkage, L_S [%]

The linear shrinkage L_S in per cent of the original dimension of the soil mass is obtained by means of the following formula /1/:

$$L_S = \left[1 - \sqrt[3]{\frac{100}{\left(w - w_s\right)R_S + 100}}\right] 100 \tag{1-15}$$

1.2.4 Strength parameters

Undrained shear strength of undisturbed cohesive soils, τ_{fu} [Pa, kPa, MPa]

The undrained shear strength of undisturbed cohesive soils is defined as the maximum shear stress that a soil sample can sustain under defined conditions with respect to loading rate and external (total) stresses permitting no drainage /3/.

Undrained shear strength of remoulded cohesive soils, τ_r [Pa, kPa]

The undrained shear strength is defined as the maximum shear stress that a soil sample can sustain under defined conditions after mechanical agitation of certain defined type /3/.

Sensitivity, S_t

The sensitivity S_t to mechanical disturbance is defined as the ratio between the shear strength (τ_{fu}) of the undisturbed sample and the shear strength (τ_r) of the remoulded sample:

$$S_t = \frac{\tau_{fu}}{\tau_r} \tag{1-16}$$

With regard to sensitivity, clays are classified in three groups: low-sensitive, medium-sensitive and high-sensitive clays (Table 1-4). Quick clay is distinguished as a special group of high-sensitive clays /1/.

Drained shear strength of soils, t_{fu} [Pa, kPa, MPa]

The shear strength of soils under drained conditions is conventionally expressed in terms of effective cohesion c' and internal friction (angle) ϕ' applying the effective stress concept. The parameters are evaluated from a set of recorded maximum shear stresses that the soil can sustain at different normal stresses under defined conditions with respect to the loading rate. The general relationship is in its simplest form expressed by Mohr/Coulomb's failure criterion. For advanced applications other failure criteria and strength parameters are used as specified in Part 3 of the document.

Table 1-4. Classification of clays with respect to sensitivity.

Designation	Sensitivity S_t according to fall-cone tests)
Low-sensitive	< 10
Medium-sensitive	10–30
High-sensitive	> 30

1.2.5 Rheological parameters

Soil compressibility. Parameters M [kPa], m and β

The compressibility of soils is often expressed by the tangent modulus M of the compression curve obtained from oedometer tests /1,3,4,5/:

$$M = m_j \sigma_j' \left(\frac{\sigma'}{\sigma_j'} \right)^{1-\beta} \tag{1-17}$$

where

m_j = modulus number
β = stress exponent
σ' = effective compression stress, kPa
σ_j = reference stress, kPa

Compression index, C_c

$$C_c = \frac{\Delta e}{\Delta \left(\log \sigma' \right)} \quad 1/\text{kPa} \tag{1-18}$$

where

Δe = change in void ratio
$\Delta\sigma'$ = change in effective compression stress (log scale)

Swelling index. Parameters a_s, M_s and S

$$M_s = \sigma' / a_s \tag{1-19}$$

$$a_s = S \Big/ \ln \left(\frac{0.8\sigma'_c}{\sigma'_{red}} \right) \tag{1-20}$$

where:

a_s = swelling index
S = "rebound" on unloading
M_s = swelling modulus
σ'_c = preconsolidation pressure
σ'_{red} = effective pressure after load reduction

as illustrated in Chapter 11.

Shear strain, γ

Shear strain is expressed as the ratio between the shear stress and the angular strain γ at simple shear (Figure 1-2). The shear modulus G is obtained from shear tests in which the shear strain is plotted as a funtion of the shear stress. It is expressed as the tangent modulus:

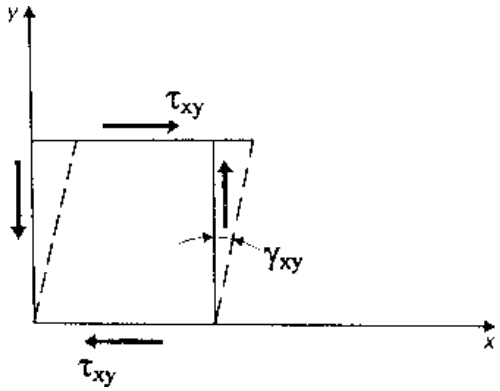

Figure 1-2. *Simple shear.*

$$G = \frac{d\tau}{d\gamma} \tag{1-21}$$

or as the secant modulus

$$G = \frac{\Delta\tau}{\Delta\gamma} \tag{1-22}$$

Shear strain rate, dγ/dt

Time-dependent shear strain under constant or non-constant volume conditions is termed creep and can be measured in direct shear tests or triaxial tests.

A general definition of creep of clays is given in Equation 1-23, /6,7/.

$$d\gamma/dt = A\ T^a\ D^b\ (t+t_o) \tag{1-23}$$

where:

A = coefficient
γ = angular shear strain
D = deviator (shear) stress
T = absolute temperature
a, b = exponents
t_o = term related to creep rate and evaluated from creep plottings

An expression for long term strain rate of a clay element assuming log time creep can be derived from Equation 1-23 /6/:

$$d\gamma/dt = \beta\ T\ D\ ln(t) \tag{1-24}$$

where:

γ = angular strain
β = strain parameter evaluated from undrained triaxial tests
D = deviator stress (σ_1–σ_3)
T = temperature

The time dependence of creep often deviates from pure log-time behaviour, at least in short-term experiments, and one can then use the relationship in Equation 1-25 /8/:

$$\dot{\gamma} = \dot{\gamma}_o e^{\alpha \frac{(\sigma_1-\sigma_3)}{(\sigma_1-\sigma_3)_{fe}}(-\alpha)\frac{(\sigma_1-\sigma_3)_0}{(\sigma_1-\sigma_3)_f}} \left(\frac{t}{t_r}\right)^n \quad (1\text{-}25)$$

where:

$\dot{\gamma}$ = creep rate
$\dot{\gamma}_o$ = creep rate at time t_r
t = time after stress change
t_r = reference time (10^5 s)
$(\sigma_1-\sigma_3)_0$ = reference deviator stress *[0.5 $(\sigma_1-\sigma_3)$]*
$(\sigma_1-\sigma_3)_f$ = deviator stress at failure

n and α = parameters derived from laboratory tests

Part 2 of this Handbook gives examples of the application of the creep laws.

Compressive strain, E, G, ν

Uniaxial compression of an elastic body of length l gives the strain $\varepsilon = \frac{\Delta l}{l}$ where Δl is the shortening. The parameters are the modulus of elasticity E and Poisson's ratio ν /5/:

$$E = \frac{3G}{1+G/3K} \quad (1\text{-}26)$$

$$\nu = \frac{1-2G/3K}{2+2G/3K} \quad (1\text{-}27)$$

$$G = \frac{E}{2(1+\nu)} \quad (1\text{-}28)$$

$$\varepsilon = \frac{1}{E}\left[\sigma_x' - \nu\left(\sigma_y' + \sigma_z'\right)\right] \quad (1\text{-}29)$$

Compressive strain rate, dε/dt

Compression occurs when the preconsolidation pressure of natural soils is exceeded and the rate of compression depends on the porewater overpressure and hydraulic conductivity. "Artificially" prepared buffers and backfills obey the same laws as natural clays, the preconsolidation pressure being the same as the effective pressure (swelling pressure). Also for these soils the rate of compression depends on the hydraulic conductivity, which is usually very low. Examples of time-dependent compression determined in the laboratory are given in this part of the Handbook.

1.2.6 Transport properties

Hydraulic (fluid) conductivity, K [m/s]

The hydraulic (fluid) conductivity is the average flow rate at percolation of a confined soil sample /7/. It is evaluated by use of Darcy's law:

$$v = \frac{Q}{A} = K \cdot i \tag{1-30}$$

where

v = flow rate (m/s)
Q = flux (m^3/s)
A = total cross section ($m^{2)}$
i = hydraulic gradient (m/m)

Occasionally another measure of fluid conductivity, i.e. *permeability* (k in m^2), is used. It is defined as $k=K\eta/\rho g$ where ρ is the density of the fluid, g is gravity and η the dynamic viscosity. Taking average values for the viscosity and density of water one finds that K expressed in m/s can be evaluated from k by multiplying the k-value (in m^2) by approximately E7.

Diffusion coefficient, D_a, D_e [m^2/s]

Diffusive ion transport is described by use of the diffusion coefficient and usually evaluated by use of Fick's law. For pore diffusion one has /9/:

$$\frac{\partial C}{\partial t} = D_a \frac{\partial^2 C}{\partial x^2} \tag{1-31}$$

$$D_e = D_a\left(\varepsilon + K_d\,\rho\right) \tag{1-32}$$

where:

C = concentration of the diffusing substance (kg/m^3)
D_a = apparent diffusion coefficent (m^2/s)
D_e = effective diffusion coefficient (m^2/s)
ε = porosity available for diffusion
K_d = sorption factor (m^3/kg)
ρ = bulk density (kg/m^3)

For the case of both pore and "surface" diffusion the effective diffusivity is given as:

$$D_e = D_a\left(\varepsilon + K_d\rho\right) + K_d\,\rho D_s \tag{1-33}$$

where:

D_s = surface diffusion coefficient

Heat conductivity, λ (W/m,K); heat capacity C_p (Ws/kg,K)

Heat transport through buffer and backfill is controlled by the thermal (heat) conductivity and the thermal (heat) capacity. The transport has the form of diffusion with the thermal diffusivity κ defined as:

$$\kappa = \lambda / \rho C_p \qquad (1\text{-}34)$$

where:

λ = heat conductivity (W/m,K)
C_p = heat capacity (Ws/kg,K)
ρ = bulk density (kg/m^3)

The thermal properties are determined as described later in this part of the Handbook.

1.3 References

/1/ **Pusch R et al, 1990.** Soil constituents and structure. Swedish Council for Building Research, Stockholm, Sweden.

/2/ **Skempton A W, 1953.** The colloidal "activity" of clays. Proc. 3rd Int. Conf. Soil Mech. a. Found. Engng., Zürich.

/3/ **Lambe T, Whitman R V, 1969.** Soil Mechanics, John Wiley & Sons, Inc.

/4/ **Janbu N, 1970.** Grunnlag i Geoteknikk, Tapir Forlag, Oslo, Norway.

/5/ **Larsson R, 1981.** Drained behaviour of Swedish clays. Swedish Geotechnical Institute Report No. 12.

/6/ **Pusch R, Adey R, 1999.** Creep in buffer clay. SKB TR-99-32, Svensk Kärnbränslehantering AB.

/7/ **Mitchell J K, 1993.** Fundamentals of Soil Behavior, John Wiley & Sons, Inc.

/8/ **Börgesson L, Johannesson L-E, Sandén T, Hernelind J, 1995**. Modelling of the physical behaviour of water saturated clay barriers. Laboratory tests, material models and finite element application. SKB TR-95-20, Svensk Kärnbränslehantering AB.

/9/ **Muurinen A, 1994.** Diffusion of anions and cations in compacted sodium bentonite. VTT Publication No. 168, Technical Research Centre of Finland, Espoo.

2 Soil characterization

This chapter deals with characterization of soils as a background of the description of their physical and chemical behaviour in the subsequent text. The various definitions and described modes of classification are of fundamental importance in applied soil mechanics and engineering geology.

2.1 Introduction

Natural soils are commonly termed mineral or organic soils depending on their composition. Further division can be made into non-weathered and weathered soils of the first-mentioned group, and into soils of different degrees of chemical degradation of the other group. The factors of importance to the physical behaviour are the following:

- Composition of solid constituents
- Particle size distribution
- Structural arrangement
- Composition of the pore solution
- Content of gas

All these factors are fundamental to sedimentary geology and have been treated in a large number of scientific reports and comprehensive textbooks. The primary purpose of Part 1 of the document is to give information on how to determine the soil physical parameters that are useful and necessary for identifying and preparing soil components for various sealing functions in repositories for radioactive waste materials. This chapter begins with a brief overview of the individual issues, continuing with more detailed treatment of matters like mineralogy and structure in the subsequent chapters.

2.2 Soil classification

2.2.1 General

Characterization of a soil is primarily made with respect to its content of solid constituents and to its geotechnical properties. The basis is the grain size, which is illustrated in Table 2-1 and discussed in detail in Chapter 6. Abbreviations for soil terms are given in Table 2-2. The figure and table refer to the recommendations of the Laboratory Committee of the Swedish Geotechnical Society /1/.

Table 2-1. Geotechnical divisions and limits of fractions /1/.

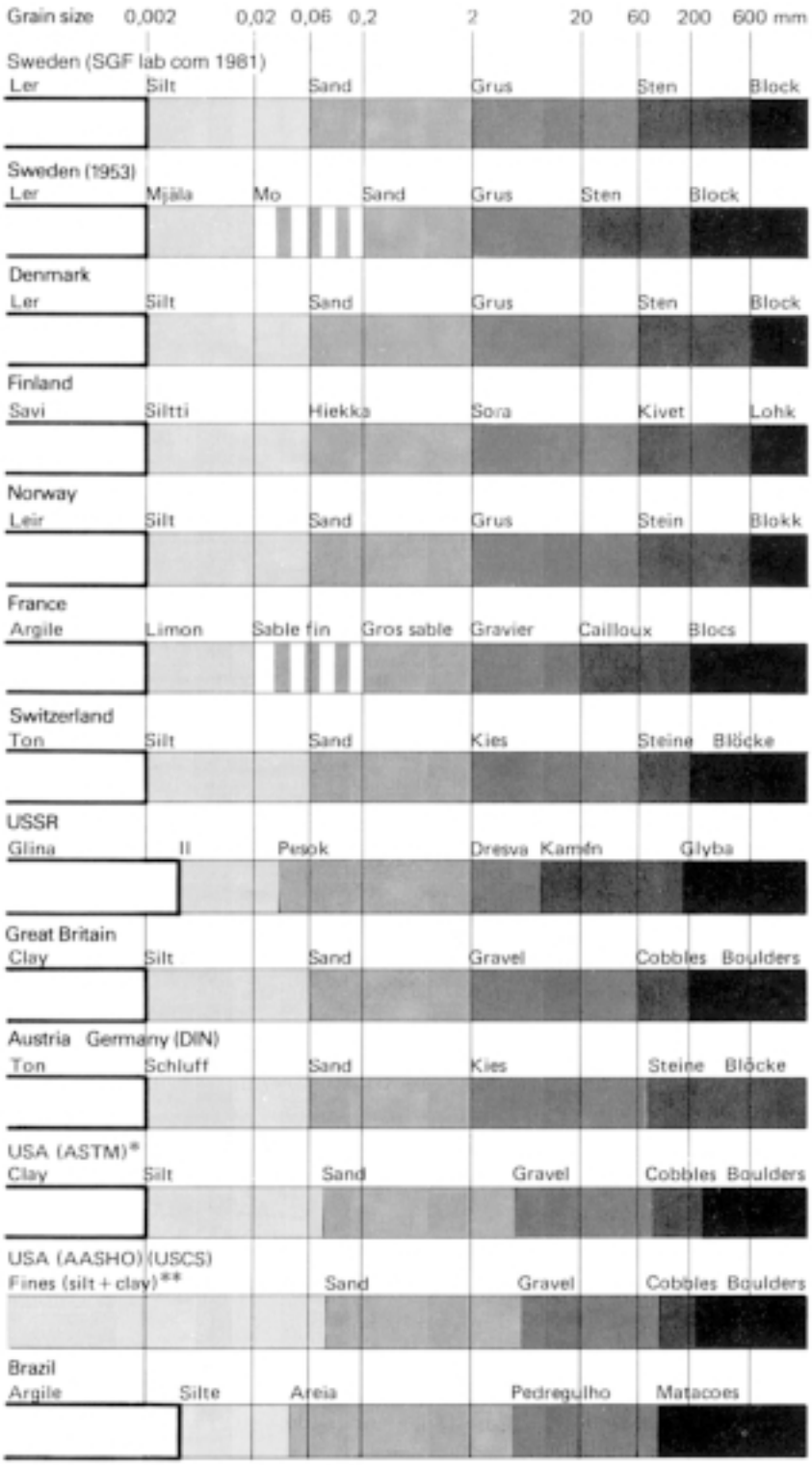

* Limit clay-silt sometimes set at 0.005
** Limit clay-silt determined by consistency properties

Table 2-2. Terminology /1/.

Main term		Derivative		Layer	
R	rock				
FR	fragmented rock				
S	soil				
T	till				
Bo	boulders				
BoT	boulder till				
Co	cobbles			co	cobble layer
CoT	cobble till				
Gr	gravel	gr	gravelly	gr	gravel layer
GrT	gravel till				
Sa	sand	sa	sandy	sa	sandy layer
SaT	sandy till				
Si	silt	si	silty	si	silt layer
SiT	silt till				
Cl	clay	cl	clayey	cl	clay layer
ClT	clay till				
SuS	sulphide soil				
SuSi	sulphide silt				
SuCl	sulphide clay				
Sh	shells	sh	shell-bearing	sh	shell layer
Lm	lake marl				
Pl	plant remains	pl	containing plant remains	pl	layer of plant remains
Pt	peat			pt	peat layer
Ptf	fibrous peat			ptf	fibrous peat layer
Ptp	pseudo-fibrous peat			ptp	pseudo-fibrous peat layer
Pta	amorphous peat			pta	amorphous peat layer
Dy	dy	dy	dy-bearing	dy	dy layer
Gy	gyttja	gy	gyttja-bearing	gy	gyttja-layer
Hu	humus, topsoil	hu	humus-bearing	hu	humus layer
F	fill				

Further symbols are the following

Symbol	Meaning
/	(between main terms) contact, e.g. Gy/Cl = contact gyttja and clay
_	(below main term) layered, e.g. SaCl = layered sand and clay
v	(before main term) varved, e.g. vCl = varved clay
d	(after main term) dry crust, e.g. Cld = dry crust of clay
( )	somewhat, e.g. (cl) = somewhat clayey
(_)	thin layer(s)
) _ (	thick layer(s)

2.2.2 Definitions

Rock – that part of the earth's crust which is characterized by brittleness and low porosity /1/. Rock can normally not be disintegrated in water except if it contains smectite.

Soil – accumulation in the surface part of the earth's crust derived from the decomposition of rock and/or the remains of living organisms. Soil can normally be dislodged by excavation.

Mineral soil matter – matter consisting of crushed or weathered rock.

Boulder fraction – grain size exceeding 600 mm.

Cobble fraction – grain size between 600 and 60 mm.

Gravel fraction – grain size between 60 and 2 mm.

Sand fraction – grain size between 2 and 0.06 mm.

Silt fraction – grain size between 0.06 and 0.002 mm.

Clay fraction – grain size smaller than 0.002 mm.

Fines – collective term for the grain fractions silt and clay.

Organic soil matter – soil matter consisting of more or less decomposed plant and animal remains. The term organogeneous soil is used to denote matter also consisting of plant and animal remains which do not readily decay, such as shell fragments.

Chemical sediment – soil consisting of shells or shell fragments from mussels or other shell-fish.

Diatomaceous earth – soil consisting of skeletal remains of diatoms.

Sedentary (autochthonous) soil – soil which has been formed in place from the original material, e.g. weathered soils, peat.

Transported (allochtonous) soil – soil which has been transported from the position of the original material by ice, water or wind.

Weathered soil – soil formed by mechanical or chemical weathering, e.g. residual soil.

Moraine (till) – soil which has been transported by glaciers and deposited in the place where the ice melted.

Sedimentary soil – soil which has sedimented in water and deposited on the bottom (aqueous sediment) or has been sedimented in air and deposited on land (eolian sediment).

Mineral soils – soils in which the mineral matter comprises the characteristic part – see below.

Organic soils – soils in which the organic matter comprises the characteristic part.

Coarse-grained soil – mineral soil in which the content of fines is less than 15% by weight of material below 60 mm.

Mixed-grain soil – Mineral soil in which the content of fines is between 15 and 40% by weight of material below 60 mm.

Fine-grained soil – mineral soil in which the content of fines is greater than 40% by weight of material below 60 mm.

Gravel – coarse-grained soil in which the gravel fraction dominates.

Silt – fine-grained soil in which the clay content is less than 20% by weight of the content of fines.

Clay – fine-grained soil in which the clay content is greater than 20% by weight of the content of fines.

Even-graded soil – soil with a uniformity coefficient C_u below 5.

Medium-graded soil – soil with a uniformity coefficient C_u between 5 and 15.

Multi-graded soil – soil with a uniformity coefficient C_u greater than 15.

Gap-graded soil – medium-graded or multigraded soil in which one or more intermediate fractions are strongly underrepresented. Gap-graded soil has usually a low coefficient of curvature C_C (usually lower than 0.5).

Peat – organic sedentary soil made up of more or less decomposed plant remains.

Dy – organic soil formed as a sediment in nutrient-poor water and mainly consisting of precipitated colloidal humid substances (dy matter).

Gyttja – organic soil formed as a sediment in nutrient-rich water and mainly consisting of more or less decomposed remains of plants and animals (detritus).

Glacial soil – soil formed of material deposited directly by a glacier or after transportation by meltwater from a glacier.

Postglacial soil – soil formed after the recession of the last ice sheet and deposited in a non-glacial environment.

Non-cohesive soil – soil with the shear strength being due to friction between the particles.

Cohesive soil – soil with the shear strength being due to both friction and cohesion between the particles.

2.2.3 Classification with respect to mode of formation

The main division with regard to the mode of formation of soils that can be used as a major or minor component in preparing backfill is based on the nature of the initial material and the environment in which it was deposited. In many countries in the northern hemisphere, a distinction is commonly made between Prequaternary and Quaternary formations. The latter are normally divided into glacial and postglacial soils. With regard to the mode of formation the soils can be classified according to Table 2-3.

Table 2-3. Classification of soils according to mode of formation /1/.

Mode of formation	Example of soil type
PreQuaternary forms	
Sedimentary, unaltered clay	Boom clay, Belgium
Sedimentary unaltered silts and sands	Scanian glass sand (Fyle, Sweden)
Weathered soils	Clay-rich residue of hydrothermally altered rhyolite rock
Converted soils	Bentonites
Quaternary forms	
Glacial	
Moraines	Gravelly sand till
Glaciofluvial deposits	Glaciofluvial soil
Fine-grained marine and lacustrine sediments	Varved clay
Postglacial	
Weathered soils	Postglacial weathered gravel
Fluvial sediments	
Basal fluvial sediments	Fluvial gravel
Lateral fluvial sediments	Fluvial sand
Delta sediments	Delta sand
Wave-washed sediments	Wave-washed sand
Fine-grained marine and lacustrine sediments	Postglacial clay
Eolian sediments	Eolian sand
Peat soils	Fen peat
Organic sediments	Gyttja, dy
Chemical sediments	Lake marl

Natural soils

Weathered soils and bentonites

We will distinguish here between soils that originate from weathered rock that has been partly or wholly decomposed to clay, and bentonites formed from volcanic ash deposited in the sea or in estuaries.

The firstmentioned soils may represent very complex strata of eroded, redeposited and chemically altered rock as well as undisturbed soil material in many deep sediments all over the world. To this group also belongs *in situ* weathered rock like laterite soils, in which the original rock structure can still be seen but in which silicates like feldspars and mafic minerals have been transformed to clay minerals. Under certain conditions rock weathering has led to relatively homogeneous, large masses of smectite-rich clay, like in Japan, and such rock is being mined for preparation of clay material for isolating toxic and radioactive wastes.

Bentonite is a geological term for smectite-rich clay formed from the glass component of volcanic ash. Bentonites usually form thin layers but beds with a thickness of a few meters are rather common. They serve, together with in situ weathered rock, as the major source of the smectite clay used in various industrial processes, like pelletization of iron ore concentrates, and is intended to be used for various sealing purposes in reposi-

tories for toxic and radioactive wate, e.g. for embedment of canisters containing highly radioactive waste. Part 2 of the document will describe a number of such materials.

Moraine (Till)

Moraines consist of material formed by soil and rock picked up and transported by advancing glaciers and deposited when the movement stopped and the glaciers melted. The mechanical agitation caused crushing and grinding, which usually gave a wide spectrum of particle size, i.e. from large blocks to fine clay. These particles typically have an angular shape. The gradation makes them suitable for preparing dense fills with low porosity, hydraulic conductivity and compressibility, especially if clay-sized particles are represented. The upper part of moraine deposits ("ablation" till) are softer than the lower parts ("lodgement" till), which were heavily compacted by the glaciers.

Sedimentary soils

Sediments originate from erosive soil or rock by wave action or flowing water. The released material was transported and deposited in rivers and estuaries or in the sea, yielding more or less regular bedding. In many cases sliding and slumping have taken place causing quick deposition of heterogeneous masses. Mechanical and chemical effects have often given the grains spherical shape and smooth grain surfaces. Bedded sediments are often characterized by a relatively uniform grain size, which means that preparation of low-permeable fills from them requires addition of other grain fractions.

Organic soils

Peat is formed from remains deposited in fens ("lowmoor" peat) or raised bogs ("highmoor" peat). Organic mud ("gyttja") originates from finely divided plant and animal remains, or colloidal humus substances, deposited on the bottom of lakes with stagnant water.

Organic soils are unsuitable for any sort of backfilling purpose. It should be noticed that pH is normally very low in organic soils and infiltration of water from such deposits into repositories is unwanted.

Artificially prepared soils

Fills

Soil mixtures, composed and compacted to form low-compressible beds of building structures, like the big silo for intermediate waste at Forsmark, Sweden, have a wide use in Europe and North America for preparing tight top covers of waste piles and they are candidate materials for backfilling underground repositories /2/. Smectite clay is often used as a sealing component and is mixed in, either by harrowing sandwiched clay and "ballast" (aggregate) soil, or by preparing mixtures in big concrete-type mixers. The performance and common preparation techniques as well as quality assurance will be treated in Part 2. Natural homogeneous smectitic soils, like the German Friedland Ton, represent an alternative to artificially prepared clay/ballast mixtures.

Precompacted blocks of soil

Blocks of highly compacted smectite clay powder or mixtures of clay powder and ballast material, like quartz powder, can be used for embedding containers with radioactive waste products and for constructing very tight plugs in underground repositories.

The ability of smectite clay to expand creates a swelling pressure on the surrounding rock or soil mass and thereby a tight contact with the confinement. The preparation of blocks of various compositions and their performance in repository environment are described and discussed in Part 2.

2.2.4 Classification according to grain size composition

The granular composition has a profound effect on the geotechnical properties of a soil. Common geotechnical classification of soils with respect to composition refers to the grain-size distribution of mineral soils and to the content of organic constituents.

Mineral soils are classified according to grain size and grain-size distribution (grain-size fractions and grading) as indicated in Table 2-4. Depending on the dominant size fractions mineral soils are divided into the four main groups specified in Table 2-5.

Table 2-4. Fractional groups.

Main groups		Sub-groups	
Designation	**Grain size, mm**	**Designation**	**Grain size, mm**
Boulder	> 600	Large boulder	> 2 000
Cobble	600–60	Large cobble	600–200
		Small cobble	200–60
Gravel	60–2	Coarse gravel	60–20
		Medium gravel	20–6
		Fine gravel	6–2
Sand	2–0.06	Coarse sand	2–0.6
		Medium sand	0.6–0.2
		Fine sand	0.2–0.06
Silt	0.06–0.002	Coarse silt	0.06–0.02
		Medium silt	0.02–0.006
		Fine silt	0.006–0.002
Clay	< 0.002	Fine clay*	< 0.0006

* The use of the designation and fine clay is mainly restricted to research

Table 2-5. Guiding values for the division of mineral soils.

Designation	Content of boulders + cobbles in wt % of total soil material*	Content of fines in wt % of material ≤ 60 mm
Boulder and cobble soils	> 40	–
Coarse-grained soils	< 40	< 15
Mixed-grained soils	< 40	15–40
Fine-grained soils	< 40	> 40

* The value of 40 per cent by weight of boulders + cobbles corresponds to 30–35 per cent by volume for the void ratio of boulder and cobble soils in natural state

The scheme for detailed classification of mineral soils given in Figure 2-1 /1/ can be used for specification of the composition of backfills and filters etc in repositories and sealing components as well as for classification of natural soils.

A special classification principle is used for designing and construction of filters and certain backfills, for which it is required that they resist piping and erosion. It depends on the grain size distribution, especially the grading, i.e. the "degree of uniformity".

With regard to grading, the coarse-grained and mixed-grained soils are divided into three groups: *even-graded soils*, *medium-graded soils* and *multi-graded soils*. The divisions are made according to the value of the uniformity coefficient $C_u = d_{60}/d_{10}$, which roughly represents the slope of the grain-size distribution curve (see Figure 2-2 and Table 2-6).

The symbol d_{60} represents the grain diameter at the weight quantity 60% on the grain-size distribution curve, and d_{10} represents the grain diameter at the weight quantity 10% on the curve (effective grain diameter).

Occasionally, the coefficient d_{60}/d_{10} is not representative of the grading, a typical example being the case when the grain-size distribution curve is uneven. In these cases, the grain-size distribution curve should always be presented. If the curve has a stepped shape, due to the fact that one or more intermediate fractions are strongly under-represented, the soil is termed *gap-graded*. Gap-graded soils usually have a high uniformity coefficient and a low value (commonly < 0.5) of the coefficient of curvature $C_c = d^2_{30}/d_{10}d_{60}$.

The sedimentary soils are usually even-graded. Wave-washed and glaciofluvial deposits can be medium-graded, especially when individual layers are mixed. Tills are commonly multi-graded.

In geological disciplines, soils are divided into the categories well-sorted, partly sorted and poorly sorted according to the value of the sorting coefficient d_{75}/d_{25}. For the well-sorted soils the sorting coefficient values of 2.5 and 3.5 correspond approximately to uniformity coefficient values of 5 and 15. The terms well-sorted, partly sorted and poorly sorted thus correspond to the terms even-graded, medium-graded and multi-graded /1/.

In English literature, division is made into poorly-graded (even-graded) and well-graded (multi-graded), and in German literature into "enggestufte" and "weitgestufte" soils. The boundary between well-graded and poorly-graded is different for gravel and sand. Thus for well-graded gravel $C_u > 4$ and for sand $C_u > 6$, in order that the designation "weitgestufte" shall apply. Furthermore, in order that soils can be designated well-graded or weitgestufte, it is required that $1<C_C<3$ /1/.

Table 2-6. Guiding values for the division of mineral soils according to the grain-size distribution.

Designation	Uniformity coefficient $C_u = \frac{d_{60}}{d_{10}}$
Even-graded	< 5
Medium-graded	5–15
Multi-graded	> 15

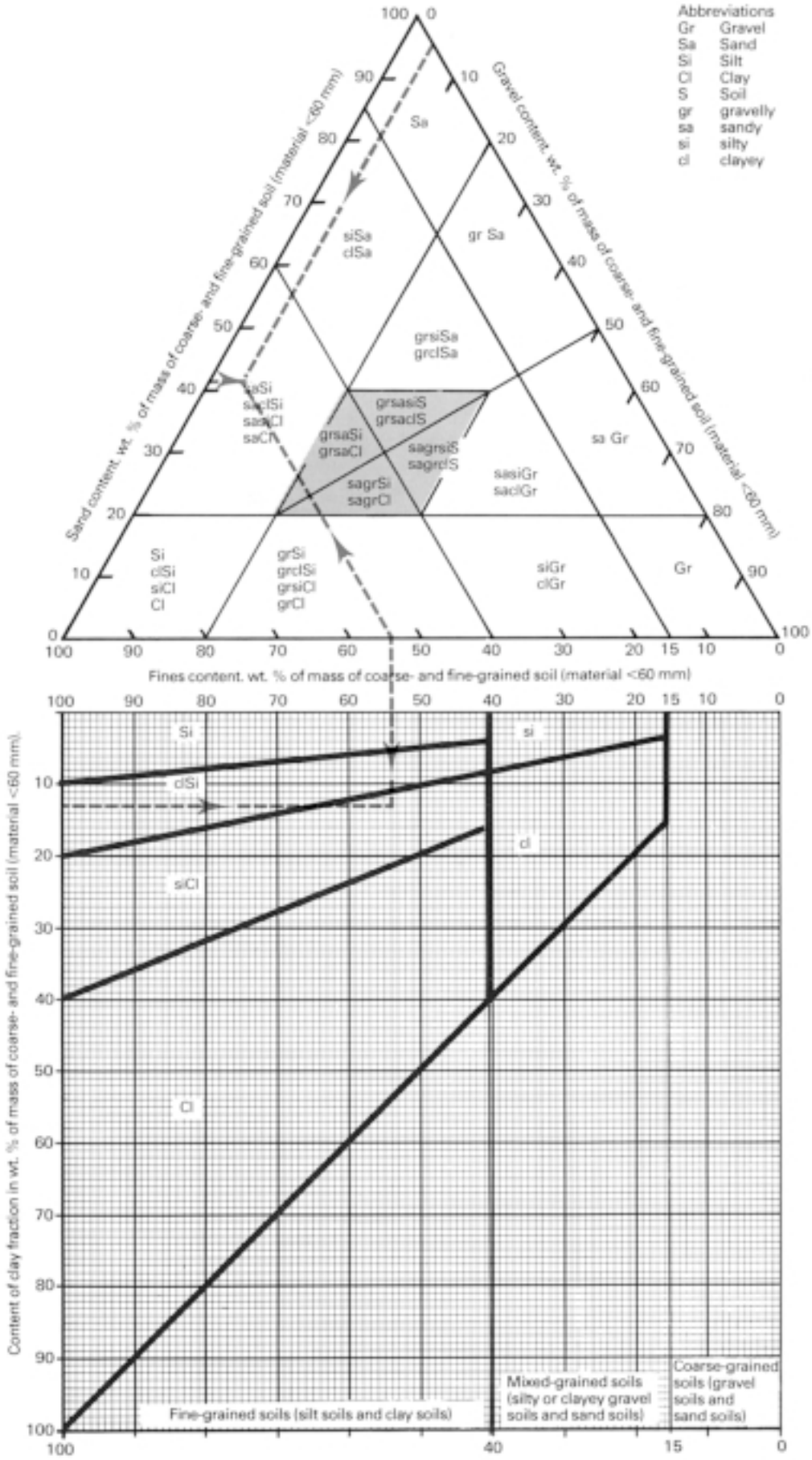

Figure 2-1. *Nomogram for classification of mineral soils /1/.*

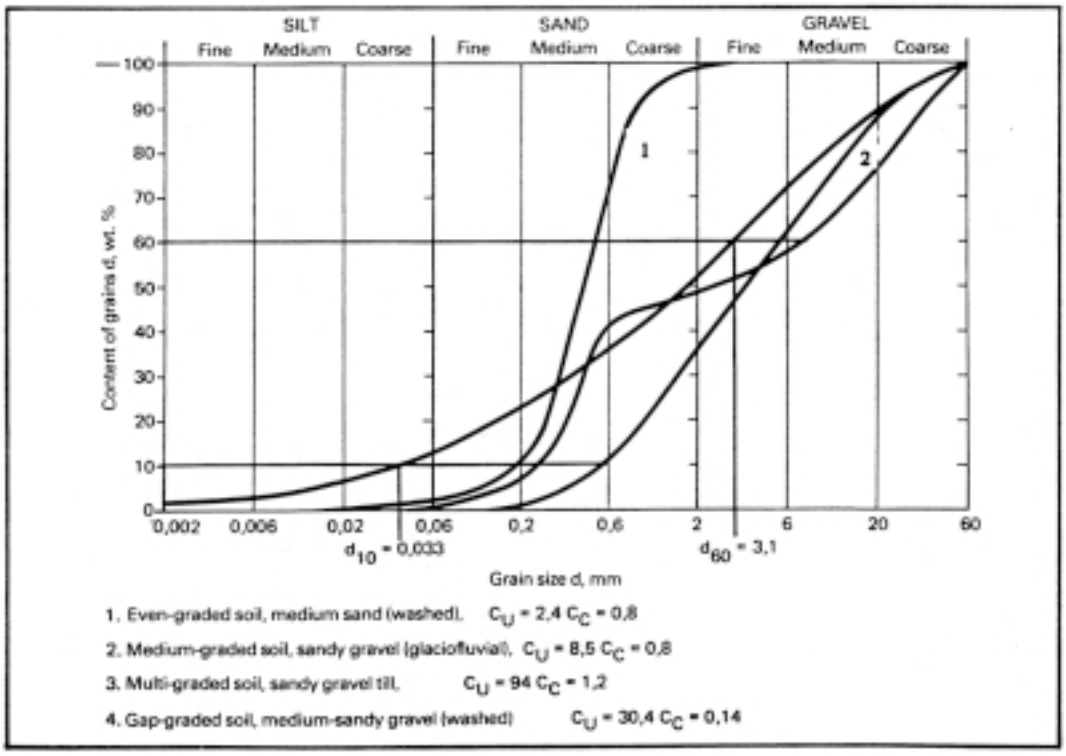

Figure 2-2. *Coefficients of uniformity, C_u /1/.*

2.2.5 Classification according to mineral composition

There does not seem to be any classification system with respect to the mineral composition in applied engineering geology in contrast to the many systems that are in use in sedimentology and general geology. From a practical point of view one can apply the principles in Table 2-7. It is based on the consistency limits, primarily the activity (see Chapter 1), and serves to give an approximate description of the performance of differently composed soils with respect to their use in repositories.

Table 2-7. Classification with respect to the impact of mineral composition and engineering performance of organic-poor soils. C=Carbonates, Q=Quartz, F=Feldspars, H=Heavy minerals, Ch=Clorite, K=Kaolinite, I=Illite, S=Smectites.

Type	Clay content, wt %	Activity number	Plasticity index	Dominant mineral	Friction angle	Plasticity	Hydr. conduct.	Therm. conduct.
I	< 5	< 0.75	5–10	Q,C,F,H, Ch,K	High	Low	High	High
II	5–20	0.75–1.25	10–30	Q,F,Ch, K,I	Medium high	Medium	Medium	Medium
III	20–60	> 1.25	10–80	I, S,Ch	Low	High	Low	Low

2.2.6 Classification according to organic content

Even a small organic content strongly affects the rheological properties of soils, and the organic constituents can also be of great importance for uptake and subsequent transport of radionuclides. Low-organic mineral soils and medium-organic soils are classified on the basis of the content and nature of organic material and of the composition of the mineral material, Table 2-8. The matter is discussed in detail in Chapter 4.

Table 2-8. Guiding values for the classification of soils on a basis of organic content /1/.

Soil group	Organic content in wt % of dry material (≤ 2 mm)	Examples of designations
Low-organic soils	2–6	Gyttja-bearing clay Dy-bearing silt (muddy silt) Humus-bearing, clayey sand
Medium-organic soils	6–20	Clayey gyttja Silty dy (silty mud) Humus-rich sand
High-organic	> 20	Gyttja (mud) Dy Peat Humus-rich topsoil

2.2.7 Classification according to geotechnical properties

Strength properties

The strength of a soil is determined by the friction between the particles, including dilatancy effects, and by precipitations creating strong bonds between the grains (cementation). For the clay fraction the strength also depends on bonding forces (sorption forces) between the strongly surface-active clay particles. Organic bonds can also contribute to the strength.

One normally distinguishes between cohesive soils and non-cohesive, i.e. friction soils. Definitions and methods for determining strength parameters are described in Chapter 11.

Undrained shear strength, τ_{fu}

For cohesive soils the undrained shear strength has been chosen as a basis of classification /1/. The determination of the undrained shear strength is one of the routine investigations of undisturbed samples of cohesive soils.

Based on the undrained shear strength, cohesive soils – mainly clays – are divided into five groups as shown in Table 2-9.

Table 2-9. Classification of cohesive soils according to shear strength /1/.

Designation	Undrained shear strength, τ_{fu}, kPa
Very soft	< 12.5
Soft	12.5–25
Medium stiff	25–50
Stiff	50–100
Very stiff	> 100

Sensitivity, S_t

Sensitivity is the ratio between the undrained shear strength of a specimen in undisturbed and in remoulded states. It is of great importance when estimating the effect on the clay of disturbance through piling, sheeting, slides, etc.

Clays are divided into four groups with respect to sensitivity as shown in Table 2-10.

The term *quick clay* is used to characterize clay with $S_t \geq 50$ for which the cone penetration with the 60g/60° cone exceeds 20 mm when the clay is remoulded.

Consistency

A cohesive soil has a plastic consistency in the remoulded state when the water content falls within certain established limits. The upper limit of the water content, at which the soil transforms from a plastic to a fluid state, is called the liquid limit w_L. The lower limit, where the soil passes from a plastic to a firmer, brittle consistency, is called the plastic limit w_P.

The matter, which is of fundamental importance for characterizing clay for repository design and construction, is discussed in detail in Chapter 8.

Table 2-10. Classification of clays according to sensitivity as determined by the fall-cone test /1/.

Designation	S_t (kPa/kPa)
Low-sensitive	< 8
Medium-sensitive	8–30
High-sensitive	> 30

2.3 References

/1/ **Karlsson R, Hansbo S, 1981.** Soil classification and identification. Doc. D8:81, Swedish Council for Building Research, Stockholm.

/2/ **Pusch R, 1994.** Waste Disposal in Rock. Elsevier Publ. Co.

3 Mineral constituents

This chapter deals with mineralogical issues of interest to repository design staffs, especially for composition and preparation of buffers and backfills. Focus is on clay minerals and their occurrence, particularly expanding ones, but rock-forming minerals are of importance as well. The section is not aimed at being a scientific document or a textbook chapter but serves to give the engineer a basis for understanding and realizing the physical and chemical behaviour of the mineral constituents of buffers and backfills. The size, shape and arrangement of the particles in such materials will be treated in Chapter 6.

3.1 Introduction

For ordinary soil mechanical purposes a detailed description of the mineral composition is usually not required, although highly plastic clays are known to require certain procedures in laboratory testing, and investigation of whether the plasticity is due to organics or to expanding clay minerals like smectites. For other purposes, as for isolation of toxic or radioactive wastes, a low hydraulic conductivity and an appreciable ion exchange capacity as well as a swelling potential are needed, for which the presence of well defined expanding minerals in sufficient quantities is required. For such isolation one also has to show that certain accessory minerals that may have a degrading effect on waste containers or on their clay embedment do not make up more than a small fraction of the total mineral content. Different minerals dominate in different size fractions, a major fact being that clay minerals have a maximum particle size of 2–5 μm and are usually much smaller than that. Bigger particles consist of rock-forming minerals, which can also make up a considerable part of the finest size fractions.

In summary, there is a need for defining methods for identifying and quantifying the mineral composition of clay materials with which this chapter deals. However, since the issue is very complex and many of the techniques and concepts are debatable we will confine ourselves to give an overview only, referring the interested reader to the vast literature on the various subjects. We will summarize practically important mineral data and describe methods for qualitative and quantitative determination of the mineral components.

3.2 Rock-forming minerals

Rock-forming minerals in natural soils including bentonites originate from degraded rock. The practically important ones belong to the silicates, sulphates, sulphides and carbonates and we will confine ourselves to list these minerals in Table 3-1 together with their diagnostic properties.

Table 3-1. Common rock-forming minerals /1/.

Mineral type	Mineral	Density kg/m³	Hardness
Silicates	Quartz	2650	7
	Feldspars		
	Microcline, orthoclase (K)	2560	6
	Albite (Na)	2620–2760	6
	Anorthite (Ca)	2620–2760	6
	Micas		
	Muscovite	2800–2900	2.5 (4⊥)
	Biotite	2800–3400	2.5
	Chlorite	2600–3300	2.5
	Mafic minerals		
	Hornblende	3000–3400	6
	Pyroxene	3200–3900	6
	Amphibole	2900–3300	5–6
Carbonates	Calcite	2710	3
	Dolomite	2850	3.5–4
Oxides, hydroxides	Iron minerals		
	Magnetite	5200	6
	Hematite	5300	5–6
Sulphides	Pyrite	5010	6–6.5
Sulphates	Gypsum	2320	2
	Anhydrite	2960	3.5

3.3 Clay minerals

3.3.1 Main minerals

Common clay mineral types are /2/:

- Halloysite
- Kandites (kaolinites, dickite, nacrite)
- Smectites (montmorillonite, saponite, nontronite, beidellite)
- Illite
- Vermiculite
- Chlorites
- Palygorskite group (attapulgite, sepiolite)

The distinction between these groups is based on crystal structure and chemistry, which also account for the variation within each group. With the exception of the halloysite and palygorskite types, the clay groups listed have a characteristic platy habit, which imparts a very high surface area to mass ratio. The crystal structure of clay minerals is responsible for a number of their characteristic chemical properties, including high cation exchange capacity. The palygorskite group of clay minerals has a fibrous habit, including large voids in the crystal structure. The large surface area and open crystal structure impart the distinctive properties of this group, including a high sorption capacity. Table 3-2 describes the crystal structures and mineral habits of major groups /2,3,4/.

Table 3-2. Generalized crystal structure and crystal properties of clay minerals (after N Chapman).

Clay mineral group	Generalized crystal structure	Layer charge deficiency	Crystal habit	Crystal properties
Kaolinite	Dioctahedral, stacks of units of 1 tetrahedral SiO sheet and 1 octahedral OH/Al sheet	0	Triclinic. Hexagonal plates, diam.: 0.1–4 μm, thickness 0.05–2 μm	Rigid, incompressible. Surface area 10–20 m^2/g
Halloysite	Dioactahedral, kaolinite-type	0	Triclinic. Tubular, diam.: 0.05–0.2 μm, wall thickn. 0.02 μm	Rigid, brittle. Surface area 35–70 m^2/g
Vermiculite	Trioctahedral, stacks of symmetric units of 2 tetrahedral SiO sheets and 1 octahedral OH/Mg sheet	0.6–0.9	Monoclinic. Irreg. shape, size several μm	Very soft. Strong expansion on heating. Surface area 800 m^2/g
Illite	Dioctahedral, stacks of symmetric units of 2 tetrahedral Si/Al/O sheets and 1 octahedral OH/Mg sheet. Potassium ions serve as glue	0.6–0.9	Monoclinic. Irreg. Shape, size 0.01–2 μm	Rel. rigid. Surface area 65–100 m^2/g
Smectite	Di- or trioctahedral, stacks of symmetric units of 2 tetrahedral Si/Al/O sheets and 1 octahedral OH/Mg, OH/Al, or OH/Fe sheet	0.2–0.6	Monoclinic. Irreg. Shape, size < 0.5 μm	Very soft. Strong expansion on wetting with gel easily formed. Surface area 800 m^2/g
Chlorite	Di- or trioctahedral, stacks of mixed-layer units of brucite and mica sheets	0.3–1.0	Monoclinic. Hexagonal plates, diam.: 0.1–4 μm, thickn. < 0.2 μm	Soft. Surface area as illite
Mixed-layer	Many combinations: smectite/ illite, smectite/kaolinite, smectite/mica. Stacks of mixed-layer units	0.2–0.6	Smectite-like	Smectite-like but moderate expansion on wetting. Surface area 100–300 m^2/g
Palygor-skite	Halloysite-like structure with Mg or Al	–	Tubular, length 0.2–0.8 μm	Rigid. Strong expansion on wetting with gel formed. Surface area like smectite

In light of the numerous clay mineral species and the difficulties inherent in attempting to analyze each group, we will only consider four major clay types: the kandite group (especially kaolinite), the illites or, rather, the hydromicas, the smectite group and the chlorite group. These four clay types are predominant in almost all natural occurrences and represent most of the extremes of properties that are of practical importance. Kaolinite and smectites are early diagenetic minerals, which are most stable at earth surface conditions, while illites and chlorites are diagnostic of higher temperature and diagenetic environments. The results of experiments and observations of these widely diverse clay minerals should be applicable to almost all types of clays and their mixtures, in a wide range of environmental conditions.

Practically all of the clay minerals are phyllosilicates (layer silicates), the structures of which are composed of well-defined sheets of linked silica/aluminum tetrahedra and aluminum/magnesium hydroxide octahedra. It is the combination of these sheets into various types of layers that distinguishes the major clay mineral groups and imparts to them many of their characteristic chemical and physical properties. Tetrahedral sheets consist of coupled, oriented silica tetrahedra sharing the three basal oxygens with nearest neighbors, and with the apical oxygens all pointing in the same direction. The linked network of the trigonal basal units of the silica tetrahedra produces a hexagonal framework, the centers of which are positions where hydrated cations are often adsorbed onto the clay mineral surface. Octahedral sheets contain linked octahedral coordination groups in which divalent and trivalent cations are enclosed by an octahedral network of oxygen and hydroxides. Octahedral and tetrahedral sheets are linked together by the apical tetrahedral oxygen replacing one of the octrahedral hydroxyls, thereby orienting the basal plane of the tetrahedra toward the other surfaces of each sheet.

3.3.2 The kandite group

The kandite group, *kaolinite*, *dickite*, *nacrite* and several hydrated forms, consist of a 1:1 layer dioctahedral structure with minimal substitution within the structure. This lack of substitution means that there is little deviation from the ideal formula, $Al_2Si_2O_5(OH)_4$ but occasionally some Fe^{3+} substitutes for Al^{3+}. The limited lattice substitution also requires very little cation adsorption in interlayer sites to balance charge deficiencies. The greatest difference among the members of the kandites is the mode of stacking and disorder of the 1:1 layers. One layer per unit cell results in triclinic kaolinite, while two stacked layers per unit cell produce the monoclinic structural varieties dickite and nacrite. The crystal lattice forms are shown in Figures 3-1 and 3-2.

Hydrogen bonding was earlier considered the major force binding kaolinite layers together but recent investigations speak in favor of OH-O electrostatic attraction, with the oxygens being bonded to cations /3/.

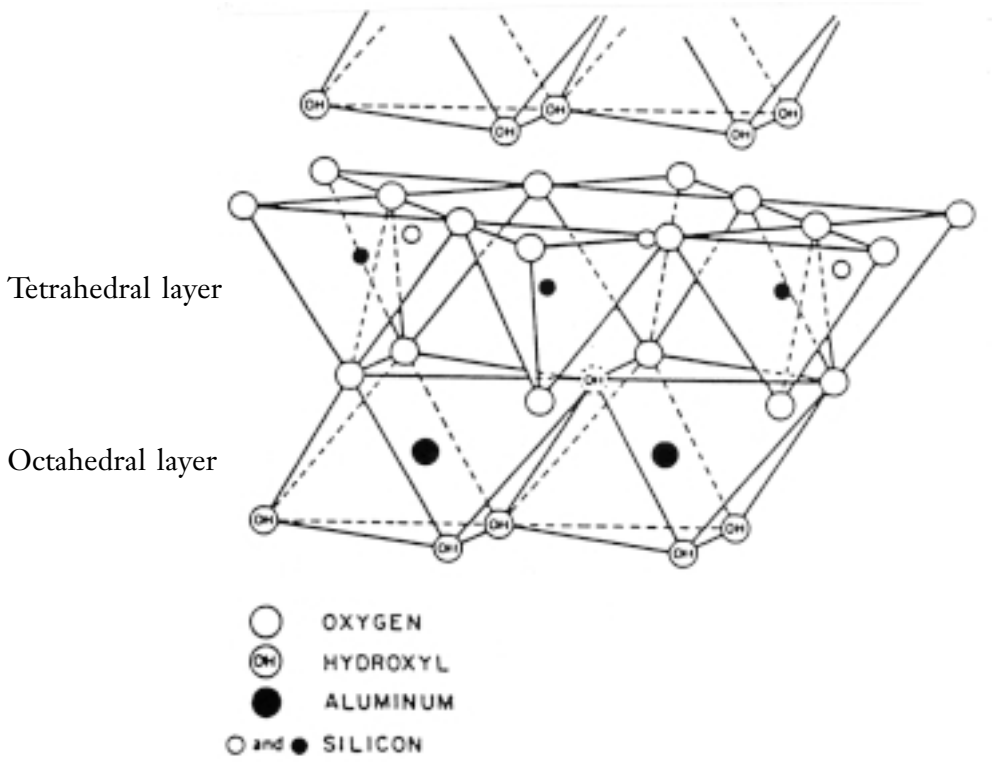

Figure 3-1. *Crystal structure of kaolinite /3/.*

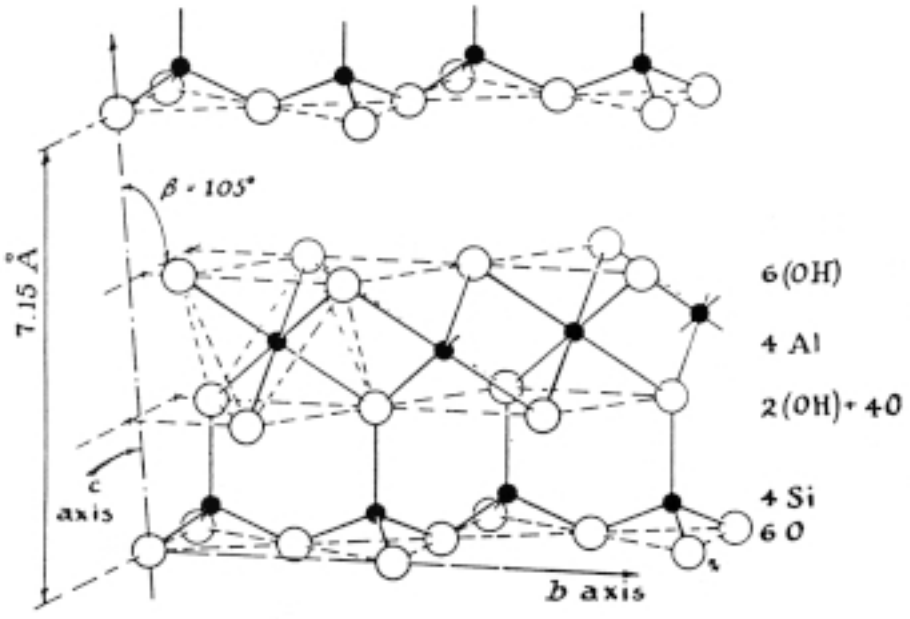

Figure 3-2*. Lattice characteristics of the triclinic kandite minerals /1/.*

3.3.3 The hydromicas ("illite")

Before discussing in detail the 2:1 clay minerals we will consider the simple 2:1 phyllosilicate *pyrophyllite* $Al_4Si_8O_{20}(OH)_4$, since its structure is similar to that of the most common smectite species montmorillonite, and since one can make use of this mineral as reference substance in quantitative mineral analyses. The structure is shown in Figure 3-3.

Pyrophyllite has no net lattice charge and no water molecules between the layers. If one of the silicons in each group of four tetrahedrons in Figure 3-3 is replaced by aluminum – leaving the octahedral layer intact – the *muscovite* structure is obtained, provided that the induced lattice charge is balanced by interlayer potassium ions (Figure 3-4). If this structure, which is represented by a formula of the type $K_2Si_6Al_6O_{20}(OH)_4$ is in turn altered so that part of the potassium is replaced by hydronium ions (H_3O^+) we obtain the mineral illite (hydromica). It has long been known that this mineral does not have any definite chemical composition but obeys the general rule:

$$M_y^I Si_{(8-y)} Al_y O_{20}(OH)_4 \left(M^{III}, M^{II} \right)_4$$

This formula, originally given by Maegdefrau /4/, has been suggested for the rock-forming micas, the hydrous micas and the smectites. M^I represents monovalent cations, while M^{II} stands for magnesium and divalent iron and M^{III} for aluminum (or trivalent iron). For y=0 the formula represents the smectite group and for y=2 it is valid for rock-forming micas. The hydrous micas have a y-value between 1 and 2, which well illustrates that this mineral represents an intermediate, not well defined stage between micas and smectites.

The layers are kept together by electrostatic forces between the potassium ions and the highly charged crystal lattices. Hydrogen bonds and dispersive (London/van der Waals) forces also contribute to link the layers together.

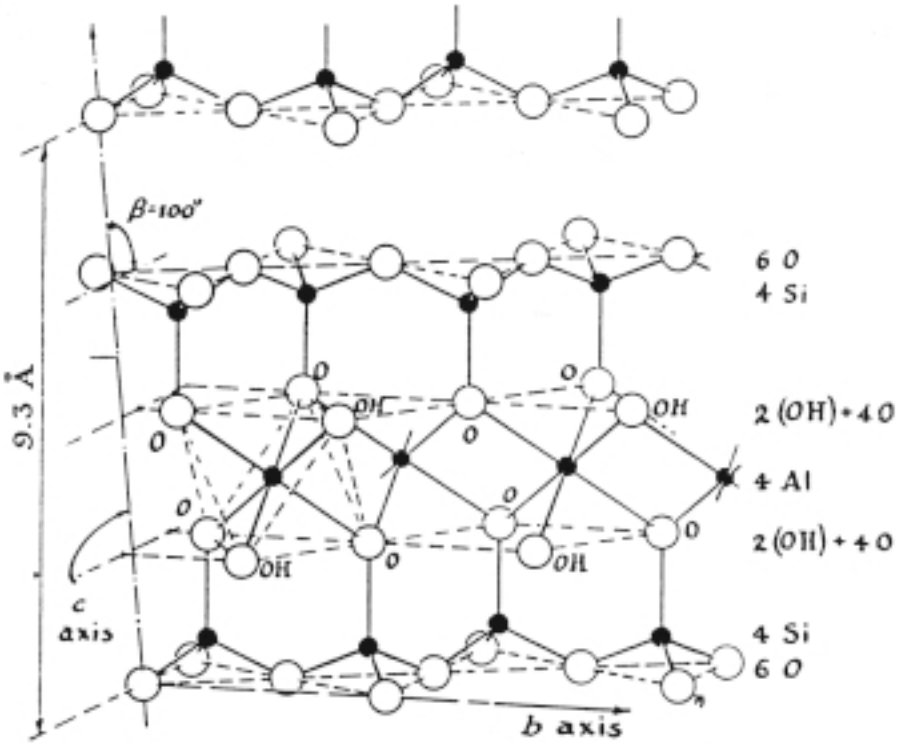

Figure 3-3. *Lattice characteristics of the monoclinic mineral pyrophyllite /1/.*

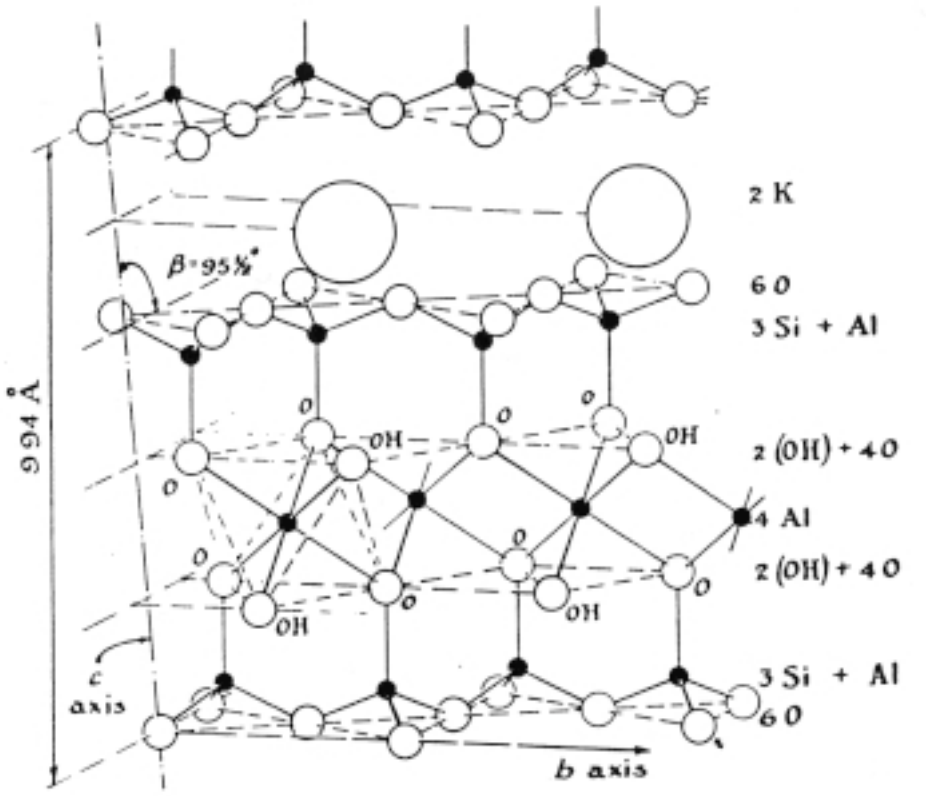

Figure 3-4. *Lattice characteristics of the monoclinic mica mineral muscovite /1/.*

3.3.4 The smectites

If we apply Maegdefrau's formula and also take silicon, aluminum and magnesium to be lattice cations and sodium as balancing adsorbed cation, we arrive at formulas which illustrate the composition of smectites, see Table 3-3.

Table 3-3. Common smectite species.

Species	Formula	Octahedral type
Montmorillonite[1)]	$(OH)_4Si_8(Al_{3.34}Mg_{0.66})O_{20}$ ↓ Na 0.66	Dioctahedral
Beidellite[1)]	$(OH)_4(Si_{7.34}Al_{0.66})Al_4O_{20}$ ↓ Na 0.66	–"–
Nontronite[1)]	$(OH)_4(Si_{7.34}Al_{0.66})Fe_4^{3+}O_{20}$ ↓ Na 0.66	–"–
Hectorite[1)]	$(OH)_4Si_8(Mg_{5.34}Li_{0.66})O_{20}$ ↓ Na 0.66	Trioctahedral
Saponite[1)]	$(OH)_4(Si_{7.34}Al_{0.66})Mg_6O_{20}$ ↓ Na 0.66	–"–

[1)] Formulas given by Grim /3/

While montmorillonite is similar to pyrophyllite, beidellite is related to hydrous mica. The general appearance of the lattice structure of the three dioctahedral smectites is shown in Figure 3-5 while Figures 3-6 and 3-7 show the detailed structural patterns of montmorillonite according to two possible, quite different models. The version suggested by Hofmann, Endell and Wilm (HEW) /5/ is the traditional structure, which is assumed to be valid for temperatures well exceeding 100°C, while that of Edelman and Favejee (EF) /5/ may represent the lattice constitution when sodium or lithium is adsorbed as balancing cations, and the temperature is lower. The matter is of great importance with respect to the hydration properties of montmorillonite.

The structural constitution of smectites has been under debate for decades and it has not yet been validated whether the structure proposed by Edelman and Favejee really exists since the matter can not be settled by XRD. This structure would yield a high cation exchange capacity without requiring lattice substitutions, a number of hydroxyls providing the negative lattice charge.

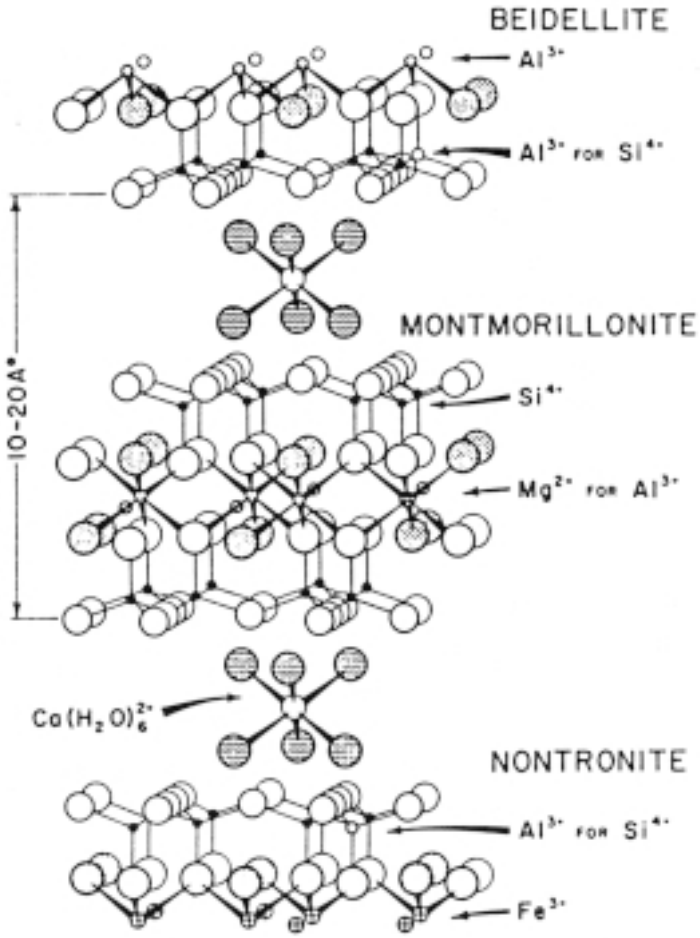

Figure 3-5. *The crystal structure of the monoclinic mineral smectite representing three common types /7/. The pictures demonstrate the special case with hydrated calcium ions located in the interlamellar space.*

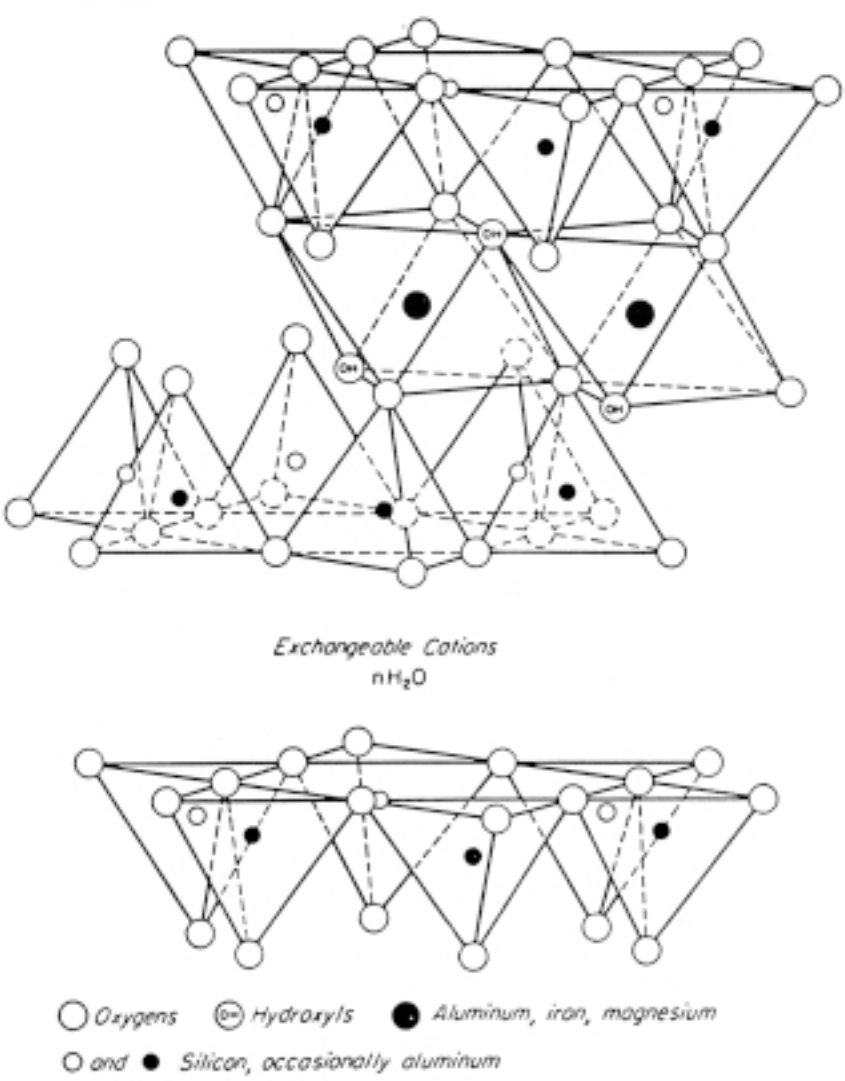

Figure 3-6. *Diagrammatic sketch of the structure of montmorillonite according to Hofmann, Endell and Wilm /3/.*

When it comes to selection of clay materials for buffers and backfills in repositories, for which smectitic clays are of primary interest, the chemical stability is of fundamental importance. Experience and geochemical analyses based on thermodynamics show that beidellite is the least stable low-charge species since uptake of potassium can make this mineral collapse and transform to illite, while saponite is considered to be the most stable form /6/.

In later years much effort has been made in chemical industry to expand the interlamellar space – "pillaring" – for increasing the amount of absorbed species of organic type. By this, effective anionic exchangers can be prepared like when smectite is treated with HDPy molecules as described in Part 2 of this Handbook. The involved processing is relatively simple and can be made on an industrial scale.

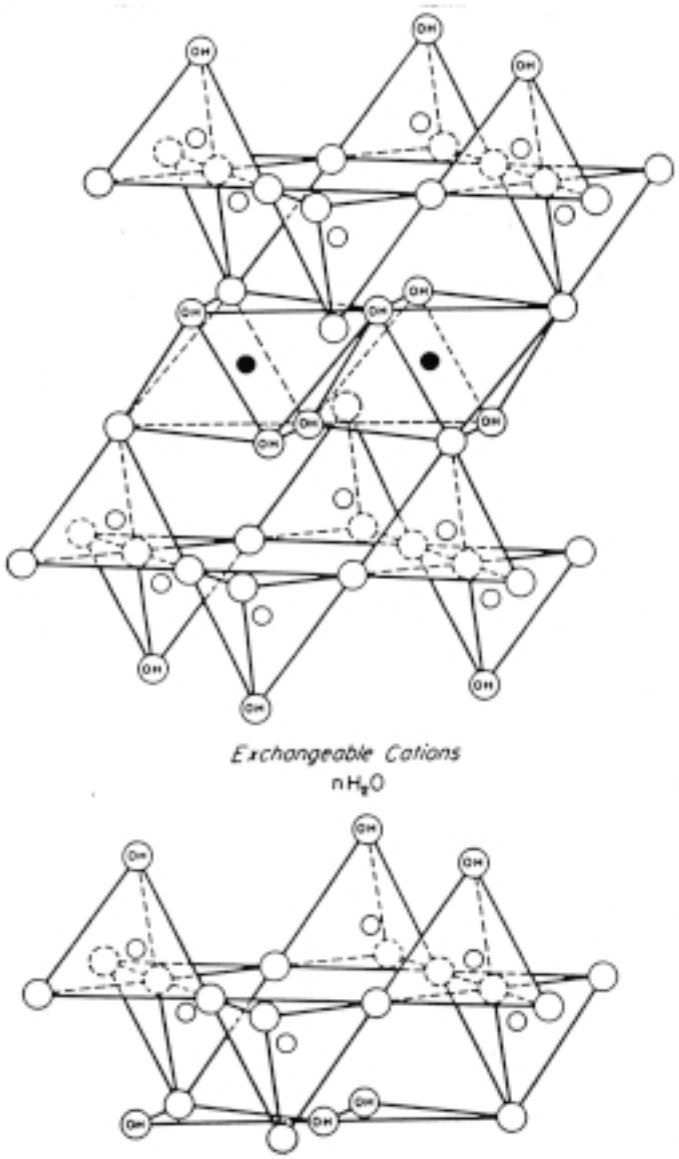

Figure 3-7. *Diagrammatic sketch of the structure of montmorillonite suggested by Edelmann and Favejee /3/.*

MAS/NMR examination of montmorillonite with respect to the coordination of ^{29}Si and ^{27}Al has given support to the existence of two crystal constitutions, i.e. the HEW and EF forms /8/. Thus, for Na clay heated up to 90°C the Si spectrum can well be representative of *trans*-coordination like in the EF model (some SiOH tetrahedrons), while heating to 130°C and more yields a change in peak pattern that would imply the ordinary *cis*-coordination (SiO tetrahedrons) of the HEW model. For the corresponding treatment of Ca montmorillonite MAS/NMR shows no change in Si coordination since HEW is valid irrespective of the temperature.

3.3.5 Chlorite

The chlorites exhibit a high degree of atomic substitution, the general formula being

$$\left(Mg, Fe, Al\right)_6 \left(Al, Si\right)_4 O_{10} (OH)_8$$

In this general formula Mg and Fe are mutually replaceable; ferric iron is often present. The structure of chlorite is illustrated in Figure 3-8. The mica layer is negatively charged and this charge is neutralized by a positive charge on the $(Mg,Al)(OH)_2$, i.e. a brucite-type layer in the chlorites thus corresponds to the potassium ions in the micas.

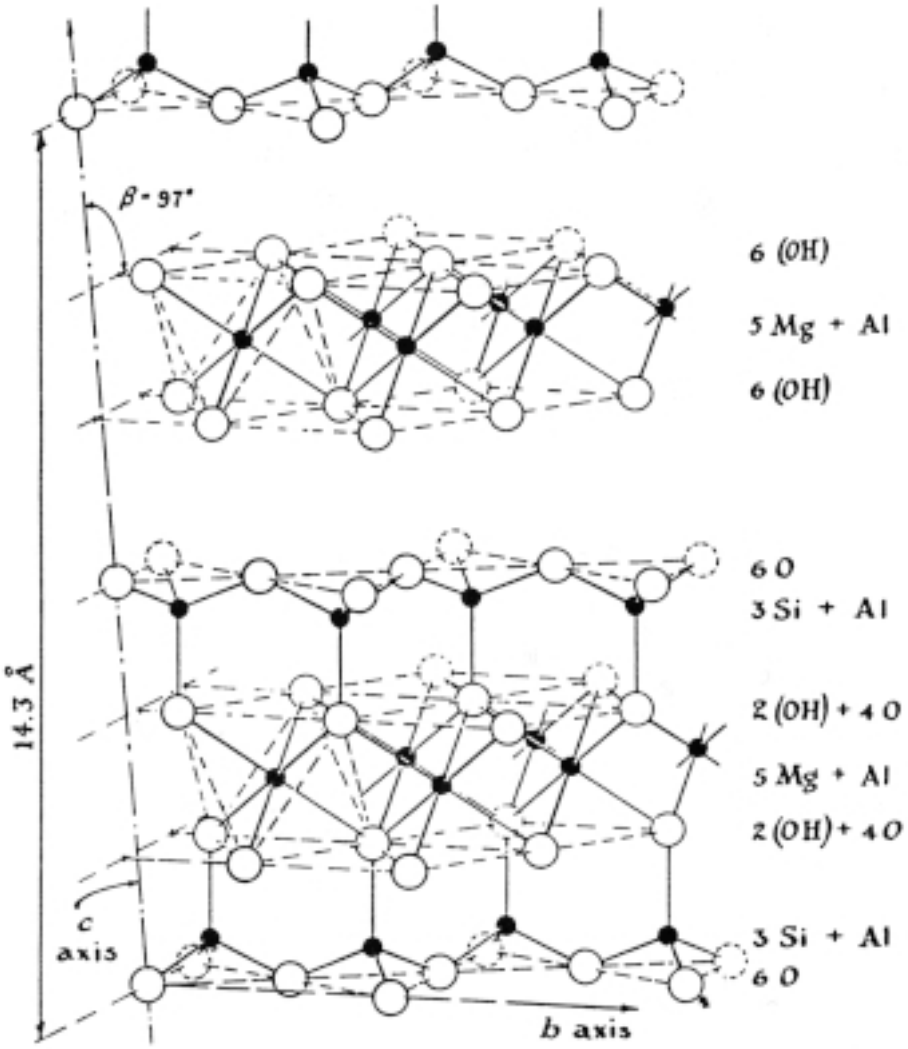

Figure 3-8. *Structure of the monoclinic mineral chlorite. A three-layer structure similar to pyrophyllite but with 5 Mg and one Al in the octahedral positions with a further octahedral layer of $Mg_5Al(OH)_{12}$ between the pyrophyllitic layers /1/.*

3.3.6 Mixed-layer minerals

After X-ray diffraction analysis (XRD) had been introduced and applied in mineralogy some 60 years ago it was early recognized that many smectite clays gave spectra that deviated from the ones corresponding to the idealized crystal structures. The discrepancy was explained by the existence of intermediate forms, i.e. mixed-layer minerals with regular or irregular ordering of smectite and illite lamellae or of smectite and kaolinite or chlorite lamellae. In recent years the existence of this sort of minerals has been seriously questioned and the odd appearance of XRD spectra instead explained by grouping of smectite and illite (or kaolinite and chlorite as well as muscovite) /7/. Since the matter is not yet settled, it has become common to use the term expandable minerals rather than mixed-layers for all species that cannot be identified as any of the smectites and that undergo changes in the crystallographic c-direction on wetting and drying or treatment with organic compounds and electrolytes of different cationic composition.

3.3.7 Appearance

Scanning electron microscopy (SEM) provides good images of the clay minerals and typical examples are given in Figure 3-9. Kaolinite and halloysite have diagnostic morphology. Illite particles in Quaternary sediments are usually irregularly shaped with thin edges, while hydrothermally neoformed illite in smectite clay often shows more regular, often lath-shaped crystals. Smectites characteristically consist of clearly discernible thin stacks of several lamellae but "mossy" appearance is not unusual either.

Suitable preparation of clay material for microscopy is essential for getting representative images. Thus, intense disintegration yields breakage of particle edges and causes dispersion of aggregates that operate as cohesive aggregates in the natural clay. Electron diffraction is helpful both for determination of crystallinity and for identification of clay minerals.

The arrangement of clay mineral particles in clay masses is of fundamental importance to the understanding of their performance and of all important processes like fluid percolation, gas penetration, ion diffusion and rheological phenomena including expansion and consolidation. These matters are dealt with in a later chapter dealing with the microstructure of natural and artificially prepared clay materials. A typical micrograph of soft montmorillonite-rich clay obtained by transmission electron microscopy of an ultrathin section of acrylate-treated impregnation for preservation of the structure is shown in Figure 3-10. It illustrates the aggregation pattern with presence of very soft clay gels in the voids between denser aggregates.

Weathering of illite and chlorite gives the porous character of degraded particles that one sees in Figure 3-10. Figures 3-11 shows how hydrothermal treatment affects montmorillonite-rich bentonite. The upper picture in this figure shows an overall view of an ultrathin section of MX-80 bentonite autoclaved at 200°C for 0.5 years, and the picture below a close-up with five areas examined with respect to the element distribution in the electron microscope with energy dispersive X-ray (EDX). The result is shown in tabular form in Figure 3-12, which exhibits amorphous colloidal silica adjacent to smectite stacks. Cristobalite and quartz commonly appear as well.

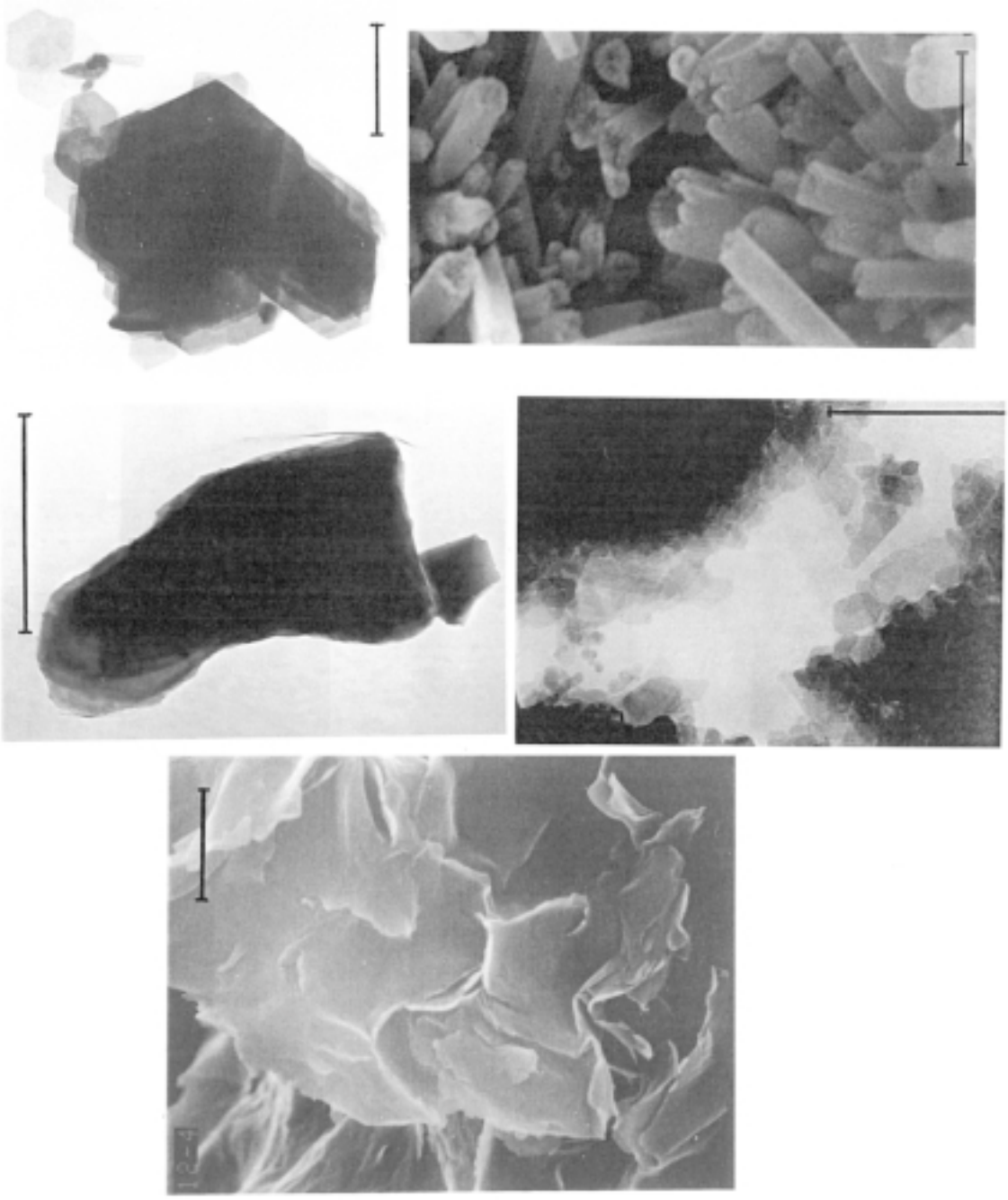

Figure 3-9. *Typical electron images of clay minerals. Upper: TEM pictures of kandite in the form of kaolinite to the left and halloysite to the right. Central: TEM pictures of illite particles. Lower: SEM picture of montmorillonite. The bars represent a length of 1 mm.*

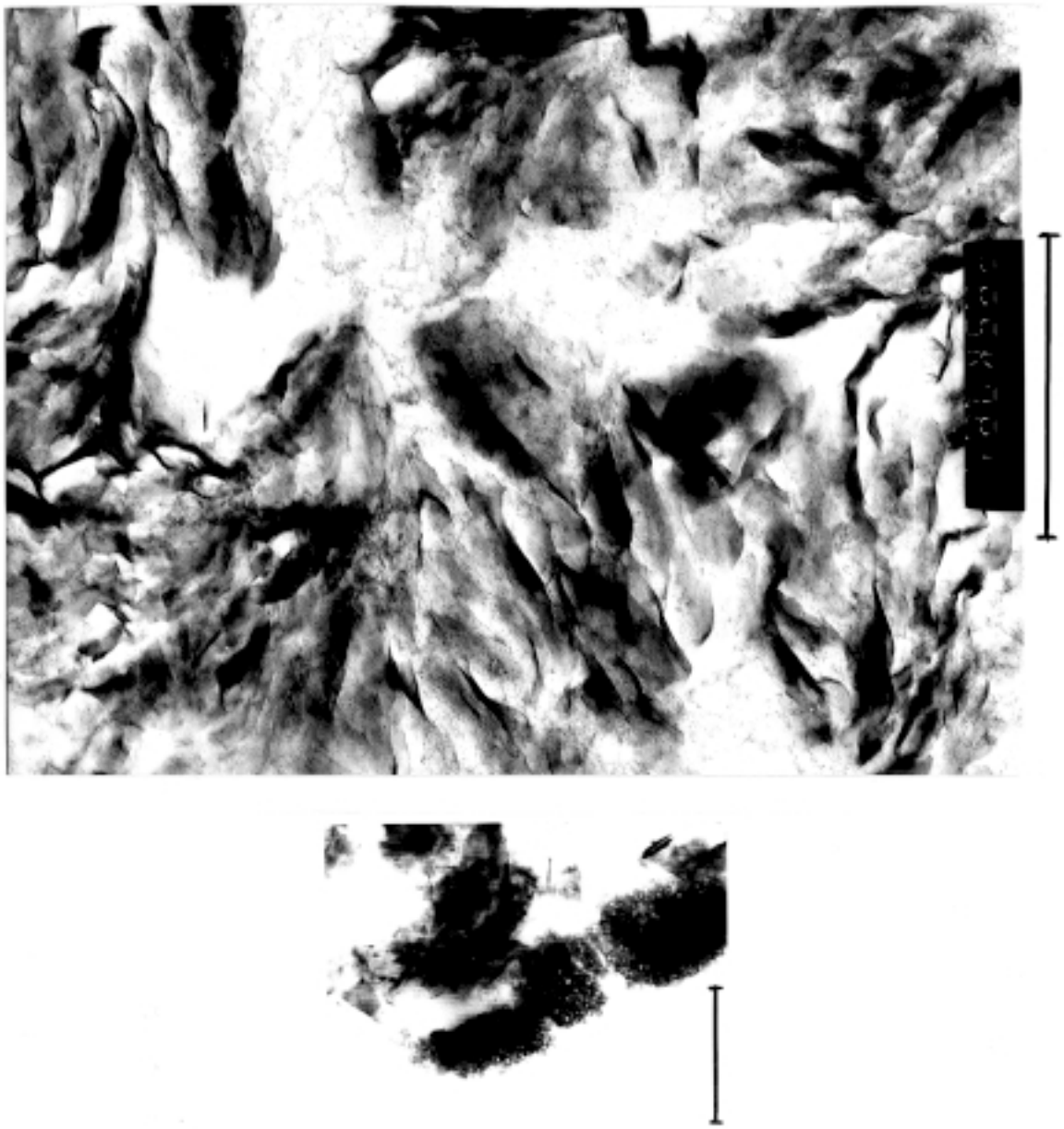

Figure 3-10. *Typical transmission electron images of elements of clay. Upper: Montmorillonite-rich clay with aggregates of stacks of lamellae and very soft clay gels in the larger voids. Lower: Weathered illite particles. The lattices loose coherence and the particles become porous and mechanically weak. The bar represents a length of 1 mm.*

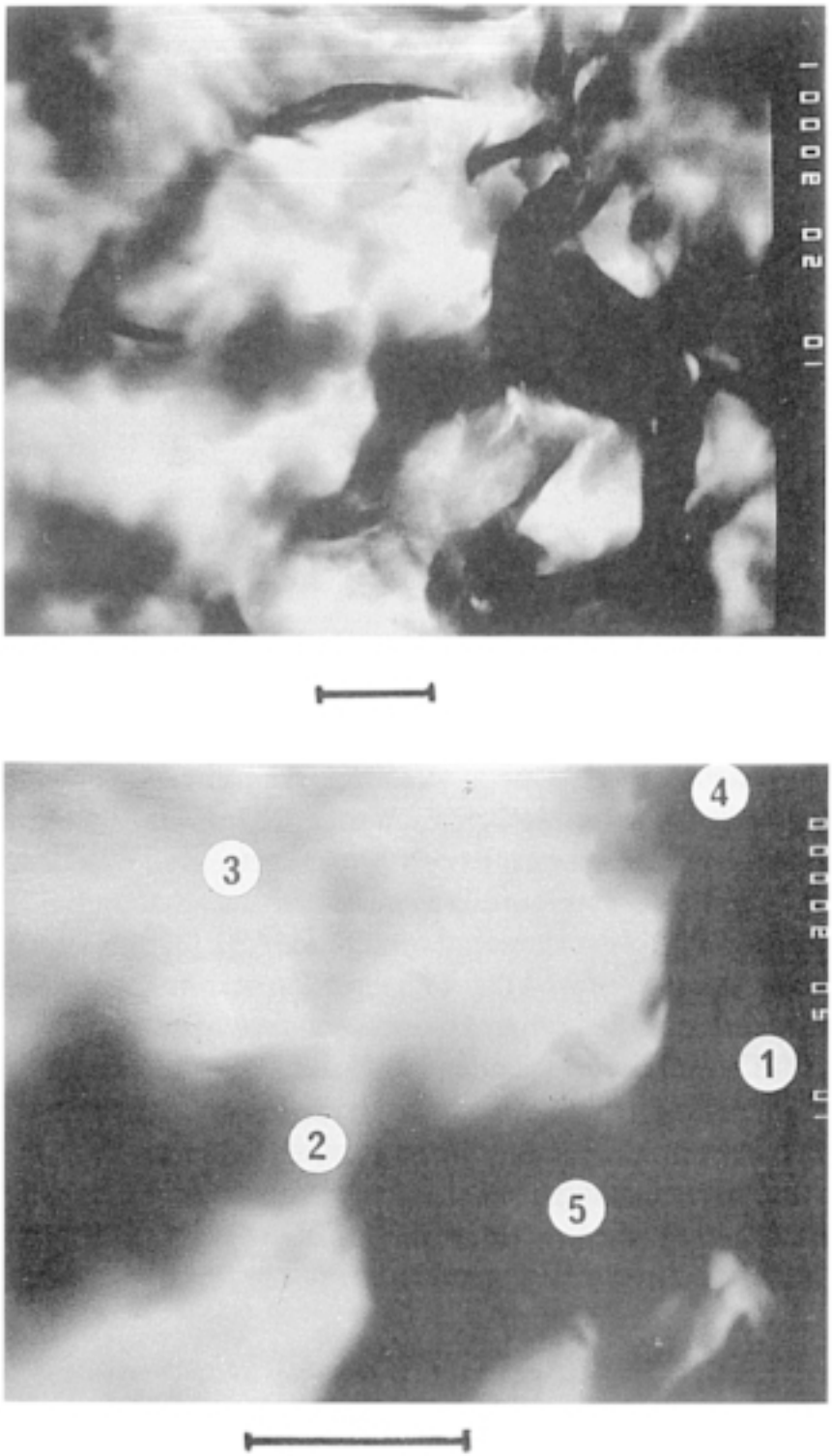

Figure 3-11. *TEM pictures showing microstructural regions for elemental analysis of bentonite that had been autoclaved at 200°C for 0.5 years. The lower picture is a close-up of the upper one, showing 5 areas selected for point element analysis. Bars represent 1 μm length.*

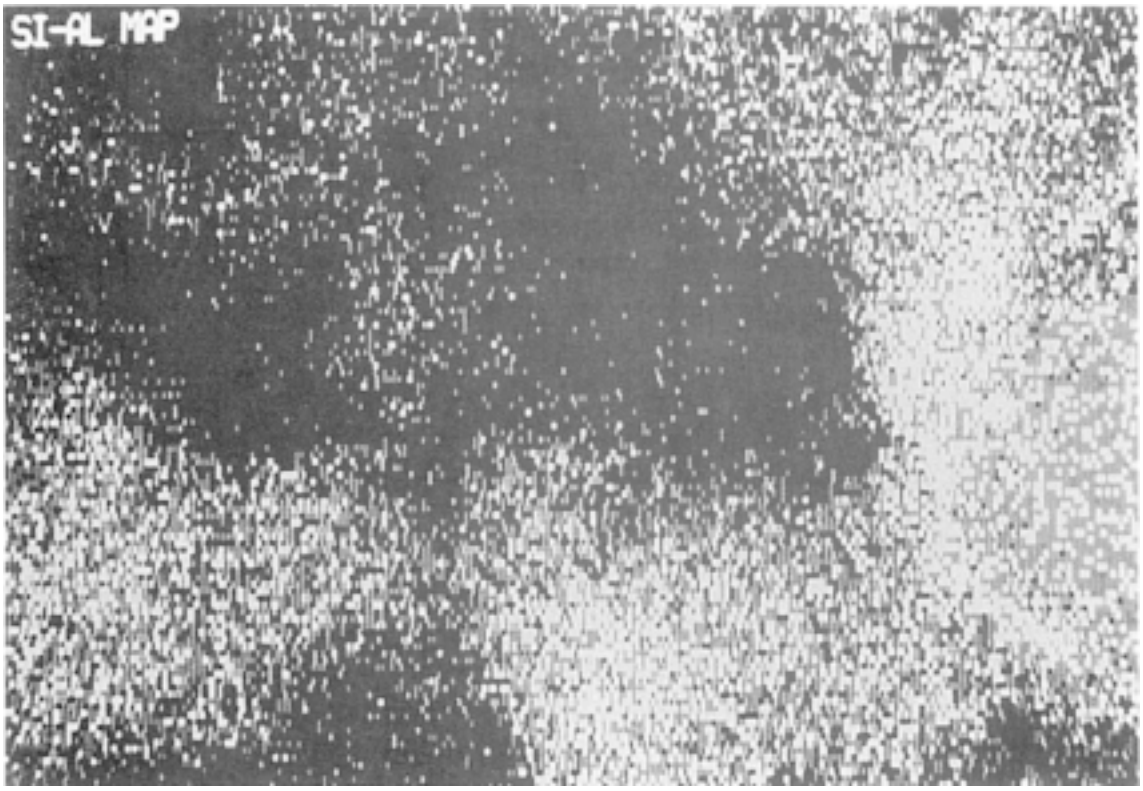

Table of atomic ratios of elements (relative to Si) obtained from the X-ray spectral data for points 1–5 in Figure 3-11 (Intensity ratios relative to Si)

Point no	Elements			
	Mg	Al	Si	Fe
1	0.00	0.05	1.00	0.01
2	0.10	0.43	1.00	0.05
3	0.10	0.38	1.00	0.04
4	0.10	0.40	1.00	0.04
5	0.07	0.39	1.00	0.04

***Figure 3-12**. Mapping of Si and Al superimposed on Figure 3-11. White areas represent the typical Sl/Al ratio of montmorillonite, while grey areas show excess Si. The grain at the right border is silica-rich and silica-enriched zones are also seen at the edges of several aggregates /6/.*

3.3.8 Occurrence

In the early sixties Charles E. Weaver /9/ concluded from X-ray analyses of the clay minerals from thousands of sediments that any of the major clay minerals can occur in abundance in any of the major depositional environments and that there is no consistent coincidence between specific clay minerals and specific depositional environments. The great majority of clay minerals in sedimentary rock are detrital in origin and strongly reflect the character of their source material, thus being only slightly modified in their

depositional environments. Only in porous and permeable sediments significant post-depositional alteration of the clay minerals were noticed by Weaver who concluded from his comprehensive study that:

- Any of the major clay mineral types, except chlorite, can occur as dominant mineral in clay strata representing similar chemical environments.
- Hydromicas, smectites, and mixed-layer minerals consisting of illite/smectite (I/S) can occur in abundance in any of the major depositional environments.
- Kaolinite is dominant mainly in fluviatile environments but can be in abundance in any formation.
- There is strong evidence from a large number of independent studies that clays are altered to some extent in fluviatile environments, but there is little direct evidence to indicate that alteration in the basin of deposition is a major factor for the ultimate mineralogic character of the clay suite. This suggests that the process of diagenesis is not as effective as is commonly thought, which is of fundamental importance for the survival of clay buffer materials in repositories. Thus, where only the pressure and temperature are changed while percolation is prevented or nearly so, no significant alteration is expected to take place provided that the temperature does not exceed about 90°C and that heating does not last for more than a few thousand years.

Kaolinite

It was early concluded that kaolinite is formed in nature by acid reactions under anaerobic conditions. It is most abundant in warm, humid climates and is a prominent constituent of oceanic sediments in the equatorial belt. The genesis of the kaolinite group of clay minerals is thus usually related to intensively weathered soil profiles in subtropical to sub-humid climates. Laboratory experiments of granite weathering at room temperature and atmospheric pressure indicate that kaolinite is the ultimate stable "pure" aluminosilicate.

Kaolinite is also found at the other upper end of the temperature spectrum, precipitating in low-grade metamorphic and hydrothermal environments at depths of up to several kilometers. Kaolinite is primarily a sedimentary mineral often incorporated in the sediment at the time of deposition. Most studies have focused on the upper limits of its stability in metamorphic terrains.

Stability relationships at surface conditions among kaolinite, aluminum hydroxides, and other aluminosilicates have been extensively evaluated with thermodynamic data. A common graphical representation of these relationships is the activity diagram where the log of dissolved silica concentration is plotted against the log of the ratio of the alkali concentration divided by that of protons (Figure 3-13). The extent of the kaolinite stability field varies with the alkali but several generalizations concerning kaolinite stability can be made. Kaolinite is favored over gibbsite, an aluminum hydroxide, by the presence of very small amounts of dissolved silica. Kaolinite is also favored over illites, montmorillonite, and feldspar phases by low $alkali^+/H^+$ ratios. This ratio is usually manifested in sedimentary environments by low pH, since this condition is often generated by decomposed organic material or hydrolysis reactions.

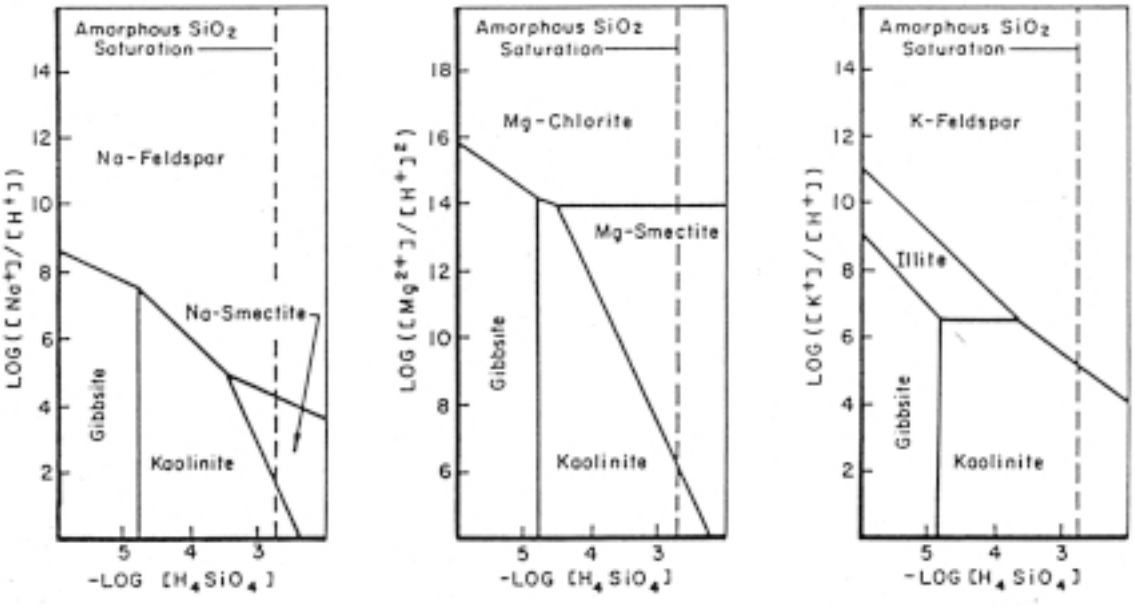

Figure 3-13. *Stability relationship diagrams for several common low-temperature clay minerals calculated for the activity of several cations (K^+, Na^+, Mg^{2+}, H^+) against silica activity, at 25°C, 1 atmosphere /9/.*

Illite (hydrous mica)

Illite is the most common clay mineral in soils, sedimentary rocks and rock undergoing low-grade metamorphism. Along with variations in chemical composition, there are several variations in crystal lattice organization.

Illite is commonly associated with chlorite, biotite, and quartz rocks that have not experienced higher temperatures than 200°C according to Velde /10/, who also stated that hydromicas dominate the argillic zone of hydrothermal alteration, generally very close to the heat source. Farther away are found kaolinite and expandable clay minerals, such as smectites, as lower-temperature alteration products /11/. However, authogenic hydromica is also found in deep sea sediments and in sandstones that have not experienced high temperatures which demonstrates that these minerals are found over a wide range of environments.

Smectites

Smectites are very common at and near the earth's surface in soil zones, on the ocean floors, as authigenic cement in shallow-buried sandstones and shales, and in certain hydrothermal zones. However, in many of these cases, the smectites under consideration are not pure, but contain a significant amount of other clay minerals. Closer investigations of many soil and diagenetic smectites indicate that they contain a small percentage of non-expandable layers interstratified within the smectite packet. The only pure smectites that have been found appear to be associated with freshly devitrified volcanic glass in recent bentonites, authigenic cement in very porous sandstones, and hydrothermal alteration products /11/.

Chlorite

The chlorite group of clay minerals is associated with a wide range of depositional environments and diagenetic grades. In shales, their appearance as authigenic minerals is first noticed around 75°C and they persist beyond 350°C. The only generalizations about chlorite composition and chemical stability that can be made at present are that Fe-rich and aluminum dioctahedral chlorites are more stable at low temperatures, while Mg-rich trioctahedral chlorites tend to be more stable at higher temperatures. Chlorite composition otherwise appears to be more dependent upon host rock and interstitial fluid chemistry than on the low temperatures found during diagenesis /12/.

In many sandstones at shallow burial depths, chlorite is present as an authigenic cement coating quartz grains /12/. The occurrence of authigenic chlorite cement is often associated with the absence of unstable components in the sandstone: rock fragments, plagioclase feldspar, and heavy minerals. Chlorite is also observed replacing feldspars and rock fragments in some sandstones. With increasing diagenetic grade, authigenic cements are replaced by certain special chlorite minerals which make up a major component of graywacke matrix.

In shales, non-detrital chlorite appears at temperatures around 75°C along with a loss of kaolinite and progressive illitization of smectite. The association of chlorite appearance with illitization is evident in Tertiary sediments of the Gulf Coast where authigenic chlorite is observed at 70°C in some Oligocene shales and at 80°C in Miocene shales. The chlorites and smectites in these shales have different Fe/Mg ratios, indicating that chloritization is a solution-reprecipitation reaction and that Mg and Fe release rates from dissolving smectite are unequal /13/.

The appearance of chlorite in many shales has been correlated with the diminished presence of kaolinite over a fairly wide range of temperatures /9/. The kaolinite-to-chlorite-reaction, though never actually observed to be a simple one-step process, is concluded to begin at temperatures as low as 100°C, while the high end of the temperature range for this reaction is believed to be around 150–200°C. Chlorite found in the kaolinite-rich claystones of Australia is associated with temperatures as high as 200–250°C. The formation of corrensite (mixed-layer smectite/chlorite) from smectite is believed to occur around 170–220°C. We conclude from this that chlorite has a wide range of compositions and is found under quite different environments, and is not easily placed on an activity diagram. Sedimentary chlorites are found in primarily alkaline waters, hence high cation/H^+ ratios, and are usually not associated with free silica.

3.3.9 Characteristic properties

The most important properties of clay minerals for use as seals, i.e. buffers and backfills in repositories are their large specific surface and hydration potential and their ability to adsorb cations – and to a certain small extent – anions. It is primarily due to lattice charge defects, and manifested by a significant cation exchange capacity. It affects their ion diffusion transport capacity and the related charge distribution is the main reason for the ability to form coherent gels. Since the size of clay mineral crystals is mostly in the interval 50 Å to 2 μm, the void size of dense clays is very small and the passages for water flow very tortuous. The hydraulic conductivity of clays, especially in dense form, is thereby very low, but the really most important factor is that a significant part of the porewater is associated with the crystal lattices, especially in smectites. At higher densities at least 50% of their porewaters is in interlamellar positions and immobile under normal hydraulic gradients.

The electrical charge conditions determine the geometrical arrangement of clay minerals and the internal force fields the rheological behaviour. The microstructure and rheology depend on the type and concentration of electrolytes in the porewater as outlined in Section 6.

3.4 Experimental

3.4.1 General

For scientific quantitative determination of the clay mineral composition of a soil or rock sample it is usually necessary to make very careful and detailed analyses, while most investigations for technical purposes require only semi-quantitative determinations. We will be concerned here with the latter type of analysis and focus on distinguishing between rock-forming minerals and clay minerals.

3.4.2 Rock-forming minerals

Rock-forming minerals in buffers

For buffers one can distinguish between the composition of the clay fraction on the one hand, and the composition of coarser fractions on the other. Accurate quantitative determination of both require separation, usually so that particles finer and coarser than 2 μm are separated. The constituents of the latter, which are still too small to be identified by determining their density and hardness, can be accurately identified by combination of four methods: 1) optical microscopy, 2) separation by use of gravity, 3) X-ray diffraction analysis and 4) chemical analysis. We will confine ourselves to describe microscopy and techniques for determining the content of carbonates and sulphur-bearing minerals, which are of major importance for the performance of buffer materials.

Microscopy using 30 μm thin sections of material embedded in Canada balsam or other suitable media and examining them in a polarizing microscope is a routine method, which makes it possible to determine accurately the composition and relative abundance of rock-forming minerals. The methods of evaluation require significant experience and application of crystallography /14/.

From a strict soil mechanical point of view most rock-forming minerals have similar properties and there is no need to distinguish between quartz, feldspars, carbonates, heavy minerals and micas. However, from the viewpoint of chemical integrity of the buffer and metal waste canisters, a significant content of potassium feldspar, mica, chlorite, carbonates and sulphur-bearing minerals is of considerable practical importance. Mineral analysis with respect to the type and amount of rockforming mineras is therefore needed for assessment of any candidate buffer material. Carbonates and sulphur-bearing minerals are of particular importance.

The approximate carbonate content can be determined by adding diluted hydrochloric acid and measuring the produced carbon dioxide since carbonate minerals give off this substance in gaseous form by such treatment. The gas bubbles can be directly observed, which gives a general indication of the content of calcium carbonate (calcite). Experience shows that if the acid has been prepared by mixing concentrated hydrochloric acid (density 1190 kg/m^3) with distilled water, in proportions 1:6, no visible gas production

takes place if the content of calcium carbonate is less than 1% of the total mineral mass, while weak and strong gas formation is seen if such minerals represent 1–3%, and 3–5%, respectively /15/. Intense and lasting gas production is caused if the content of calcite exceeds 5% by weight. A more accurate method is to use a device like the one in Figure 3-14 for determining the carbonate content. The CO_2 gas produced in the reactor vessel (1) fills the rubber bladder (2) in vessel (3) and displaces the corresponding amount of air and water in the pipette (4). Concentrated HCl solution is poured into the reactor vessel and the reaction maintained until the gas production ceases. For calcium carbonate the stochiometric reaction gives a mass ratio $CaCO_3/CO_2$ of 2.27, which means that the amount of $CaCO_3$ per liter CO_2 is 4.18 g at room temperature.

Dolomite (calcium/magnesium carbonate), which is usually much less common than calcium carbonate, can only be dissolved in hot, concentrated hydrochloric acid. A way to distinguish between calcite and dolomite is hence to determine firstly the amount of CO_2 at room temperature and then proceed by heating the reactor vessel to boiling temperature. It should be mentioned that hydrogen peroxide, which is sometimes used in the preparation of soil samples for determination of the organic content, can dissolve some of the carbonate content.

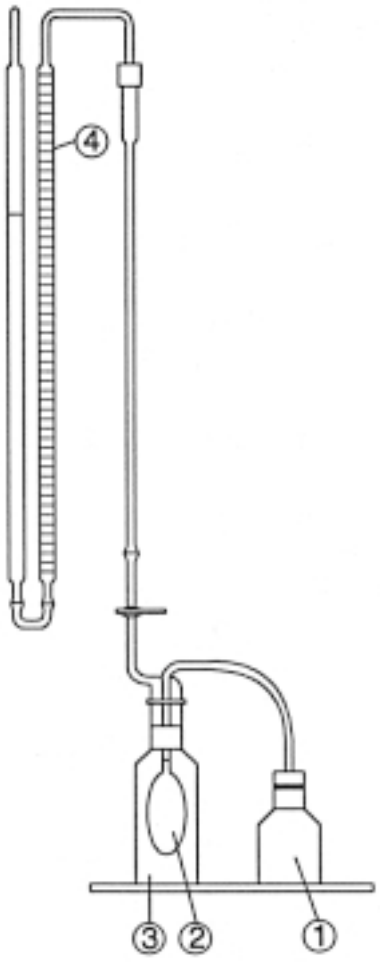

Figure 3-14. *Simple device for measuring carbon dioxide released from HCl-treated sample. The components are termed in the text.*

Sulphur-bearing minerals may have an impact on the corrosion of canisters with highly radioactive waste and also on the formation of cementing agents like gypsum and anhydrite. It may therefore be required that the amount of sulphate and sulphide minerals, primarily pyrite, is determined and a number of techniques have been proposed for quantitative analysis. The method employed by the Swedish State Power Board is sufficiently accurate for most purposes. The procedure is the following:

- Disperse 0.030 kg of finely ground soil or rock material, dried at 105°C, in 0.300 kg of distilled water. After ultrasonic treatment for 5 minutes, the dispersion is left to rest for 24 hours.
- Centrifugation is made and 10 ml decanted. 40 ml distilled water is added so that the weight of the solution becomes 0.050 kg.
- Filtration and de-airing under vacuum is made by use of 3 μm glass filters.
- Analysis by spectrography or chromatography. Evaluation of the content of total sulphur C in ppm in the sample is made using the expression:

$$C = \frac{X \cdot 10^{-6} \cdot m_w \cdot 5}{m_s} \cdot 100\% \qquad (3\text{-}1)$$

where

X = content of SO_4^{2-} in ppm given by the instrument
m_w = mass of added water (300 g recommended)
m_s = mass of dry clay

Ballast

The mineralogy of ballast grains is rather easily determined since macroscopic crystals in grains larger than a millimeter can usually be identified through their appearance, hardness and optical properties. Naturally, the mineralogy of ballast prepared from crushed rock is easily characterized by identifying the rock type. Very careful characterization, i.a. for determining the relative amounts of K-bearing and Na- or Ca-bearing feldspars, requires optical microscopy and XRD analysis of crushed and finely ground material. XRD analysis is required for determining the degree of weathering.

3.4.3 Clay minerals

Simple estimates

For the present purpose we are particularly interested in finding the mass proportions of the minerals in the clay fraction. It is true that some of the clay minerals, like kaolinite, may be represented in the fine part of the silt fraction as well, but most of the other clay minerals are not and only the clay fraction is usually examined for qualitative and quantitative determination of the clay minerals. Such an analysis starts by separating minus 2 μm particles through sedimentation of ultrasonically treated suspensions, which can be used directly for the mineral analysis (cf Chapter 6). The remainder, containing the rock-forming minerals, can be used for corresponding analysis as indicated in Section 3.4.2.

While a sufficiently accurate determination of the mineral composition of the silt and sand fractions can be made by use of a polarizing microscope, combined with chemical analysis of carbonates and S-bearing minerals, other methods are required for qualitative and quantitative determination of the mineralogy of clays. Simple methods using organic dyes, which are adsorbed to different degrees by different clay minerals, have been tried and are still being used, but since many of them are hazardous by producing cancer they should be abandoned with the exception of Methylene Blue, which is used as an indicator of the smectite content in the industrial processing of bentonite.

The best way of qualitative and (semi)quantitative determination is to combine four individual techniques:

1. Chemical analysis
2. X-ray diffraction spectrometry
3. Cation exchange capacity (CEC) measurement
4. Determination of the consistency limits ("activity")

In addition, it appears that much valuable information on the microstructure and mineralogy of clays, particularly as to geotechnically pertinent variations in clay samples, can be gained from electron microscope images of suitably prepared specimens /16/. Methods for preparation of clay material for microstructural investigation and evaluation are described in Chapter 6.

Chemical analysis

Spectroscopy using coupled plasma-atomic emission spectrometry (ICP-MS) is one method among several alternatives that is applied to soil minerals dissolved in $LiBO_2$ melt. The relative concentrations of the most important elements Si, Al, Fe, Ca, Mg and Na are given explicitly by the instrument. Characteristic compositions are given in Table 3-4.

The whole issue of chemical characterization of the clay fraction is very intricate and derivation of a structural formula requires that one follows procedures like the ones proposed by i.a. Newman and Brown /17/.

Table 3-4. Typical composition of clay minerals (weight%).

Mineral	SiO_2	Al_2O_3	Fe_2O_3	CaO	MgO	Na_2O	K_2O
Kaolinite	44–46	28–40	0–1.5	0–0.8	0–0.15	0–0.1	0–0.2
Illite	48–54	18–21	4–5	0.3–1.7	1.5–3	0.2–0.3	6–8
Montmorillonite	52–60	17–20	3–6	0.8–1.1	4.5–5.5	1.3–1.5	0.02–0.04
Beidellite	59–65	29–36	0.2–0.5	0.1–2	0.1–3	0.1–4	0.05–0.50
Saponite	40–55	3–6	0.5–12	0.5–3	15–32	0.01–3	0.05–0.40

X-ray diffraction analysis

The most commonly applied technique for identifying clay minerals is X-ray diffraction analysis. The principle is that monochromatic X-rays directed into a clay sample prepared by compaction or sedimentation become diffracted and yield a spectrum of reflections with peaks that are determined by the crystal lattice (Figure 3-15). Nowadays, identification of the various mineral components is made by use of computer technique /18/. Preparation of samples and conducting XRD tests as well as evaluating diffractograms are delicate matters and requires access to special equipment and trained staffs. In practice, such investigations have to be performed by mineralogical laboratories at universities or special enterprises. Here, we will confine ourselves to give a condensed description of a preparation technique that is recommended and some basic data of general interest for qualitative and semi-quantitative determination of the clay mineral content. Quantitative analyses are very difficult and time-consuming and require special training and considerable experience. Specimens are prepared in two alternative ways /18/:

1a) Dispersion in distilled water and sedimentation on sample holder under vacuum for obtaining "oriented" samples. This procedure is suitable for qualitative and quantitative clay mineral analysis. Separate analyses are often made of the size fractions < 0.5 μm, < 1 μm and 1–2 μm.

1b) Sample preparation as in par. 1a adding a droplet of ethylen glycol for uptake in interlamellar positions, by which a defined expanded state is obtained (cf Figure 3-15).

2) Compaction of air-dry powder in sample holder. This is suitable for getting information on the overall mineral composition of the material.

The XRD test is performed by rotating the sample holder so that it is exposed to the X-ray beam at different angles as in Figure 3-15. Reflected waves hit the counter for recording, yielding the generalized type of spectrum in the figure.

The two different specimen preparations are helpful in evaluating the mineral composition (cf Figure 3-16).

The 2θ-angle refers to the spacing of different atomic planes in the crystal lattices and there are characteristic sets of peaks that are diagnostic for a large number of minerals as indicated in Figure 3-17. Commonly, however, the spectra are more complex and show overlapping peaks that are common to two or more minerals (Figure 3-18). Diagnostic peaks are listed below for XRD obtained when CuK_α radiation and Ni filter are applied /18/:

Kaolinite. The kaolinite group of minerals is identified by the well defined regular basal sequence of 7.13 Å, 3.57 Å, and 2.39 Å peaks. The transition from well-crystallized to poorly crystallized kaolinite is shown by a broadening and weakening of the reflections and a tendency for adjacent reflections to fuse into one. A high area/height ratio of the 7 Å peak is taken as indicative of poorly crystallized kaolinite and/or finely crystalline kaolinite. The lack of clearly discernible kaolinite "doublets" (spacings of 4.17 Å and 4.12 Å) or "triplets" (spacings of 2.55 Å, 2.52 Å, and 2.49 Å, 2.37 Å, 2.33 Å, and 2.28 Å) is taken as indicative of poorly crystallized material.

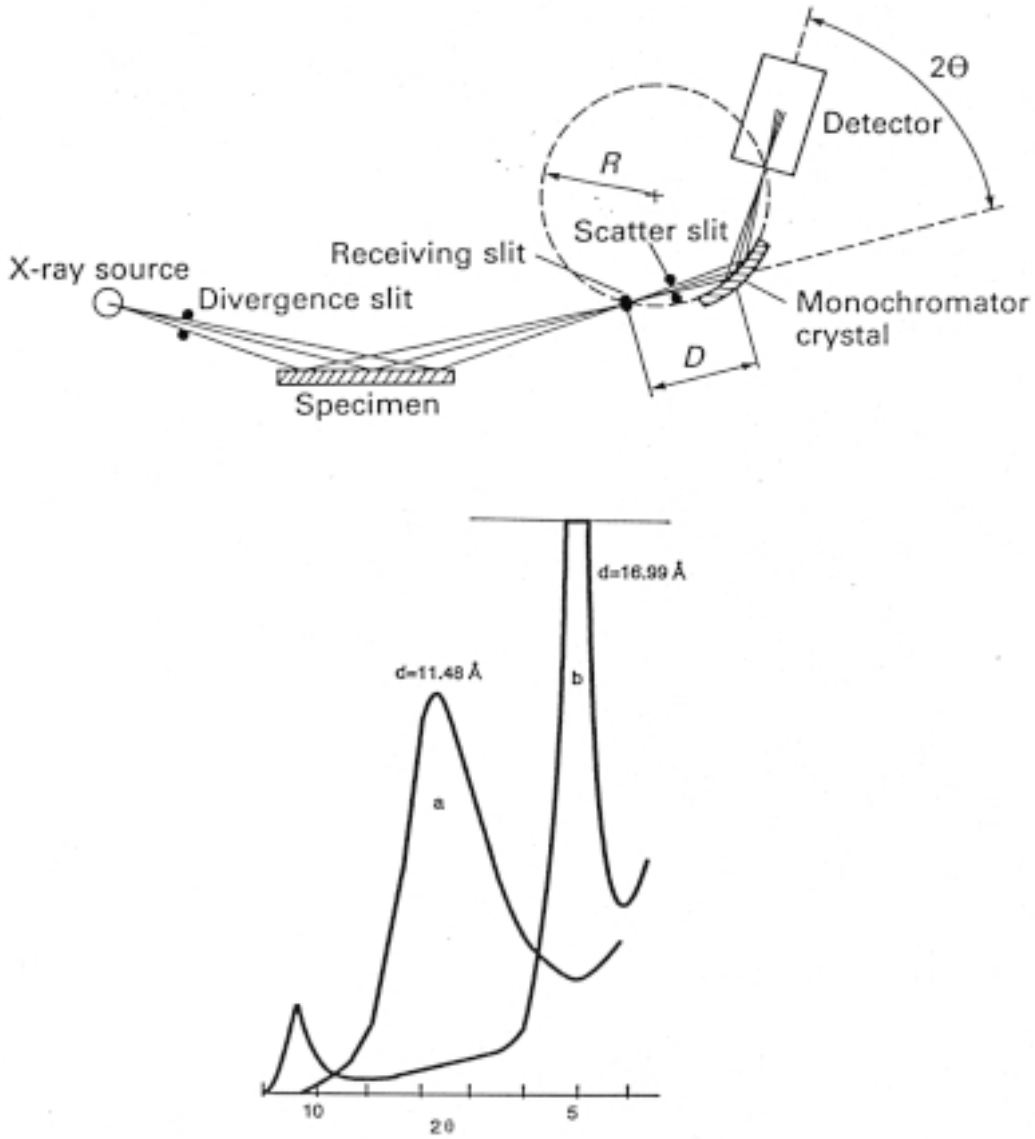

Figure 3-15. *Principle of XRD test. Upper: Rotation of sample holder exposes the sample to the radiation beam at different angles and reflected waves hit counter for recording (Philips information sheet). Lower: Example of XRD spectrum obtained for montmorillonite without (a) and with ethylene glycol treatment (b) for determining lattice expansion.*

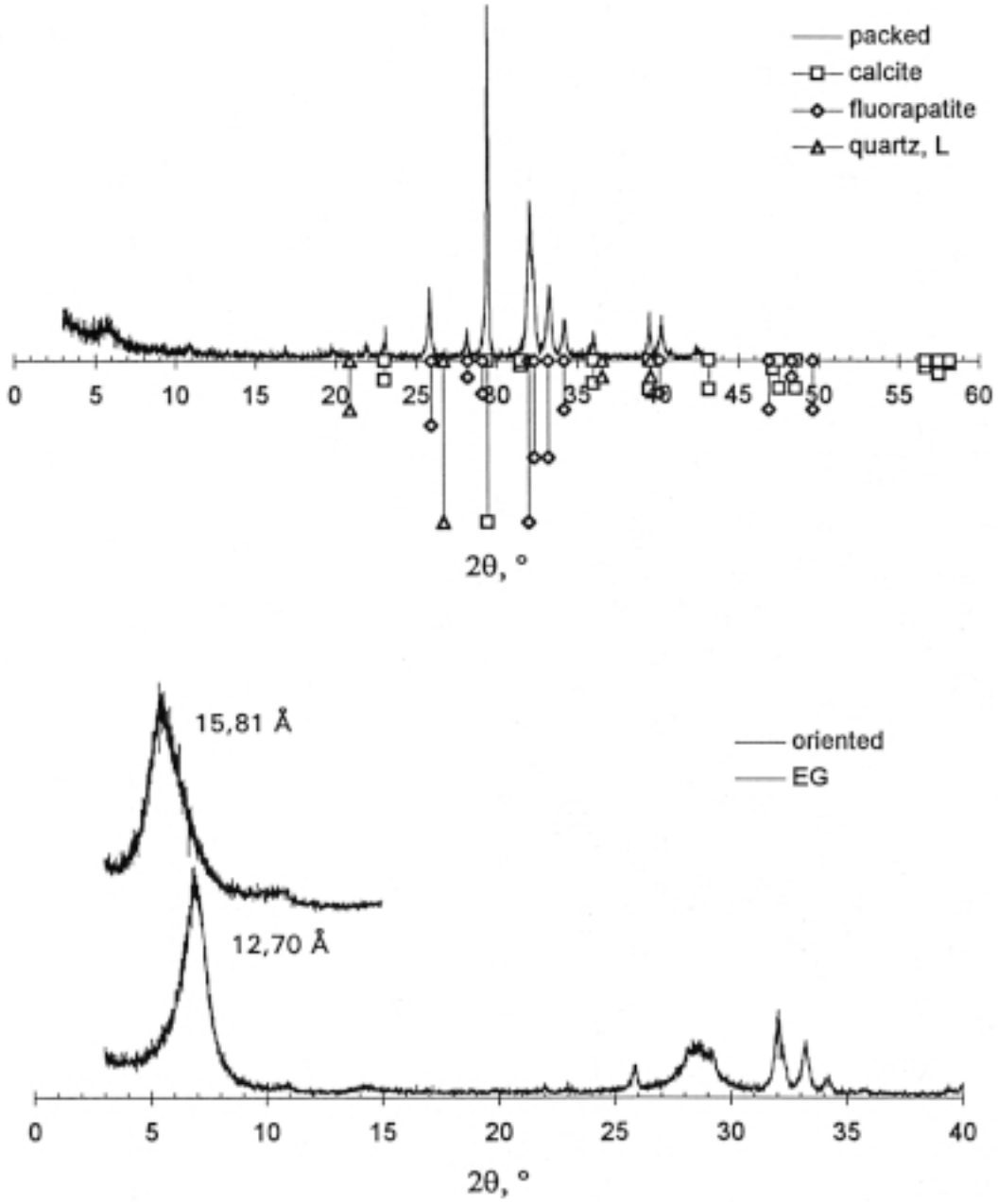

Figure 3-16. *Example of XRD spectra of a soil sample containing calcite, apatite and small amounts of smectite. Upper: spectrum of unsorted, packed material. Lower: spectrum of oriented material from the clay fraction of the same samples. The curve above shows the spectrum after ethylene glycol treatment.*

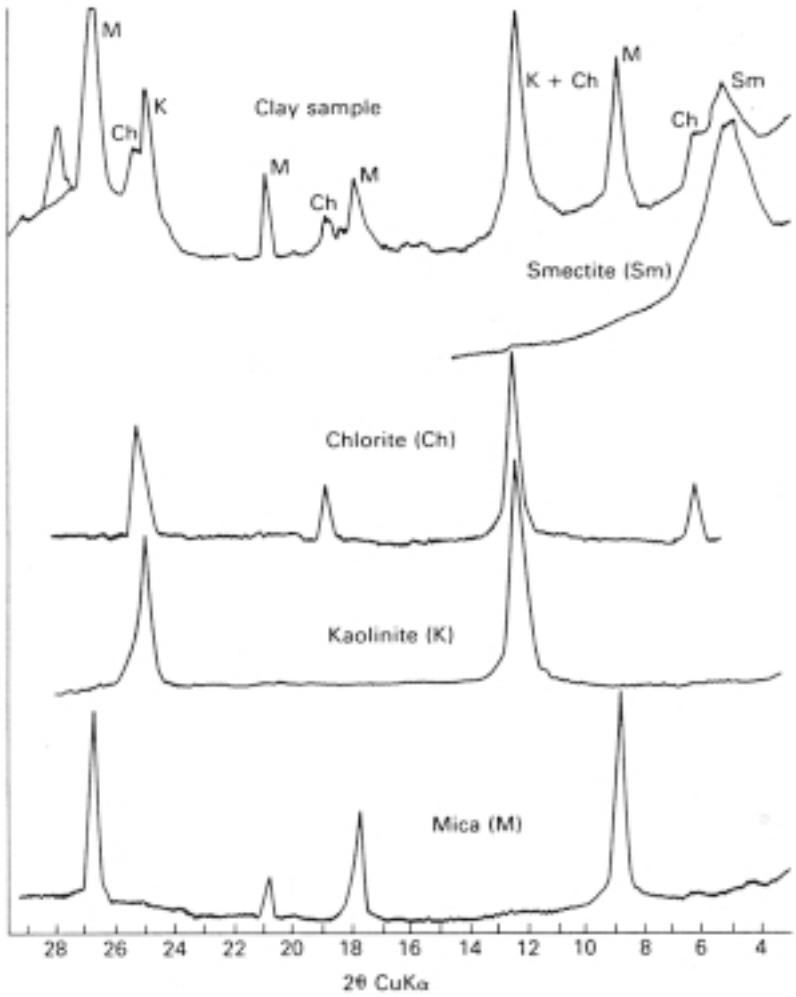

Figure 3-17. *Example of XRD spectra of a sample composed of 4 major minerals and of the individual mineral components after separation. Notice that while the smectite-component gives a very clear and high although broad peak it is partly masked by the chlorite in the mixed state. The actual smetite content was about 15% by weight.*

Chlorite. Chloritic clay minerals may be confused with the kaolinite minerals because many of the diffraction peaks of these two groups coincide. The first- and third-order chlorite reflections (14 Å and 4.7 Å, respectively) will serve to indicate the presence of chlorite. However, the iron-rich chlorites frequently give only weak first- and third-order reflections. In such cases it is often necessary to conduct further tests. Kaolinite, heated to 600°C, tends to loose its crystalline character, whereas well-crystallized chlorite is only partially dehydrated at this temperature, causing increased intensity of the 14 Å reflection. Treatment with warm, dilute HCl can also be used to take advantage of the higher solubility of chlorite in this acid.

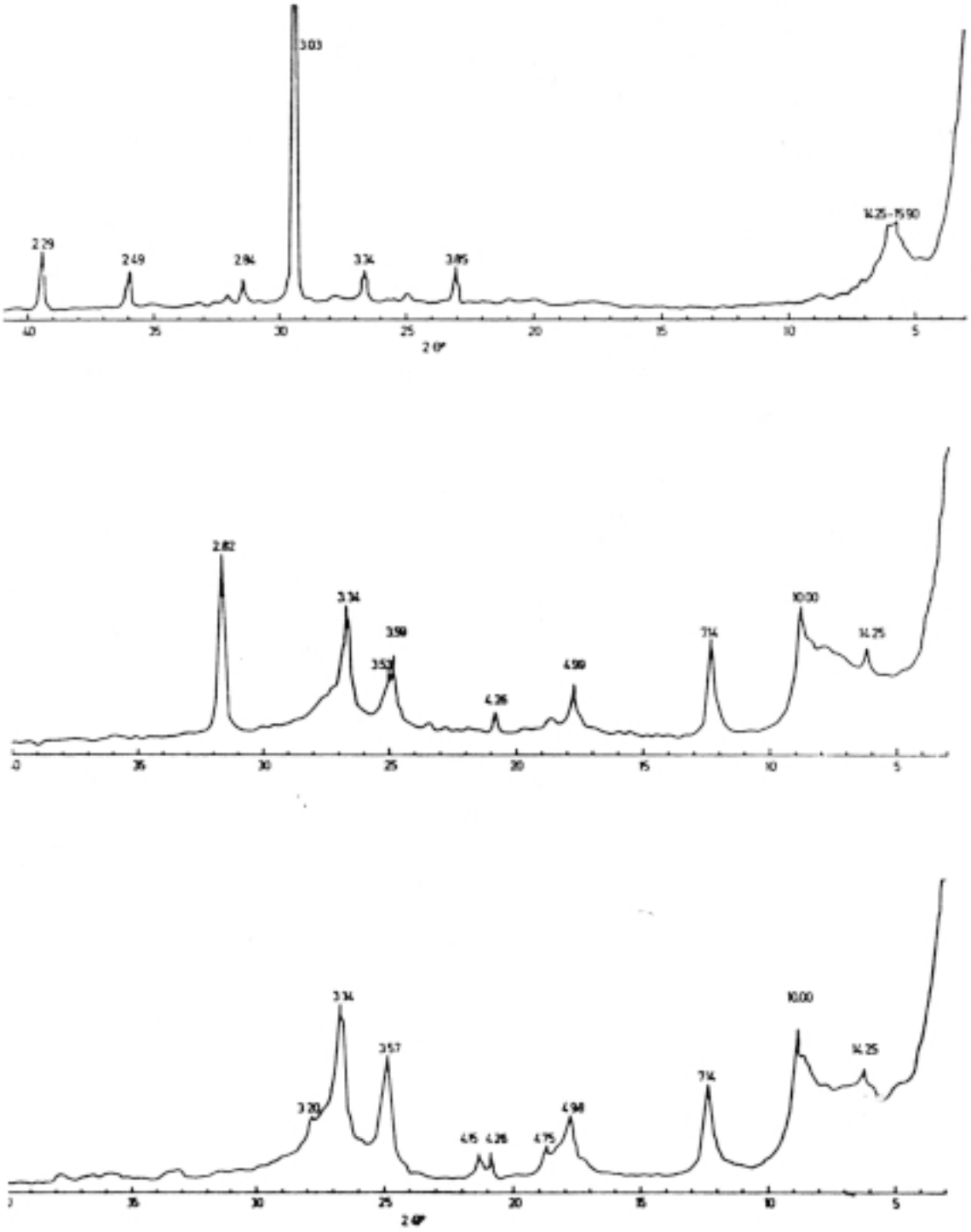

Figure 3-18. *Example of XRD spectra of oriented specimens. Upper: Cretaceous bentonite with calcite and montmorillonite as major minerals. Central: Tertiary London Clay with illite as dominant clay mineral and moderately abundant montmorillonite and kaolinite. Lower: Røsnaes clay dominated by montmorillonite and with relatively abundant illite and kaolinite.*

If a 14 Å peak does not develop after heating samples to 600°C, chlorite is considered to be an unimportant constituent and the 7 Å peak attributed principally to kaolinite. This interpretation is usually supported by the presence of a 7 Å peak after treatment with warm dilute HCl.

Illite. This group exhibits an integral sequence of basal reflections at approximately 10 Å, 5 Å and 3.3 Å. The 10 Å peak is typically asymmetrical toward the low angle region and the 3.3 Å peak is asymmetrical toward the high angle region. The lack of symmetry is taken as an indication of small particle size, variation in the interlayer cation and/or occasional slight interlayer hydration.

Smectites. The smectite group of minerals is identified by basal reflection (001) peaks at approximately 12 to 15 Å (untreated sample), 17 Å (glycolated sample) and 10 Å (heated sample). The c-axis dimension is not fixed but varies with the type of exchangeable cation occurring between the silicate layers and the size of the polar molecules occurring between the silicate layers. Under ordinary RH conditions a montmorillonite with Na^+ as exchangeable ion frequently has one interlayer of molecular water and a c-axis spacing of 12.5 Å; with Ca^{2+} there are frequently two molecular water layers and a c-axis spacing of about 15.5 Å. Ethylene glycol expands the lattice of montmorillonite to 17 Å and heating to 250°C decreases the lattice spacing to approximately 10 Å.

Interstratified ("Mixed-layer") clay minerals. Three major types of mixed-layer clay minerals have been defined in the literature: 1) regularly interstratified clay minerals, 2) randomly interstratified clay minerals, and 3) segregated mixed-layer clay minerals.

1) The regularly interstratified mixed-layer clay minerals exhibit "superlattice" characteristics. They give high (001) spacings and a regular series of sharp higher order reflections with spacings that are submultiples of the (001) spacing. The large (001) spacing represents a composite of the (001) spacings of the interstratified clay minerals.

2) If the mixture is a random interstratification of layer clay minerals, a nonintegral series of reflections is obtained from the basal planes. The reflections occur at positions where the reflections from the individual components nearly coincide, and they vary in intensity, shape and position, according to the relative proportion of the constituents in the mixed-layer structure.

3) The segregated mixed-layer clay minerals are characterized by a varying proportion of cation density within individual crystallites and from crystallite to crystallite. The diffraction peak of the major clay mineral is generally simply altered in shape and intensity by the development of secondary layers of different composition within the crystallite of the major mineral. It has been stated that segregated mixed-layer clay minerals may be composed of a clay mineral in various states of hydration. The illite structure is often partially "degraded" by interlayer hydration. If the layers collapse with heating or expand with ethylene glycol treatment, they may be called smectite /19/.

A number of auxiliary techniques have been developed for evaluation of complex spectra, i.a. Reynolds method for synthesizing spectra of differently composed mineral assemblages that can be compared with those obtained in the tests /20/. One example of the appearance of such a computer-derived spectrum is shown in Figure 3-19 /21/. The application of this and similar techniques require that a suitable reference mineral is mixed in like pyrophyllite or dolomite with typical reflection patterns.

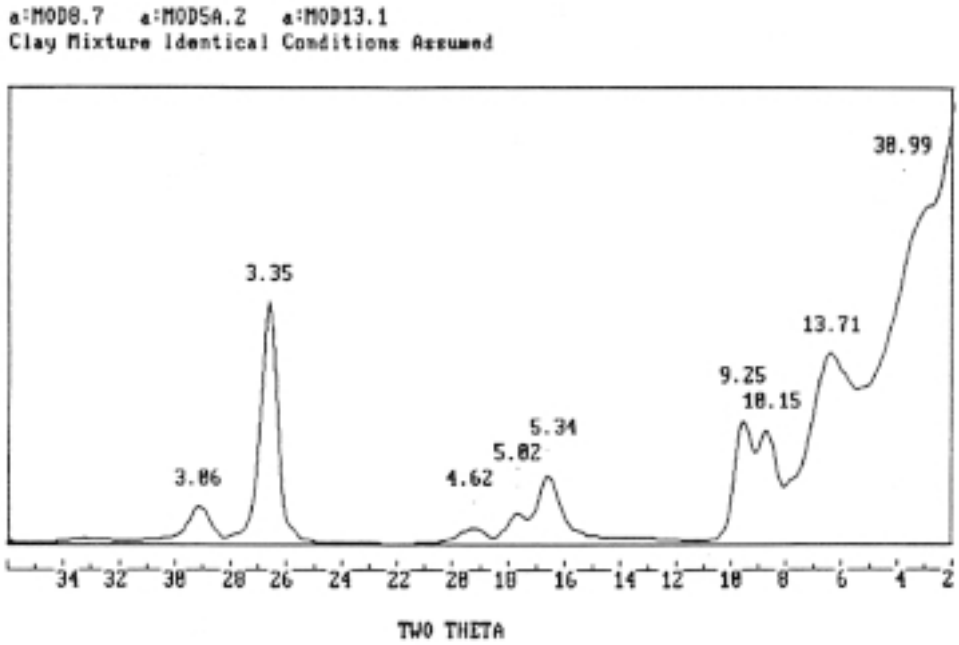

Figure 3-19. *Synthetic XRD/EG spectrum for 70% illite/smectite (I/S) with K^+ in the hydrous mica, + 20% illite, + 10% pyrophyllite. Smectite forms 40% of the mixed-layer minerals. Pyrophyllite was added for the quantitative analysis /20/.*

Cation exchange capacity, CEC

The ability of clay minerals to adsorb cations is a diagnostic property and this ability is defined as the cation exchange capacity. Typical values, expressed in terms of meq/100 g dry material are given in Table 3-5.

Among several techniques proposed in the literature, Chapman's method is recommended because of its relative simplicity. This technique involves exchange of the initially adsorbed cation by NH_4^+ by repeated washing with ammonium acetate solution. The supernatants are saved for analysis of the initially adsorbed cations /17/. Repeated washing with isopropyl alcohol to remove excess NH_4^+ is made and treatment with NaCl solution is finally made for complete saturation with sodium.

Quick checking of the smectite content

The activity number a_c defined in Chapter 1 [$a_c = (w_L - w_P)/I_c$] is useful as a quick and relatively safe method for estimating the smectite content /22/. It is essentially a measure of the water-adsorption potential of the minerals in the clay fraction, and typical values are given in Table 3-6.

In the case of very smectite-rich clays, and particularly for commercially available bentonites, the liquid limit is a sufficiently sensitive measure of the smectite content. Thus, typical liquid limit values of high-quality sodium and calcium bentonite are 500 and 100%, respectively.

Table 3-5. Cation exchange capacity (CEC) of common pure minerals /17/.

Mineral	CEC, meq/0.100 kg
Zeolites	100–300
Vermiculite	100–150
Montmorillonite	80–150
Chlorite	5–50
Hydrous mica (illite)	10–40
Kaolinite	3–15
Feldspar	~ 1
Quartz	~ 1

Table 3-6. Activity values of different minerals /22/.

Mineral	Activity
Quartz	≈ 0
Calcite	0.18
Mica (muscovite)	0.23
Kaolinite[1]	0.33
Kaolinite[1]	0.46
Illite	0.90
Ca-montmorillonite	1.5
Na-montmorillonite	7.2

[1] Different investigations

The Methylene Blue test is also valuable for quick testing of the smectite content and it is the standard method of many mineral-producing companies. The description is given some space here because of the wide-spread use of the techniques.

Principle of the Methylene Blue test

The method is virtually a cation exchange capacity test although the potential to adsorb methylene blue and cations of other types is not necessarily the same; the firstmentioned is commonly somewhat less than the actual cation exchange capacity. A clay sample intended for testing must firstly be treated with hydrogen peroxide for removal of other dye-adsorbing components like organics (lignosulfonates, lignites, cellulosic polymers and polyacrylates, etc). Methylene Blue solution is then added to a suspension of the clay and acidified until saturation is noted by the formation of a “dye halo” around a drop of solids placed on filter paper as illustrated in Figure 3-20.

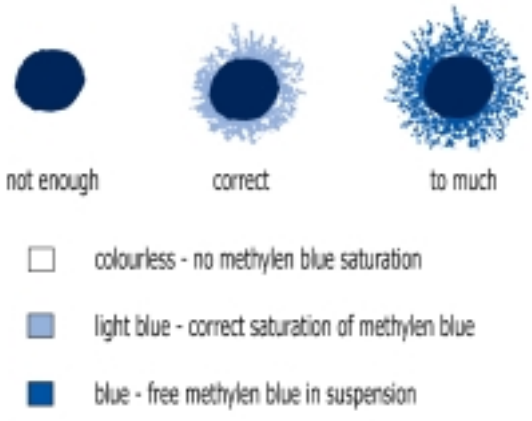

Figure 3-20. *Appearance of halo at treatment with methylene blue (Zwahr).*

The detailed laboratory procedure is as follows:

1. Prepare solution of 10 g of Methylene Blue in 1 liter of distilled water.
2. Treat the soil with 3% hydrogen peroxide, wash with distilled water and dry the soil at 105°C.
3. Prepare suspension of 7.5 g of sieved soil (< 50 μm) in 50 ml distilled water.
4. Add Methylene Blue solution to the suspension in increments of 5 ml. Transfer drops of suspension to a filter paper for visual examination.
5. When the blue tint halo spreading from the spot is detected, shake the flask for 2 minutes and place another drop on the filter paper. If the blue ring is again evident, the final endpoint has been reached. If the blue ring does not appear, then continue as before until a drop taken after 2 minutes shows the blue tint halo.
6. The smectite content is evaluated by calculating the methylene blue capacity according the following expression:

$$\text{Methylene Blue Capacity} = \frac{\text{Methylene Blue, g}}{\text{100 g suspended soil}}$$

The Methylene Blue Capacity (MBC) is in the range of 5–30 depending on the content of clay-sized particles and of smectite minerals. Figure 3-21 shows a classification scheme of expandability versus MBC.

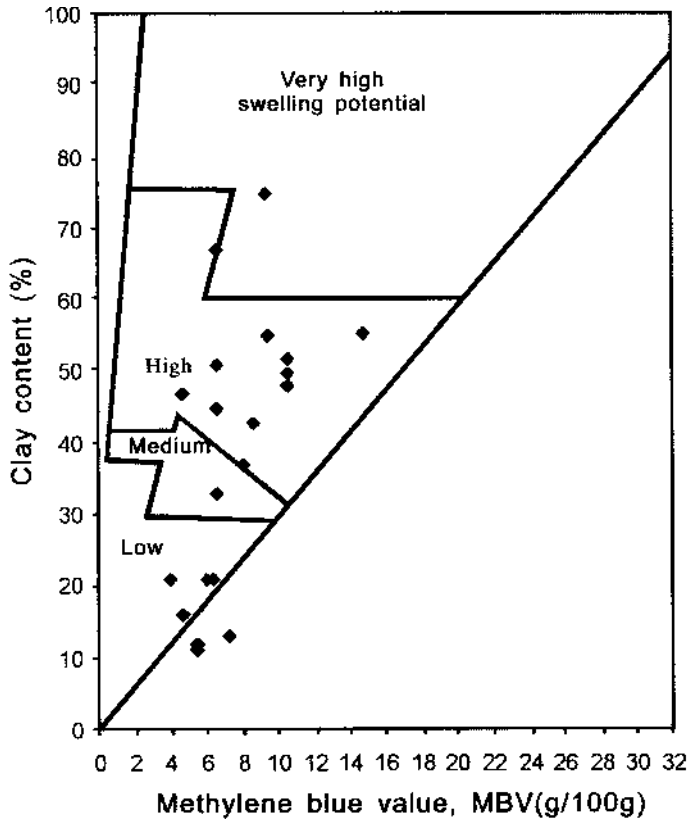

Figure 3-21. *Classification chart of the swelling potential with examples of data for clays with a smectite content ranging from 15 to 55% [after Erguler and Ulusay].*

3.5 References

/1/ **Berry L G, Mason B, 1959.** Mineralogy. W.H. Freeman and Co., San Fransisco and London.

/2/ **Meyer D, Howard J J, 1983.** Evaluation of clays and clay minerals for application to repository sealing. Technical Report OH43201, Office of Nuclear Waste Isolation, Battelle Memorial Institute, Columbus.

/3/ **Grim R E, 1953.** Clay Mineralogy. McGraw-Hill Publ. Co., London.

/4/ **Maegdefrau E, 1941.** Die Gruppe der Glimmerartigen Tonmineralien. Sprechsaal für Keramik, Glas und Email, Vol. 74 (pp. 1–38).

/5/ **Forslind E, Jacobsson A, 1975.** Clay-Water Systems. Water a Comprehensive Treatise, Vol. 5, Ed. F. Franks, Plenum Press, New York and London, ISBN 0-306-37185-5.

/6/ **Pusch R, Güven N, 1990.** Electron microscopic examination of hydrothermally treated bentonite clay. Engng. Geology, Vol. 28 (pp. 303–314).

/7/ **Borchardt G A, 1977.** Montmorillonite and other smectite minerals. Minerals in Soil Environment (Ed:s Dixon et al). Soil Sci. Soc. America, Madison, Wisconsin, U.S.A.

/8/ **Pusch et al, 1991.** Final Report of the Rock Sealing Project. Sealing Properties and Longevity of Smectite Clay Grouts. Stripa Project, Technical Report 91-30, Svensk Kärnbränslehantering AB.

/9/ **Weaver C E, 1979.** Geothermal alteration of clay minerals and shales: Diagenesis, ONWI-21, Office of Nuclear Waste Isolation, Battelle Memorial Institute, Columbus, Ohio.

/10/ **Velde B, 1985.** Clay Minerals. A physico-chemical explanation of their occurrence. Developments in Sedimentology, No. 40, Elsevier Publ. Co.

/11/ **Eberl D, Hower J, 1976.** Kinetics of illite formation. Geological Society of America Bulletin, Vol. 87.

/12/ **Wilson M D, Pittman E D, 1977.** Authigenic clays in sandstones. Recognition and influence on reservoir properties and paleo-environmental analysis. J. Sedim. Petrology, Vol. 47.

/13/ **Weaver C E, Beck K C, 1971.** Clay-water-diagenesis during burial: How mud becomes gneiss. Geol. Soc. America, Spec. Paper 134.

/14/ **Kleber W, 1962.** Einführung in die Kristallographie. VEB Verlag Technik, Berlin.

/15/ **Pusch R, 1974** Soil constituents and structure. Performance and interpretation of laboratory investigations, part 3. Swedish Council for Building Research (in coop. with the Laboratory Comm. Swed. Geot. Soc.).

/16/ **Smart P, Tovey N K, 1981.** Electron Microscopy of Soils and Sediments: Examples. Clarendon Press, Oxford (ISBN 0-19-854515-0).

/17/ **Newman A C D, Brown G, 1987.** The chemical consitution of clays. Chemistry of clays and clay minerals. Ed. A.C.D. Newman. Mineralogical Society, Monograph No. 6, Longman Scientific & Technical (ISBN-0-582-30114-9).

/18/ **Hardy R, Tucker M, 1988.** X-ray powder diffraction of sediments. Techniques in Sedimentology, Ed. M Tucker. Blackwell Scientific Publications.

/19/ **Nadeau P H, Bain D C, 1986.** Composition of some smectites and diagenetic illitic clays and implications for their origin. Clays and Clay Minerals, Vol. 34, (pp. 455–464).

/20/ **Reynolds R C, 1985.** Principles and techniques of quantitative analysis of clay minerals by X-ray diffraction methods. AIPEA conf.

/21/ **Pusch R, Karnland O, 1988.** Geological evidence of smectite longeviy. The Sardinian and Gotland cases. SKB TR-88-26, Svensk Kärnbränslehantering AB.

/22/ **Skempton A W, 1953.** The colloidal “activity” of clays. Proc. 3rd Int. Conf. Soil. Mech. a Found. Engng., Zürich.

4 Organic constituents

This chapter deals with organic matter in soils. It affects the rheological properties of soils in general and in repositories they may produce gas and serve as nutrients for bacteria. As for organic colloids, bacteria may carry radionuclides from leaking canisters to the biosphere.

Focus is on characterization of organic constituents and of practical methods of quantifying them. The matter of organics in soils is a scientific discipline per se and the present section only gives some basic information related to the performance of buffers and backfills.

4.1 Introduction

The organic content of natural soils, including bentonites, consists of macroscopic matter like roots, carbon particles, and more or less decomposed fragments of plants and animals and microscopic objects, like microorganisms (bacteria and fungi), organic molecules and compounds. We will confine ourselves here to consider sedimentary clay soils deposited in the sea or in estuaries, a group of soils that comprises the particularly interesting bentonites /1/.

The origin of the microorganisms and their products found in present clay soils dates back to the time of soil formation. The microfauna in marine or strongly brackish environments where bentonites were formed mainly consists of unicellular protozoa, nematodes and crustacea, while the microflora is made up of fungi, bacteria and algae. Among the protozoa large numbers of foraminifers, radiolaries, flagellates and infusion animals are represented, many of which have shells or skeletons. The nematodes are represented by microscopic eelworms. Microscopic organisms belonging to the group Crustacea form the majority of zoo plankton.

In cold oceans, such as those in which glacial clays were deposited, the dominating members of the microflora are silicic algae (diatoms). In warmer seas with depths smaller than about 200 m, autotrophic blue-green algae are frequent and such species may therefore have been common under certain periods of the deposition of glacial clays and when bentonite-producing ashfall took place in central Europe. Fairly large numbers of bacteria and fungi were and are still present in the oceans.

The frequency and composition of microorganisms vary strongly. Generally, considerable amounts are present in arctic sea-water while the number of different species is restricted. In our time bacteria and algae have production maxima in springtime and in the autumn in coastal areas due to the contribution of nutrient salts which are brought to the sea by melting snow and ice in springtime and by the rains in the autumn. The same conditions probably occurred throughout the Quaternary and Mesozoic eras. The present density of microorganisms in the oceans can be illustrated by the number of bacteria, which varies in the range of 10^3 –$3 \cdot 10^5$ per cm^3 at depths down to 50 m below the water surface while the number of fungi is very much smaller /1/. In ancient cold oceans the content of bacteria was probably of the same order of magnitude as in

present time but the amount of fungi (dead, dormant or alive) may have been greater than today in local areas due to richer occurrence of fragments of vegetation, which was brought to the sea by rivers /1/.

The present concentration of microorganisms in the sedimentary top layer of shelf areas in the oceans has been estimated to be at least 10^8 to 10^{12} per kilogram of moist sediment /1/. If all these microorganisms are considered to be bacteria with a volume of 10^{-15} m^3, their combined volume would correspond to about 0.01% to 100% of the pore volume of the sediment. It follows from this that the microorganisms may be of great importance for the physical properties of many sediments.

4.2 Primary organic species

Organisms in fine-grained sediments

Living microorganisms were active already when the oldest commercially exploited bentonites were formed in Ordovician time. Bacteria, and to a smaller extent fungi, colonized suspended mineral and organic particles and thereby changed the size, shape and sedimentation rate of these particles. Partial or complete destruction of the settling particles took place in those cases where they acted as nutrients. In other cases colonization caused an increase of the particle size. An important effect was aggregation of particles by the action of fungi, the hyphae of which kept particles together /1/. The same effect was caused by slime spores of fungi, various bacteria and many other microorganisms with filamentous extentions or fibrous shape (Figures 4-1 to 4-4). The surface properties of fungi and bacteria are of special importance since they determine the interaction with clay minerals.

The construction unit of fungi is the hypha, which forms a system termed mycelium. The hyphae are hollow tubes with a diameter of 3–10 μm and, generally, with a cell wall material of chitin, which is a polysaccharide based on the acetyl derivative of the nitrogen-containing amino sugar, glucosamine. Other organic matter, such as spores and bacteria, have cell walls of proteins and chitin, often accompanied by a considerable proportion of lipid substances (fatty acids). Flagella of bacteria are mainly made up of protein. The surface properties are dependent upon the balance of hydrophilic and hydrophobic groups of long-chain molecules which constitute the cell wall material. Among the hydrophilic groups may be included –OH, $–NH_2$, $–SO_3$, –COO, $–NH_3$ and C=0. Important common hydrophobic groups are the radicals $–CH_3$ and $–C_6H_5$.

In cell walls of proteins, chitin and lipid, as well as in cellulose, hydrophilic regularly spaced groups are separated by hydrophobic groups and water adsorption therefore takes place in the form of local clusters of organized water. Hydroxyl groups may be responsible for the primary adsorption /1/. Probably there are large differences in the organization and stability of the adsorbed water.

Under usual conditions of growth and at pH near neutrality most bacteria carry a negative electric surface charge. This results in the adsorption of cations to the surface of the bacteria. As in the case of clay particles, aggregation of bacteria and establishment of cohesive forces take place depending on the nature and concentration of electrolytes present.

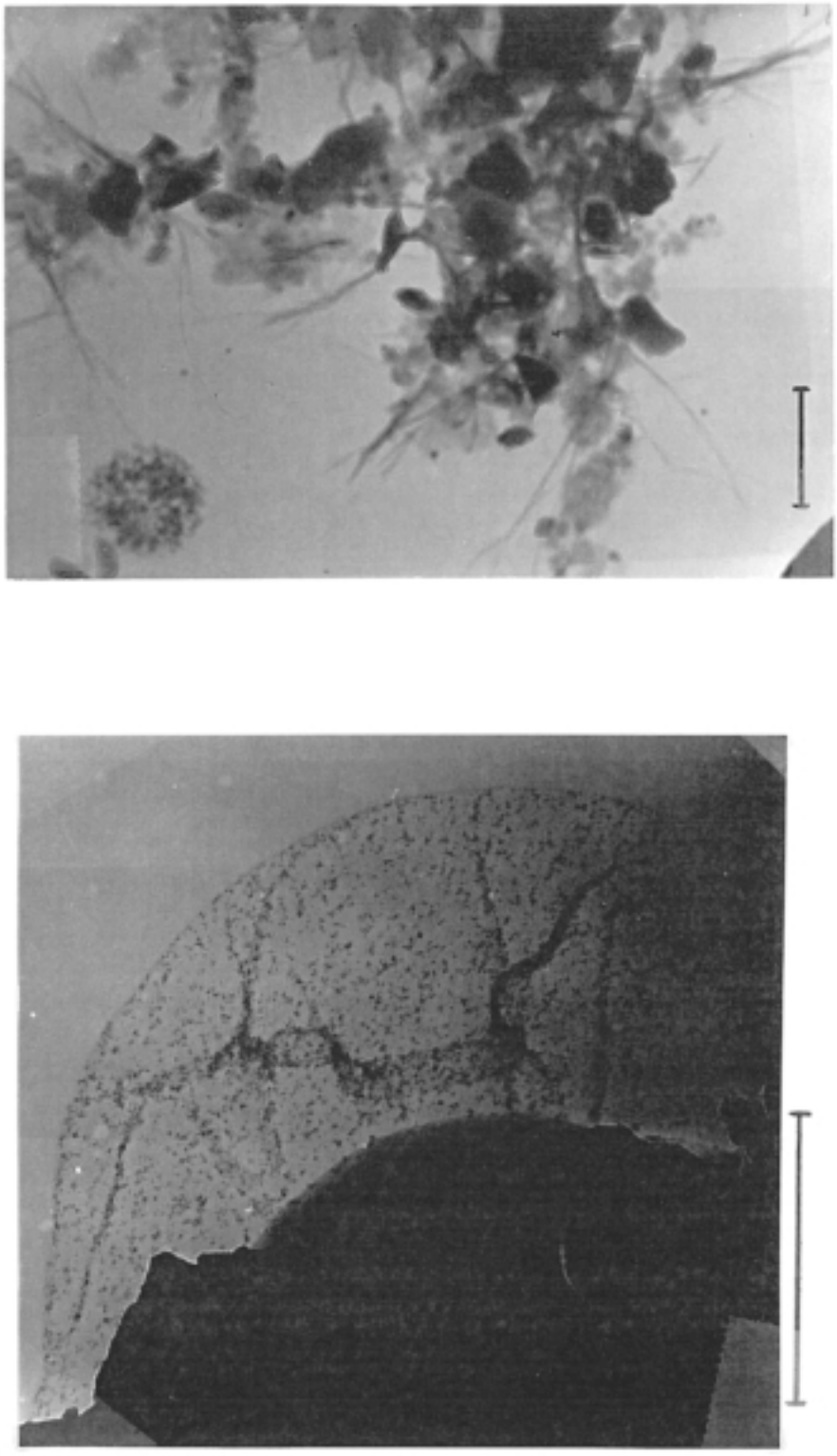

Figure 4-1. *TEM pictures of organic substance associated with clay particle aggregates. Electron micrograph of dispersed illitic clay. Upper: Fibrous species serving as reinforcement. Lower: Colloidal organic tissue with adsorbed about 100 Å large electron-dense nodules, probably ion compounds. The bars represent a length of 1 μm /1/.*

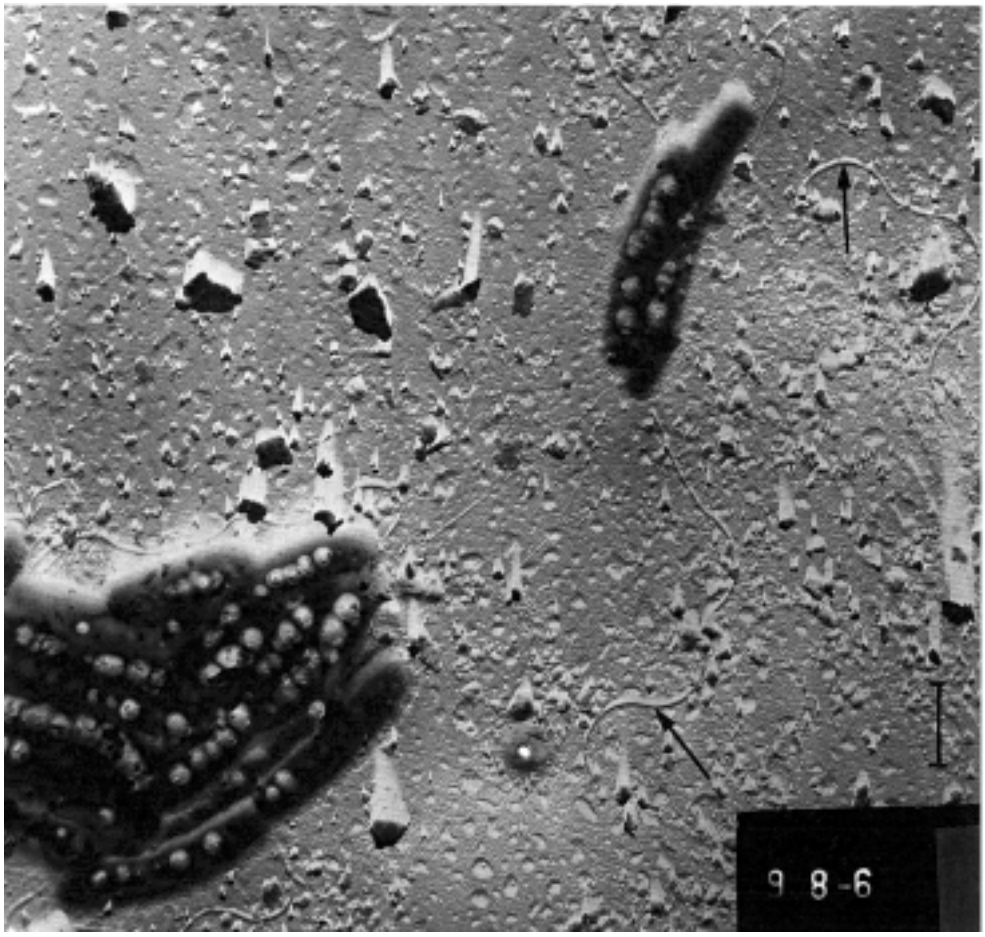

Figure 4-2. *TEM picture of bacteria in post-glacial clay. Electron micrograph of dispersed clay material from 2 m depth at Skå-Edeby. (Post-glacial, muddy brackish-water clay). The bar represents a length of 1 μm /1/.*

Attraction and bonding also occurs between microorganisms and clay particles. Thus, bacteria may sorb and form protein-clay complexes but for various reasons, such as unfavorable geometrical orientation of larger organisms and the presence of hydrophobic groups in the cell walls, the bonding between microorganisms and clay partices, which depends on pH and type of electrolyte in solution, is probably not very strong /1/.

Due to combined effects of mechanical and physico/chemical coupling between organic matter and mineral surfaces, the sedimenting units in the formation of sedimentary clay consisted of clay particle aggregates in and around which organic matter was enclosed or attached.

Consolidation of natural sediments under their own weight, which grew parallel to the increased overburden, caused reduction in void size and less space for larger animals and finally also for bacteria to move and this brought them into dormant state and finally caused their death because of lack of nutrients. This issue is of importance in assessing the possibility of microbes to survive and multiply in buffers and backfills as discussed in Chapter 6, which deals with their microstructure.

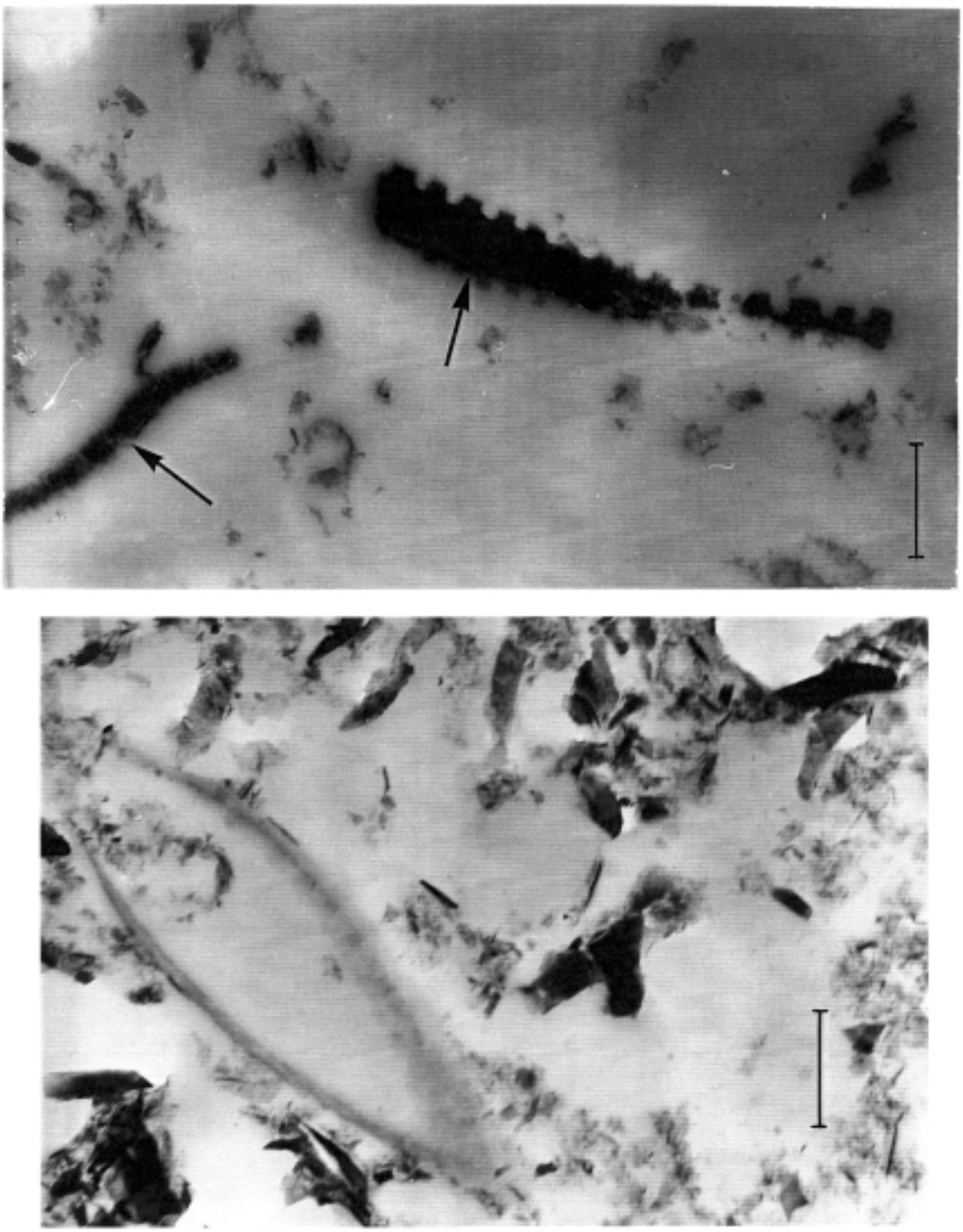

Figure 4-3. *TEM pictures of objects of organic origin in soft illitic clays. Transmission electron images of ultrathin sections. The bars represent a length of 1 μm.*

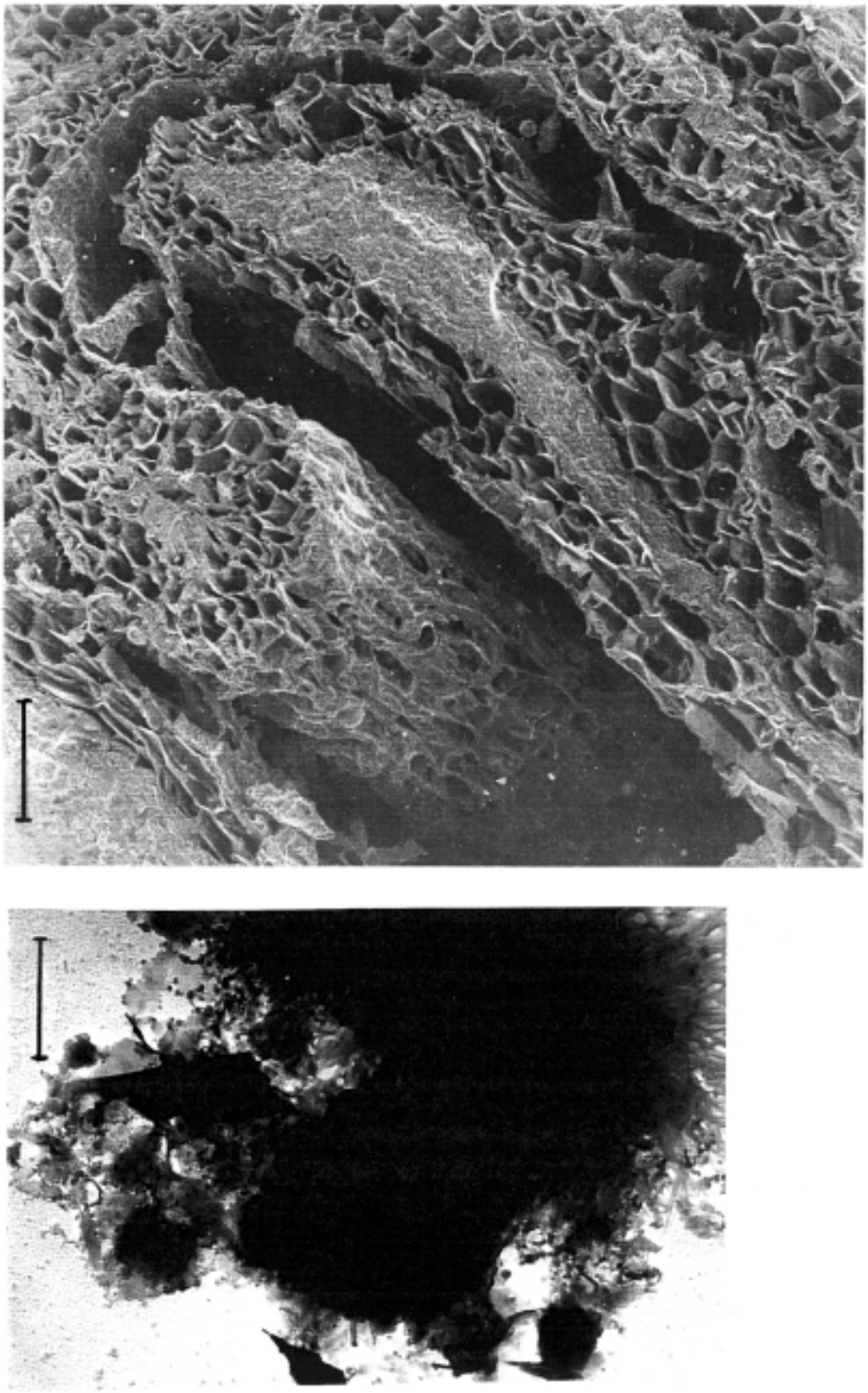

Figure 4-4. *Electron micrographs of organic residues in soils. Upper: SEM picture of cellulose tissues. Lower: TEM picture of humus substance. the upper bar represents a length of 100 μm, the lower 1 μm.*

Organisms in smectitic clays for use as buffer and backfill

Since the conditions were the same for formation of any ancient non-smectite and smectitic sediment the expected content of organic material is also similar. Fish fossils, for example, are found in the Cretaceous Fish bentonite in Denmark and many commercially exploited bentonites have an organic content of at least 1000 ppm. Phosphatic microfossils like *conodonts* are relatively abundant in the Ordovician Kinnekulle bentonites and have served as temperature indicators /2/. Kerogene in and adjacent to bentonites, like in Gotland, validates the presence of organic material from the start of sedimentation /3/.

4.3 Secondary organic matter in sediments

Residual organic matter made up of degraded microorganisms and of products of their activity are termed secondary organic matter here.

The microorganisms, sedimented together with the clay particles, were exposed to a new environment when locked in the sediment. Many of the bacteria and fungi continued to live by utilizing nutrients in their immediate vicinity but since their mobility was largely hindered, the majority of these organisms subsequently died or turned into a dormant state by the lack of nutrients. Certain enzymes may have persisted a long time in the absence of active microorganisms, thereby contributing to the supply of available nutrients. The action of living organisms was that of catalysts causing the oxidation of organic matter to simple inorganic compounds /1/. Organic acids and gases were also growth products.

Chemo-autotrophic nitrifying bacteria were responsible for the transformation of ammonia (liberated by ammonifying microorganisms during decomposition of organic remains) into nitrites, which were subsequently oxidized by other bacteria to form nitrates. Molecular nitrogen could be reduced to ammonia, when organic compounds of nitrogen, and eventually proteins, were synthesized. When a fungal hypha or a bacterial cell had exhausted its zone of enzymic erosion, no more energy-supplying carbon compounds could be obtained and the organisms died. Its proteins were broken down by ammonifying bacteria to ammonia, and the nitrogen thus set free was directly absorbed by a new generation of microbes. Similar processes released phosphorous matter and sulphur in mineral form /1/.

As the organisms died, they added to the sediment products derived from the autolysis of their body substance. All these products may include all or many of the characteristic substances that make up humus. Also, owing to a lack of suitable identification techniques, microbial cells, both living and dead, commonly masquerade as humus. Thus, humus substances in glacial clay appear to range from fairly low molecular weight compounds to humic high molecular compounds. The most important representatives are humic acids, fulvic acids and humus, which represent humic acids closely bound with the mineral part of soil. Humic and fulvic acids have similar principles regarding their structure and it is reasonable to believe that fulvic acids are primary forms of humic acids or products of their destruction. Humus substances comprise at least 80–90% of the organic part of mineral soils /1/.

The simple structural units of humus, such as phenol and amino acids, are readily decomposed, yet polymerization takes place in soil containing microorganisms. Humus molecules are thought to be rapidly polymerized from free radicals formed enzymically in an environment devoid of microorganisms capable of decomposing the molecules. Such an environment occurs within all cells shortly after their death, when autolytic enzymes are active but external microbial attack has not yet started. After microbial attack humic molecules are released and become quickly sorbed at clay surfaces where they are protected from microorganisms, particularly in pores less than 1 μm in diameter. This indicates the importance of the density of the clay for organic activity, which can be illustrated by applying microstructural models.

Applying generalised microstructural models /4,5/, one finds that in montmorillonite-rich clay evolved from highly compacted MX-80 bentonite powder, the maximum size of gel-filled voids in clay with a bulk density of 2130 kg/m^3 is 5 μm, while the voids in the clay gel filling is only about 300 Å, i.e. 0.03 μm. This is significantly less than required for letting a bacterium move through the clay. For a bulk density of 1850 kg/m^3 the corresponding space is about 0.06 μm which is also too small to let bacteria through. However, for bulk densities of 1570 kg/m^3, the aperture is about 0.12 μm, which means that certain bacteria may move through bentonite-poor backfills, particularly since the degree of homogeneity of the clay component is not very high. Spores can get through smaller space.

The composition of the major components of humic substance, the humic acids, varies somewhat from soil to soil as concluded from various studies, see Table 4-1.

Humic acids contain several functional groups, namely carboxyl (COOH), phenol and alcohol (OH), methoxyl (OCH_3), carbonyl (C-O) and quinone (C=0). The hydrogen of carboxyl and phenol groups can be exchanged against various bases. The molecular structure is formed by aromatic (hydrophobic) and aliphatic (hydrophilic) side chains (Figure 4-5).

The composition of the humic substance in clays suggests various types of interaction with the mineral particles. Humic acids, for instance, are adsorbed on clay particle surfaces through hydrophilic groups. This may produce a protective envelope, which acts as a barrier against aggregation of particles. This is probably the case when the soil contains sodium humates as, possibly, in quick clays, where such substances consequently act as dispersive agents /6/. On the other hand, humus is also known to have a cementing ability. This is the case when polyvalent cations are present, forming irreversible gel complexes with the humic acid. A similar cementing effect has been observed for other organic molecules, such as cellulose and polyacrylonitrile, which were used in the former USSR for improvement of drilling muds /7/. Possibly the functional groups of COOH side chains become bonded to clay mineral lattices, which can occur through exchange of clay-adsorbed cations to the proton of the carboxyl group.

Table 4-1. Examples of chemical composition of humic substance /1/.

Elements and element ratios						
C* %	H %	N %	O %	C:N	C:H	O:H
52.62	3	3.5	32	14	10	8
52.62	4.5	4.5	39	19	22	10.5

* Theoretical reference

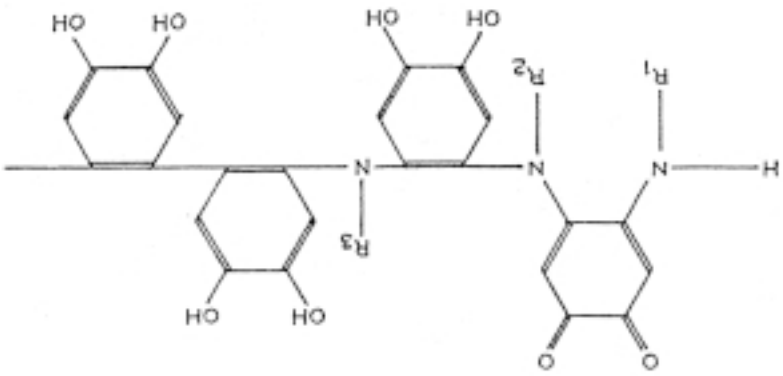

Figure 4-5. *Hypothetical arrangement of soil-type humic acids forming polymers containing phenols and amino acids /1/.*

Bonds between COO and exposed Al ions in the clay mineral lattices may also be established (Figure 4-6). Experience shows that it is difficult to disperse some of the humic substances in the soil /1/. The explanation may be that they are tightly bound to mineral surfaces or that they are protected from dispersion by being co-precipitated with hydrated inorganic oxides or hydroxides.

Regarding organic molecules other than humic substances, several investigations have shown that such molecules with a net positive charge can replace inorganic cations adsorbed on clay particle surfaces /8/. Besides electrostatic attraction, hydrogen bonding e.g. between carbon atoms and hydroxyl groups of the basal planes of clay particles, and van der Waals forces may be active. Thus, organic phosphorous compounds, enzymes and other proteins, with or without net charge, have been found to sorb within the crystal lattice of expanding clay minerals as well as on kaolinite and illite. Probably the size and structure of large organic molecules distort the organization of water close to the clay particle surfaces thereby facilitating their approach to the minerals, which leads to close contact and strong attraction, at least in those cases where the molecules can orient favourably.

A special case, which is exemplified by the EG treatment for identifying expanding clay minerals (Chapter 3), is the adsorption of organic molecules in the interlamellar space of smectites. This matter has become important in the use of clays for isolating organic waste materials from the biosphere and it is related to the formation of clay complexes with aliphatic compounds which have polar groups. The organic material can enter the interlamellar space in the form of positive ions, as the alkylammonium and methylene blue ions. Amines can also be adsorbed because of protonation of the oxygen of the carbonyl group /9/. Ion-dipole and co-ordination bonding can take place of ventral molecules, and hydrogen bonding is important for the adsorption of all molecules containing OH, NH_2 and NH_3 groups. Certain complexes, like the high-molecular-weight compounds that can occupy a large interlamellar space by being oriented perpendicularly or at a steep angle, are thought to be bound by van der Waals forces (Figure 4-7). π-bonding and covalent bonding can also take place, the latter when mixing dry montmorillonite with certain organic substances like diazomethane.

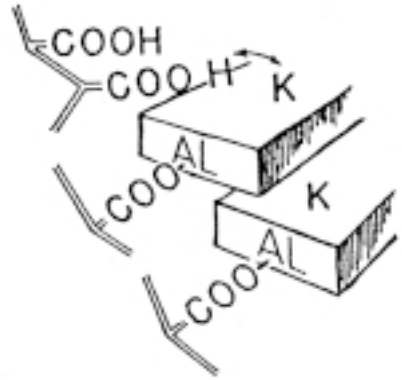

Figure 4-6. *Bond mechanism of organic molecules and clay mineral particles /8/.*

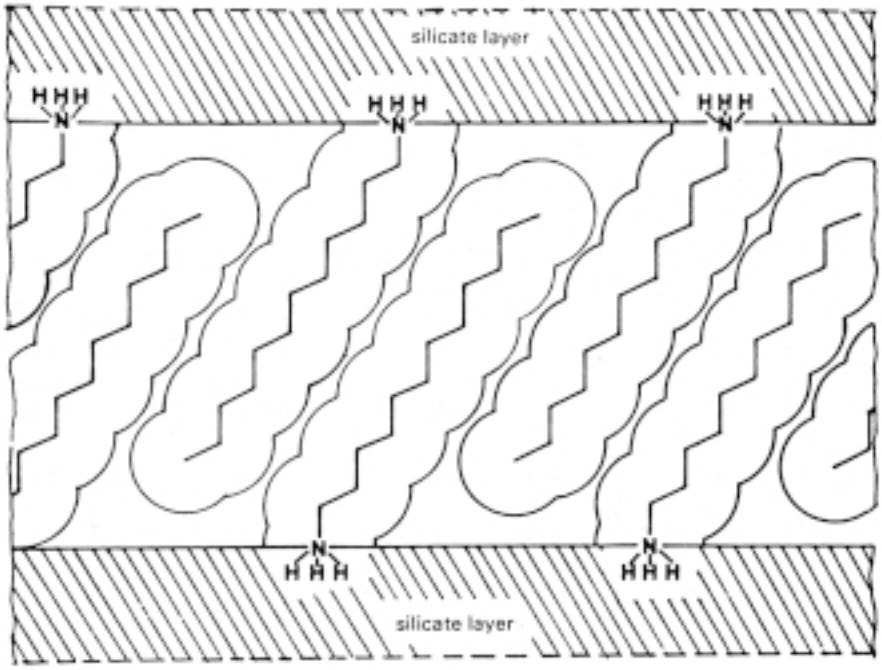

Figure 4-7. *Paraffin-like structure of the alkyl chains adsorbed in interlamellar space /10/.*

The interlamellar water and the nature of the exchangeable cation play a central role in the adsorption process. Thus, hydrates of cations of high field strength, like Ca, Mg, Al are much more dissociated than water in bulk, and can therefore protonate organic molecules so that they are retained in cationic form. Initially adsorbed metal cations stay in the interlamellar space when neutral organic molecules enter this space and establish bonds with these molecules via water molecules.

It has not yet been demonstrated what the mechanisms are that control the uptake of organic molecules in the interlamellar space when a dense bentonite clay is exposed to organic molecules. It is expected, however, that while such uptake takes place easily in laboratory experiments in which organic liquids are mixed with a dilute smectite dispension, spontaneous penetration of the smectite by organic molecules, requiring dehydration of the interlamellar space, may be difficult at high bulk densities.

4.4 Implications with respect to the performance of organics in buffers and backfills

A high organic content, i.e. representing more than about 2% of the total solid mass by weight, affects the rheological properties of soils, enhancing creep and delaying consolidation (Figure 4-8). Even more important is the possible risk of organic colloids being formed in the buffers and migrating out into the surroundings carrying radionuclides. The charge properties of both such organics and of clay minerals cause intimate interaction which minimizes the risk of colloid transport, particularly at high densities of the buffer, but it may still be necessary to keep the organic content significantly lower than 2% by weight; 2000 ppm being a current upper limit according to SKB's concept. This requires access to standardized techniques for determining the organic content in the quality assurance process. A recommended technique is described below.

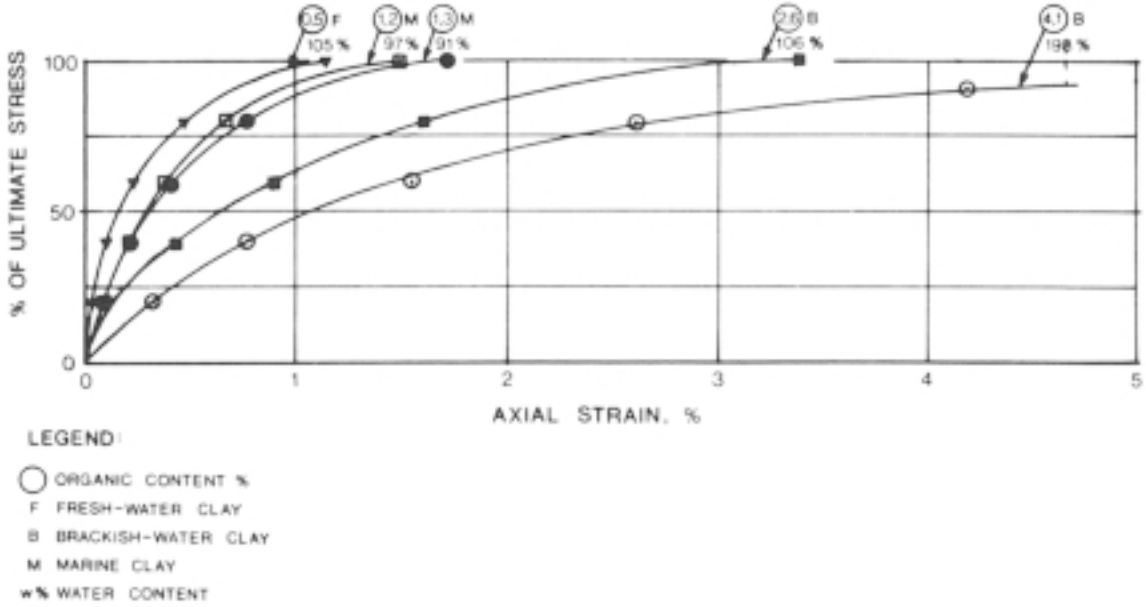

Figure 4-8. *Axial strain at unconfined compression of clay samples with different amounts of organic matter /1/. Organic content values in weight percent encircled.*

4.5 Experimental

4.5.1 General

There are several routine methods for determining the organic content but we will confine ourselves here to describe a relatively simple and accurate wet combustion technique that is currently used by the Swedish Geotechnical Institute /11/.

4.5.2 Experimental

Equipment

- Oven
- Mortar with pestle
- Colorimeter with optic light filter for the wave length interval 600–640 μm
- Electronic balance with ± 0.01 accuracy
- Erlenmeyer flasks of glass (500 ml)
- Pipettes (20 and 40 ml)
- Fume-cupboard
- Chemicals
  - Potassium dichromate ($K_2Cr_2O_7$) solution prepared by dissolving 86 g in 1 liter of distilled water
  - Sulphuric acid
  - Glucose (water-free)
  - Distilled water

Performance

- Select representative 50 g samples for double tests and dry them at 105°C.
- Grind the dried soil and extract about 10 g specimens for the determination.
- Calibrate the colorimeter by using glucose solutions with different content of organic carbon. A solution with 1% weight percent of carbon is prepared by dissolving 2.5 g glucose in 97.5 g of distilled water.

  Glucose solutions are prepared in Erlenmeyer flasks, by mixing 1 to 6 g of the 1% glucose solution with 20 ml $K_2Cr_2O_7$ solution adding subsequently 40 ml concentrated H_2SO_4. After 15 minutes, 200 ml of distilled water are added. A solution with no glucose is also prepared. Colorimeter readings of all the mixtures are taken after 12 hours, yielding a calibration curve of the type shown in Figure 4-9. The scale-factor $s = m_{ko}/k_o$ is evaluated.
- Solutions with soil material instead of glucose are prepared and colorimeter readings made as in the calibration process.

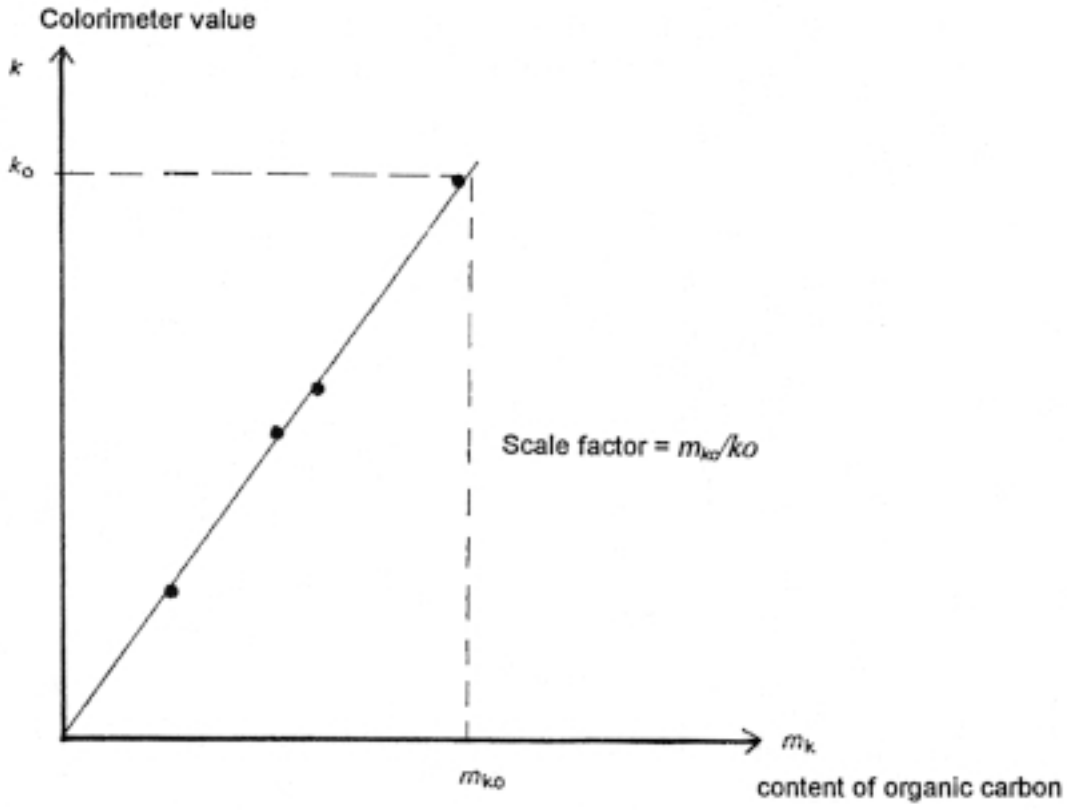

Figure 4-9. *Calibration curve for colorimeter.*

Evaluation

The organic content is obtained from the expression in Equation (4-1):

$$g_0 = \left(ks/Am\right) - 0.002 \qquad (4\text{-}1)$$

where

g_0 = organic content with A weight percentage carbon of the total solid mass. A can usually be taken as 58%
k = colorimeter reading
s = scale factor ($s = m_{ko}/k_o$)
m = solid mass in the flask

4.6 References

/1/ **Pusch R, 1973.** Influence of organic matter on the geotechnical properties of clays. Nat. Swed. Build. Res. Council, Document D11:1973.

/2/ **Pusch R, 1983.** Stability of deep-sited smectite minerals in crystalline rock – chemical aspects. SKBF/KBS Technical Report. Svensk Kärnbränslehantering AB.

/3/ **Pusch R, Karnland O, 1988.** Geological evidense of smectite longevity. The Sardinian and Gotland cases. SKB TR-88-26, Svensk Kärnbränslehantering AB.

/4/ **Pusch R, Karnland O, Hökmark H, 1990.** GMM – A general microstructural model for qualitative and quantitative studies of smectite clays. SKB TR-90-43, Svensk Kärnbränslehantering AB.

/5/ **Pusch R, 1999.** Mobility and survival of sulphate-reducing bacteria in compacted and fully water saturated bentonite – microstructural aspects. SKB TR-99-30, Svensk Kärnbränslehantering AB.

/6/ **Söderblom R, 1966.** Chemical aspects of quick-clay formation. Engng. Geol. Vol 1(16). Elsevier Publ. Co. (pp. 415–431).

/7/ **Kachinskii N A, 1966.** Mechanical and microaggregate composition of soils. Akademiya NAUK USSR. Israel Progr. Sci. Translations, Jerusalem.

/8/ **Gerasimov I P, Glazovskaya M A, 1965.** Fundamentals of soils science and geography. Akademiya NAUK USSR. Israel Progr. Sci. Translations, Jerusalem.

/9/ **MacEwan D M C, Wilson M J, 1980.** Interlayer and intercalation complexes of clay minerals. Crystal Structures of Clay Minerals and Their X-ray Identification (Ed. G.W. Brindley), Mineral Soc. Monograph No. 5, London.

/10/ **Lagaly G, Weiss A, 1969.** Determination of the layer change in mica-type silicates. Proc. Int. Clay Conf. 1969, Tokyo, Vol. 1. Israel University Press, Jerusalem (pp. 61–80).

/11/ **Larsson R, Nilsson G, Rogbeck J, 1985.** Bestämning av organisk halt, karbonathalt och sulfidhalt i jord. Rapport No. 27, Swedish Geotechnical Institute, Linköping.

5 Porewater chemistry

This chapter gives some basic statements concerning the porewater chemistry. The issue is extremely complex and comprehensive and is of importance for a number of physical and physico/chemical processes and properties like smectite stability, microstructural constitution and rheological behaviour. In the condensed chapter, focus is on practical experimental determination of the electrolytic composition of the porewater of buffers and backfills.

5.1 General

pH, Eh and the content of dissolved ions are the major chemical parameters of the porewater. They depend on the interaction with the water phase of the surroundings and on the interplay between the porewater and mineral phase of the soil and may hence be different in parts of the soil/water system as discussed in Chapter 6, "Soil Structure". Relevant data represent some sort of average that can be recorded by direct or indirect methods.

5.2 The electrochemical potential

The distribution of charges in a soil/water system is governed by the potentials that arise around the electrified mineral/water interface. They reflect the inhomogeneities in the molecular environment of the interface and are described by the electrochemical potential of a charged species and can be measured by determining the electromotive force developed across a pair of electrodes that behave reversibly to the charges species /1/.

Equation (5-1) gives the expression for the electrochemical potential difference μ for a species:

$$\bar{\mu}[i] = \xi_0 + RT\,ln(i) + Z_i F\phi \qquad (5\text{-}1)$$

where

ξ_0 = basic term that depends on pressure, temperature and chemical nature of the species
i = activity of the species
R = molar gas constant
T = absolute temperature
ϕ = electric potential to which [i] is subjected

The first two terms represent a purely chemical part and the third one a purely electrostatic part containing the potential ϕ.

Equation (5-1) can be used to demonstrate that the Galvani potential difference between two electrodes is a measurable quantity. If charged species cannot traverse an interface freely, the interface is called polarizable, while the opposite conditions imply that zero electrochemical potential difference exists across it. In soils, the former are typical in clay/water systems while the latter are represented by hydrous oxide solids.

5.3 pH

pH is a designation of the activity of the hydrogen ion in a solution or the acidity of a solution, expressed as:

$$pH = -log\{H^+\} \tag{5-2}$$

$$\{H^+\} = \frac{\{H_3O^+\}}{\{H_2O\}} \tag{5-3}$$

In pure water H_3O^+ ions and OH^- ions are present in equal concentrations. H_3O^+ is the concentration of all more or less hydrated hydrogens, including those in interlamellar positions in smectites.

A special case of great importance is represented by the pH conditions created through interaction of air and water. Carbon dioxide emanating from the air is dissolved and exists in two forms: dissolved CO_2 and the hydrated version H_2CO_3.

The pH of the porewater in smectitic clay cannot be accurately defined or determined since the density of protons is different in the interlamellar space and in the voids between the clay aggregates and it varies with the distance from the clay mineral surfaces.

Typical values of Na smectite clay are in the interval 8<pH<11, while for Ca smectite pH is commonly in the interval 7–8. Considerable changes in pH is produced by altering the porewater chemistry because of cation exchange that governs the amount of H_3O^+ in exchange positions. Heating also affects pH because thermally enhanced dissolution of silicates yields the charged species H_4SiO_4.

5.4 Eh

The redox potential Eh is a measure of the ability of a chemical system to oxidize another, interacting one. It is expressed in volts, referring to neutral conditions. Systems with higher Eh can oxidize systems with lower Eh /2/.

Eh determines i.a. the form in which iron exists and vice versa. Thus, the low Eh in sediments with stagnant porewater where microbic processes contribute to the creation of reduced conditions and where organic detritus of various sorts can be enriched and

preserved, iron and various other compounds exist in reduced form. The content of hydrogen sulphide tends to be high in this sort of environment but inflow of oxygen-rich "ventilated" groundwater causes precipitation of many species, usually forming high valency compounds of low solubility.

The Eh conditions in canister-embedding buffer clay are of great practical importance since they determine the nature and rate of corrosion of the metal canister. The importance as to the smectite clay is that Eh determines the chemical state of dissolved elements like copper and cobalt and also silica, which become enriched under stagnant groundwater conditions and yield ion exchange and precipitation of cementing compounds.

Eh of groundwater can be determined in situ by measuring the potential between two electrodes, Au and Pt, and a reference electrode /3/. The problem is the risk that samples taken for Eh-determination become oxidized during transport and handling. The only way to get reasonably relevant Eh-values is to insert electrodes in the sample in a glovebox with inert gas. No commercially available standard equipment is available for this purpose.

5.5 Electrolyte content

The electrolyte content of the porewater in smectitic clays depends on the chemical interaction between the clay minerals and the porewater. As for pH the electrolyte content cannot be adequately defined and determinaded for smectitic clays. Thus, it follows from the preceding text on electrochemical potentials and the description of clay microstructure (Chapter 6) that the ions in the porewater are not homogeneously distributed in smectite clays: the interlamellar space is occupied by exchangeable cations and the basal planes of the stacks of flakes hold electrical double-layers with hydrated cations that are rather strongly bound to the negatively charged mineral surfaces (Figure 5-1).

The diagrams in Figure 5-2 illustrate that analysis of expelled porewater gives a change in pH as well in the concentrations of Na and K /4/. The initial water content of the Na montmorillonite-dominated clay was 1000%, while compression at 1 MPa gave a water content of 37%. 50 MPa reduced the water content to 18%.

The firstmentioned technique, i.e. to disperse a small amount of soil into a larger quantity of distilled water, which is then analyzed with respect to the content of electrolytes, is very common and can be recommended for routine testing. Usually, the dispersion and testing is made under aerobic conditions, which is of course simpler than to work in a glove-box with inert gas. However, the latter environment should be used when possible. It should be added that a general measure of the electrolyte content can be obtained by recording the electrical resistivity of expelled porewater or of undisturbed samples into which electrodes are inserted.

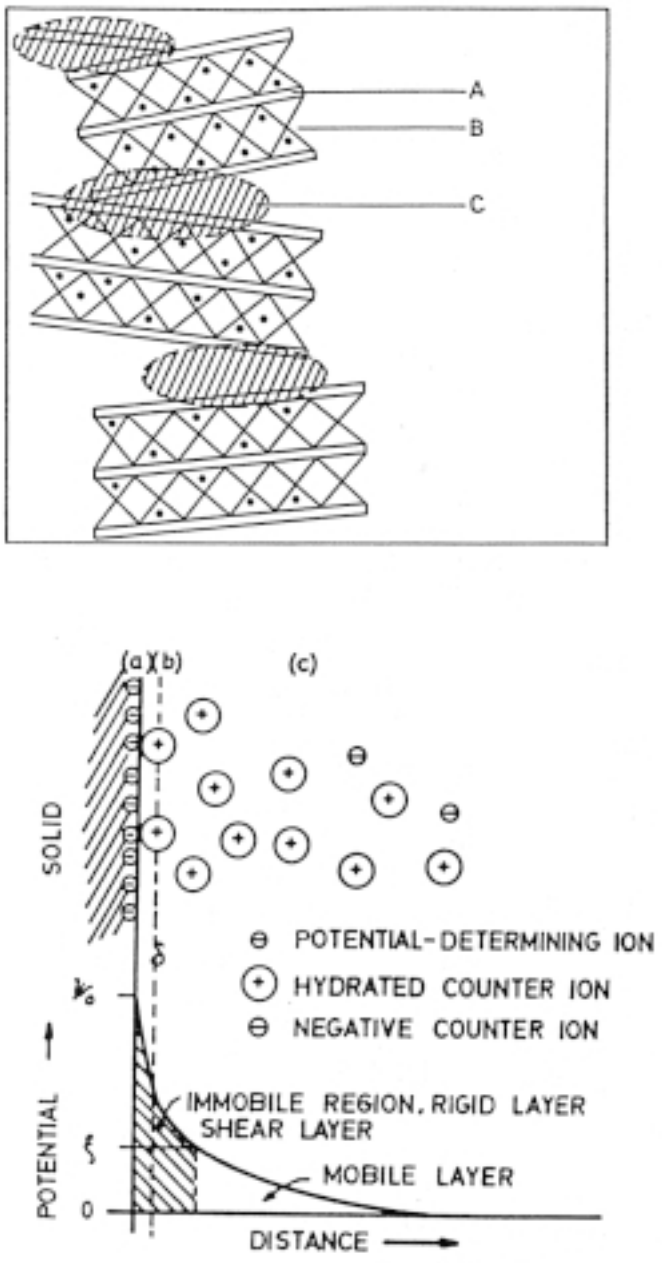

Figure 5-1. *Heterogeneous distribution of ions in the porewater of smectite clays. Upper: A) Stacks of flakes with B) interlamellar water with cations and C) stack "contacts" with electrical double-layers (cf Figure 11-23 to 11-25). Lower: Electrical double-layer with the electrical potential varying with the distance from the mineral surface. Only cations are present in the immobile (Stern) layer and the innermost part of the mobile layer.*

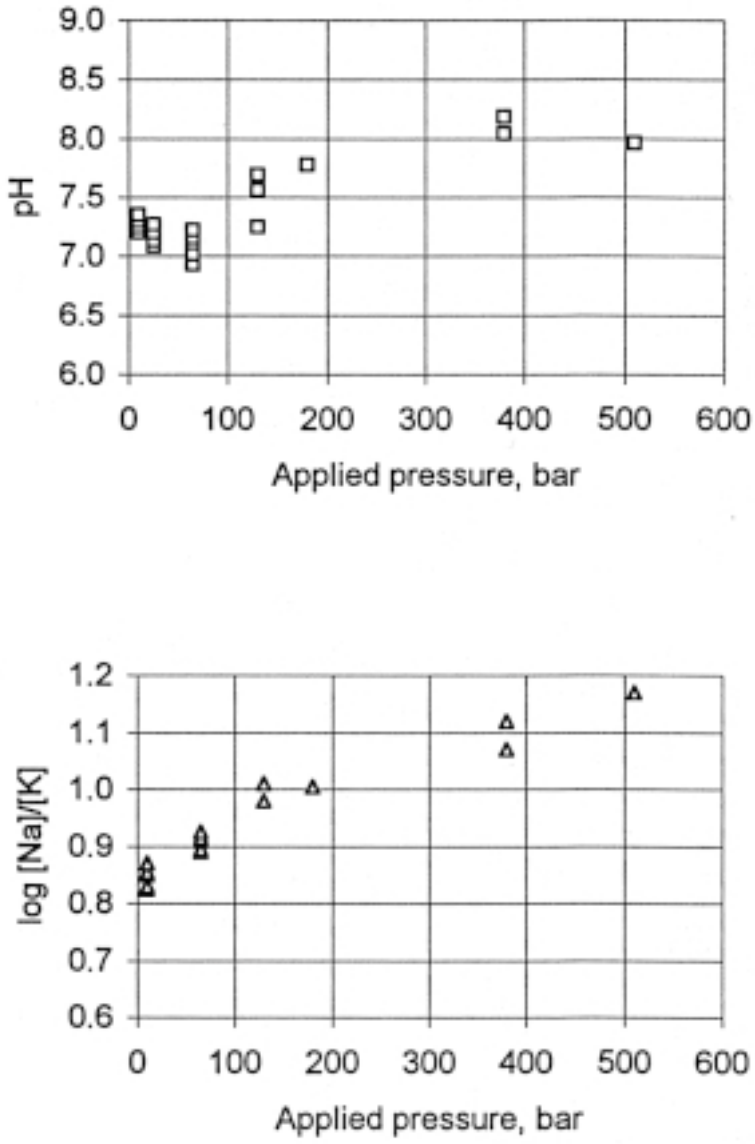

Figure 5-2. *Change in pH and Na/K ratio in porewater expelled at successively increased pressure /4/.*

5.6 Experimental

5.6.1 pH

General

Measurement of pH is most accurately made by potentiometric measurement of the electromotive force of an element in which an electrode potential is a function of $\{H^+\}$. The most simple principle is offered by utilizing the *hydrogen gas electrode* but the most practical way is to use a *glass electrode*. For quick but less accurate estimation of the pH one can use various types of *indicators*. We will confine ourselves to describe pH-measurement by use of glass electrodes in this chapter.

pH can be measured by titration of expelled porewater or by use of a pH-meter with glass electrode. The latter method implies that pH is determined by measuring the electrical potential between a solution with known pH, contained in a glass electrode, and the soil sample wetted by adding distilled water to become semifluid. This technique is recommended and is described below. Titration of expelled porewater has the disadvantage that pH of the fluid is altered if it is exposed to the atmosphere.

Expulsion of porewater from soft soil samples can be made with ordinary oedometer equipment (cf Chapter 9) but very high pressures are required for getting sufficiently large water samples from dense smectite clay. Figure 5-3 illustrates equipments that have been used for this purpose. The filters ("sinter") must be mechanically strong and have voids less than 0.05 mm for minimizing transport of particles. For larger soil samples heat will be produced that may require cooling.

Equipment

A common pH-meter equipped with glass electrode is shown in Figure 5-4. The complete equipment in addition the pH-meter consists of the following units:

- 500 ml glass vessel for dispersion of soil sample
- Spatula
- Ultrasonic dispersion apparatus

Performance

The soil sample is ultrasonically dispersed in water for 10 minutes, using the same amount of solid soil and distilled water. The dispersion is left to homogenize for a few hours and the measurement is then performed by lowering the glass electrode, filled with a standard solution of known pH, into the dispersion. pH readings are taken after a few minutes.

Evaluation

The readings give the actual pH of the porewater, the accuracy usually being ± 0.5 units.

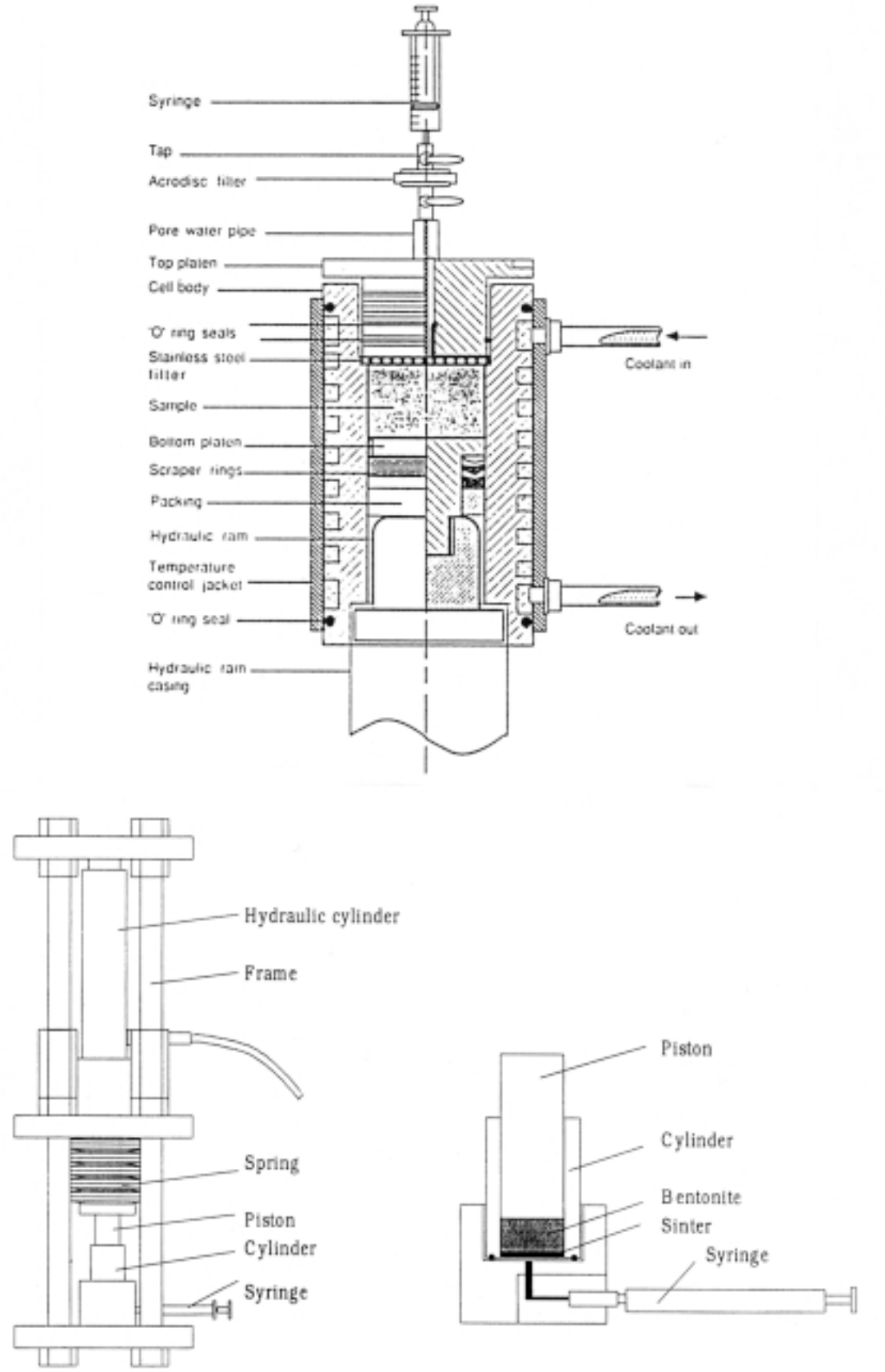

Figure 5-3. *Schematic picture of devices for squeezing porewater from soil samples. Upper: Rigid apparatus with cooling facility /5/. Lower: Equipment for expelling porewater from 20 mm diameter bentonite samples /6/.*

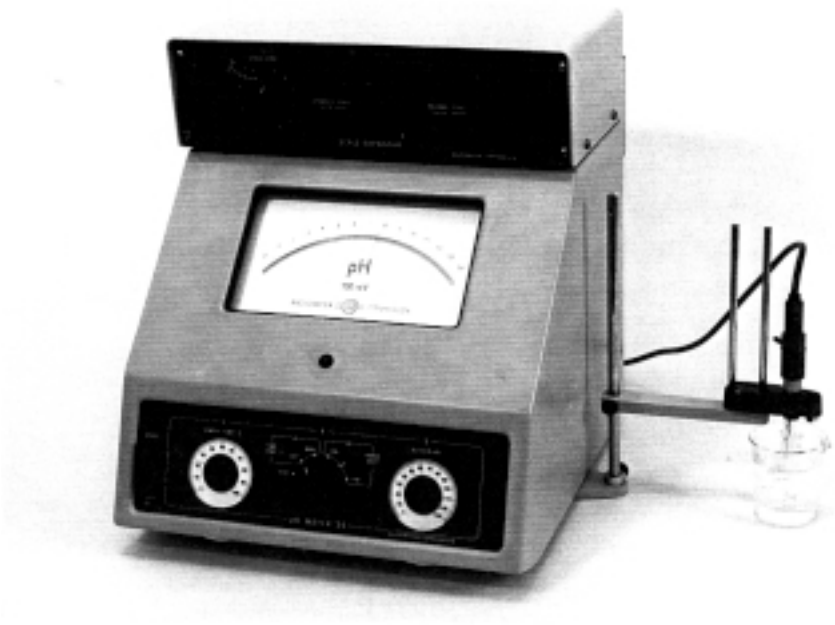

Figure 5-4. *Standard equipment for pH determination using glass electrodes.*

5.6.2 Porewater composition

Any attempt of direct measurement of the total and relative concentrations of ions in the porewater by inserting ion-selective gauges or by extracting porewater will only give average values that depend on the soil/water mass ratio. Hence, the two methods that are usually applied, i.e. dispersion of a representative amount of soil in a larger volume of water and chemical analysis of the solution, or compression of soil to expel porewater that is then analyzed, do not give information on the distribution of the various ions in the soil.

Equipment and performance

Determination of the content of cations dissolved in the porewater is most suitably made by spectroscopy using inductively coupled plasma – atomic emission spectrometry (ICP-AES), plasma-optical emission spectrometry (ICP-OES), or mass spectrometry (ICP-SMS). Fluoride is determined by use of an ion selective electrode and all other anions by ion chromotography using autosamplers. A standard performance is *EPA-method 200.7.*

Solid organic components can be identified by microscopy and dissolved organic substances identified by paper chromatography. In modern chemical analysis nuclear magnetic resonance (NMR) and similar techniques are used for quick and reliable determination. All these techniques are highly specialized and the analyses have to be made by well equipped laboratories. They will not be described here.

Evaluation

Data from chemical analysis of porewater are given in protocol form showing concentration in mg/l (ppm) for most cations and anions (Ca, Fe, K, Mg, Na, S, Si; Cl and SO_4), while the concentration of elements like Al, As, B, Ba, Cd, Co, Cr, Cu, Li and Sr are usually in μg/l (ppb).

The accuracy depends on the amount of fluid – small amounts need addition of distilled water by which the accuracy drops. Extraction of samples from natural soil layers causes exposure to carbon dioxide, which will generate carbonitization and a change in ion concentration. Exposure to oxygen will significantly change pH of sulphidic soils. In general the accuracy is on the order of ± 10%.

5.6.3 Precipitation from porewater

Many investigations of fluid transport mechanisms in soils, particularly buffers and backfills, involve introduction of tracers for identifying pathways and adsorption of ionic species. This requires spot analysis using electron microscopy (EDX), which is a highly specialized technique for sample preparation and investigation of very thin specimens. Figure 5-5 illustrates the outcome of a study using scanning electron microscopy of a smectitic clay sample in which an uranium-doped solution was injected. Major elements including U are seen in the left EDX spectrum. The right spectrum was obtained from a reference solution for calibration purposes.

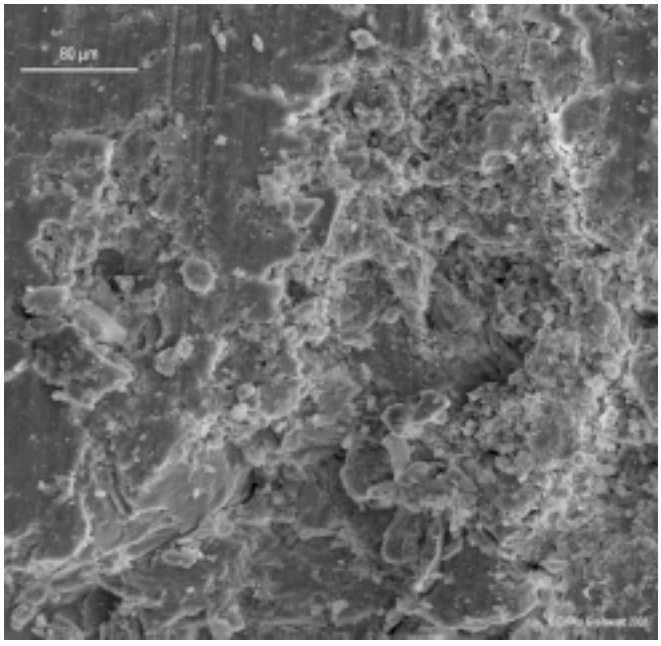

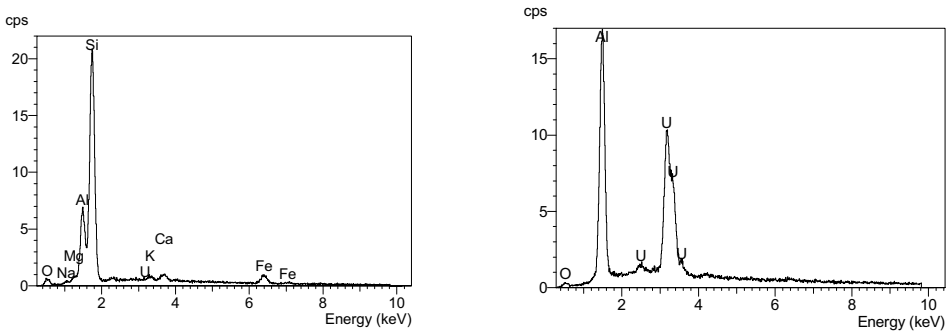

Figure 5-5. *SEM-EDX examination of MX-80 samples with a dry density of 1510 kg/m³ into which uranium acecate solution had been injected. Upper: SEM picture (250x magnification). Lower left: U-traces in the analyzed area. Lower right: Calibration test with uranium solution on an aluminum sample holder /7/.*

5.7 References

/1/ **Sposito G, 1984.** The Surface Chemistry of Soils. Oxford University Press/ Clarendon Press, Oxford.

/2/ **Grenthe I, Stumm W, Laaksoharju M, Nilsson A-C, Wikberg P, 1992.** Redox potentials and redox reactions in deep groundwater systems. Chemical Geology, Vol. 98, (p. 131).

/3/ **Wikberg P, 1991.** Laboratory Eh simulations in relation to the redox conditions in natural granitic groundwaters. Proc. OECD/NEA Workshop on Sorption Processes, Interlaken, October 1991 (p. 217).

/4/ **Touret O, 1988.** Structure des argilles hydratees thermodynamique de la deshydratation et de la compaction des smectites. Dr. thesis Unversity Louis Pasteur, Strasbourg.

/5/ **Entwisle D C, Reeder D, 1993.** New apparatus for pore fluid extraction from mudrocks for geochemical analysis. Chapter 15 in Geochemistry of Clay-pore Fluid Interactions (Ed. D.A.C. Manning et al), Chapman & Hall, London (SBN 0-412-48980-5).

/6/ **Muurinen A, 1999.** In: Microstructural and chemical parameters of bentonite as determinants of waste isolation efficiency. Final Report Contract No F14W-CT95-0012, European Commission, Brussels.

/7/ **Pusch R, 2001.** Can the water content of highly compacted bentonite be increased by applying a high water pressure? SKB TR-01-33, Svensk Kärnbränslehantering AB.

6 Soil structure

This chapter deals with the geometry of soil constituents and their arrangement, i.e. the microstructure. Focus is on the size and shape of mineral particles. The meaning and determination of the specific surface area and of the microstructural constitution are major subjects.

6.1 Introduction

The granulometry, the interaction with porewater and the arrangement of soil constituents, primarily mineral particles, determine the physical properties of soils. They make up the soil structure with which this chapter deals. Focus is on the following issues:

- Grain size
- Grain shape
- Grain surface area
- Fabric ("Microstructure")

6.2 Granulometry

6.2.1 Size

For many purposes, particularly in industrial chemistry, one has tried to define the size of an individual particle by using a "mean diameter", expressed for instance as a function of the dimensions of the particle, as a function of the particle volume, or as a function of the area of the projected image of the particle when placed in the most stable position. Such a "mean diameter" can be used for estimating the (specific) surface area and the statistical distribution of the particle size /1/.

Since description of the shape of individual clay particles involves determination of the dimensions of the particles, it is suitable to express the size as a function of them /2/. The definitions of particle size given by Krumbein /3/ are most suitable; the characteristic dimensions are measured as shown in Figure 6-1. **a** the long diameter is the longest intercept. **b**, the intermediate diameter, is the measure of the widest part of the "maximum projection plane". The direction of **b** is perpendicular to the long axis. **c**, the short diameter, is the measure of the widest part when the particle is rotated 90° from the position shown in the figure illustrating the measure **b**. The three diameters are mutually perpendicular but do not necessarily intersect at the same point.

Particle size as a principle should be expressed as a function of the dimensions **a**, **b** and **c**. However, since **c** is often small compared with **a** and because **a** and **b** generally are of the same order the **a**-value gives sufficient information about the size and we can confine ourselves to defining the *particle size as the* **a**-*value, that is the longest diameter* /1/.

6.2.2 Size determination

The long diameter can be measured directly on grains larger than about 5 mm by use of micrometer screws while that of smaller grains must be measured using optical or electron-optical microscopes. Figure 6-1 shows definition of particle dimensions and a photo of gravel with easily estimated grain dimensions.

Figure 6-2 shows an example of the variation in size of clay particles as derived from transmission electron microscopy (TEM).

Rational size determination does not allow for individual measurements and sieving was introduced more than 100 years ago for practical determination of the size and shape of granular material. Figure 6-3 illustrates the most common type of equipment for sieving.

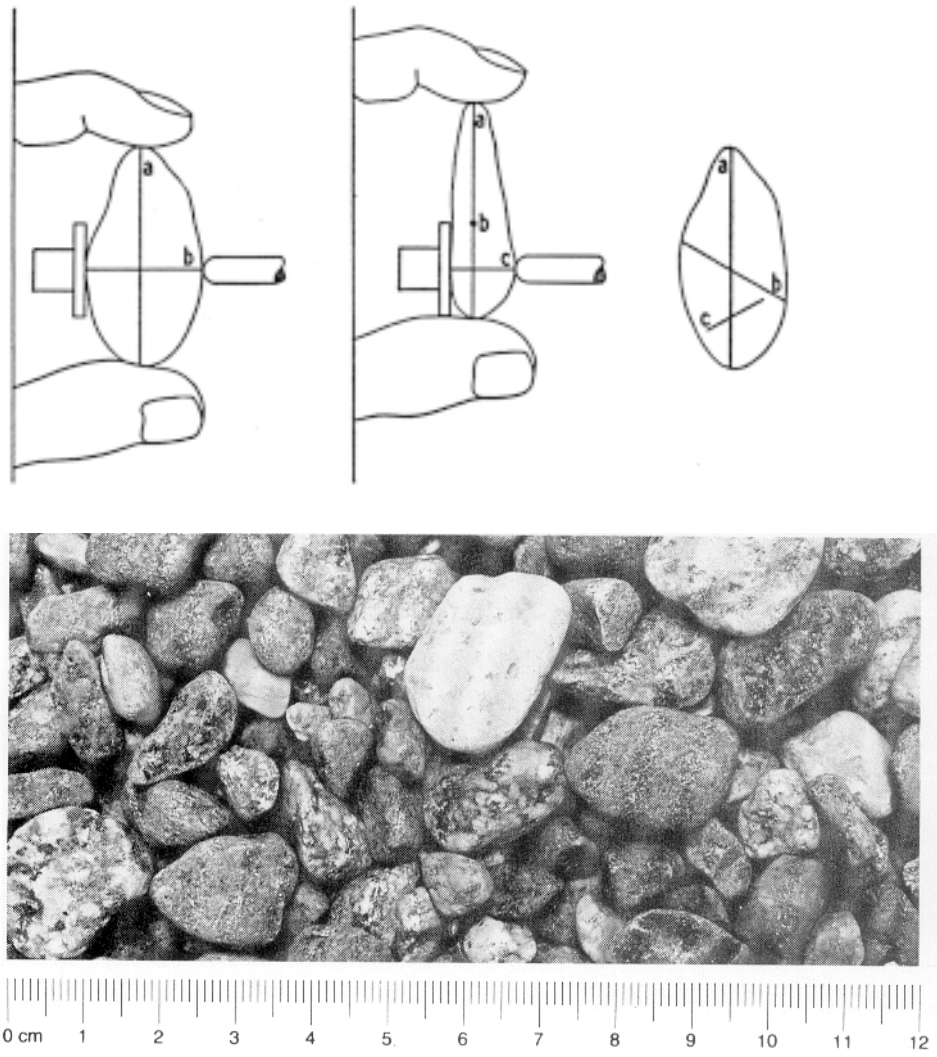

Figure 6-1. *Definition of particle dimensions /3/ and the appearance of gravel.*

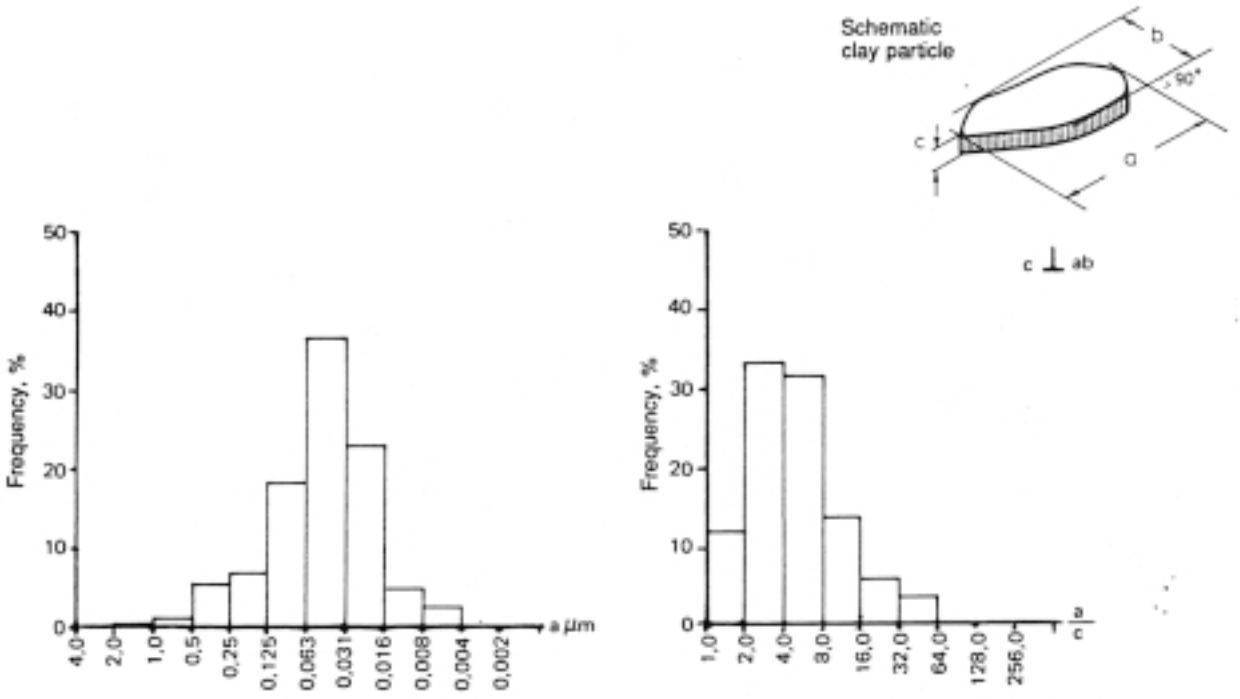

Figure 6-2. *Histogram of clay particle size expressed in terms of the maximum diameter (a), and of clay particle shape expressed in terms of the ratio between the largest and the smallest diameters (a/c), respectively.*

The size of boulders and cobbles are determined in the field by direct measurements or by sieving using gratings. The size of grains passing gratings is equal to or smaller than the free width of the opening between the bars. A traditional method of estimating anisotropy of boulders and cobbles is to perform sieving using first square mesh sieves and then gratings. This gives a measure of how splintery the particles are, using the parameter $F = \frac{s}{t}$, where s = is the square mesh aperture and t the width of the grating. The evaluation is shown in Figure 6-4. For ordinary, "good" crushed rock F is 1.20–1.35 while very splintery material has $F > 1.40$. The volume of boulders is at least 0.1 m^3 (mass about 0.25 t) and for large boulders at least 4 m^3 (mass about 10 t).

Boulders, cobbles and gravel normally consist of more or less rounded rock fragments, each particle usually consisting of several minerals. Sand and silt grains normally consist of single crystals, commonly quartz, feldspar, heavy minerals and mica.

The grain-size distribution of the coarse fractions gravel and sand is determined by sieving with the particle size taken to correspond to the free width of the mesh opening (*d*). Table 6-1 gives examples of standard mesh sizes.

The grain-size distribution of the fine fractions silt and clay (fines) is determined by sedimentation of dispersed soil. It is made by applying Stoke's law using actually recorded settlement rates. The fine grains are assumed to be spherical and their size is therefore given in terms of the equivalent (Stoke) diameter.

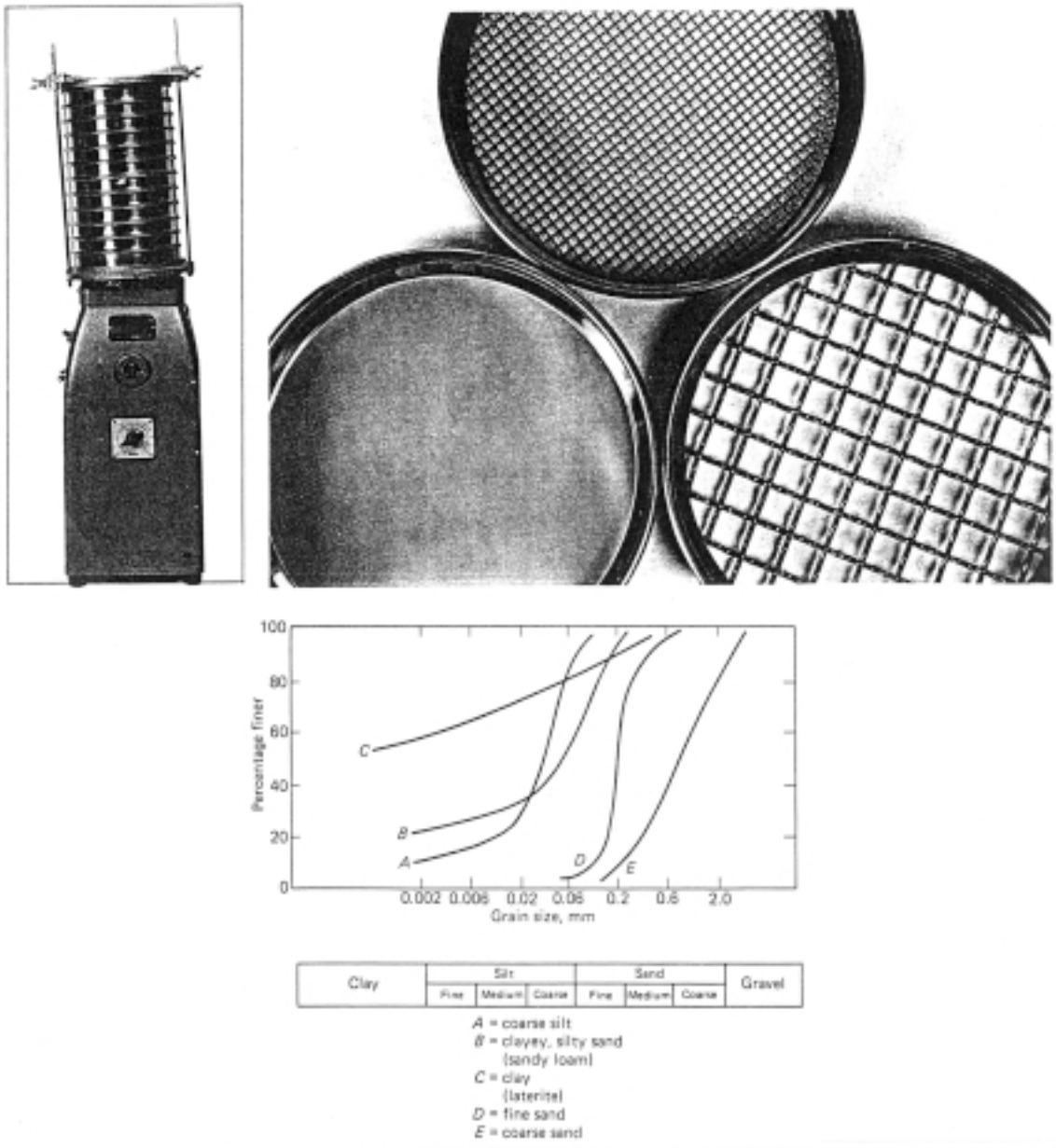

Figure 6-3. *Sieving. Upper: Vibrator and square mesh sieves. Lower: Example of grain size distribution evaluated from sieving.*

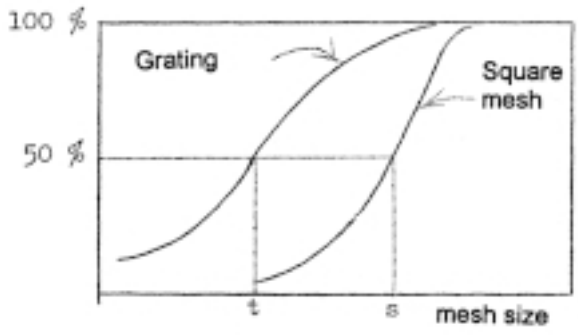

F *is evaluated from the expression:*

$$\log s - \log t = \log \frac{s}{t} = \log F$$

Figure 6-4. *Sieve diagrams for evaluation of F.*

Table 6-1. Standard mesh size, mm.

International (ISO/R565)	American (ASTM:E11-61)	Swedish
0.063	0.063	0.063
–	0.074	–
0.125	0.125	0.125
–	–	0.200
0.250	0.250	0.355
0.355	0.354	–
0.500	0.500	0.630
1.0	1.0	1.0
2.0	2.0	2.0
4.0	4.0	4.0
5.6	5.66	–
6.3	6.35	6.3
8.0	8.0	–
11.2	11.2	11.2
16.0	16.0	–
–	19.0	–
20	–	20.0
22.4	22.6	–
–	26.9	–
31.5	32.0	31.5
45.0	45.3	–
–	53.8	–
63.0	64.0	63.0
–	76.1	–
90.0	90.5	–
–	107.6	–
125.0	–	125.0

Clay particles primarily consist of clay minerals but fine particles of rock-forming minerals are usually also present, like quartz and feldspars, which are relatively abundant even in smectite-rich bentonites.

Preparation of soils for grain size analysis can alter the original size of many particles. This matter is discussed later in the present chapter.

The techniques in Table 6-2 are commonly used for determining the grain size distribution of silts and clays.

Sedimentation analysis is based on the principle that particles settling in a fluid of known viscosity move at a rate that depends on their size.

The *light-penetration* granulometry of modern type makes use of one or several laser beams that penetrate the suspension, which is constrained in a thin cell. Diffraction and refraction take place to an extent that depends on the grain size and density of the suspension. The method appears to underestimate the content of clay-sized particles and calibration by sedimentation analysis is required.

Table 6-2. Techniques for determination of the size of fine particles.

Method	Principle of evaluation	Particle size, μm
Sedimentation analysis	Stoke's law	0.5–100
Light-penetration analysis	Density measurement	0.1–500
Coulter-counter	Flow of suspension through fine holes with defined diameters	0.1–100

The *Coulter-counter* method simply implies measurement of the fraction of particles dispersed in a suspension that pass through holes with different, defined sizes. This method gives grain size distributions that tend to underestimate the content of clay-sized particles.

Although the conventional sedimentation analysis is the most time-consuming method – the required time for a complete test is about 1 day compared to 15 minutes for laser light measurement – it gives the most reliable results and we will therefore confine ourselves to describe a common version of this method, i.e. the hydrometer technique.

The settling rate of dispersed particles in sedimentation analysis is defined by Stoke's law:

$$v = \frac{h}{t} = \frac{(\rho_s - \rho_w)g}{18\eta} \cdot d^2 \qquad (6\text{-}1)$$

where

v = settling rate (m/s)
h = settling distance (m)
t = settling time (s)
ρ_s = grain density (kg/m^3)
ρ_w = water density (kg/m^3)
η = water viscosity (kg/m, s)
d = grain diameter (m)
g = gravity (m/s^2)

If a centrifuge is used to accelerate the settling, which is suitable for particle size that is smaller than 1 μm, gravity g in the formula is replaced by the acceleration produced by the machine.

In the course of the sedimentation process, which starts immediately after stirring of the suspension has stopped, the concentration of particles and thereby the density of the suspension changes with the time and depth. Down to a certain depth h only particles finer than d will be present (Figure 6-5) and the relative amount of these grains can be calculated using the ratio of the density of the suspension at this depth and the original density. The simplest procedure to determine the density is to use the hydrometer, i.e. a glass body that sinks to a depth where the buoyancy of the suspension balances the weight of the glass body.

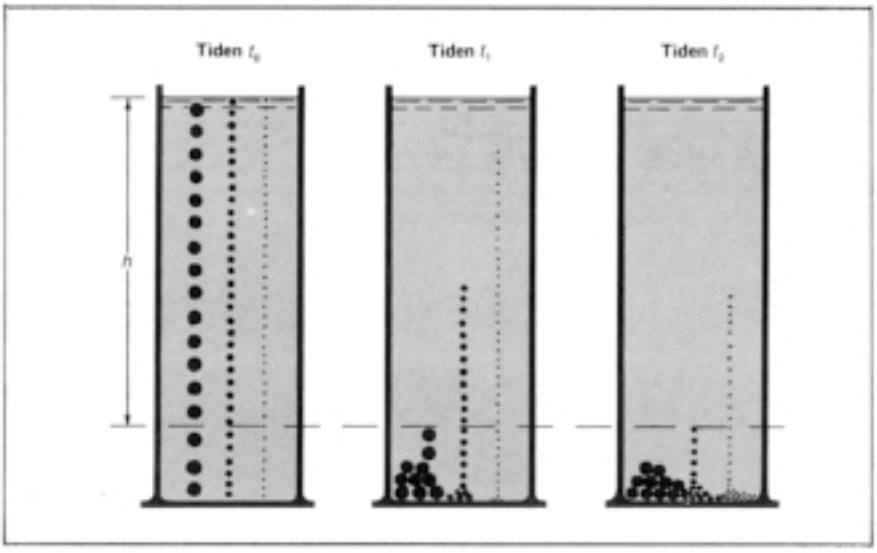

Figure 6-5. *Schematic picture of the change of particle size distribution in the course of the particle settling ($t_2>t_1>t_0$).*

A number of factors combine to yield an error in the evaluated particle size. Firstly, Stoke's law is valid only for spherical particles, which is far from correct for clay particles (cf Figure 6-2). Secondly, Brownian movement and physico/chemical interaction of the particles cause deviation from pure Stoke-type settling. Thirdly, larger grains cause turbulence and disturb the settling of finer particles. Adding to this the disturbance caused by bringing the glass body into the suspension (Figure 6-6), it is clear that the evaluated grain size distribution is not very accurate. However, sedimentation analyses give a value of the "equivalent Stoke diameter" of the particles that is acceptable for practical purposes, i.e. for soil categorization and characterization.

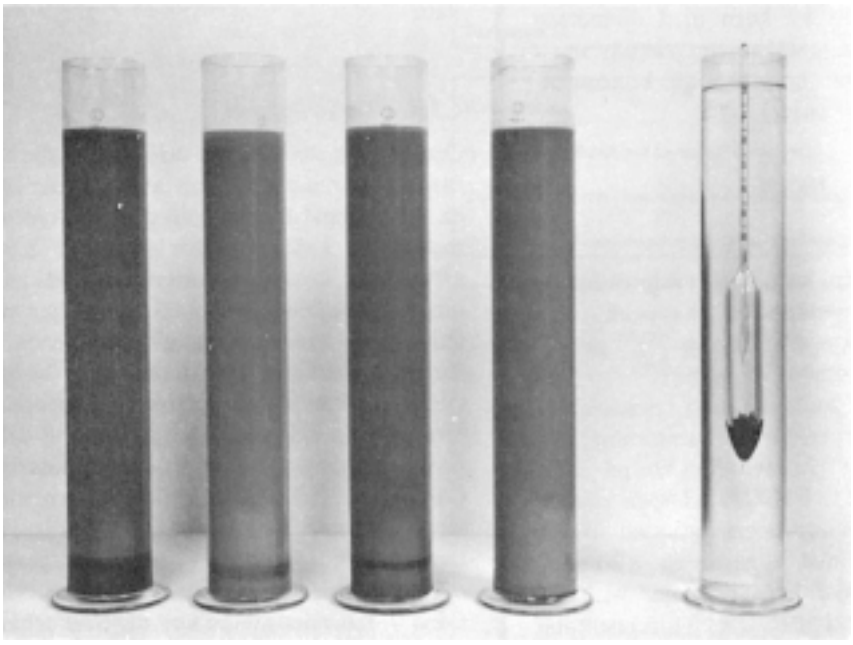

Figure 6-6. *Hydrometer and 1 liter sedimentation vessels with suspensions.*

6.2.3 Shape

The shape of mineral particles is of importance in the preparation of mixtures of clay and coarser material, i.a. for backfilling purposes in repositories. One distinguishes between the general shape of the grains expressed in terms of "sphericity" or "shape factor", i.e. the deviation from the shape of a sphere, and the sharpness of the grains, which is termed roundness and describes the radius of curvature of the edges. The splintery factor, defined earlier in this chapter, is a special measure of the general shape of crushed rock fragments.

The *sphericity S* /1/ is defined as in Equation (6-2):

$$S = \sqrt[3]{\frac{b \cdot c}{a^2}} \tag{6-2}$$

where a, b, c are the grain diameters defined in Section 6.2.1.

The *shape factor* C_f is defined as in Equation (6-3) /4/:

$$C_f = \frac{\sum_1^n W_i / \rho}{\sum_1^h \frac{\pi}{6} a_i^3} \tag{6-3}$$

where W_i = mass of one grain with density ρ and large diameter a_i.

The *roundness R* /2/ is defined as in Equation (6-4):

$$R = \frac{\Sigma r / R}{N} \tag{6-4}$$

where

r = the radius of curvature in the plane of observation (Figure 6-7)
R = radius of the inscribed circle in the plane of observation
N = number of edges

Mineral particles belonging to different size fractions often exhibit quite different shapes and degrees of roundness. While clay-sized particles are typically thin and flat, quartz silt grains of glacial origin are less bladed but still far from spherical. They appear to have a low roundness, similar to that of moraine or crushed rock (Figure 6-8). Glacial and river-transported sand and gravel as well as beach sand commonly have a roundness of 0.2–0.3, dropping with the grain size. Coarser material in eskers and beach gravel are among the best rounded soils. They may have a roundness of up to 0.8–1.0 (Table 6-3).

Figure 6-9 gives examples of the relation between sphericity and roundness. Figure 6-10, finally, shows five defined roundness grades which can be used for classification purposes /5/. They are related to the roundness as indicated in Table 6-3 /6/.

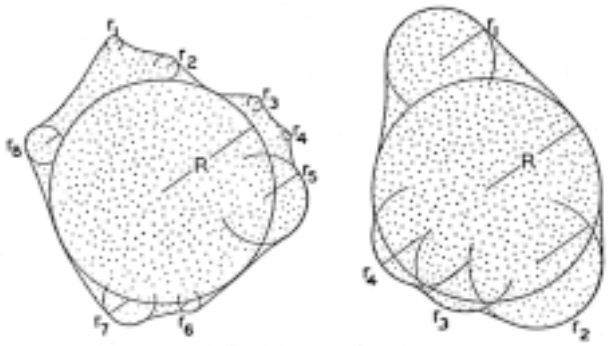

Figure 6-7. *Examples of pebble shape /3/.*

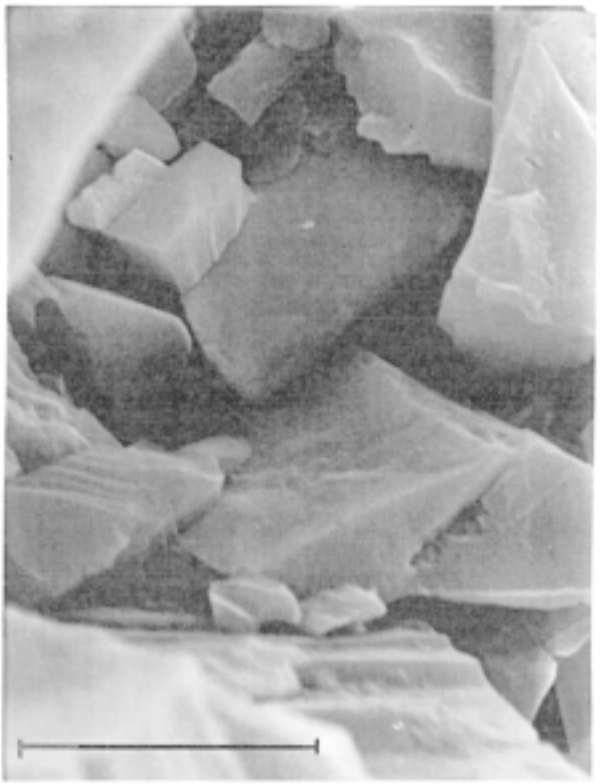

Figure 6-8. *Silt grains (quartz) of glacial origin. The length of the bar represents 10 μm.*

Table 6-3. Roundness grades /6/.

Grade term	Class limits	Geometric mean
Angular (A)	0–0.15	0.125
Subangular (B)	0.15–0.25	0.200
Subrounded (C)	0.25–0.40	0.315
Rounded (D)	0.40–0.60	0.500
Well rounded (E)	0.60–1.00	0.800

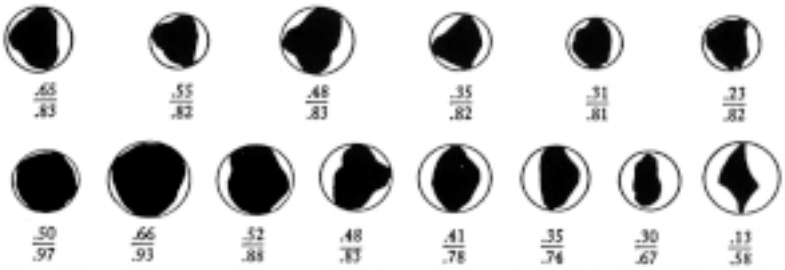

Figure 6-9. *Images of particles to show differences between roundness and shape. Figure above the line shows R and the one below gives S /2/.*

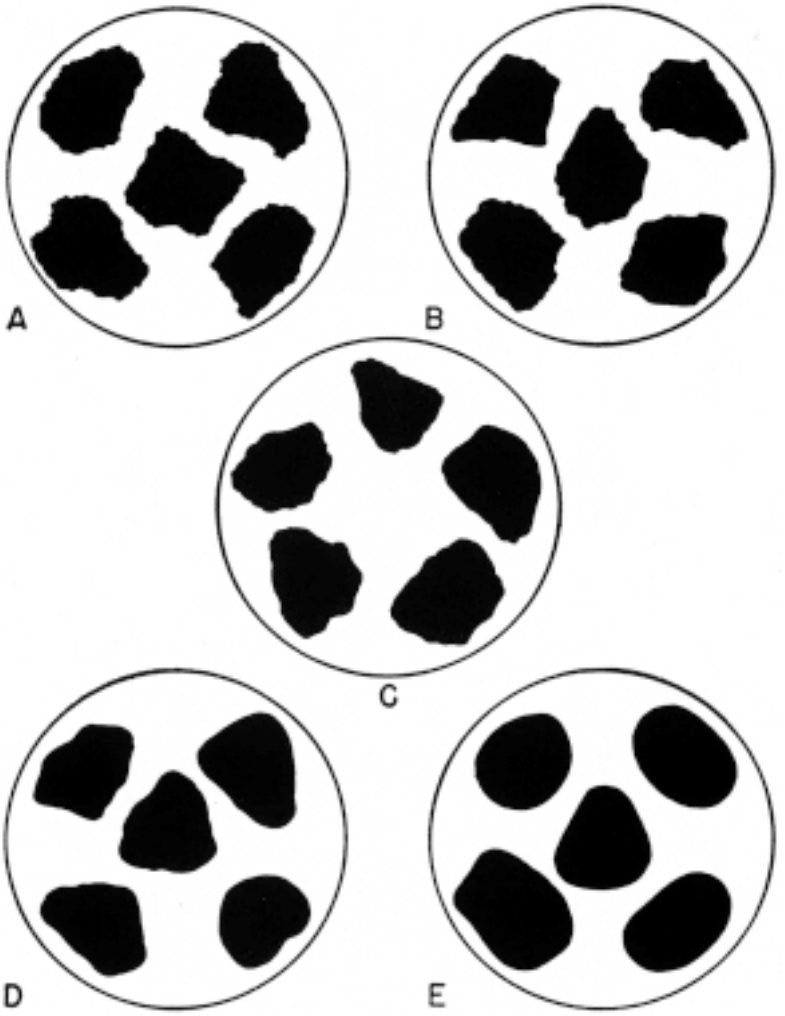

Figure 6-10. *Chart to show roundness classes. A) Angular, B) Subangular, C) Subrounded, D) Rounded, E) Well rounded /3/.*

6.2.4 Accuracy

A very important question is how effectively one should disperce soil material for proper grain size and shape determination. Wet samples normally need rather moderate treatment while dry ones must be crushed and disintegrated by intense agitation. Especially in the latter case the treatment may break down primary particles, like stacks of smectite or kaolinite flakes, while the physical behaviour of the soil may in fact be controlled by aggregates of such particles. Different preparation methods may therefore be required depending on what the purpose of the investigation is. Applied sedimentology offers several alternatives.

6.2.5 Specific surface area

Determination of the specific surface area is of considerable help in the identification of expandable minerals and in estimation of the degree of cementation of expandable clays. The determination of the specific area is made by determining the *external* and *internal* surface areas. The former is determined by measuring the adsorption of non-polar gases like nitrogen, which cannot enter the interlamellar space. The internal surface can be determined by measuring the total surface area using water and subtracting from it the separately determined external surface area. The procedure recommended here stems from Madsen and Kahr /8/.

External surface area – BET technique

In 1938 Brunauer, Emmet and Teller introduced a multilayer-adsorption theory that can be used for determining the external surface area of fine-grained soils /7/. One finds that the following equation of the BET isotherm applies:

$$\frac{P}{V\left(P_o - P\right)} = \frac{1}{CV_m} + \frac{C-1}{CV_m} \cdot \frac{P}{P_o} \qquad (6\text{-}5)$$

where

P = vapor pressure
P_o = vapor pressure at saturation
V_s = volume of minerals
V_m = volume of monolayer
C = constant

Plotting of $P/ V_m(P_o–P)$ yields a straight line $y = a+bx$ with the intercept $a = 1/C\ V_m$ and the inclination $B = (C–1)/CV_m$.

The external surface area A_e can be calculated as the ratio of the area of a layer of gas molecules (A_g) divided by the total mineral mass (m_s), which yields:

$$A_e = \frac{V_m/\rho_g}{V_s/\rho_s} \qquad (6\text{-}6)$$

where

ρ_g = density of the gas
ρ_s = density of the minerals

Internal surface area

Performing the experiment with water vapor after saturating the clay with calcium, which gives a well defined interlamellar water/ion constitution, one gets the following form of Equation (6-5):

$$\frac{P}{W\left(P_o - P\right)} = \frac{1}{CW_m} + \frac{C-1}{CW_m} \cdot \frac{P}{P_o} \tag{6-7}$$

where

P = water vapor pressure
P_o = water vapor pressure at saturation
W = mass of adsorbed water
W_m = mass of monomolecular water layer
C = constant

putting $a = 1/CW_m$ and $b = (C–1)/CW_m$ one gets:

$$b / a = \frac{(C-1)CW_m}{CW_m} = C - 1 \tag{6-8}$$

or $C = \frac{b}{a} + 1$

Now, since $W_m = 1/aC$ one has:

$$W_m = 1/(a+b) \tag{6-9}$$

Since 1 g of water represents a monolayer for a total surface of 3500 m^2, we get the total specific surface area A_{tot} as:

$$A_{tot} = \frac{3500}{a+b} m^2/g \tag{6-10}$$

From this we get the internal surface area A_i from Equation (6-11):

$$A_i = A_{tot} - A_e \tag{6-11}$$

Comments

Typical values of the external and internal surface areas are given in Table 6-4, from which one finds that these areas serve as diagnostic parameter values for different clay minerals. Furthermore, if the tests turn out to give only a small difference between the external and internal areas, and X-ray diffraction analysis (XRD) on well dispersed material has shown that smectite is the dominant clay mineral, it can be concluded that cementation agents hold the stacks of flakes together sufficiently firmly to prevent interlamellar hydration.

Table 6-4. Typical specific surface area data of clay minerals.

Mineral	Specific surface area, m^2/g	
	External	Internal
Kaolinite	10–15	10–15
Illite	100–150	100–150
Smectites	100–150	800–1000

6.3 Clay microstructure

6.3.1 Structure-forming factors and processes

Natural soils

Using modern terminology the term clay microstructure refers to two fundamental properties of sediments: the fabric and the physico/chemistry /9/. Clay fabric is defined as the orientation and arrangement or spatial distribution of the solid particles and the particle-to-particle coupling. The physico/chemistry relates to the interparticle forces in the sediment which result from both the physical interactions arising from gravitational forces and the electrical nature of the particles and the surrounding fluid. The interaction of fine particles that are forced together under overburden pressure leads to mineral/mineral contacts and to gel formation with water separating colloidal particles. Organic material has a significant influence on the strength of interparticle bonds in clay sediments /10/.

The evolution and character of the microfabric in development of sedimentary deposits was explored by Terzaghi and Casagrande who proposed primitive microstructural models to help explain the bonding and mechanical sensitivity of cohesive sediments. When electron microscopy was introduced in the midst of the 20th century more advanced models were proposed that could explain the mechanisms involved in consolidation and shearing /13,14,15/. Early models of microfabric were developed on the basis of simplified assumptions of the physical chemistry of the fine-grained minerals (single platelets) but the presence of multiplate particles (domains) as the predominant fundamental particle type has been accepted in the last 10–20 years (Figure 6-11). A domain is defined as a multiplate particle composed of parallel or nearly parallel plates that may be stacked either as sheets in a book or with an offset or stair-step arrangement. In illitic clays they are known to be formed by shearing and by compression and operate as unstable "slip" units (Figure 6-11), which tend to repel each others and transform to yield gel structure of the "edge-to-edge" or "edge-to-force" types (Figure 6-12). It is considered to have significant structural integrity and to behave in a functional sense as a unit particle for a finite period of time under an applied stress regime /15/. Thus, it is important to note that "a particle" can be defined in terms of size and morphology as well as of function.

The sources of energy associated with the processes and mechanisms are the determinants of clay and shale microfabric signatures. The major fundamental processes active in the continuum include (1) physico/chemical, (2) bioorganic, and (3) burial diagenesis /16/.

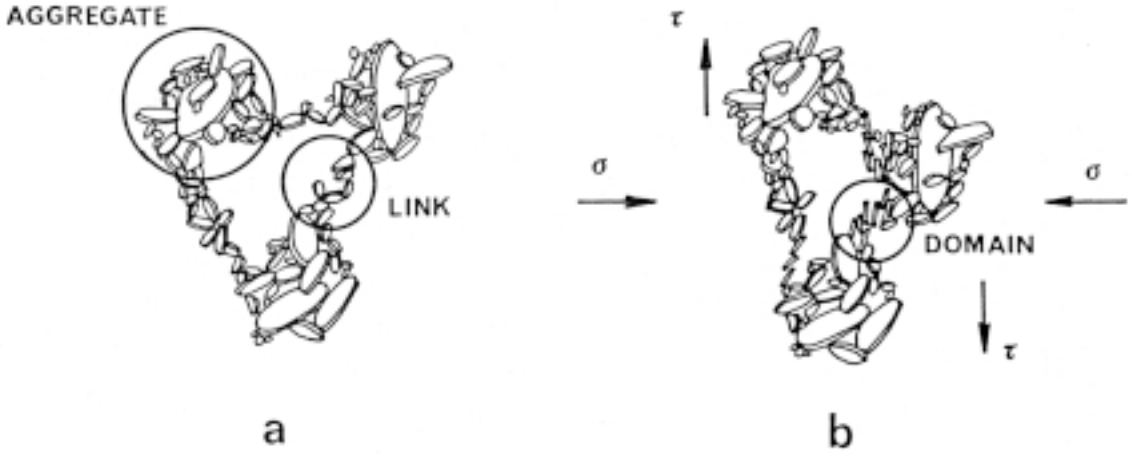

Figure 6-11. *Schematic picture of failure process. a) Natural microstructural pattern. b) Breakdown of particle links resulting in domain formation (σ represents consolidation pressure and τ shear stress) /14/.*

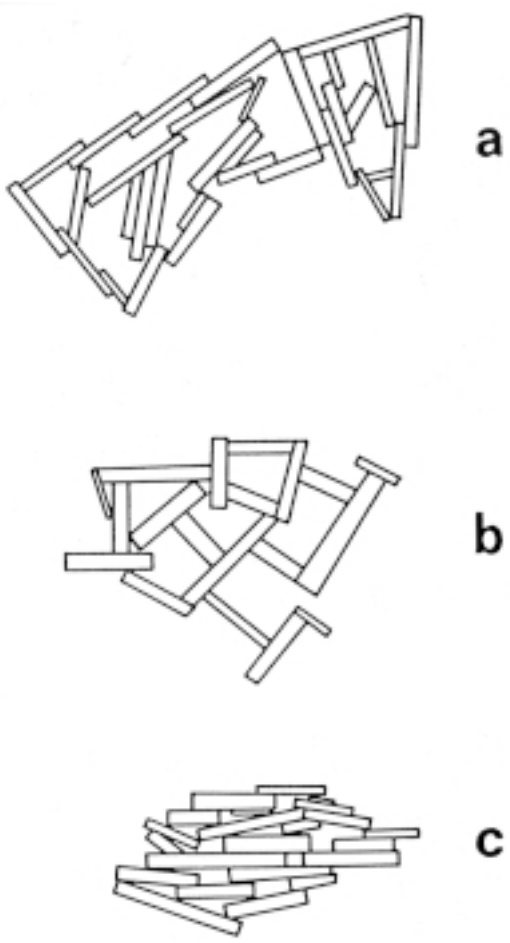

Figure 6-12. *Particle arrangement as a function of water salinity. a) Salt-flocculated. b) Non-salt flocculated. c) Dispersed (after Lambe).*

Clay gels

The same electrochemical forces that are responsible for the chemical bonding that holds particles together internally also bind particles to one another. At a point of contact between two particles of the same material, the bonding is similar to and possibly even indistinguishable from that within the bulk material, i.e., covalent and ionic bonds, hydrogen bonds, London-van der Waal's attraction /14,15/.

For particles in near contact the electrochemical forces of greatest importance are electrostatic interactions ("dipole"-type) and van der Waal's attraction, the latter existing between all sorts of particles. The force between two particles increases as the particles are moved closer together and as their area of overlap increases. Electrostatic interactions exist between electrically charged particles; particles of opposite charge attract each other and those of the same charge repel. The magnitude and even the sign of the electrical charge on a particle in water may be quite sensitive to the pH of the system and on the types and concentrations of dissolved salts. This sensitivity to the composition of the surrounding aqueous medium results from the sorption of ions from water onto the particle surface and the release of ions from the particle to water as indicated in Chapter 5 on porewater chemistry. Thus, the surface charge of the particles is balanced by the net charge of the mobile ions surrounding it in the aqueous medium yielding electrical double-layers with a net surplus of ions with charge opposite to the particle charge and of total charge equal to the particle charge. As two clay particles in a water suspension approach one another, the repulsive interaction between the two clouds of positive charges tends to prevent the particles from approaching one another sufficiently closely for shorter range van der Waal's attraction to pull them together, but pressure – grain pressure or "effective" pressure – can force them together sufficiently close to make such attraction effective (Figure 6-13).

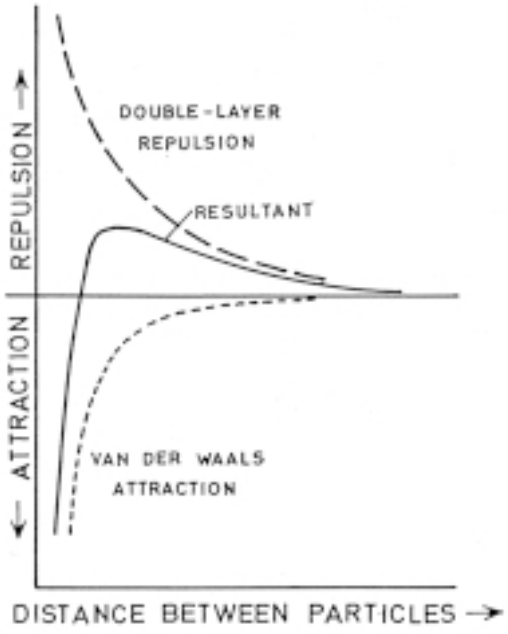

Figure 6-13. *Forces between basal surfaces (001) of parallel clay minerals as a function of interparticle distance, according to double-layer theories.*

In smectites, the individual lamellae are held together by cations and, when these consist of Li or Na, by interlamellar water lattices according to various investigators /16,17/. The "stacks" consisting of lamellae, usually 3–5 in Na smectite and on the order of 10 in Ca smectite, behave as coherent bodies in contrast to the apparently similar "domains" in sheared clay. The term "stack" is reserved for stable units of parallel flakes in any clay material.

When clay particles are free to form a microstructural pattern without any geometrical restraint and with no external forces altering their virgin arrangement, like in the formation of shallow sediments, the charge distribution and magnitude determine the nature of this pattern. Thus, as the salt content of the water increases, the distance of separation of the positive charges from the particle surfaces decreases and the particles have a greater probability of approaching sufficiently close to permit aggregation. In principle, therefore, there is a fundamental difference between clay microstructure formed in electrolyte-poor and in salt water, respectively. The former is characterized by a more homogeneous pattern with small, closely located particle aggregates, while a marine clay sediment typically consists of large aggregates separated by larger voids (Figure 6-14).

This causes a significant difference in hydraulic and gas conductivities as we will see in Chapter 9. The detailed arrangement of primary particles (including smectite stacks) varies due to the influence of the water chemistry and to the distribution and magnitude of the particle charge, as well as to the space offered for formation of clay gel fillings in voids between dense aggregates. In nature the rate of settlement played a major role. Figure 6-15 shows a number of possible structural arrangements /8,16/.

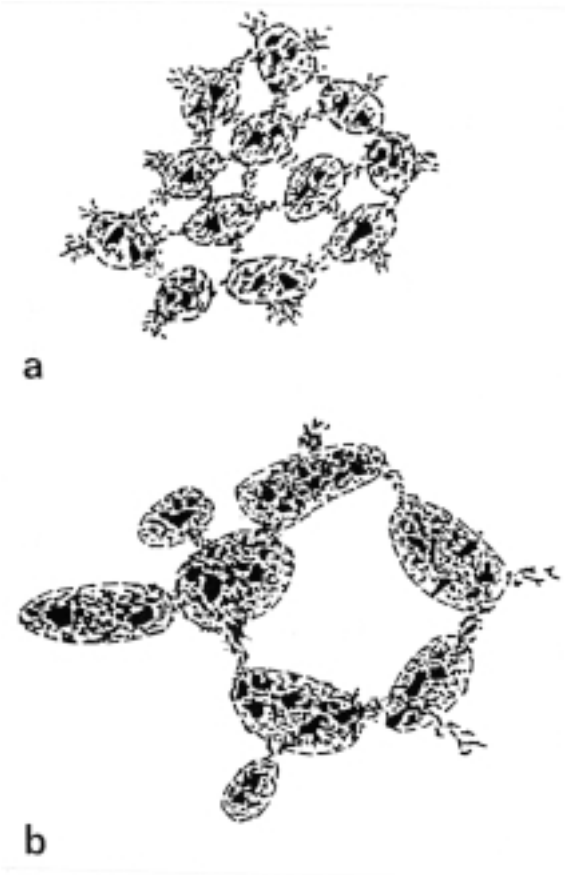

Figure 6-14. *Schematic clay particle arrangement. a) Clay deposited in fresh water having relatively porous aggregates and small voids. b) Marine clay with large, dense aggregates separated by large voids /14/.*

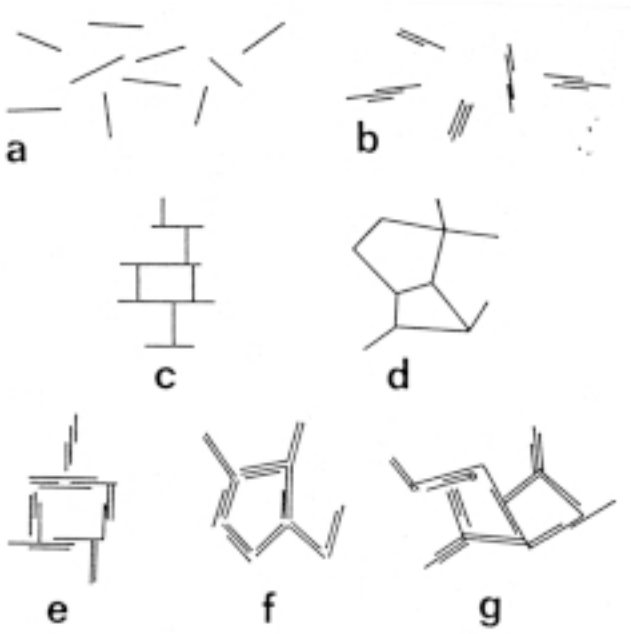

Figure 6-15. *Various modes of particle association in clay gels /8/.*

Artificially prepared buffers and backfills

Consolidation and shearing induce microstructural changes as indicated in Figure 6-11, and so does compaction of clayey material that is not water saturated, i.e. the smectitic soils from which buffers and backfills are commonly prepared.

Blocks of buffer material, like those intended for embedding canisters in various concepts, and for plugging purposes, are prepared by compressing granulated commercial bentonite powder. Such grains can have different size distributions and organisations depending on the required density and degree of water saturation of the compacted blocks (Figure 6-16).

When compacting such bentonite powder under pressures of 50–150 MPa, the granules deform and establish firm contacts but voids exist and their size varies over a large range. When the blocks are exposed to water, the system of interconnected air-filled voids is first filled with water, which secondarily is absorbed by the very hydrophilic granules. Their internal structure is characterized by a rather high degree of particle orientation if they originate from strongly preconsolidated natural bentonite beds (Figure 6-17) but since the granules are oriented at random when filled in compaction cells like oedometers, the degree of particle orientation in the blocks is largely at random. However, in uniaxially compacted clay prepared from bentonite granules air pockets may remain that have the character of very fine fisssures oriented normally to the compression direction.

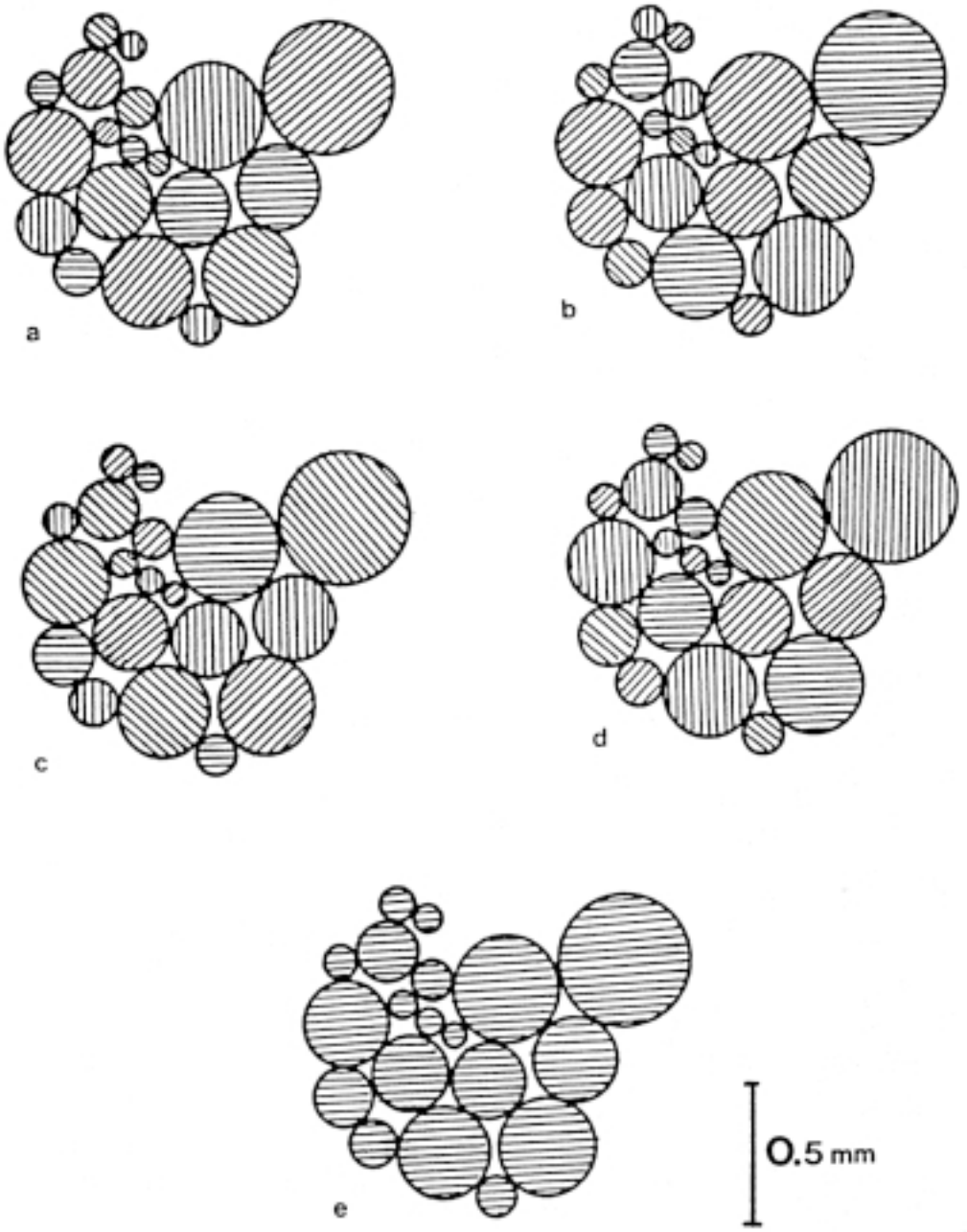

Figure 6-16. *Assumed variation in orientation of MX-80 grains in compacted bentonite powder. a), b), c) and d) are plausible, while e) is not /17/.*

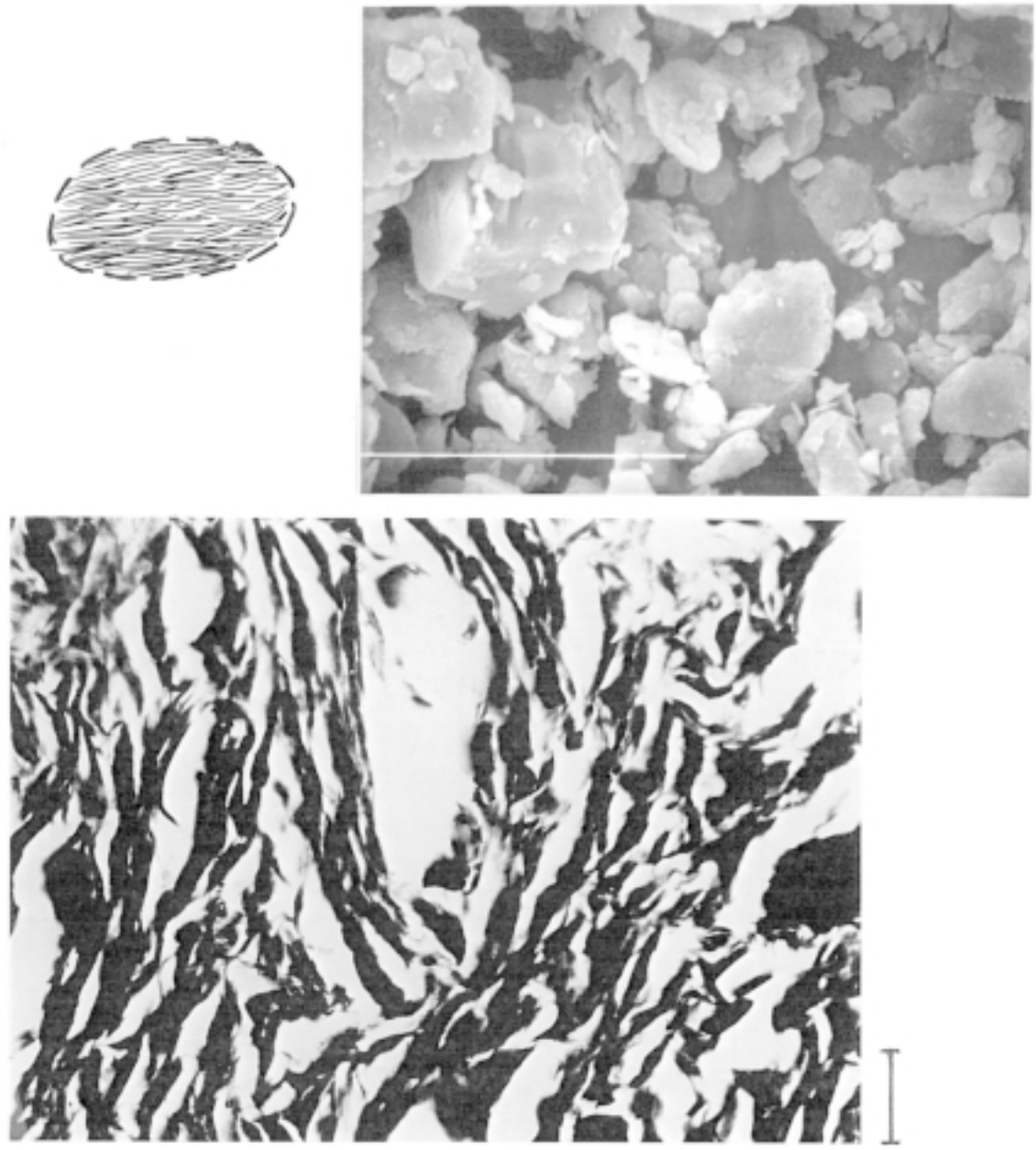

Figure 6-17. *Dense smectite clay. Upper left: Schematic build-up of smectite stacks in bentonite granule. Upper right: SEM picture of bentonite granules (length of white bar is 1 mm). Lower: TEM picture of smectitic Tertiary London clay (length of bar is 1 μm).*

The maturation process, which is primarily characterized by expansion of the granules, also comprises exfoliation of stacks from the surface of the granules. The released stacks are free to be rearranged and they are known to create clay gels in the voids between the granules as indicated in Figure 6-18.

Preparation and compaction of mixtures of smectite-poor bentonites involve intense mechanical agitation of two basically different soil types: the smectitic component, usually bentonite, and the ballast component, which consists of rock-forming minerals, primarily quartz and feldspars. This main structure-forming mechanism is the same as when clayey moraines were formed in nature, i.e. shearing and kneading under high normal stresses, which is known to produce the characteristic microstructural pattern shown in Figures 6-19 and 6-20. The first picture shows a dense arrangement of clay-poor moraine with a bulk density of 2200 kg/m^3, while the second one shows an equally dense moraine clay with up to 20% clay content of which about half is made up of smectites. In this latter clay the soft clay particles are seen to be squeezed between the hard coarser grains, yielding a relatively homogeneous matrix with voids up to about 1 µm in the matrix. The pressure has been about 2 MPa, exerted by the glaciers in the latest ice age.

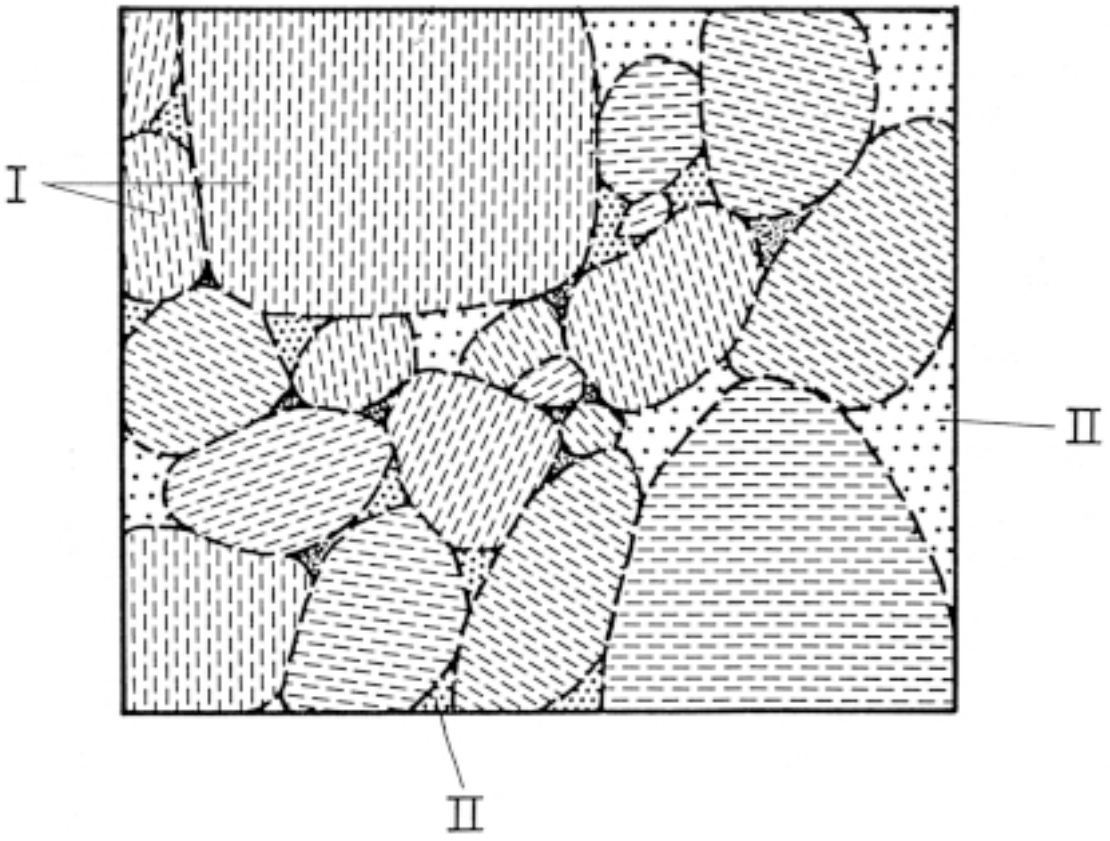

Figure 6-18. *Generalized microstructural pattern of Na montmorillonite clay formed from powder grains. I is expanded grain (1–3 interlamellar hydrates), II external pores with gels of different densities. The edge length of the picture is in the range of 0.1–2 mm /17/.*

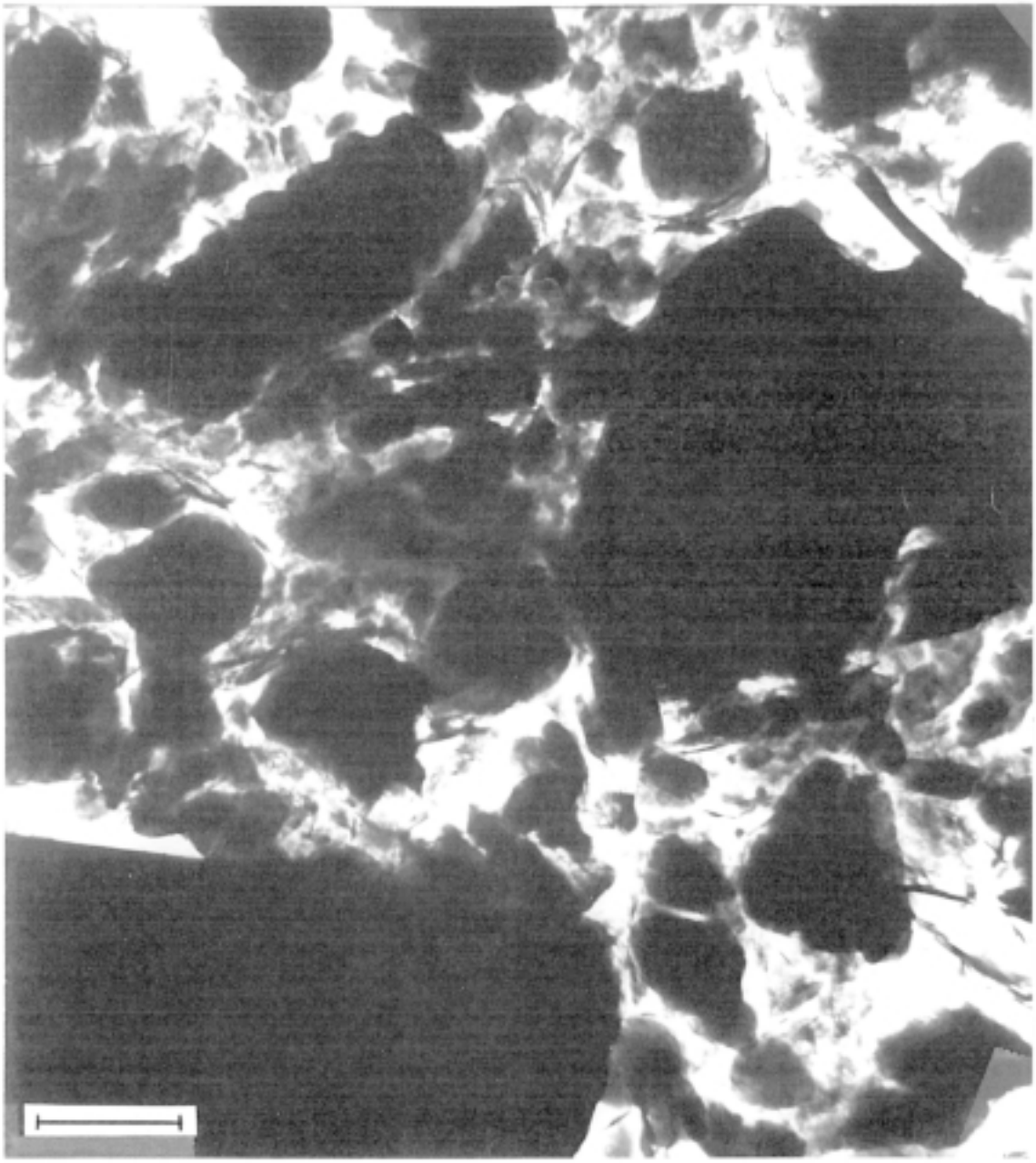

Figure 6-19. *TEM picture of moraine clay. The length of the bar is 1 μm.*

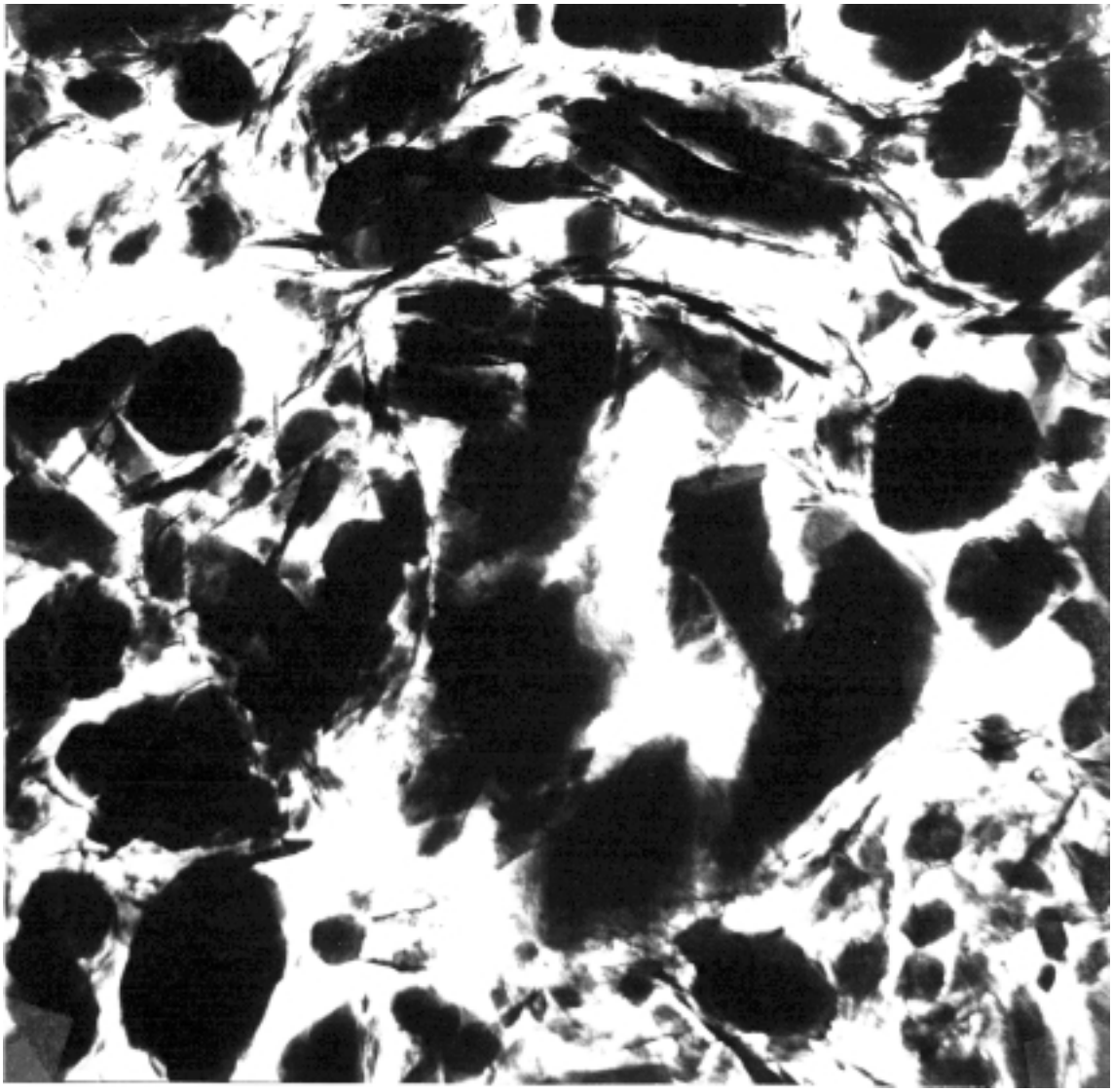

Figure 6-20. *TEM picture of moraine clay with 20% clay content, half of which is smectite. The horizontal edge of the micrograph is 5 μm.*

Such effective homogenization cannot be produced by field compaction of bentonite/ ballast mixtures if ordinary vibratory rollers or pneumatic compaction tools are used but the difference may not be very significant if densities (saturated conditions) of about 2200 kg/m^3 can be reached. The matter is further discussed in Part 2 where techniques for preparation, application and compaction of backfills will be described. Microstructural modeling is treated in Part 3.

6.4 Experimental

6.4.1 Scope and comprehension

In this section a number of methods for laboratory determination of the size and shape of particles and of their arrangement in undisturbed soil are described. The various techniques are selected according to the principle that they must be simple and give reasonably accurate, reproducible results, and to be applicable also in field laboratories.

6.4.2 Granulometry

General

It can be debated whether one should try to obtain maximum disintegration of the soil sample to be investigated. For certain purposes it is certainly recommended that different dispersion methods are applied, but in order to make the results of grain size determinations comparable both when samples are tested by one and the same laboratory and by different laboratories, a standard procedure must be defined. Two such preparation methods are recommended for investigation of common, natural soils, one proposed by the Laboratory Committee of the Swedish Geotechnical Society /18/, and the other by Müller-Vonmoos /19/.

Preparation

The most effective disintegration technique is described below. Humus, precipitated salt, cementing carbonate- and ion-compounds are removed by using hydrogen peroxide, acid ammonium oxalate and hydrogen chloride solution.

The soil material is dispersed in a solution of sodium hexametaphosphate $(NaPO_3)_6$ that is prepared by dissolving 13.3 g of this substance in 1000 ml of distilled water. Alternatively, sodium pyrophosphate ($Na_4P_2O_7$) is used for preparing the solution. 1/10 of any of the prepared solutions is added to the air-dry soil, which should represent 25–50 g (< 2 μm) and the suspension is then agitated for 3 minutes by a propeller mixer like British Standard 1377:1967 or ASTM:D422-63. The suspension is left to rest during the night and is then used for the sedimentation analysis after repeated agitation for some minutes.

Equipment

- Sieves (0.063 mm, 2 mm and 20 mm mesh)
- Oven for drying at 105°C
- Centrifuge, 2000–3500 rpm
- Glass vessels, 500 ml
- Mortar with rubber pestle
- Dispersing solutions
- Bowls and dishes, 200–500 ml

Performance

If the soil sample contains solid aggregates it is first treated with ammonium solution (1 part concentrated commercial ammonium solution and 10 parts of distilled water). The suspension is transferred to the 0.063 mm sieve and stirred under flowing water. Material passing through the sieve is collected and put in a bowl for drying in the air. The soil remaining on the sieve is also collected for separate analysis.

Humus is removed by adding 10% hydrogen peroxide solution to the air-dry soil in the bowl to form a slurry, which is heated by putting the bowl in a water-bath. The mixture is evaporated to almost dry conditions and the procedure is then repeated until no more foam is formed. After this, the soil is stirred up in distilled water and centrifuged twice until the fluid is free from suspended particles.

Iron compounds are dissolved and removed by putting humus-free soil in a glass vessel and adding a solution prepared by mixing 12.5 g $H_2C_2O_4$, 25 g $(NH_4)_2C_2O_4$ and 1000 ml distilled water to yield a slurry. Continuous stirring for one day is made, whereafter the solution is removed by a pipette and the soil stirred up in distilled water and centrifuged twice until the fluid is free from suspended particles.

Carbonate serving as cement is removed by treating the sample with a solution of 0.05-n hydrogen chloride solution. The air-dry soil is mixed with this fluid to form a slurry which is stirred continuously for a few hours, after which washing with distilled water is made by centrifugation as in the humus- and iron treatment.

Commercial bentonites or other smectite-rich soils do not require pretreatment except if the carbonate content is significant. The preparation for sedimentary analyses involves air-drying of the samples at room temperature and crushing in the mortar to yield pieces smaller than 2 mm /19/. 5 g of the material is put in 0.01% sodium hexametaphosphate and agitated by ultrasonic treatment for 6 minutes (20 kHz, amplitude 9–34 μm, 700–800 W). Saturation with sodium can be made by use of Dowex ion exchange /19/, but repeated washing with the dispersion fluid using centrifugation is commonly sufficient. The washed clay is freeze-dried and 1 g is then dispersed in 50 cm^3 salt-free, distilled water by ultrasonic treatment (28 μm amplitude). Water is added to a total suspension volume of 100 ml to which 67 ml acetone is added stepwise. 10 ml samples are used for the sedimentation analysis, which is performed in a centrifuge using a special procedure that we will not go into here.

Determination of the grain size distribution

For natural soils one commonly needs to perform both sieving and sedimentary analysis. For *sieving* the following applies.

Equipment

- Complete series of sieves, assembled and attached to a vibrator
- Balance with 1 g accuracy and 5 kg capacity
- Oven
- Bowls

Performance

A suitable amount of soil (100 g for fine sand, 200 g for coarse sand and 500–2000 g for very coarse sand and gravel) dried at air temperature after preceding treatment procedures is poured on the upper, coarsest sieve. The sieving time should be 5–15 min. The individual sieves are weighed and the mass of soil left on them is calculated.

Evaluation

The mass of soil on each sieve is determined by weighing and its fraction of the total mass is plotted in the grain size diagram (Figure 6-3).

For *sedimentation analysis* the soil material finer than a certain size, usually 0.063 or 0.200 mm, i.e. all soil material that has passed these sieves, is investigated. The following applies.

Equipment

- Balance with 0.1 g accuracy for hydrometer analysis
- Oven for drying at 105°C
- Dispersion liquid. 13.3 g $Na_4P_2O_7$ or $(NaPO_3)_6$ is dissolved in distilled water
- Bowls
- 1000 ml glass vessels for sedimentation
- Hydrometer, density scale from –2 g/l to + 60 g/l calibrated for $\rho_s = 2650$ kg/m^3 and $\rho_w = 1001.33$ kg/m^3 at 20°C
- Chronometer
- Thermometer

Performance

The suspension is poured into a 1 liter vessel (Figure 6-6). The suspension is stirred and the hydrometer submerged for making the first reading. Readings are then made after 1, 2, 4, 10, 20, 50, 100, 200 and 400 minutes, and a final reading after 24 hours. After each measurement the hydrometer is removed and put in a 1000 ml vessel filled with distilled water. Since the viscosity of water is very sensitive to temperature, the laboratory must be kept at practically the same temperature throughout the testing (± 0.5°C).

Evaluation

According to the hydrometer method the hydrometer is submerged into the 1 liter vessel containing the suspension, which is thereby displaced so that the true falling height becomes:

$$h = h_R - \frac{V}{2A} \tag{6-11}$$

where:

h_R = distance between the surface of the suspension and the center of the hydrometer, cm
V = volume of the hydrometer, cm^3
A = cross section area of the vessel containing the suspension

Stoke's equation can be written as:

$$d = \sqrt{\frac{18\eta}{(\rho_s - \rho_w)g}} \cdot \sqrt{\frac{h}{t}} \tag{6-12}$$

Combining Equations (6-11) and (6-12) one gets:

$$d = \sqrt{\frac{18\eta}{(\rho_s - \rho_w)g}} \cdot \sqrt{\frac{h_R - \frac{V}{2A}}{t}} \tag{6-13}$$

Equation (6-13) can be taken as a basis for deriving a nomogram for easy evaluation of the grain size for each hydrometer reading and time of sedimentation (Figure 6-21, upper diagram).

The hydrometer readings give the concentration of particles of different size in the suspensions. Evaluation is made by use of the following expression:

$$P = \frac{W}{W_{tot}} \cdot 100\% \tag{6-14}$$

where:

P = content of particles with a size smaller than the size d evaluated from the nomogram, expressed in weight percent of the total mineral mass
W = hydrometer reading (g per liter suspension)
W_{tot} = total mineral mass in the suspension (g per liter suspension)

P is then adjusted to be related to the *total* mineral mass, which is the same figure as W_{tot} if the mineral mass in the suspension represents the entire sample. If only a fraction of the sample is represented, e.g. the material passing the sieve used for the separation of material used for the sedimentation analysis, P is corrected to represent the actual fraction of the total mineral mass. This gives the continuous grain size curve in Figure 6-21 (lower diagram).

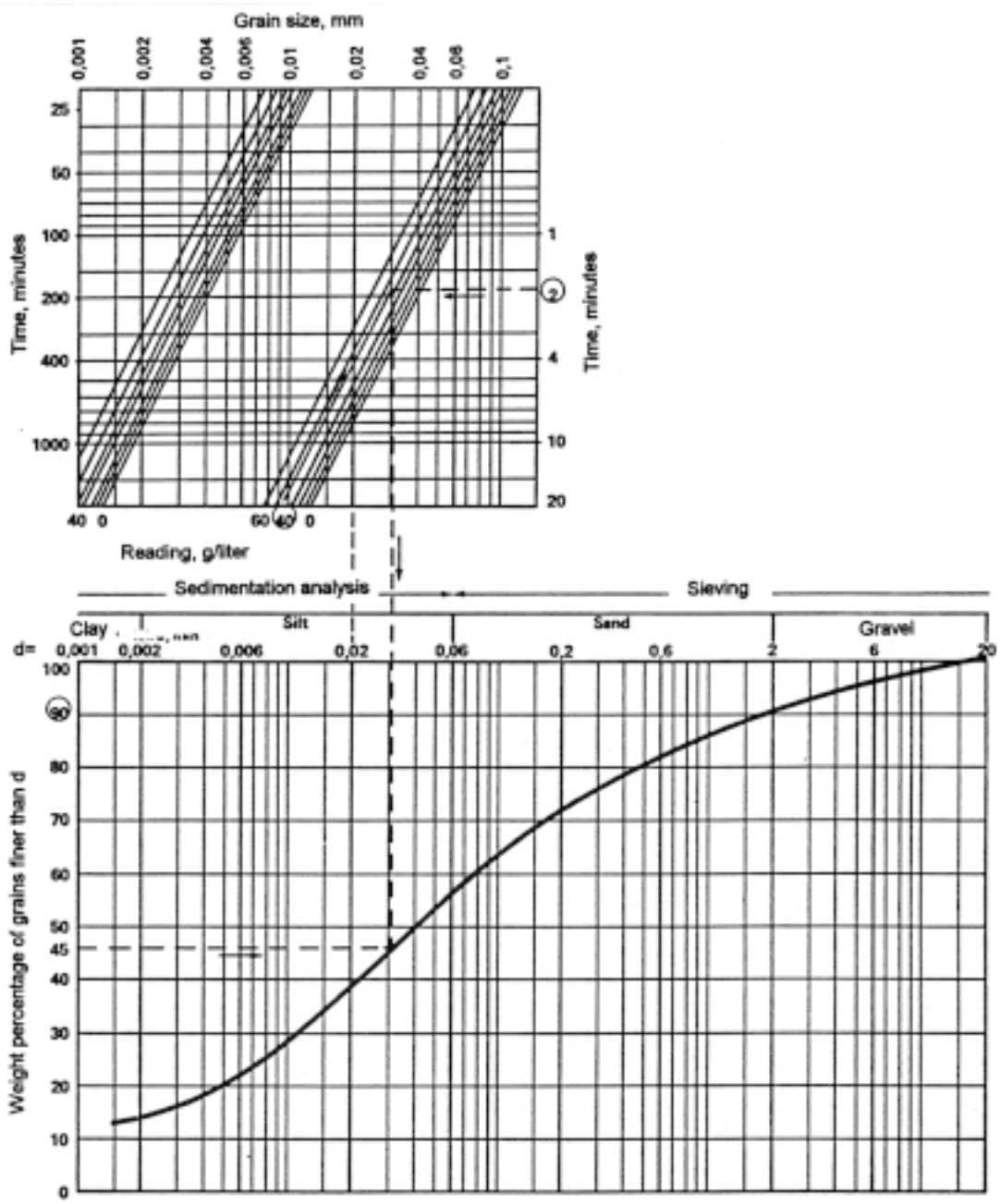

Figure 6-21. *Plotting of grain size. Upper: Nomogram for evaluation of the maximum grain size d that is in the suspension after different periods of time. Lower: Size distribution curve resulting from sieve and sedimentation analyses.*

6.4.3 Microstructure

Great help in identification of clay minerals and characterization of the arrangement of mineral particles is offered by microstructural analyses. Both optical microscopy and electron microscopy can be applied, the main techniques being the ones described in Table 6-5. The microscopes, microtomes and other equipment required for microstructural anlayses belong to specially equipped laboratories (geological department of universities and special companies) with trained staffs and they are not further described here. However, the sample preparation techniques deserve a short presentation as general information.

Table 6-5. Microscopic techniques.

Radiation	Technique	Magnification, times	Resolution	Specimen thickness
Ordinary light	Dark-field	< 2 000	1 µm	30 µm
"Polarized" light	Transmission	< 1 000	2 µm	30 µm
Electron beam	Transmission (TEM)	< 100 000	5–10 Å	300–500 Å
Electron beam	Scanning (SEM)	< 100 000	50–100 Å	Surface

A special technique used in conjunction with transmission TEM and scanning electron microscopy SEM can be applied for quantitative determination of the relative amounts of a number of elements in small parts of a specimen image. The technique, termed EDX, can be used for analyzing parts of the surface as small as 70 Å x 70 Å and the results are given as in Figures 3-12 and 5-4 /20/.

Preparation

Preparation of specimens is most important since artifacts are easily introduced /21/. For SEM, freeze-drying is the best method but it must be realized that it causes collapse of expanded stacks of flakes and thereby some change in void size. However, the general structural features and characteristic particle morphology is preserved /22/. For both optical microscopy and TEM the soil is best prepared in the following fashion /21/.

1. A prismatic specimen with a base area of approximately 25–50 mm^2 and a length of approximately 10 mm is cut from a clay sample with a thin steel wire or, in the case of hard clay, with a sharp knife. The clay sample should be cut in such a way that the orientation of the individual clay layers in situ can be defined.

2. The sample is stored in 50% ethyl alcohol for 30 min and in 70% alcohol for 5 min and thereafter in 90% alcohol and finally in 99.5% alcohol for 5 min each.

3. The sample is stored in a monomer consisting of 85% butyl methacrylate and 15% methyl methacrylate for 45 min. This process is repeated once.

4. The sample is stored for 90 min in a solution consisting of 98% monomer and 2% 2.4-dichlorbenzoylperoxide (EWM) catalyst. Thereupon the sample is placed in a gelatin capsule, which is filled with monomer and catalyst.

5. After polymerization by storing the sample for 15 hours in an oven at 60°C the gelatin capsule is washed off with water. The sample can then be trimmed and cut. The trimming is done in such a way that the original orientation of the thin sections obtained in the microtome can be defined.

After trimming the acrylate-treated specimens, they are cut by using a precision microtome equipped with a diamond knife (Figure 6-22). The liquid in its collecting trough should be a 10% acetone solution. The sections are picked up and placed on carbon coated 150–400 mesh grids.

The majority of all sections cut from smectite-rich clay can be used by this procedure. However, when the diamond edge meets coarser particles, like in smectite-poor backfill material, they may be pushed up in front of the edge and cause a disturbance. The sections which appear to be intact can be selected by observing the cutting process in the eye-piece of the microtome.

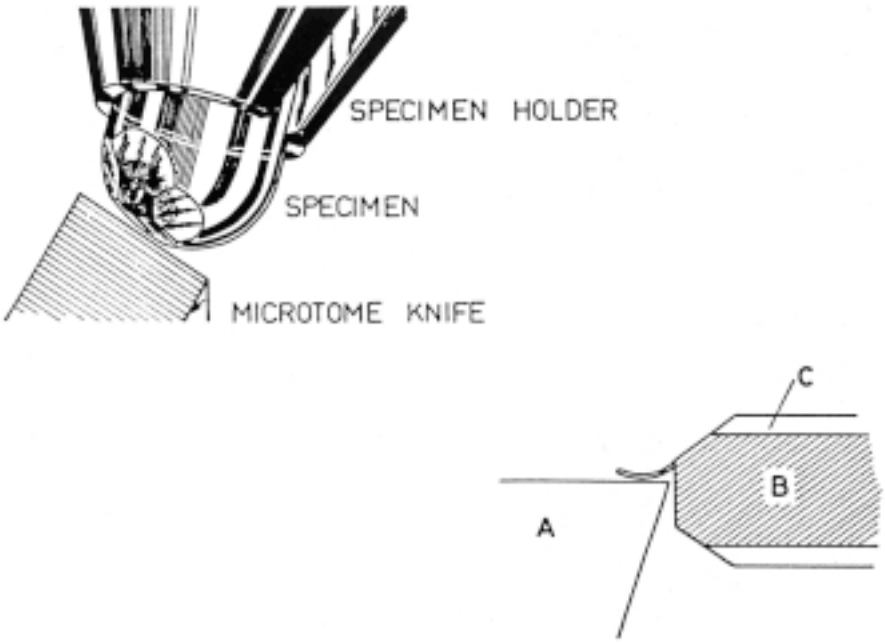

Figure 6-22. *Ultrathin sectioning. Upper: Embedded clay specimen trimmed for sectioning. Lower: Close-up view of knife and specimen. A is the knife, B the plastic-treated clay specimen and C external plastic.*

Comparison of micrographs of natural, wet illitic clays taken by use of high-voltage microscopy (HVM) and obtained by use of the described preparation method indicates that this method does not significantly alter their microstructure /21/. HVM is made with the samples being contained in closed cells or humid atmosphere in the TEM. Current investigation of smectite-rich clays indicates that they also have their major microstructural features preserved when the preparation method described is applied.

Evaluation

Micrographs can be used for the following purposes:

1. Characterization and determination of the size and shape of individual small grains.
2. Characterization and determination of microstructural constitution (contact between particles, orientation of particles, aggregation and void properties).
3. Quantification of permeable and non-permeable parts of cross sections.
4. Chemical analysis for identification of minerals and precipitations.

1) and 2) can be evaluated from all kinds of microscope techniques. Figure 6-23 gives examples of SEM micrographs that can be used for characterization of individual grains and mutual contact. 3) can be evaluated from microscopy of thin sections as will be described in Chapter 9 and in Part 3 of this Handbook. The evaluation is strongly dependent on the thickness of the specimens as illustrated by Figure 6-24. For adequate quantitative determination of permeable and non-permeable parts of sections of clay the specimens need to be very thin and practically representing 2-dimensional cross sections for TEM analysis. This requires use of ultramicrotomy since the specimen thickness must be less than 500 Å Examples of TEM micrographs for this purpose are shown in Figures 6-25 and 6-26. 4) can be made by use of SEM (cf Figure 5-5) and TEM.

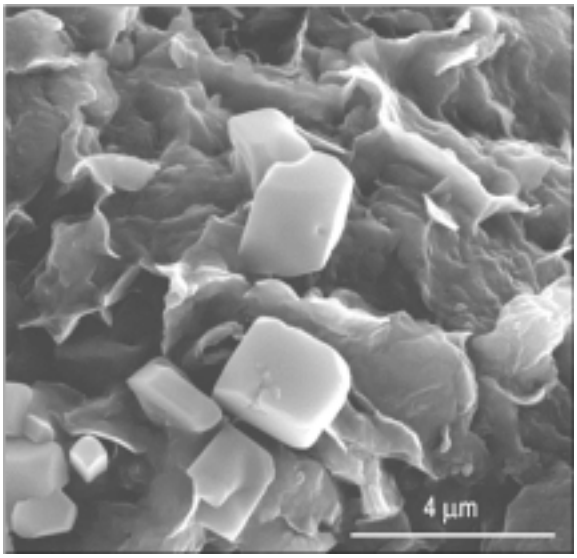

Figure 6-23. *Example of SEM micrograph from which grain characteristics can be derived. NaCl crystals are seen embedded in smectite matrix.*

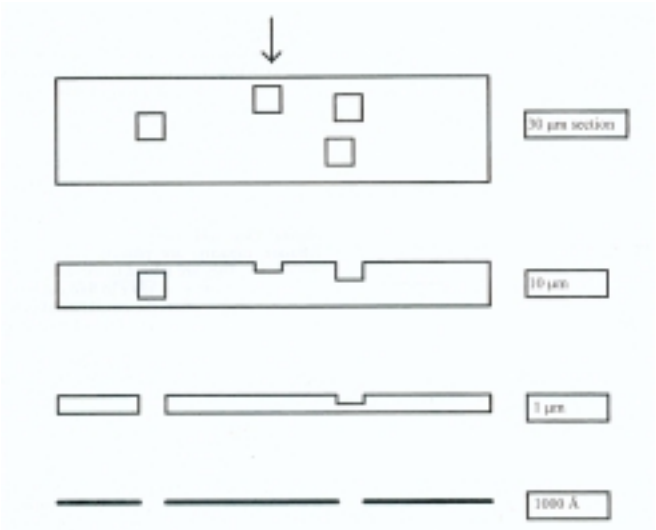

Figure 6-24. *Clay films with different thickness prepared from material with the same void population. Thicker films make identification of smaller voids less accurate /23/.*

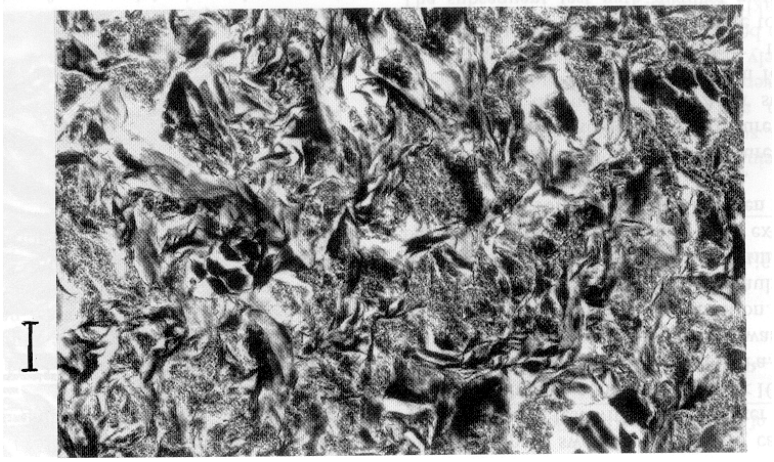

Figure 6-25. *Microstructural pattern of smectitic clay (Friedland Ton) as vizualised by 500 Å ultrathin section using TEM. Density 1900 kg/m³ at complete water saturation. The darkest parts are dense particles of rock-forming minerals, mainly chlorite, medium-gray parts are mainly mixed-layer and montmorillonite clay minerals, while white parts are open voids. The bar is 1 μm long. The permeable fraction of the cross section is represented by the white and light-greyish parts.*

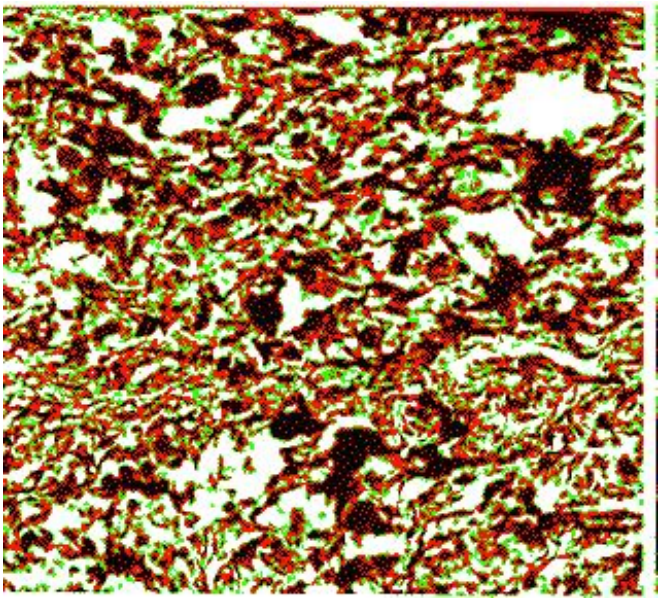

Figure 6-26. *Digitalized TEM micrograph (300 Å) of MX-80 clay with 1800 kg/m³ density. Black objects: rock-forming minerals, red: dense impermeable clay matrix, green: soft, permeable clay matrix, while white parts are open voids. Width of micrograph is 3 μm.*

6.5 References

/1/ **Pusch R, 1962.** Clay Particles. Nat. Swedish Build. Res. Council, Stockholm.

/2/ **Wadell H, 1932.** Volume, shape and roundness of rock particles. J. Geol., Vol. 40.

/3/ **Krumbein W C, 1941.** Measurement and geological significance of shape and roundness of sedimentary particles. J. Sedim. Petr., Vol. 2, No. 2.

/4/ **Andreasson L, 1973.** Kompressibilitet hos friktionsjord. D. Thesis Chalmers University of Technology, Gothenburg, Sweden.

/5/ **Russell R D, Taylor R E, 1937.** Roundness and shape of Mississippi River Sands. Journ. Geol., Vol. 45.

/6/ **Pettijohn F J, 1949.** Sedimentary Rocks. Harper & Brothers, New York.

/7/ **Brunauer S, Emmet P H, Teller E, 1938.** Adsorption of gases in multimolecular layers. J. Am. Chem. Soc., Vol. 60 (pp. 309–319).

/8/ **Madsen F T, Kahr G, 1992.** Wasserdampfadsorption und spezifische Oberfläche von Tonen. Deutsche Ton- und Tonmineralgruppe, Tagungsband zur DTTG-Tagung 1992 in Hannover.

/9/ **Bennett R H, Bryant W R, Hulbert M H, 1991.** (Eds). Microstructure of Fine-grained Sediments. Frontiers in Sedimentary Geology. Springer Verlag. (ISBN 0-387-97339-7 and 3-540-97339-7)

/10/ **Pusch R, 1973.** Influence of organic matter on the geotechnical properties of clays. Nat. Swed. Build. Res. Council, Document D11:1973.

/11/ **Terzaghi K, 1925.** Erdbaumechanik auf Bodenphysikalischer Grundlage. Franz Denticke, Leipzig und Wien.

/12/ **Casagrande A, 1932.** The structure of clay and its importance in foundation engineering. Journal of Soc. Civil Engrs., Vol. 15.

/13/ **Rosenqvist I Th, 1959.** Physico-chemical properties of soils: soil-water systems. J. Soil Mech. a. Found. Div., Proc. Am. Soc. Civ. Engrs., Vol. 85 (pp. 31–53).

/14/ **Pusch R, 1970.** Clay Microstructure. Document D8:1970. Nat. Soc. Swed. Build. Res. Council., Stockholm.

/15/ **Bennett R H, O'Brien N R, Hulbert M H, 1991.** Determinants of clay and shale microfabric signatures: Processes and Mechanisms. Ch. 2. Microstructure of Fine-grained Sediments. Frontiers in Sedimentary Geology. Springer Verlag. (ISBN 0-387-97339-7 and 3-540-97339-7)

/16/ **Van Olphen H, 1965.** An Introduction to Clay Colloid Chemistry. Interscience Publishers.

/17/ **Pusch R, Hökmark H, Börgesson L, 1987.** Outline of models and water gas flow through smectite clay buffers. SKB TR-87-10, Svensk Kärnbränslehantering AB.

/18/ **Stål T et al, 1972.** Kornfördelning. Nat. Swed. Building Res. Council, Rep. B2:1972, Stockholm.

/19/ **Müller-VonMoos M, 1971.** Zur Korngrössenfraktionierung tonreicher Sedimente. Beiträge zur Geologie der Schweiz, Nr. 54, Leeman AG, Zürich.

/20/ **Pusch R, Güven N, 1990.** Electron microscopic examination of hydrothermally treated bentonite clay. Engineering Geology, Vol. 28, 1990 (pp. 303–314).

/21/ **Pusch R, 1967.** A technique for investigation of clay microstructure. J. Microscopie, Vol. 6 (pp. 963–986).

/22/ **Tovey N K, Yan W K, 1973.** The preparation of soils and other geological materials for the SEM. Proc. Int. Symp. on Soil Structure, Gothenburg 1973 (Swedish Geol. Soc., Stockholm, 1973).

/23/ **Pusch R, 1999.** Experience from preparation and investigation of clay microstructure. Eng. Geol. Vol. 54 (pp. 187–194).

7 Density, water content and porosity

This chapter deals with the most important constitutional parameters of buffers and backfills, the density, water content and porosity. The various components have different densities, which are commonly expressed as averages. For explaining the influence of the microstructural features on the bulk physical properties of smectitic soils, the spacial distribution of clay density and porosity need to be quantified as discussed in Chapter 3.

7.1 Introduction

The density, water content and porosity are intimately related soil properties of fundamental importance for the behaviour of soils. They will be discussed in this chapter, and the laboratory procedures for determining the various parameters will be described.

7.2 Density

7.2.1 General

The five density concepts referred to in soil physics have been defined in Chapter 1 of this part of the Handbook and they are /1/:

- Bulk density
- Dry density
- Specific (grain) density
- Porewater density
- Gas density

The bulk density ρ of soil, which is commonly expressed in kg/m^3, is determined by a number of factors, primarily the amount of solid particles per volume unit and their density ρ_s, and the degree of water saturation S_r. The amount of solid particles per volume unit, which is most important, is a function of the mode of formation of the soil and of the grain size distribution as well as of the stress history both for natural deposits and artificially produced buffers and backfills. The amount of solid particles is also related to other common soil physical data like the dry density ρ_d, porosity n, void ratio e, water content w, and degree of water saturation as given by Equations (7-1) to (7-18).

Water saturated conditions are represented by the following expressions:

$$\rho = \rho_{sat} = \frac{V_p \rho_w + V_s \rho_s}{V_p + V_s} \tag{7-1}$$

or

$$\rho_{sat} = \frac{w + 1}{w / \rho_w + 1 / \rho_s} \tag{7-2}$$

and

$$w = \frac{\rho_w \cdot V_p}{\rho_s \cdot V_s} \tag{7-3}$$

which can be written as:

$$w = \frac{\rho_w (\rho_s - \rho_{sat})}{\rho_s (\rho_{sat} - \rho_w)} = \frac{\rho_w (\rho_s - \rho_{sat})}{\rho_s \cdot \rho'} \tag{7-4}$$

Submerged and fully water saturated conditions are represented by:

$$\rho' = \rho_{sat} - \rho_w \tag{7-5}$$

and

$$V_{\rho d} = V_{\rho_{sat}} - V_{p\rho w} \tag{7-6}$$

Unsaturated conditions are represented by:

$$V_{\rho d} = V_{\rho_{sat}} - V_{p\rho w} \tag{7-7}$$

$$V_p = \frac{m}{\rho} - \frac{m_s}{\rho_s} \approx \frac{m_w + m_s}{\rho} - \frac{m_s}{\rho_s} = \left(\frac{w+1}{\rho} - \frac{1}{\rho_s} \right) m_s \tag{7-8}$$

from Equations (7-7) and (7-8) the degree of water saturation $S_r = V_w / V_p$ is obtained:

$$S_r = \frac{w \rho \rho_s / \rho_w}{\rho_s (w+1) - \rho} \tag{7-9}$$

The relationship between the water content w and the bulk density at different degrees of water saturation S_r is illustrated by Figure 7-1 for ρ_s = 2700 kg/m^3, which is typical of smectite minerals.

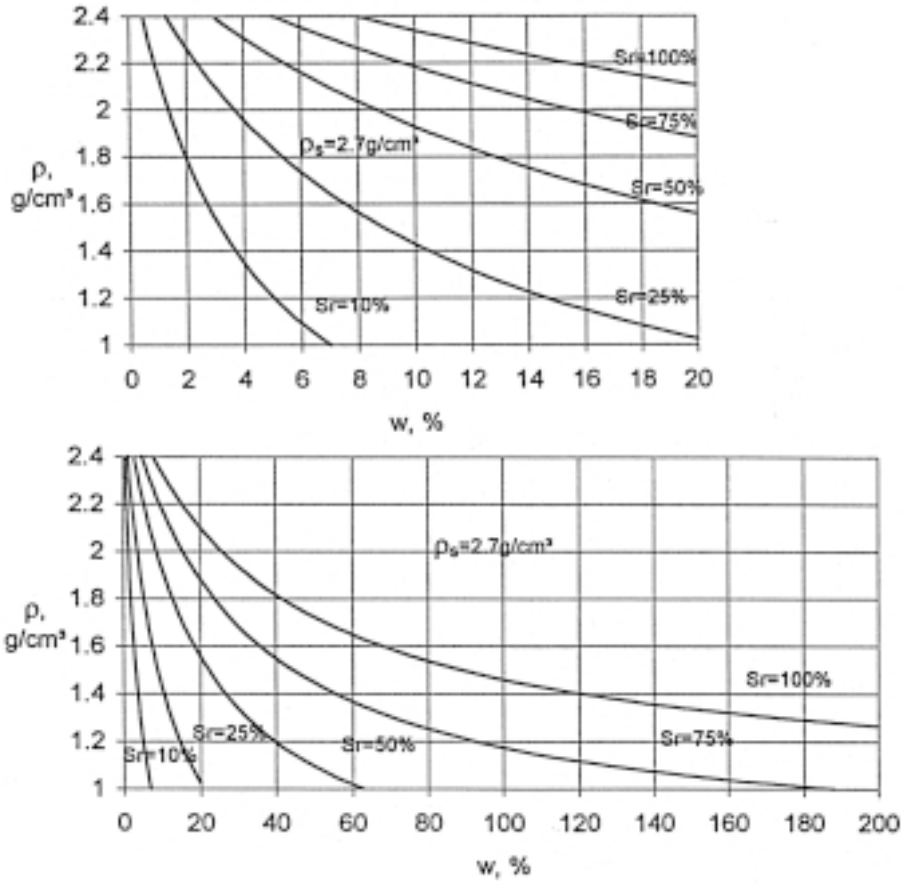

Figure 7-1. *Bulk density as a function of the water content at different degrees of water saturation for ρ_s = 2700 kg/m^3.*

The expression for the void ratio $\left(e = \frac{V_p}{V_s}\right)$ is:

$$\rho_s V_s + \rho_w V_w + \rho_g V_g = \rho\left(V_s + V_p\right) \tag{7-10}$$

yielding

$$1 + w + \frac{\rho_g V_g}{\rho_s V_s} = \frac{\rho}{\rho_s}\left(1 + e\right) \tag{7-11}$$

or

$$e = \frac{\rho_s\left(w+1\right)}{\rho} - 1 \tag{7-12}$$

The relationship between void ratio and bulk density at different degrees of water saturation is illustrated by Figure 7-2 for ρ_s = 2700 kg/m^3.

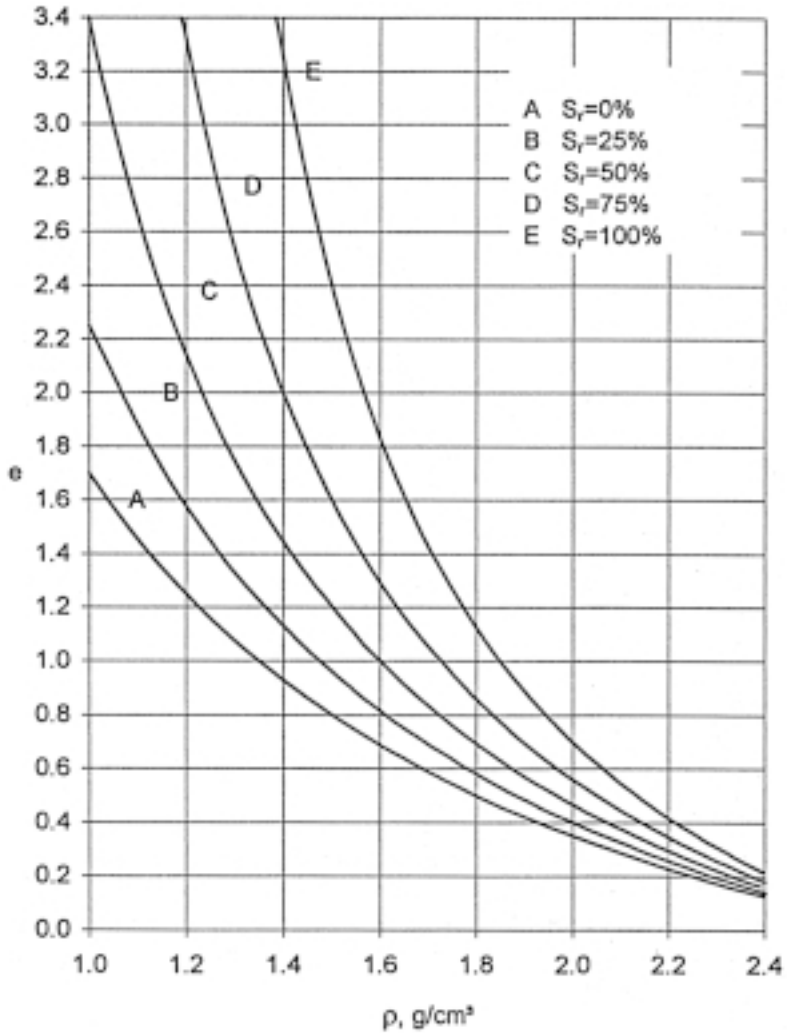

***Figure* 7-2.** *Bulk density as a function of the void ratio at different degrees of water saturation for ρ_s = 2700 kg/m³.*

Completely water saturated soil is represented by:

$$V_{\rho d} = V_{\rho_{sat}} - V_{p\rho w} \tag{7-13}$$

and

$$\rho_d = \frac{m_s}{V} = \frac{\rho_s V_s}{V_s + V_p} = \frac{\rho_s}{1+e} \tag{7-14}$$

from which the following relationship is obtained:

$$e = \frac{\rho_s}{\rho_d} - 1 \tag{7-15}$$

The void ratio is usually in the interval 0.7–3.0 for natural clay and silt soils. It controls the hydraulic conductivity as well as the strength and stability of the particle skeleton.

The porosity n, which is defined as $\frac{V_p}{V}$, is related to the void ratio as given by Equation (7-16):

$$e = \frac{n}{1-n} \tag{7-16}$$

which, with Equation (7-12), yields:

$$n = 1 - \frac{\rho}{\rho_s(w+1)} \tag{7-17}$$

Completely water saturated conditions are represented by:

$$n = \frac{\rho_s - \rho_{sat}}{\rho_s - \rho_w} = \frac{w}{w + \rho_w / \rho_s} \tag{7-18}$$

7.2.2 Bulk density

Influence of grain size distribution

The grain size distribution is very important for the bulk density as illustrated by the extreme cases of moraine (till) with a typical strong variation of the grain size, and sand which may have practically only one grain size (Figure 7-3). Combined compression and shearing causes the particles in the first type of soil to move into stable positions with minimum void space while the uniformly sized grains of the second type of material cannot be brought into denser arrangement than corresponding to a porosity of about 20% irrespective of the pressure and shear strain. Moraines hence have very small voids that form tortuous passages, which gives a low hydraulic conductivity, while sands have wider, interconnected voids, which give them a high conductivity. Applying this principle, artificial mixtures of low compressibility and low hydraulic conductivity should be prepared from mixtures of different size fractions.

Influence of organic content and gas content

The strong hydration potential of organic material leads to a very low bulk density of shallow sediments, which makes them highly compressible. Degradation of organic matter produces gas like methane and carbon dioxide (cf Chapter 4).

Influence of smectite content

Like organic constituents, smectite clay particles have a strong hydration potential and give the soil a low bulk density at low overburden pressure. Thus, while compression of a water saturated moraine-type soil under an effective pressure of 0.1 MPa yields a bulk density of about 1800 kg/m^3, a sample of Na bentonite with about 80% smectite clay

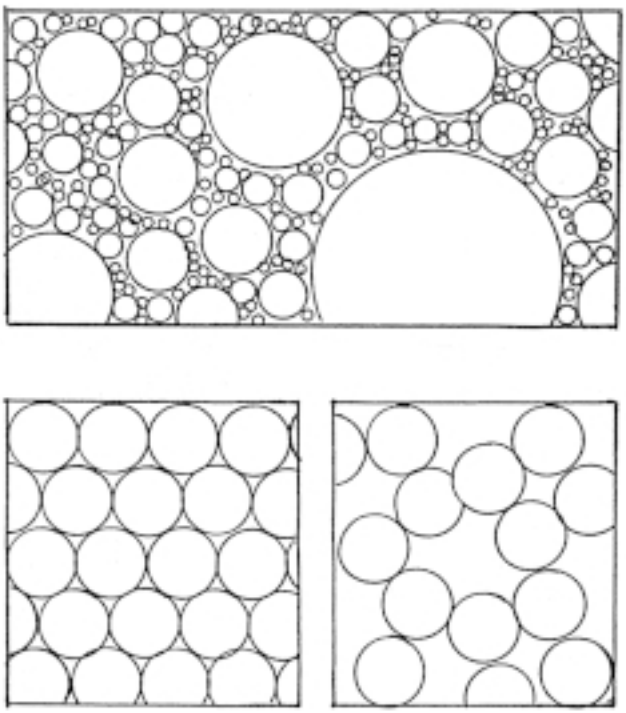

Figure 7-3. *Visualization of porosity n. Upper: Dense particle arrangements in moraine (n down to 15%). Lower: Sand with uniformly sized particles in dense, stable arrangement (n ≈ 25%) and in unstable form (n ≈ 40%).*

has a bulk density of only about 1500 kg/m^3 at saturation because this type of clay has a swelling pressure that balances the external pressure at this low bulk density.

Colloid-chemical factors determine the distance and arrangement of clay particles under different chemical porewater conditions and thereby the compressibility, strength and bulk density (cf Chapters 6, 9 and 11).

Influence of mineral composition

The bulk density is a function of the density ρ_s of the mineral constituents, which means that bulk density data of different soils are not directly comparable unless these constituents are the same (cf Chapter 3). A typical example is the case with pure bentonite (ρ_s=2700 kg/m^3) and bentonite mixed with graphite (ρ_s=2200 kg/m^3). It is therefore recommended to refer to the void ratio or the porosity rather than to the density when describing the physical state of a soil.

Influence of mode of formation

The grain size distribution, mineral composition and bulk density of sedimentary soils are determined by the mode of formation. Hence, a slow sedimentation rate of fine particles causes loose layering and a low bulk density, while quick deposition, i.a. in the form of slumping or slides, yields a low void ratio and high bulk density.

Deposition of clay, particularly smectite, in fresh water and salt water give quite different degrees of aggregation and thereby different void size distributions (cf Chapters 6 and 9). This has a considerable effect on the hydraulic conductivity.

Influence of stress history

The stress history after deposition of natural soils and of artificially prepared mixtures has a most important effect on the void ratio and bulk density. Thus, compression under the own weight of a soil mass produces a reduction in void size and an increase in bulk density that are directly related to the compressibility of the soil.

Loading and unloading of laboratory samples gives changes in density, water content and porosity that strongly affect the transport- and stress/strain properties that are used for characterizing the soil from a rheological point of view. The changes are related to altered particle arrangement and orientation as discussed in Chapters 9 and 11.

Influence of drying

Desiccation of fine-grained soils like in shallow natural clay or in hot parts of a buffer clay sets up capillary forces yielding a negative pore pressure and hence an increased effective stress, by which compression takes place. This leads to a high bulk density but it is not uniform since fissures and open fractures are also formed in the clay matrix unless an external pressure of sufficient magnitude is applied. Desiccation is associated with chemical effects, like precipitation of dissolved substances, which also raise the mechanical strength (cf Chapters 3 and 11).

Influence of freezing and thawing

Fine-grained soils can remain largely unfrozen at temperatures below 0°C since part of the porewater is associated with the mineral phase and the porewater electrolytes cause freezing-point depression. Smectites remain largely unfrozen even at low temperatures as illustrated by Table 7-1. The freezing process involves migration of unfrozen water to larger voids where it freezes and forms ice lenses that grow as long as water can move in from the surroundings. The soil particles accumulate in dense layers separated by parallel ice sheets that are oriented perpendicularly to the freezing direction. The soil layers become denser than in the unfrozen soil and freezing during winter can in fact be used for consolidating soft soil provided that a load is applied that causes expulsion of the water that is set free at thawing.

Where frost can reach down to a repository, only a very small fraction of the porewater of smectite-rich dense buffer will freeze while backfills with low clay contents may have their structure changed and ice lenses formed.

Table 7-1. Unfrozen water w_u in weight percent /2,3/. The dry density of the unfrozen water saturated soil ranged between 1700 kg/m^3 for the silt and gravel to 800 kg/m^3 for the illite and bentonite.

Soil	–1°C	–2°C	–5°C	–10°C	–20°C
Gravel	3	2	1	< 1	0
Silt	5	4	3	2	0
Kaolinite	28	22	10	6	–
Illitic clay	20–60	15–30	10–18	8–17	–
Wyoming bentonite	90	45	40	36	> 30

Influence of compaction of soil material

Compaction of soil brings the particles together to reach stable positions with a void ratio and bulk density that is determined by the energy input and the mobility of water and soil particles. Thus, compaction on the "wet" side of optimum (9–11% for the morainic soil in Figure 7-4) produces porewater overpressure, which prevents the particles from moving into a denser arrangement, while compaction on the "dry side" of optimum prevents dense layering by generating strong capillary forces. Compaction at a very low water content can yield a density that is on the same order of magnitude as at the optimum water content (Figure 7-4). The fact that compaction is usually made at a water content that is lower than at full saturation, makes it suitable to refer to the dry density or to the void ratio for characterizing the physical state of the soil.

7.2.3 Dry density

General

The dry density is related to the bulk density according to Equation (7-19):

$$\rho_d = \frac{\rho}{1+w} \tag{7-19}$$

At complete water saturation and ρ_s = 2670 kg/m^3, the dry density can be expressed by Equation (7-20):

$$\rho_d = \frac{\rho_{sat} - 1}{0.63} \tag{7-20}$$

This measure of density is widely used in road and dam construction and in foundation engineering, and it is commonly used for characterization of the degree of compaction by comparing it with the density obtained at standard laboratory compaction tests. The density that can be obtained for smectitic fills is exemplified by the preparation of the bottom bed of the big silo for intermediate waste in the SFR repository at Forsmark /5/.

Influence of grain size distribution, organic and gas contents, mineral content etc

The dry density is affected by the same factors as the bulk density, except that the water content and the degree of water saturation do not appear explicitely in the mathematical expressions of the dry density.

7.2.4 Specific (grain) density

The density of the solid constituents of a soil is defined as:

$$\rho_s = \frac{m_s}{V_s} \tag{7-21}$$

where:

m_s = solid mass
V_s = volume of mass

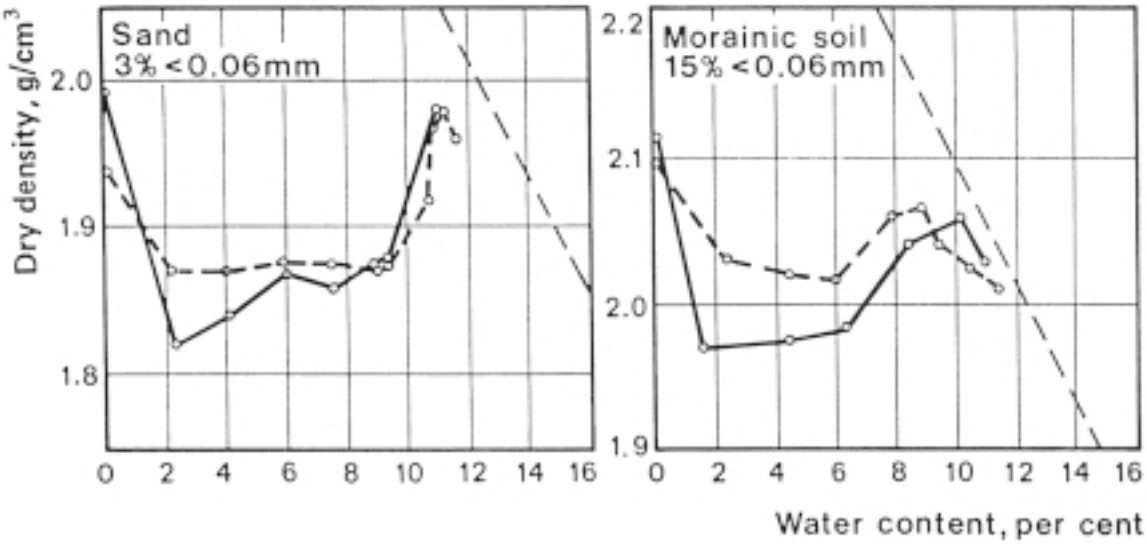

***Figure** 7-4. Dry density at compaction of two types of soil showing maximum density at almost zero water content and a second maximum at optimum water content. The steep broken curves represent 100% degree of water saturation /4/.*

The specific density depends on the type of minerals and organic substance in the soil. Separation of minerals with different densities can be made by use of liquids with different densities but for most practical purposes it is sufficient to get an average value of the density of the solid constituents including the fine voids and fissures that may exist in them.

7.3 Porewater density

The density of porewater (pore fluid) is defined as:

$$\rho_w = \frac{m_w}{V_w} \tag{7-22}$$

where:

m_w = mass of water
V_w = volume of water

The density of the porewater is commonly taken as 1000 kg/m^3 but in many contexts, as in the evaluation of piezometer measurements and the determination of the grain density, the density has to be known with greater accuracy. The factors that influence the density of the porewater is 1) temperature, 2) content of dissolved material ("salt"), and 3) content of colloids. As will be discussed in Section 7.5, different types of porewater in smectite clays turn out to have different densities, which may cause difficulties in evaluating the degree of water saturation.

The influence of temperature on the density of water is illustrated in Table 7-2 for distilled water.

Table 7-2. Density of distilled water as a function of temperature.

Temperature, °C	Density, kg/m³
15	999.1
20	998.2
25	997.1
30	995.7
35	994.1
40	992.2
50	988.0
60	983.2
70	977.7
80	971.2
90	965.3
95	961.9

The density of seawater at 10°C is known to be 1035 kg/m^3 with its usual chemical composition. For other compositions and concentrations, the true density is suitably determined by extracting porewater and measuring its density by use of an aerometer. The location of the meniscus on the scale gives the density with an accuracy of about 1 kg/m^3. The contribution to the bulk water density of dispersed organic and inorganic matter is normally much less important than that of dissolved substances.

7.4 Gas density

The density of any gas contained in soil samples is determined by its pressure and temperature. The amount of gas in a soil sample can be evaluated from the degree of water saturation but the gas pressure cannot be readily determined unless a syringe is inserted without causing leakage along it. For smectite-rich clay compacted in the laboratory and saturated with water by applying a high backpressure on the confining filters, the gas pressure at equilibrium is estimated to be equal to the porewater pressure.

7.5 Water content

The water content[3] gives the ratio of the mass of porewater and the mass of solid substances:

$$w = \frac{m_w}{m_s} \tag{7-23}$$

[3] Synonymous to the less commonly used “water ratio”

The water content is routinely determined in all sorts of soil physical and mechanical laboratory investigations. Natural soils are commonly completely water saturated at depth but samples extracted at large depths usually contain gas that is dissolved in the porewater, which means that it turns to gaseous form by the pressure release caused by bringing the samples up to the ground surface. Shallow soils often contain considerable amounts of gases; air, methane, and carbon dioxide, especially at and above the groundwater table. This means that the degree of water saturation S_r, defined by Equation (7-24), may be low:

$$S_r = \frac{V_w}{V_p} \tag{7-24}$$

where:

V_w = volume of water
V_p = pore volume

Water is in different physical form in different parts of soils, especially in smectite clays. Practically all soils have a monomolecular film of water attached to the grain surfaces (Figure 7-5) and this water has a different physical form than free water.

For a smectite sample, the wide distribution of void size means that the various porewater components play different roles. Determination of their relative amounts requires heating to different temperatures. The water in the large voids is lost at about 100°C, the water in fine capillaries at 105°C or slightly more, while the last hydrate of the interlamellar water is lost at temperatures appreciably higher than 105°C /6/. The best method to quantify the amounts of different water components is nuclear magnetic resonance a typical result of such an investigation being shown in Figure 7-6. This technique requires access to advanced equipment and highly specialized laboratory staff of physical departments of universities and research institutes.

This sort of investigation, NMR, gives measures of the proton mobility, which is different for free water, adsorbed water and water constituting the mineral lattices (hydroxyl groups), /7/. The basic idea is that movement of protons is equivalent to stress relaxation following basic concepts for visco-elastic bodies. The measurement is made by locating the sample in a constant oscillating radiofrequency magnetic field while varying a polarizing magnetic field through the resonance frequency. A voltage is thereby induced in a receiver coil and it is recorded as a modulated RF signal, which can have the form of a proton resonance wide line, the width of which gives the spin-spin coherence time T_2. This parameter represents the time required for the protons to come back to equilibrium after being reoriented, which naturally is much longer for non-associated free water (2.3 seconds) than for adsorbed water (micro- to milliseconds).

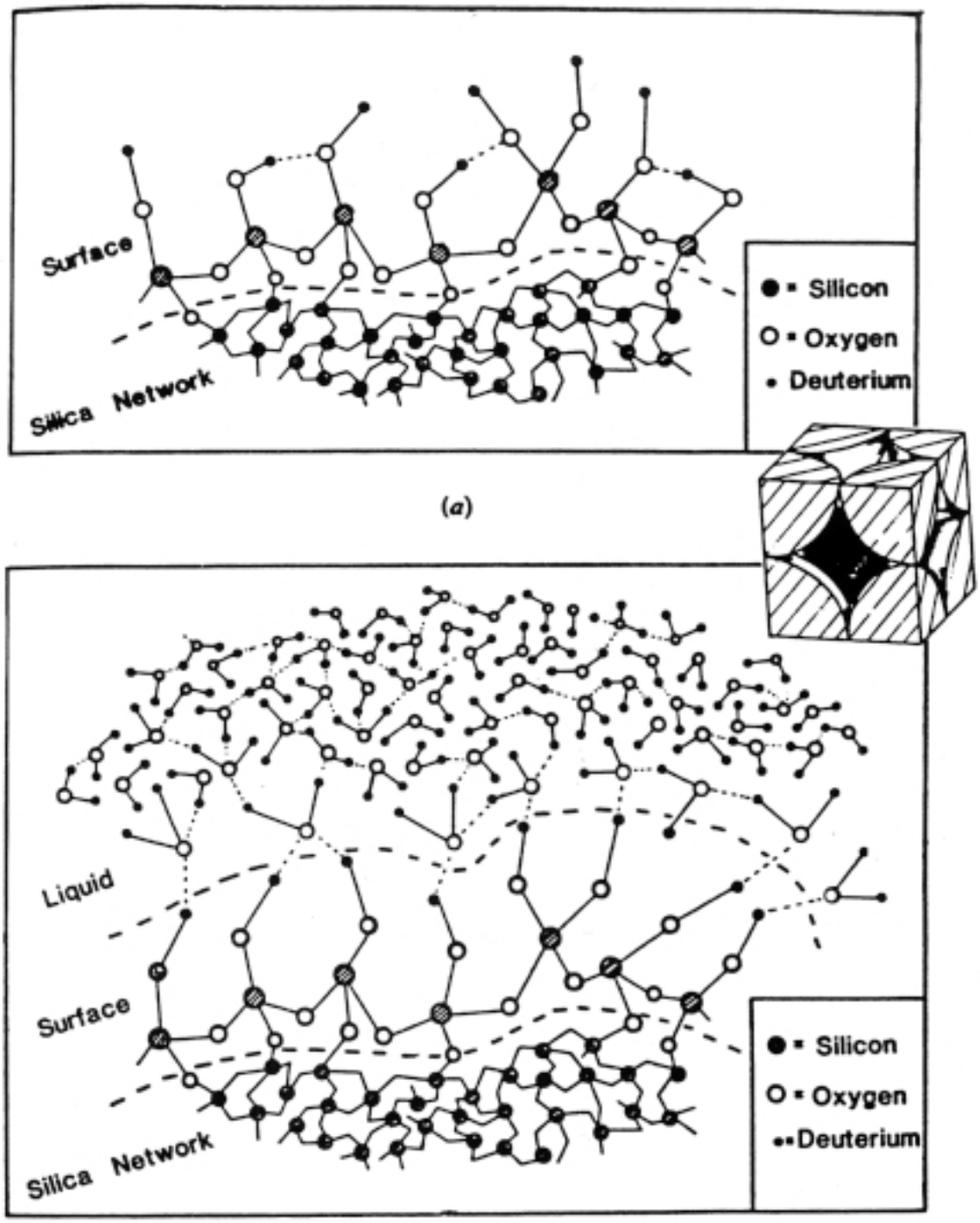

Figure 7-5. *Schematic diagram illustrating (a) the hydroxylated silica surface and (b) the structure at the water interface (after Steytler, Dore and Wright).*

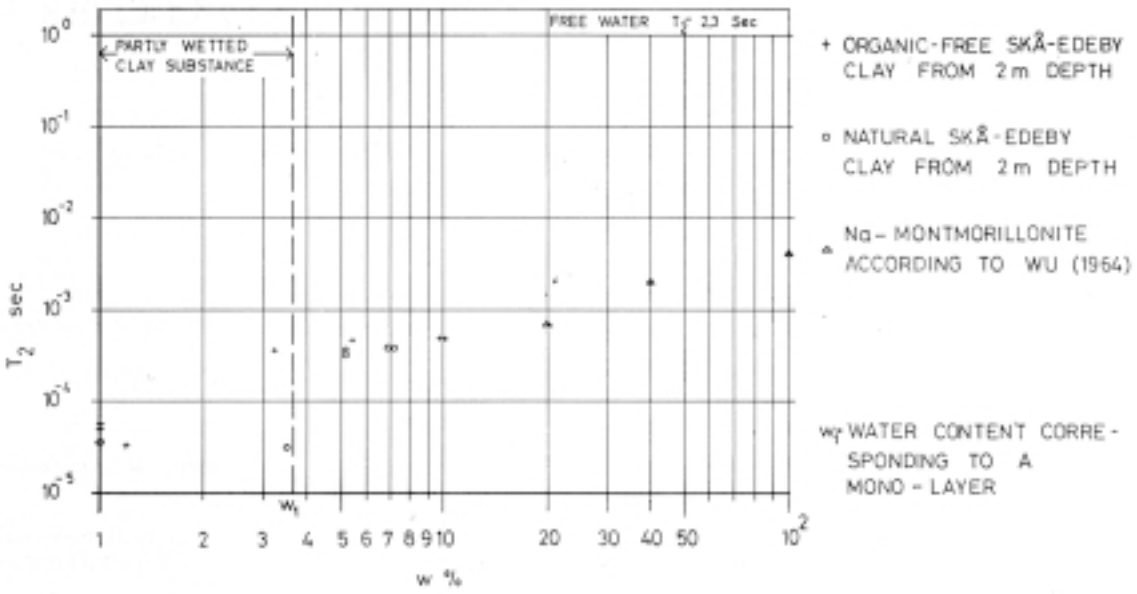

***Figure* 7-6.** *Example of relation between the spin-spin coherence time T_2 and the water content of illitic clay with and without organic material (Skå-Edeby) and of Na montmorillonite /8/. The spin-spin coherence time is very low even at a bulk water content of 100%, which indicates that a considerable fraction of the porewater of the soft illitic clay has a higher viscosity than free water. For both the illite and the smectite with 20% water content practically all the porewater is immobile.*

Figure 7-7 gives a graphical illustration of the different types of water in smectitic clays, the two major components being the "external" water contained in voids between stacks of lamellae, and the interlamellar, or "internal", water held between the lamellae in the smectite stacks. The latter type of water is sometimes termed pseudo-crystalline. The ratio between the "internal" and "external" water of smectite clays is illustrated for montmorillonite by the diagram in Table 7-3 (cf Part 2 of this Handbook).

The one-molecular water layer on the surfaces of practically all mineral grains is maintained even at heating to about 100°C. They hydrate quickly when exposed to ordinary laboratory atomsphere after drying, which means that very small mineral particles become associated with a water hull that is large compared to their size. Heating to 100–150°C gives a fairly well defined mass value, representing a dehydration state with only a small amount of "internal" water in smectite clay. By increasing the temperature under conditions that allow for desiccation, interlamellar water and intra-crystalline hydroxyls are released from clay minerals at diagnostic temperatures as indicated by Figure 7-8.

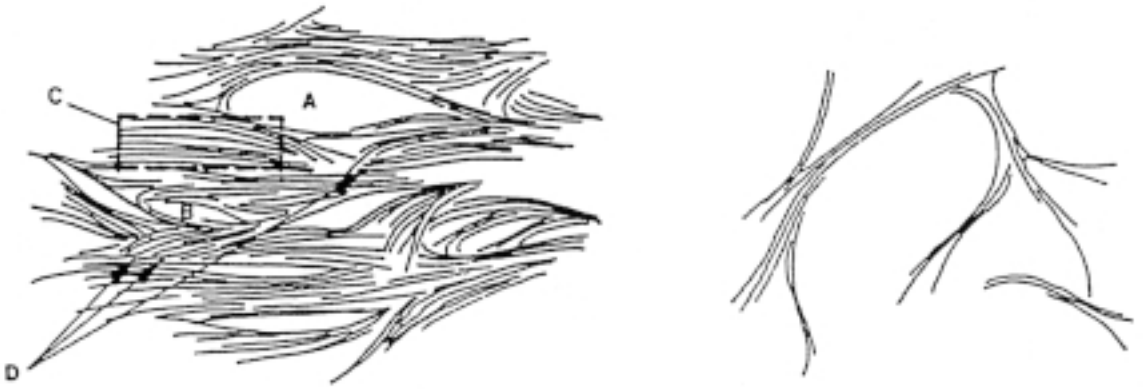

***Figure** 7-7. Microstructural features of smectite clays (1). Left: Dense clay with A) large and B) small void with "external water", C) stack of flakes, D) Interface between stacks. Right: Expanded Na smectite clay gel with practically only external water /5/.*

Table 7-3. Volume fraction of interlamellar water in smectite clay in percent of total water content.

Smectite (100%)	Density at water saturation, kg/m³					
	1200	1440	1600	1800	2000	2200
Na montmorillonite	12	26	55	83	93	96
Ca montmorillonite	8	17	29	50	87	96

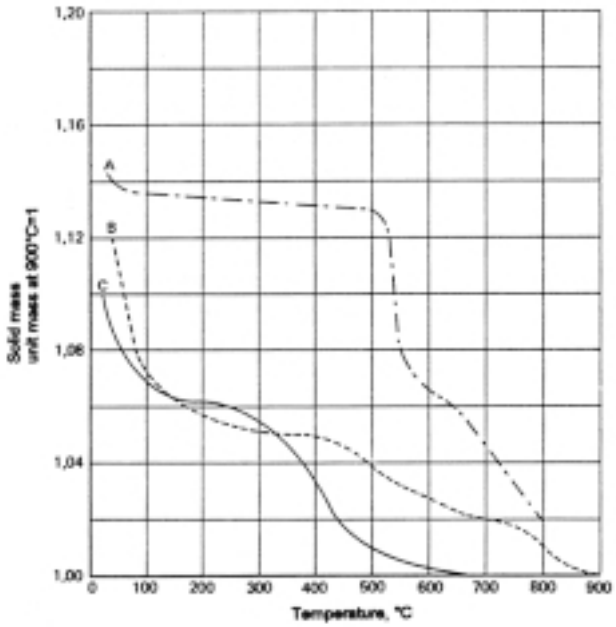

***Figure** 7-8. Loss in mass by dehydration of chlorite (A), expanding clay minerals (B), and illite (C), /9/. The variable on the vertical axis m/m_{ref} is the ratio between the mass at the respective mass and the reference mass at 900°C.*

7.6 Experimental

7.6.1 Bulk density and dry density

Determination of the bulk density is a routine procedure for undisturbed clayey samples extracted by use of standardized piston samplers. For clay-free materials one can use piston samplers with back-valves but for shallow sampling, as for determining the density in the course of a backfilling campaign including application and compaction of artificially prepared soil mixtures, one uses "balloon" techniques, which make it possible to excavate a well defined volume of soil and measure the mass /4/.

In this chapter procedures will be described for determination of the bulk and dry densities of undisturbed samples confined in sampling tubes, and ways of determining the density of samples with an irregular shape. Field measurements are described in Part 2 of this Handbook.

Equipment

- Balance with 1 g accuracy and 2 kg capacity for ordinary tube samplers. For small irregularly shaped samplers an electronic precision balance with 0.01 g accuracy and a hook for hanging samples below the balance is used.
- Sliding caliper.
- Ruler with millimetre scale.
- Extruder.
- Cutting tool with metal string.
- Sample holder of wire net for hanging samples. The net is equipped with a loop by which it can be hung in the balance.
- Glass beaker containing napthalene or other oil insoluble in water.
- Tap grease.

Performance

- Remove rubber lids from the sampling tube; if the sample does not fill the tube extrude the sample so that a plane surface can be cut.
- Measure the length and diameter of the sample.
- Weigh the tube with soil using an empty tube as tare.

Evaluation (tube samples)

The volume V of the sample is calculated and its mass m read on the scale of the balance:

The bulk density is $\rho = \frac{m}{V}$ (7-25)

For determining the dry density the water content w must be determined as described later in this chapter. This yields:

$$\rho_d = \frac{m_s}{V} = \frac{m_w / w}{V} \qquad (7\text{-}26)$$

Performance (irregular samples)

Evaluation of the volume of an irregularly shaped soil sample is best made by determining its weight in air and in a liquid of known density. The liquid must not penetrate into the sample and it should evaporate after removing the sample from it. Napthalene is suitable for the purpose /1/.

- Determine the density ρ_2 of the napthalene by use of an aerometer. It is approximately 760 kg/m^3.
- Hang the sample holder in the balance and weigh the holder, first in air (m_1) and then in paraffine oil (m_2).
- Place the soil sample and weigh sample + holder, first in air (m_3) and then in naphtalene (m_4), (Figure 7-9).

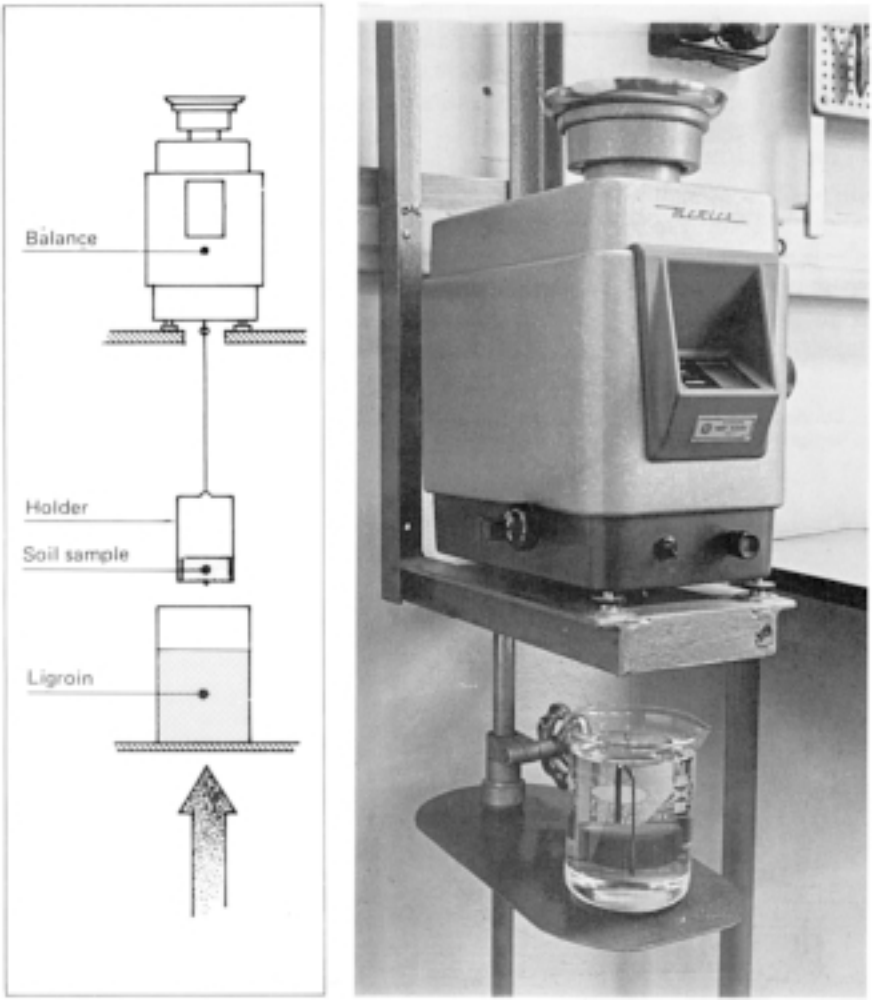

Figure 7-9. *Determination of the volume of the sample by weighing.*

Evaluation (irregular samples)

The volume of the sample holder is $(m_1–m_2)/\rho_2$ and that of the sample $(m_3–m_4)/\rho_2$. The bulk density $\rho = m/V$ is obtained by use of Equation (7-27):

$$\rho = \frac{m_3 - m_1}{m_3 - m_4 - m_1 + m_2} \cdot \rho_2 \qquad (7\text{-}27)$$

As for tube samples we get, for a known value of the water content, the expression in Equation (7-26) for the dry density.

7.6.2 Grain density

The grain or specific density should be determined by use of pycnometer technique. Using water, some penetration will take place into voids and fissures that are exposed at the grain surfaces through which the evaluated density will be intermediate to the true density of the crystal lattices and the density of the grains including all voids. Using high-viscous liquids like certain types of silicon oil, the problem with penetration into the fissures is avoided /1/.

Equipment

- Pycnometer 25–250 cm^3 (Figure 7-10)
- Distilled water
- Heat source (gas heater or electric cooker)
- Electronic balance with 0.01 g accuracy
- Oven for drying at 105°C
- Thermometer with 1°C reading accuracy
- Vacuum pump
- Exsiccator with silica gel
- Mortar with pestle
- Spatula
- Water bath

Performance

- Samples are taken with due respect to observable structural heterogeneities like lamination with different grain size. Two samples are extracted for each determination.
- Weigh the pycnometer (m_1).
- Fill the pycnometer with distilled water, read the thermometer and weigh the filled pycnometer.
- Evaluate the density of the water by use of Table 7-1.

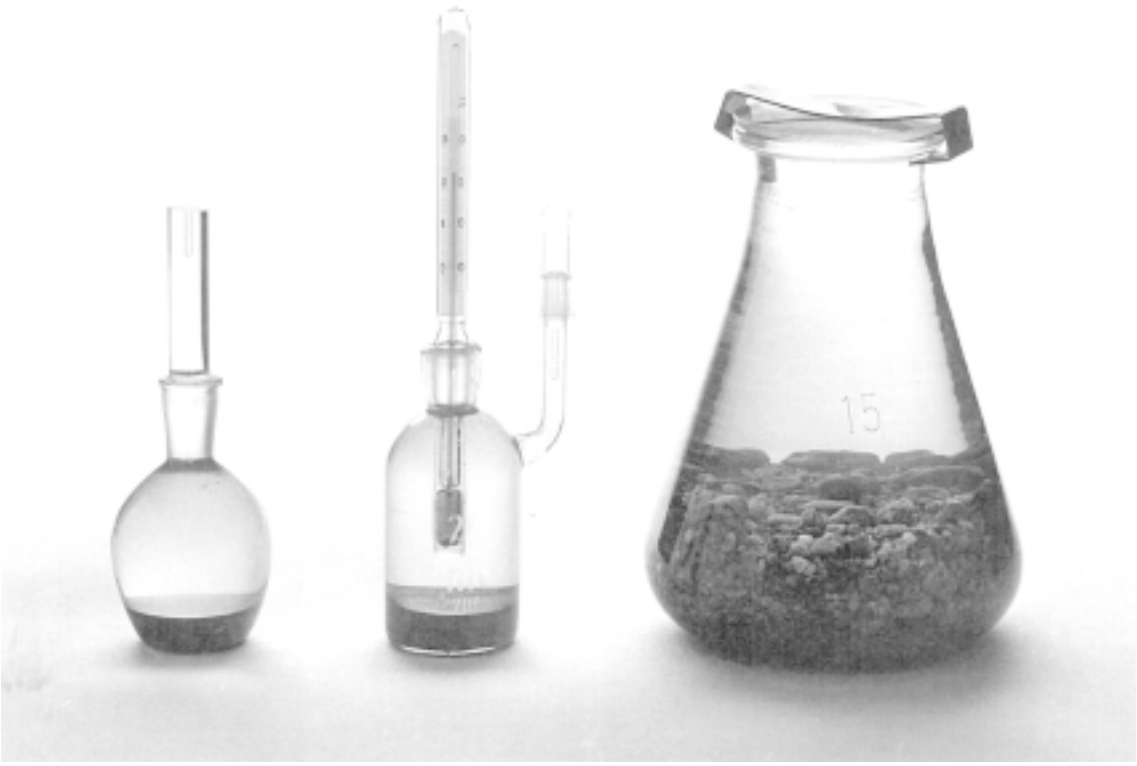

Figure 7-10. *Pycnometers.*

- Dry the soil sample, which should be about 20 g for clay and 50 g for coarser material, at 105°C for 24 hours and grind it by use of a mortar. Dry the ground powder at 105°C for a few hours and transfer it to the empty pycnometer.
- Weigh the pycnometer with dry soil (m_3).
- Fill the pycnometer with distilled water so that the water level is a couple of centimeters above the soil surface. Drive out air from the suspension by connecting the pycnometer with a vacuum pump until all air bubbles have been removed. Add distilled water to the measuring mark indicating a known volume.
- Remove drops and moisture on the outside of the pycnometer and weigh it (m_4).

Evaluation

Taking the density of the water in the pycnometer to be ρ_w at the prevailing temperature, its volume V_{pyc} is:

$$V_{pyc} = \frac{m_2 - m_1}{\rho_w} \tag{7-28}$$

One also has:

$$m_s = m_3 - m_1 \tag{7-29}$$

The volume of the water in the soil-containing pycnometer is:

$$\frac{m_4 - m_3}{\rho_w} \tag{7-30}$$

and the volume of the solid soil material is hence:

$$V_s = V_{pyc} - \frac{m_4 - m_3}{\rho_w} \tag{7-31}$$

From this the grain density, or the specific density, is obtained:

$$\rho_s = \frac{m_s}{V_{pyc} - \frac{m_4 - m_3}{\rho_w}} \tag{7-32}$$

7.6.3 Porewater density

The density of expelled porewater can be accurately determined by measuring the mass of dissolved matter using hydrometer technique (cf Chapter 3).

7.6.4 Water content

The evaluation of the water content, i.e. the ratio of the mass of water (m_w) and of the solid substances (m_s) is made by using the relation in Equation (7-33):

$$m = m_w + m_s = m_2 - m_1 \tag{7-33}$$

where

m = total mass
m_w = mass of water
m_s = mass of solid substance

Equipment

- Oven (150°C) with accurate thermostat (±1°C)
- Balance ±0.01 g
- Sample holder
- Exsiccator

Performance

The water content is determined by weighing the soil sample in its holder before (m_3) and after drying at 105°C for 24 hours (m_1). The sample holder is weighed separately (m_2).

Evaluation

The mass m_s of the solid substance, i.e. of the dry soil, is obtained from the expression:

$$m_s = m_3 - m_1 \tag{7-34}$$

The water content is hence obtained by applying the expression:

$$w = \frac{m_w}{m_s} = \frac{m_2 - m_3}{m_3 - m_1} \tag{7-35}$$

Accuracy

The accuracy of water content determinations strongly depends on the temperature, drying time and treatment of the soil after oven drying. Certain ovens do have a variation in temperature in different parts of as much as 10%, and it is not unusual that the actual temperature level deviates from the selected 105°C scale value. Such deviations can give a net error of a few percent units, but unsufficient drying time is normally more important, yielding values that can be several percent units too low.

In conjunction with large field experiments or constructions there is need for quicker determination of the water content of high numbers of samples and drying in microwave ovens or by use of lamps and other heaters is often used. They do not give the same values as the standard method and need careful calibration.

7.6.5 Degree of water saturation

According to Equation (7-9) the degree of water saturation is obtained from:

$$S_r = \frac{w\rho\rho_s}{\left[\rho_s(w+1) - \rho\right]\rho_w} \tag{7-36}$$

It is hence required that the water content and grain density as well as bulk density are known and that the porewater density also has to be determined. For clayey samples with well defined volume as for undisturbed samples taken by use of piston samples or from oedometers one has:

$$S_r = \frac{m_w}{\left(V - \frac{m_s}{\rho_s}\right)\rho_w} \tag{7-37}$$

where:

m_w = mass of water
m_s = mass of solid matter

V = total volume
ρ_s = grain density
ρ_w = water density

The accuracy of the evaluated degree of water saturation primarily depends on the accuracy of the determination of the mass of water and the density of the solid substance. For smectite clays the density of the water has been a matter of dispute and data in the range of 800–1200 kg/m^3 have been reported in literature. Since density values of smectite minerals have been reported to range between 2300 and 2800 kg/m^3 considerable uncertainties respecting the true degree of water saturation my arise. In recent years the matter has been investigated in some detail and it turns out that at least for montmorillonite clay one arrives at reasonably correct S_r-values by putting ρ_s = 2780 kg/m^3 and ρ_w = 1000 kg/m^3. The true figures may, however, be different.

7.6.6 Porosity and void ratio

General

The fraction of the total soil volume that represents voids is expressed as porosity (n), i.e. the ratio of the pore volume and total volume of a soil sample, or void ratio (e), i.e. the ratio of the pore volume and the volume of the solid components. Neither of them can be determined with any accuracy by direct measurement, such as microscopy of thin sections of the soil, but the size of individual voids in small specimens can be determined with some precision and the average porosity roughly estimated using such techniques (Chapter 9). In practice, the porosity and void ratio are derived from other soil data as given by Equations (7-38) and (7-39):

$$e = \frac{\rho_s(w+1) - \rho}{\rho} \tag{7-38}$$

$$n = 1 - \frac{\rho}{\rho_s(w+1)} \tag{7-39}$$

where:

ρ = bulk density
ρ_s = grain density
w = water content

For completely water saturated soil one has:

$$e = \frac{w\rho_s}{\rho_w} \tag{7-40}$$

$$n = \frac{w}{w + \frac{\rho_w}{\rho_s}} \tag{7-41}$$

where:

ρ_w = density of porewater

7.7 References

/1/ **Pusch R, and the Laboratory Committee of the Swedish Geotechnical Society, 1990.** Soil constituents and structure. Performance and interpretation of laboratory investigations, part 3. Swedish Council for Building Research.

/2/ **Anderson D M, Pusch R, Penner E, 1978.** Physical and thermal properties of frozen ground. In: Geotechnical Engineering for Cold Regions. Eds: O B Andersland, D M Anderson. McGraw-Hill Book Company.

/3/ **Pusch R, 1979.** Unfrozen water as a function of clay microstructure. Eng. Geol., Vol.13 (pp. 157–162).

/4/ **Fagerström H, and the Laboratory Committee of the Swedish Geotechnical Society, 1973.** Packningsegenskaper. Revised issue 1973. Swedish Building Council.

/5/ **Pusch R, 1994.** Waste Disposal in Rock. Elsevier Publ. Co.

/6/ **Pusch R, Karnland O, Hökmark H, 1990.** A general microstructural model for qualitative and quantitative studies of smectite clays. SKB TR-90-43, Svensk Kärnbränslehantering AB.

/7/ **Forslind E, Jacobsson A, 1972.** Water, a comprehensive treatise (Ed. Franks). Ch. 4. Clay-water systems, Plenum, New York.

/8/ **Pusch R, 1970.** Clay Microstructure. Doc. D8:1970. Nat. Swed. Build. Res., Stockholm.

/9/ **Grim R E, 1953.** Clay Mineralogy. McGraw-Hill Publ. Co., Ltd.

8 Consistency

This chapter deals with the physical state of soils. Handling, preparation and compaction of soils, as well as classifying them with respect to their general performance, require that one determines the "consistency limits". In many cases soil description includes comparison of the water content with these limits, as for classifying soils with respect to their sensitivity to mechanical disturbance. The consistency limits are of fundamental importance for the definition of suitable backfills in repositories and the matter is therefore given considerable space here.

8.1 Introduction

Clayey soils can be characterized and classified by determining the water content for certain well defined physical conditions and these water contents are termed consistency limits. They serve as particularly good characteristics of soils in general and smectite clays in particular with special respect to use in radioactive waste repositories. The matter of consistency is therefore given considerable space in this document.

Very extensive examination of the consistency properties of fine-grained soils was made in the beginning of the 20th century by the Swedish soil chemist Albert Atterberg /1,2/. He investigated how the consistency – primarily the stiffness and the plasticity of the soil – changed with the water content and defined characteristic consistency states. The water content yielding transition from one consistency state into another were called consistency limits. Atterberg worked out special methods for the determination of the consistency limits and indicated how they could be used for classification of fine-grained soils. Atterberg's methods are still used, though with certain modifications.

The most important consistency limits are the liquid limit, the plastic limit and the shrinkage limit. The liquid limit, which is a measure of the ability of a soil to hydrate and adsorb water, can be determined according to two, principally different methods, i.e. the percussion method (percussion liquid limit) and the fall-cone method (fall-cone liquid limit). The percussion method was worked out by Atterberg and has later been further developed, primarily by Casagrande /3/. Internationally, the percussion method is the one most used.

The fall-cone method was introduced in 1915 in conjunction with evaluation of slope failures in Sweden. By this method it is possible to determine, in addition to the liquid limit, also the shear strength of the soil sample for the undisturbed state, as well as the sensitivity. These determinations are normally included in routine testing of fine-grained soils in Sweden.

The Swedish fall-cone method is primarily used in Scandinavia and to some degree in Canada. Other fall-cone methods are used for determination of the liquid limit in France, Great Britain, India, Russia and eastern European countries.

Symbols and definitions used in this chapter are given in Chapter 1.

8.2 Consistency states

Following common praxis, the term 'consistency' refers primarily to the degree of stiffness and plasticity of a soil in the remoulded state. From a physico-chemical point of view, the consistency of a soil depends on the internal bonds between the soil particles and the interaction between particles and porewater. A characteristic of cohesive soils is that, within certain water content limits, they have a *plastic consistency* in the remoulded state. At lower water contents they have a stiff consistency and at higher water contents they turn liquid. As an intermediate state between the solid and plastic consistency a *semi-solid consistency* is distinguished.

A soil sample with a solid consistency is non-plastic and brittle rupture occurs at a small deformation.

A soil sample having a plastic consistency is mouldable and maintains its shape after deformation.

A soil sample having a liquid consistency deforms and flows under its own weight. The water content limits corresponding to the boundaries between the solid/semi-solid, semi-solid/plastic and plastic/liquid consistency states are called shrinkage limit, plastic limit and liquidity limit, respectively (Figure 8-1). These consistency limits are collectively called the Atterberg limits.

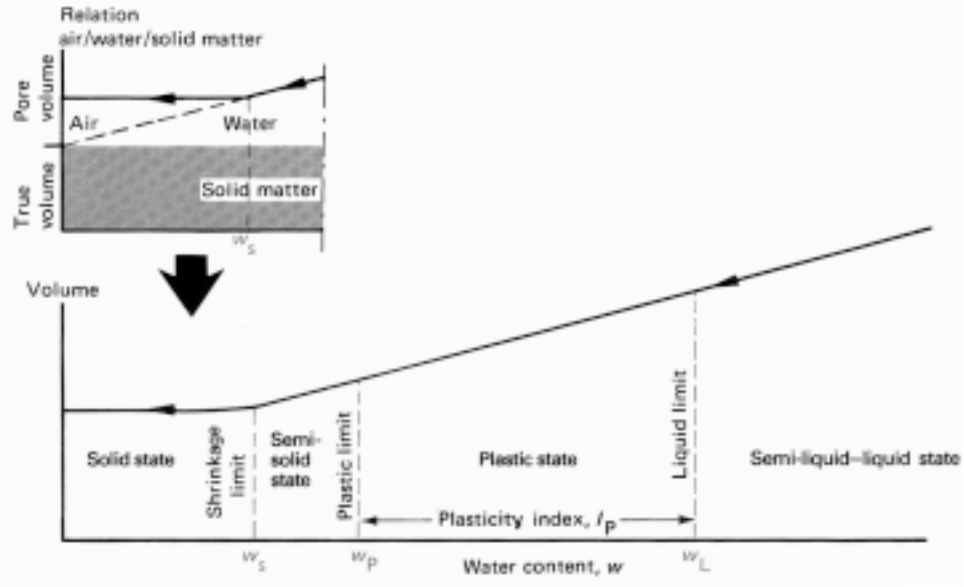

Figure 8-1. *Consistency states and limits.*

8.3 Consistency limits

8.3.1 Definition

The values of the consistency limits depend on the hydration potential of the soil in remoulded form. This ability is primarily controlled by the content and nature of clay minerals and organic colloids, and by the electrolyte content of the pore water.

The *shrinkage limit* w_S is defined as the water content at which an initially saturated soil sample ceases to shrink when dried. At further desiccation, air starts to penetrate the pores. At the same time the colour of the sample becomes lighter. The shrinkage limit can be determined for remoulded samples as well as for undisturbed samples.

The *plastic limit* w_P is defined as the lowest water content at which a remoulded soil sample can be rolled to a 3 mm thick thread without crumbling.

The *liquid limit* w_L can be determined according to the percussion method (percussion liquid limit) or the fall-cone method (fall-cone liquid limit).

The *percussion liquid limit*, determined by Casagrande's liquid limit device /3,4,5/, is defined as the water content at which a remoulded soil sample, placed in the cup of the device and divided into halves by a V-shaped groove, has such a consistency that the gap between the two sample halves close over 13 mm (½") length along the bottom of the groove when the cup is allowed to fall 10 mm 25 times.

The *fall-cone liquid limit* (earlier called the fineness number), determined by the fall-cone method, is defined as the water content at which a remoulded soil sample has such a consistency that the penetration of a 60 g/60° fall-cone is 10 mm (shear strength 1.7 kPa). The fall-cone liquid limit agrees with the percussion liquid limit for many soils but not for smectite-rich materials. According to British Standard, the (cone) liquid limit is defined as the water content at 20 mm penetration with an 80 g/30° cone.

8.3.2 Preparation of samples

The preparation method worked out at the U.S. Public Roads /6/ is generally used and it has been accepted as standard method by the American Society for Testing Materials (ASTM) /7/, and other organizations. According to this method, one starts with air-dry samples, which are disintegrated by intense mechanical agitation using a rubber-covered pestle and then sieved using a mesh opening of 0.42 mm. The material passing through the sieve is used for determining the consistency limits after mixing it with distilled water. The initial dry condition should be obtained by letting the fresh samples desiccate in laboratory atmosphere, while the use of hot air (drying oven, hair-drier etc) to reduce the water content is unsuitable.

When storing samples, even in sealed tubes, the consistency properties can change to a large extent depending on the influence of biological factors (fungi and bacteria) as well as oxygen and carbon dioxide.

When remoulding a soft undisturbed clay sample, breakdown of the structure of the soil skeleton takes place. The rate and degree of such destruction depends, besides the input energy, on the water content of the sample and on the electrolyte content of the pore water.

After remoulding, successive thixotropic strength regain takes place due to establishment of bonds between adjacent particles that move into equilibrium positions driven by attractive forces and Brownian movement. The thixotropic strength increase has a considerable influence on the consistency limits of smectite clays and quick clays.

The remoulding is normally carried out manually by means of a spatula and should be continued until the consistency of the sample stops changing. It should be made such that air bubbles are not formed in the sample.

Due to the breakdown of the structure when remoulding, the shrinkage limit of a remoulded sample is usually considerably lower than that of an undisturbed sample. The shrinkage limit for undisturbed samples of high-sensitive clays, and for undisturbed samples of medium-sensitive clays near the plastic limit is appreciably higher than the plastic limit, while the shrinkage limit for remoulded samples is considerably lower than the plastic limit.

Sedimentary clays have, in their natural undisturbed state, a more or less anisotropic structure (single particles or aggregates of particles are, to a predominant degree, oriented in the horizontal direction) and therefore shrink more in the vertical than in the horizontal direction on drying. For compacted clay powders intended for buffers in repositories the anisotropy is usually not very significant.

8.4 Liquid limit

8.4.1 Percussion liquid limit

General

Since Atterberg made his first attempts in 1911, a hemispherical cup has been used for determining the percussion liquid limit. The soil is applied in the cup and cut to form two separate halves which come together again by applying a certain number of blows; the corresponding water content being the liquid limit. While Atterberg mixed air-dried soil and water to an extent that made the sample fluid, the procedure is now somewhat different. Thus, according to the Public Roads /4/, distilled water should first be added to an extent that makes the initially dry sample plastic and additional water then gradually mixed in until the criterion of closing the groove between the two halves over 13 mm length is fulfilled after a defined number of percussions. The maximum thickness of the sample should be 10 mm. The method used by the Public Roads (called Manual Method) and the Casagrande method (called the Mechanical Method), have been recommended as standard procedures by ASTM and other organizations.

The Casagrande Method

Casagrande's liquid limit device is shown in Figure 8-2 /5,6/. It consists of a stand with a detachable brass cup, in which the sample is applied. A grooving tool is part of the device.

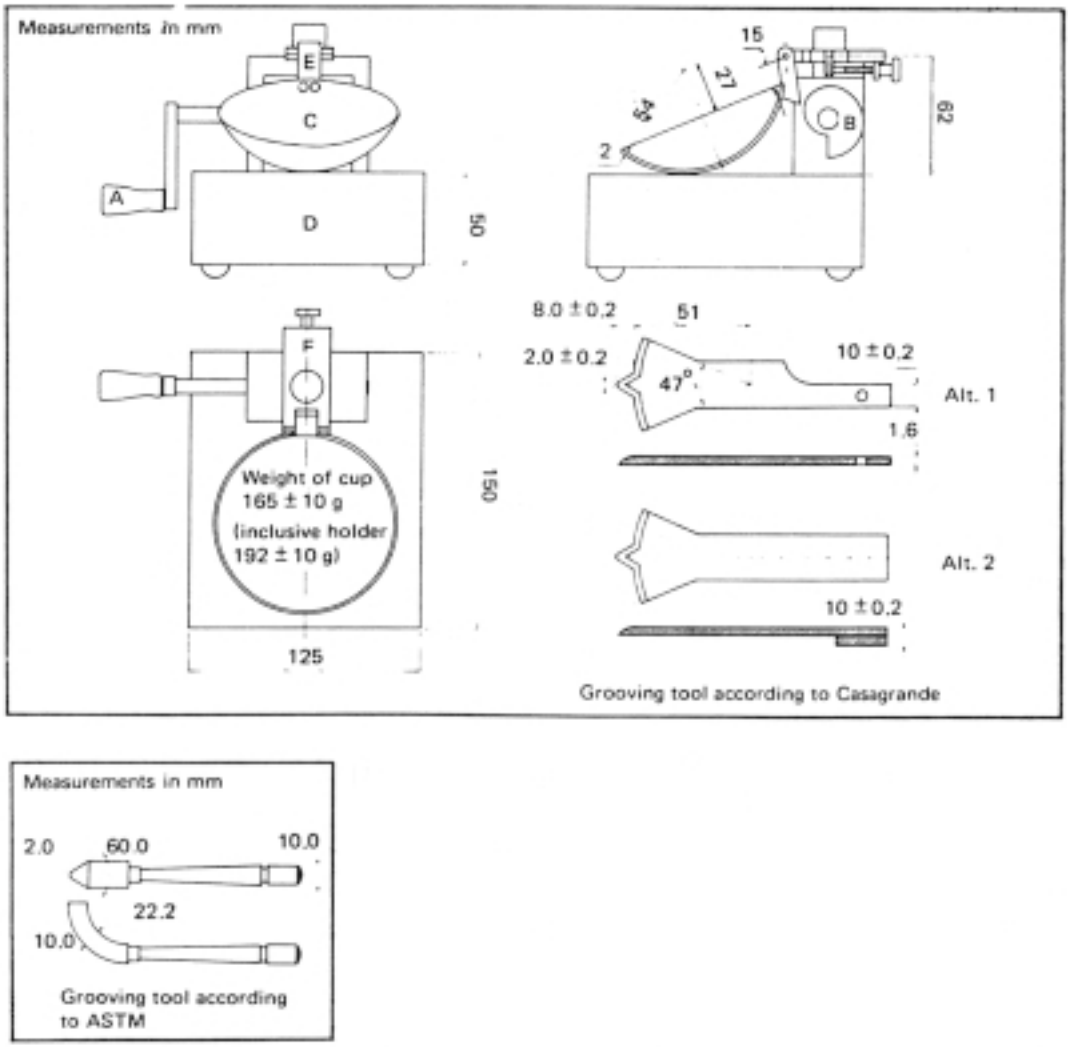

Figure 8-2. *Casagrande's liquid limit device with recommended tolerances /4/.*

The device works in the following way: When turning the crank A, the cam B lifts the cup C to a certain height. The cup then falls instantly to the base D of the stand. The cup is attached to arm E, which is mounted in bearings in the plate F with a steel pin. The plate F is displaceable for correcting the height of the fall. The flow of the soil to close the groove is shown in Figure 8-3.

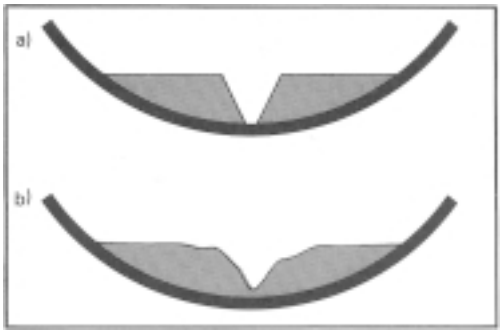

Figure 8-3. *Sample a) before and b) after flowing together when determining the liquid limit by the percussion method.*

The cup should be positioned so that the height of the fall is 10 mm. This means that the point of the cup that is in contact with the base should be 10 mm above the base after the cup has been lifted to its uppermost position by the cam (Figure 8-4). It should be observed that the distance between the lowest point of the cup and the base is then less than 10 mm since the cup moves along a circular orbit. The adjustment is made by means of the gauge on the handle of the grooving tool (Figure 8-4).

According to British Standard, the base should be made of rubber, but BS rubber gives, according to investigations made by Norman /7,8/, 6–8%, higher values of the liquid limit than devices with an "ebonite" or "Micarta" base, which are recommended.

In Figure 8-2 Casagrande's grooving tool is shown as well as the ASTM tool. Casagrande's tool is to be preferred because the ASTM version does not give a defined depth of the groove. It should be made of hardened steel in order to minimize wearing.

When determining the liquid limit according to the Casagrande method, a series of trials are made with different water contents of the remoulded soil sample. The number of percussions required is counted and the relation between the water content and the corresponding number of percussions plotted in a semi-logarithmic graph (Figure 8-5). The flow curve is approximately a straight line obeying the expression in Equation (8-1):

$$w = I_F \cdot \log\ n + C \qquad (8\text{-}1)$$

where:

w = water content
I_F = constant called flow index
n = number of percussions
C = constant

The flow curve indicates the slope of the flow curve and is defined as the decrease of the water content within one cycle on the logarithmic scale (number of percussions 10 to 100). On the whole, the value of flow index increases with an increasing value of the liquid limit.

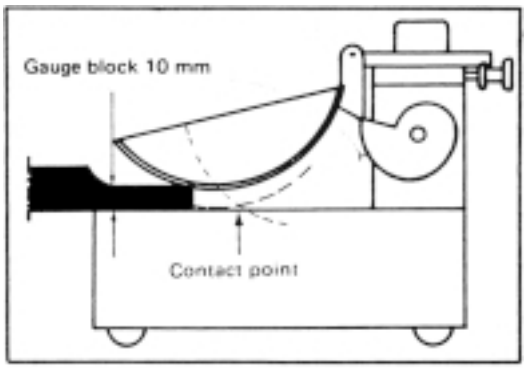

Figure 8-4. *Adjustment of height of fall in Casagrande's liquid limit device.*

The liquid limit is evaluated by means of the flow curve and is defined as the water content corresponding to 25 percussions (Figure 8-5).

Simplified methods – so called one-point methods – are generally used today to determine the percussion liquid limit. According to these methods, it is sufficient to determine only one point on the flow curve representing the number of percussions required for various water contents, for evaluating the liquid limit. It is required, however, that the water content of the sample is not too different from the liquid limit.

In the U.S., three different one-point methods have been worked out, viz. at Waterways Experiment Station (WES) /8/, Washington State Highways /9/ and Public Roads /7/. A general conclusion is that the number of percussions for groove closure should be restricted to the range of 22 to 28 percussions to get equal accuracy with respect to the multi-point method.

The Public Roads method presupposes that the flow curves in a semi-logarithmic graph converge towards a certain point on the axis for the number of percussions. The empirical Equation (8-2) has been derived for evaluation of the liquid limit:

$$w_L = \frac{w_n}{1.419 - 9.3 \ \log n} \tag{8-2}$$

where:

n = number of percussions
w_n = water content at n percussions

The WES Method, which is the most commonly applied method internationally, presupposes that the flow curves in a double-logarithmic graph are straight lines with the same inclination, which gives the relation in Equation (8-3):

$$w_L = w_n \left(\frac{n}{25} \right)^{\tan\beta} \tag{8-3}$$

where

$\tan\beta$ = inclination of the flow curve

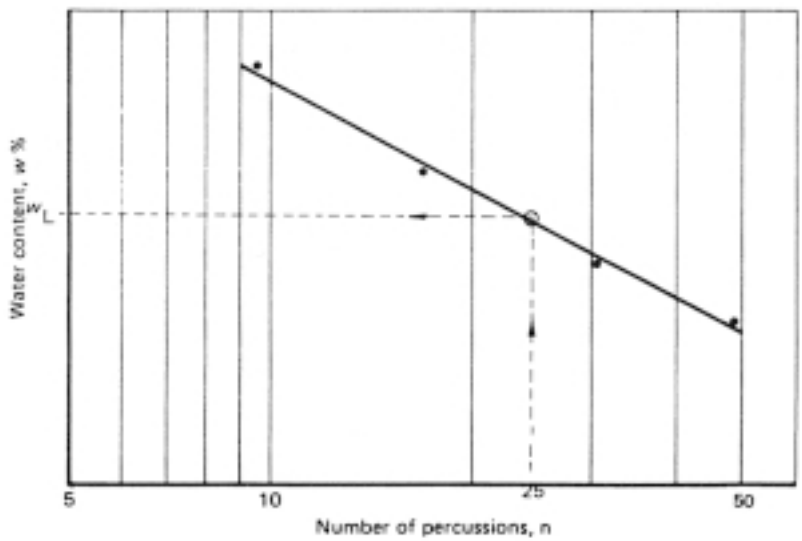

Figure 8-5. *Evaluation of the percussion liquid limit by means of the flow curve.*

In the investigation carried out by WES /8/, which comprised 767 samples with liquid limits from 17% to 147%, the value of *tan*β varied between 0.027 and 0.235, with an average of 0.121.

According to WES, the evaluation of w_L should be made by means of a nomogram where the *tan*β is taken as 0.121 and the number of percussions is within the range 15–41, and w_L in the interval 20 to 150%.

Figure 8-6 shows the change of w_L for certain changes (Δ *tan*β) of *tan*β in relation to the number of percussions *n*. As shown in the figure, the value of w_L is changed by approximately 5% for Δ *tan*β = 0.10, when the number of percussions is 15 to 41.

The value of *tan*β has been determined for Swedish clays and found to be 0.12 (428 samples) /11/. For sedimentary inorganic clays, the mean value of *tan*β was found to be equal to 0.13 (310 samples) and for clayey tills 0.17 (18 samples). For organic soils (organic clay, gyttja and amorphous peat) the mean value has been found to be 0.09 (78 samples). Equation (8-3) can be written as:

$$w_L = K_n \cdot w_n \tag{8-4}$$

where the coefficient K_n depends on the value of *tan*β and the number of percussions *n*. For *tan*β = 0.13 and *tan*β = 0.09 and *n* = 15–41 the value K_n is obtained by means of Table 8-1.

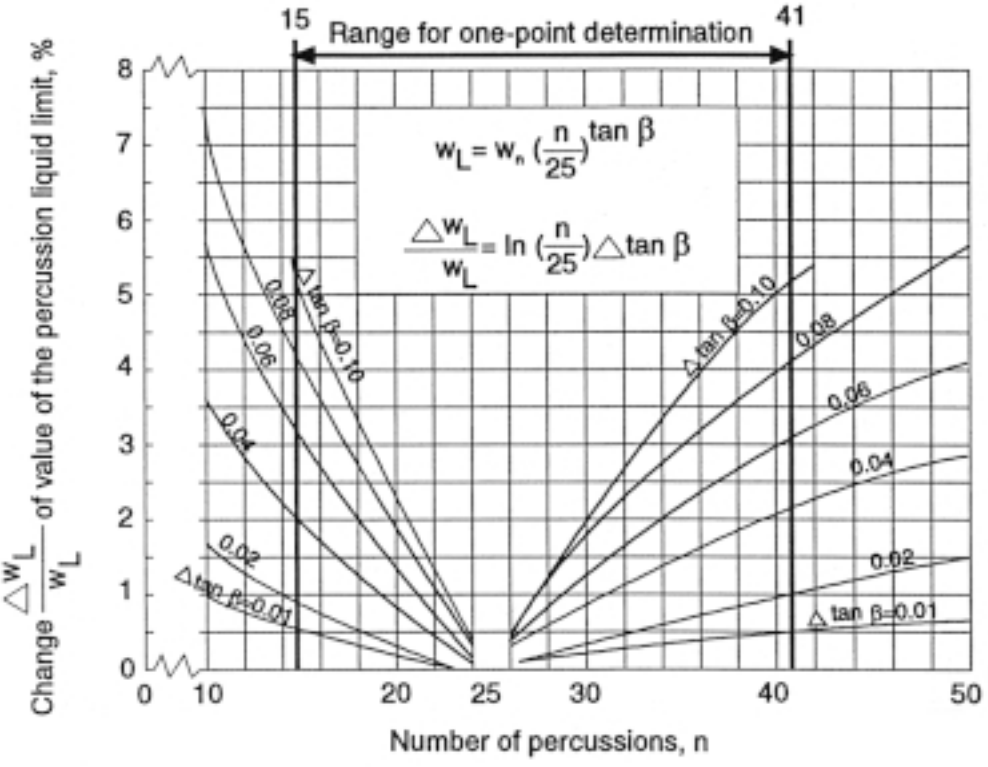

Figure 8-6. *Percentage change of value of percussion liquid limit w_L for different values of Δtanβ. (According to the U.S. Waterways Experiment Station, /8/).*

Table 8-1. Relation between number of percussions and the coefficient K_n in formula $w_L = K_n \cdot w_n$ where $K_n = (n/25)^{\tan\beta}$

Number of percussions *n*	Coefficient K_n *tan*β= 0.13	Coefficient K_n *tan*β= 0.09	Number of percussions *n*	Coefficient K_n *tan*β= 0.13	Coefficient K_n *tan*β= 0.09	Number of percussions *n*	Coefficient K_n *tan*β= 0.13	Coefficient K_n *tan*β= 0.09
15	0.936	0.955	24	0.995	0.996	33	1.037	1.025
16	0.944	0.961	25	1.000	1.000	34	1.041	1.028
17	0.951	0.966	26	1.005	1.004	35	1.045	1.031
18	0.958	0.971	27	1.010	1.007	36	1.049	1.033
19	0.965	0.976	28	1.015	1.010	37	1.052	1.036
20	0.971	0.980	29	1.019	1.013	38	1.056	1.038
21	0.978	0.984	30	1.024	1.017	39	1.060	1.041
22	0.984	0.989	31	1.028	1.020	40	1.063	1.043
23	0.989	0.993	32	1.033	1.022	41	1.066	1.046

Determination of percussion liquid limit

For routine testing sufficient accuracy is generally obtained by using the one-point method, while multi-point determination should be used when great care has to be taken.

The following equipment is required (see Figure 8-7):

- Casagrande's liquid limit device with grooving tool.
- Mixing cup of porcelain, plastic or other suitable material with a hemispherical shape and with a diameter of approximately 10 cm.
- Spatula with a blade 70 mm long and 20 mm wide.
- Spray bottle (preferably of plastic) with distilled water.
- Unglazed paper of the type used for typing.
- Drying cans equipped with lids. Volume about 25 cm^3.
- Balance with 0.01 g accuracy. Preferably an electronic precision balance.
- Drying oven with thermostatic control. Temperature 105°C.

When preparing mixed-grained soils, the following additional equipment is required:

- Mortar with a rubber-coated pestle.
- Sieve with 0.40 mm mesh opening The measure may be up to 0.42 mm.

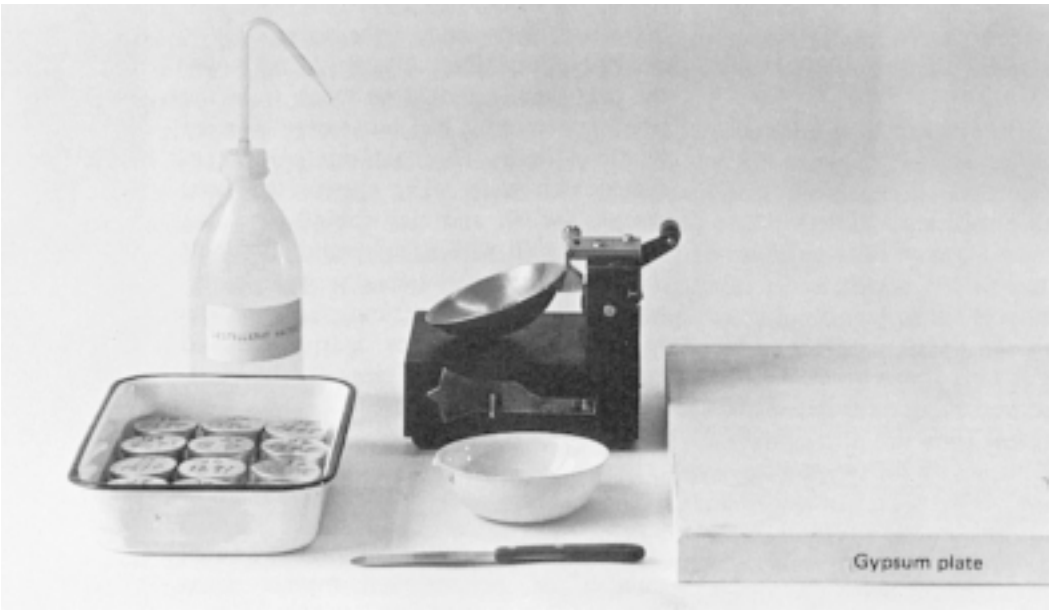

Figure 8-7. *Percussion liquid limit device with auxiliary equipment.*

For determination of the percussion liquid limit of fine-grained mineral soils and organic soils, about 100 cm^3 of fresh soil is required.

The air-dried sample is crushed in the mortar by means of the rubber-coated pestle and sieved by use of the 0.40 mm sieve. About 100 g of the material that has passed the sieve is mixed in the mixing cup with distilled water to yield a plastic consistency. The sample should then be left for a couple of hours, or preferably till the next day, to give the water time to spread homogeneously in the soil before the liquid limit is determined. In the meantime, the cup should be covered in order to prevent water evaporation.

"One-point" procedure

- Remould the soil sample in the mixing cup carefully with the spatula.
- Place a part of the sample in front of the cup of the liquid limit device (see Figure 8-8).
- Smoothen the sample in the brass cup with the spatula so that the surface of the sample becomes parallel to the base and level with the lowest part of the edge of the cup. The maximum thickness of the sample will then be about 12 mm. Move the excess soil back to the mixing cup.
- Make a groove with the grooving tool through the sample in the direction away from the hinge (Figure 8-8a). The tool should be kept perpendicular to the bottom of the cup with the edge moved forwards. Make sure that the groove is smooth (Figure 8-8b). Air bubbles can have a disturbing influence.
- Turn the crank of the device at an even rate of about 2 revolutions per second until the two sample halves have flowed together over about 13 mm (½") length at the bottom of the groove (Figure 8-8c). Meanwhile, count the number of percussions. The one-point method is valid for 15–41 percussions.

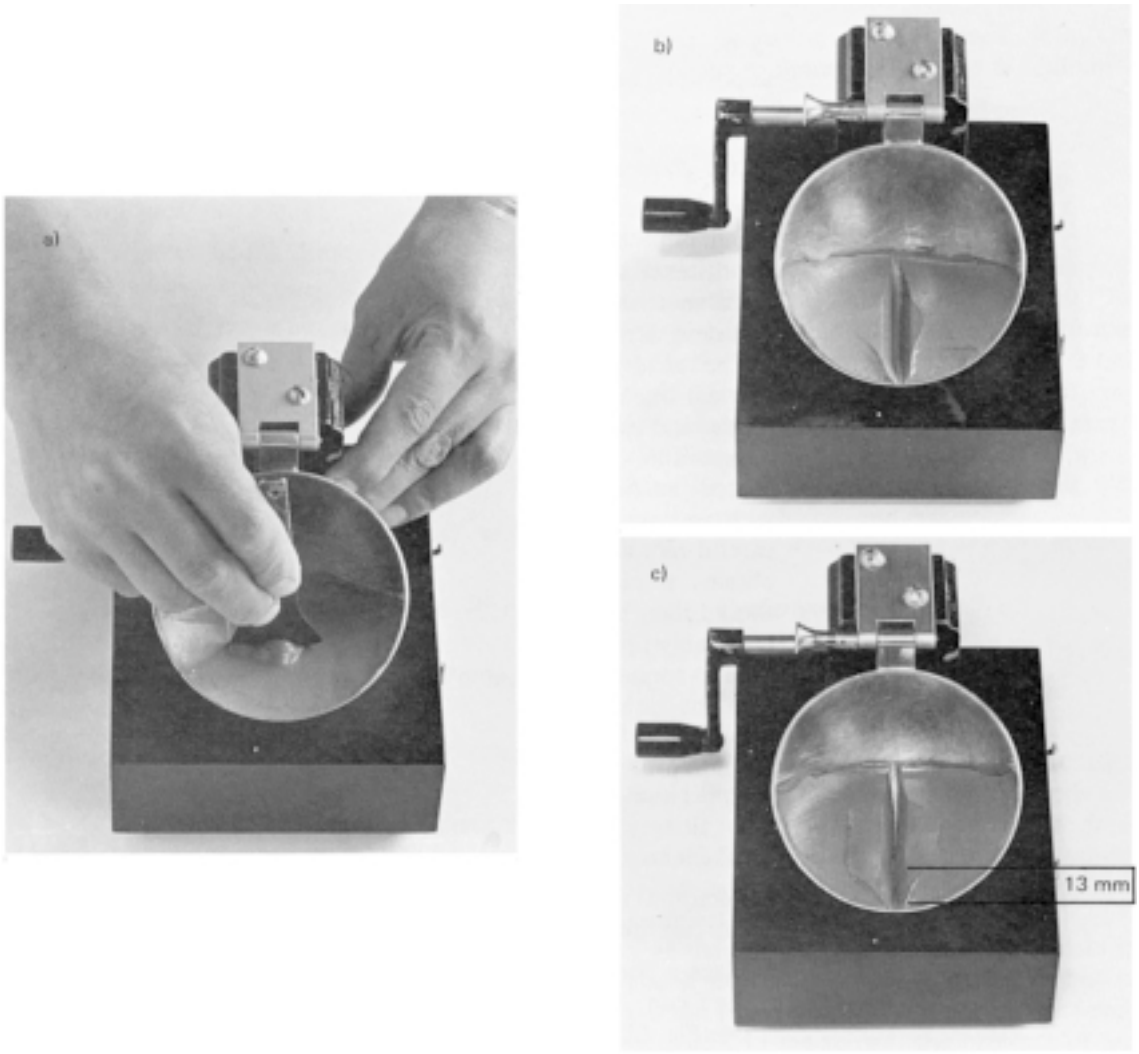

Figure 8-8. *Steps in the determination of the percussion liquid limit. a) Cutting a groove. b) Groove before the sample has flowed together. c) Groove after the sample has flowed together.*

If the number of percussions is less than 15 or more than 41, the water content of the sample has to be adjusted (reduced or increased as the case may be), so that the number of percussions falls within the interval of 15–41 on subsequent testing.

Before the water content is adjusted, two 20 g specimens are extracted for determination of the water content.

If the water content has to be increased, the sample in the brass cup is transferred back to the mixing cup and the entire sample diluted with distilled water and carefully remoulded with the spatula.

If the water content has to be reduced, the whole sample is spread on the paper, which absorbs water relatively quickly. The sample is then moved back to the mixing cup and carefully remoulded with the spatula.

Before further trials are carried out, the brass cup and the grooving tool must be cleaned.

- Count and record the number of percussions required to close the groove over 13 mm length and cut out a 10–20 g sample for water content determination.
- Repeat the determination by using the second sample.
- If the two determinations do not give almost the same number of percussions, additional determinations should be made.
- Determine the water content.

"Multi-point" procedure

The determinations are performed as described above for at least three different water contents (different numbers of percussion) of the remoulded sample. The number of percussions for groove closure should be above and below 25 and in at least three determinations the number of percussions for groove closure should be within the range 15 to 41. The water content of only one extracted 10–20 g sample is sufficient for each determination.

Special considerations

For certain soils, the groove cannot be obtained by means of the tool, because the sample deforms and slips along the bottom of the cup. It is then suitable to cut the groove with the spatula or a knife.

A general note is that exposure to air should be minimized for avoiding drying and oxidation, which can cause a drop in liquid limit.

Evaluation of "one-point" procedure

- The water content of each part-sample is evaluated.
- The liquid limit w_L is obtained by Equation (8-4). For inorganic clay and silt soils, except smectite clays, $tan\beta = 0.13$ while for organic soils and smectite clays $tan\beta = 0.09$. The average value is rounded off to the closest whole number.

  If the difference between the two values exceeds 2% units when the average is less than 40%, or if the difference exceeds 5% units of the average value when the average value exceeds 40%, an additional test should be made.

  The results are suitably reported by filling in standard forms of the type shown in Figure 8-9.
- The water content is evaluated and the values obtained plotted against the corresponding percussions for groove closure (Figure 8-5).

  The liquid limit w_L is obtained as the water content corresponding to 25 percussions on the flow curve. The value is rounded off to the closest whole number.

  The results are reported in the same manner as in the "one-point" procedure (Figure 8-9).

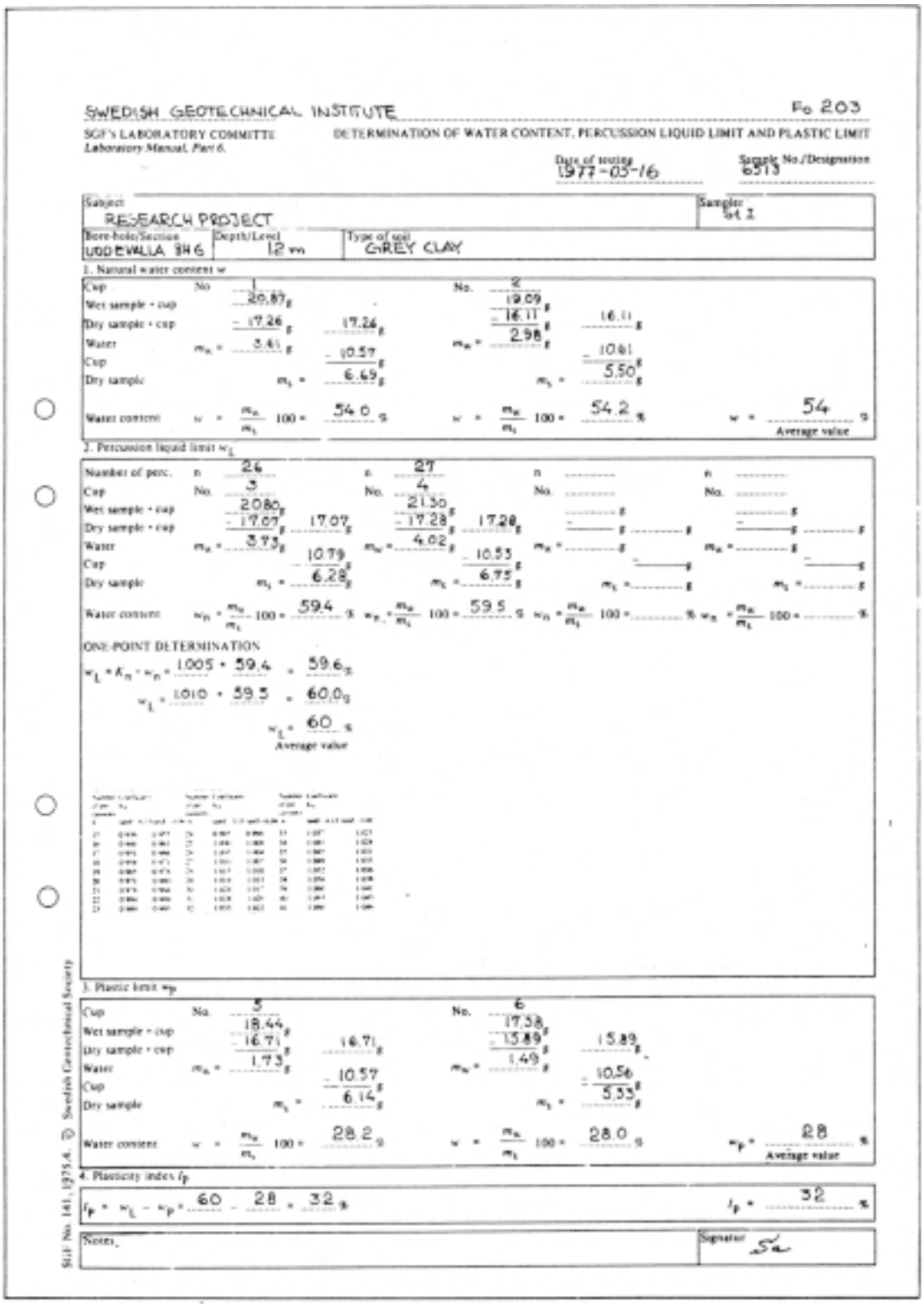

SWEDISH GEOTECHNICAL INSTITUTE — Fo 203

SGI's LABORATORY COMMITTEE — DETERMINATION OF WATER CONTENT, PERCUSSION LIQUID LIMIT AND PLASTIC LIMIT

Laboratory Manual, Part 6.

Date of testing: 1977-05-16 — Sample No./Designation: 6513

Subject: RESEARCH PROJECT — Sampler: St 2

Bore-hole/Section: UDDEVALLA 3H6 — Depth/Level: 12 m — Type of soil: GREY CLAY

1. Natural water content w

Cup No.	1			No.	2			
Wet sample + cup	20.87 g				19.09 g			
Dry sample + cup	17.26 g	17.24 g			16.11 g	16.11 g		
Water m_w	3.61 g			m_w	2.98 g			
Cup	10.57 g				10.61 g			
Dry sample m_s	6.69 g			m_s	5.50 g			
Water content $w = \frac{m_w}{m_s} 100$	54.0 %			$w = \frac{m_w}{m_s} 100$	54.2 %		w = 54 % Average value	

2. Percussion liquid limit w_L

Number of perc.	n	26		n	27		n	
Cup	No.	3		No.	4		No.	
Wet sample + cup	20.80 g			21.30 g				
Dry sample + cup	17.07 g	17.07 g		17.28 g	17.28 g			
Water m_w	3.73 g			m_w	4.02 g			
Cup	10.79 g			10.55 g				
Dry sample m_s	6.28 g			m_s	6.75 g			
Water content $w_n = \frac{m_w}{m_s} 100$	59.4 %			$w_n = \frac{m_w}{m_s} 100$	59.5 %		$w_n = \frac{m_w}{m_s} 100$	%

ONE-POINT DETERMINATION

$w_L = K_n \cdot w_n = 1.005 \cdot 59.4 = 59.6$ %

$w_L = 1.010 \cdot 59.5 = 60.0$ %

w_L = 60 % Average value

3. Plastic limit w_p

Cup	No.	5		No.	6			
Wet sample + cup	18.44 g			17.38 g				
Dry sample + cup	16.71 g	16.71 g		15.89 g	15.89 g			
Water m_w	1.73 g			m_w	1.49 g			
Cup	10.57 g			10.56 g				
Dry sample m_s	6.14 g			m_s	5.33 g			
Water content $w = \frac{m_w}{m_s} 100$	28.2 %			$w = \frac{m_w}{m_s} 100$	28.0 %		w_p = 28 % Average value	

4. Plasticity index I_p

$I_p = w_L - w_p = 60 - 28 = 32$ %

I_p = 32 %

Notes: — Signature: Sa

SGI Info No. 141, 1975-6. © Swedish Geotechnical Society

Figure 8-9*. Form for reporting results. Determination of water content, percussion liquid limit and plastic limit /1/.*

8.4.2 Fall-cone liquid limit

General

The fall-cone apparatus (Figure 8-10) consists of a stand with a vertically adjustable arm in which a fall-cone can be hung. As a rule, the apparatus is equipped with four different cones, the mass/cone angle being 400 g/30°, 100 g/30°, 60 g/60° and 10 g/60°, respectively. In the test, the stand-arm is moved down so that the tip of the cone touches the levelled surface of the soil sample. The cone is then released and penetrates the sample, the drop being recorded by means of a millimeter-graded scale.

A theoretical interpretation of the fall-cone test based on studies of the fall motion of the cone has been worked out by Hansbo, yielding the relationship between the undrained shear strength τ_{fu}, of the soil sample, the mass m of the cone and the cone penetration i given by Equation (8-5), /11/:

$$\tau_{fu} = K\frac{mg}{i^2} \tag{8-5}$$

where:

K = constant, depending on the cone angle and, to a certain extent, also on the type of soil
m = mass of cone
g = acceleration of gravity

By calibration with a laboratory vane apparatus, the value of the constant K for a remoulded sample has been set at K = 0.8 for 30° cones and K = 0.27 for 60° cones /10/.

Among several methods proposed for evaluating the liquid limit the one introduced by Karlsson is preferred /10/. According to this method the consistency curve can be approximated to a straight line obeying Equation (8-6):

$$w_L = M \cdot w_i + N \tag{8-6}$$

where:

$$M = \frac{1.8}{1.8 + 2\log\frac{i}{10}}$$

$$N = \frac{34 \cdot \log\frac{i}{10}}{1.8 + 2 \cdot \log\frac{i}{10}}$$

w_i = the water content of the remoulded sample at the cone penetration i mm

The applicability of this evaluation method is limited to cone penetrations from 7.0 to 14.9 mm with the 60 g/60° cone. The values of M and N are obtained by means of Table 8-2.

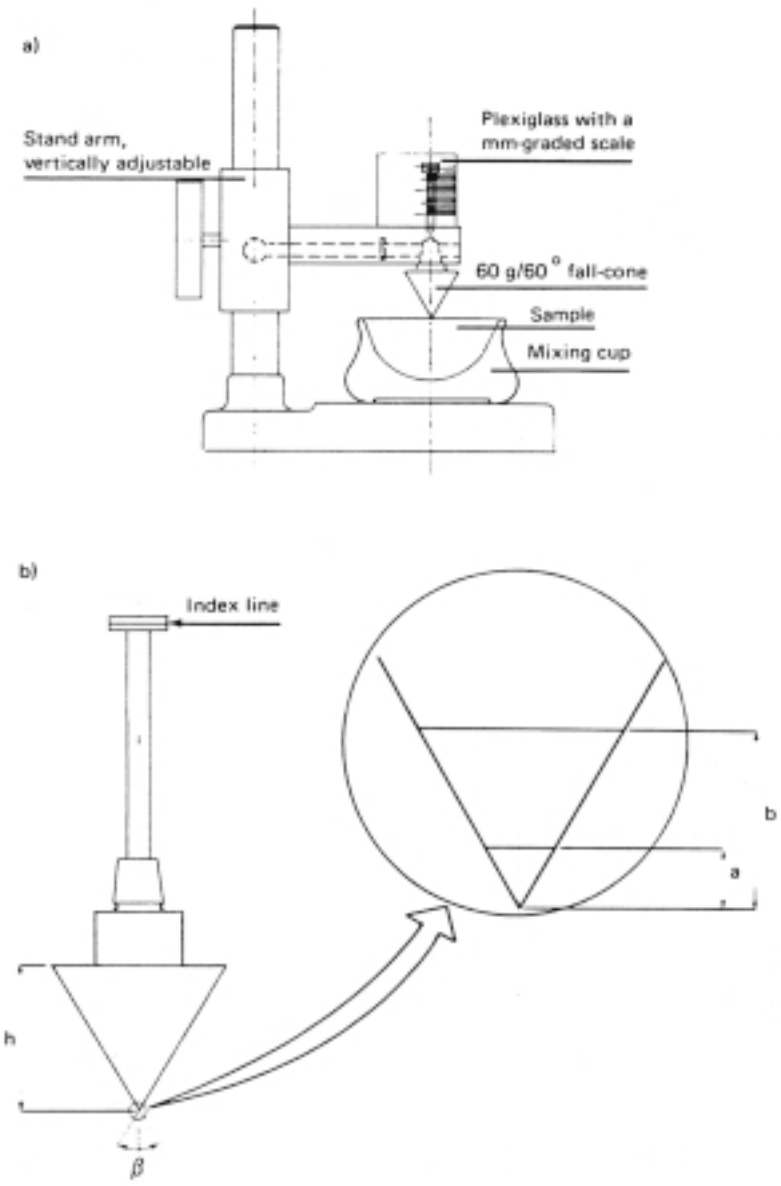

Height, h mm	Deviation from geometrical apex		Cone angle β degrees	Mass g
	Manufacturing tolerance a, mm	Wear tolerance b, mm		
≥ 20	0.1	0.3	60 ± 0.2	60 ± 0.6

Figure 8-10. *Fall-cone apparatus. a) Principle. b) 60 g/60° fall-cone with recommended tolerances according to the Swedish Geotechnical Society (SGF).*

Table 8-2. Relation between cone penetration i (60 g/60°) and factors M and N in the formula $w_L = M \cdot w_i + N$.

i, mm	M, N	0	1	2	3	4	5	6	7	8	9
7	M	1.21	1.20	1.19	1.18	1.17	1.16	1.15	1.14	1,14	1.13
7	N	−3.5	−3.4	−3.2	−3.0	−2.9	−2.7	−2.6	2.5	−2.3	−2.2
8	M	1.12	1.11	1.11	1.10	1.10	1.09	1.08	1.07	1.07	1.06
8	N	−2.1	1.9	−1.8	−1.7	−1.6	−1.4	−1.3	−1.2	−1.1	−1.0
9	M	1.05	1.05	1.04	1.04	1.03	1.03	1.02	1.01	1.01	1.00
9	N	−0.9	−0.8	−0.7	−0.6	−0.5	−0.4	−0.3	−0.3	−0.2	−0.1
10	M	1.00	1.00	0.99	0.99	0.98	0.98	0.97	0.97	0.96	0.96
10	N	0	0.1	0.2	0.2	0.3	0.4	0.5	0.5	0.6	0.7
11	M	0.96	0.95	0.95	0.94	0.94	0.94	0.93	0.93	0.93	0.92
11	N	0.7	0.8	0.9	0.9	1.0	1.1	1.1	1.2	1.3	1.3
12	M	0.92	0.92	0.91	0.91	0.91	0.90	0.90	0.90	0.89	0.89
12	N	1.4	1.4	1.5	1.5	1.6	1.7	1.7	1.8	1.8	1.9
13	M	0.89	0.88	0.88	0.88	0.88	0.87	0.87	0.87	0.87	0.86
13	N	1.9	2.0	2.0	2.1	2.1	2.2	2.2	2.2	2.3	2.3
14	M	0.86	0.86	0.86	0.85	0.85	0.85	0.85	0.84	0.84	0.84
14	N	2.4	2.4	2.5	2.5	2.5	2.6	2.6	2.7	2.7	2.7

Determination of the fall-cone liquid limit

The fall-cone liquid limit can be obtained by either one-point determination or multi-point determination. For routine testing sufficient accuracy is generally obtained by the one-point method, while greater accuracy requires “multi-point” determination. For smectite-rich clays the latter is required.

Equipment (see Figure 8-11)

- Fall-cone apparatus with a 60 g/60° cone.
- Mixing cups of plastic or other suitable material with a diameter of about 60 mm and a depth of about 30 mm (Figure 8-12).
- Spatula with a blade about 70 mm long and 20 mm wide.
- Spray bottle (preferably of plastic) with distilled water.
- Unglazed paper of the type used for typewriting.
- Drying cans equipped with lids. Volume about $2{,}5 \cdot 10^4$ m^3.
- Balance with 0.01 g accuracy. Preferably an electronic precision balance.
- Drying oven with thermostatic control. Temperature 105°C.

When preparing mixed-grain soils, the following additional equipment is required:

- Mortar with a rubber-coated pestle.
- Sieve with 0.40 mm mesh opening.

Figure 8-11. *Fall-cone liquid limit device with auxiliary equipment.*

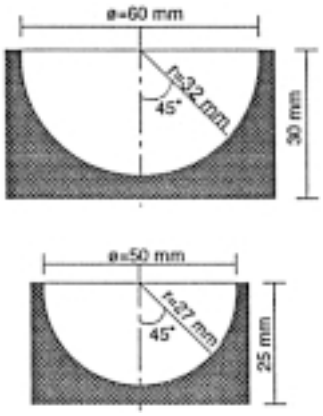

Figure 8-12. *Mixing cups of plastics. a) Normal amounts of soil. b) Small amounts of soil.*

For the determination of the fall-cone liquid limit of mixed-grain soils, for instance till, approximately 100 g of air-dried material, which has passed the 0.40 mm sieve, is required. Coarse-grained layers should have been removed as when the Casagrande method is used.

The air-dried sample is crushed in the mortar by means of the rubber-coated pestle and sieved through the 0.40 mm sieve. About 100 g of the material that has passed is mixed with distilled water in the cup until the soil obtains plastic consistency. The sample should then be left for a couple of hours, or preferably till the next day, to let the sample homogenize before the determination of the liquid limit is made. In the meantime, the cup must be covered in order to prevent water evaporation.

"One-point" determination

- Remould the soil sample in the mixing cup carefully by means of the spatula. The sample should fill the cup completely.
- Smoothen the sample flush with the edge of the cup by means of the spatula. Move the excess soil to an empty cup.
- Mount the 60 g/60° cone in the stand of the fall-cone apparatus and place the mixing cup centrally under the cone.
- Bring the stand arm down so that the tip of the cone just touches the surface of the soil sample.
- Check that the index line on the cone shaft coincides with the zero line of the millimetre-graded scale.
- Release the cone.
- Read the cone penetration within 0.1 mm. The cone-point method is valid for 7.0 to 14.9 mm cone penetration.

If the cone penetration is less then 7.00 or more than 14.9 mm, the water content of the sample should be adjusted (increased or reduced as the case may be) so that the cone penetration at subsequent testing falls within the interval of 7.0 to 14.9 mm.

Before the water content is adjusted, two 20 g specimens are extracted for determination of the original water content.

If the water content has to be increased, the sample in the cup is transferred back to the mixing cup and the entire sample is then diluted with distilled water and carefully remoulded with the spatula.

If the water content has to be reduced, the whole sample is spread on the paper, which absorbs water relatively fast. The sample is then moved back to the mixing cup and carefully remoulded with the spatula.

Before further trials are carried out, the cup must be cleaned.

- Read and record the cone penetration and extract a 20 g specimen from the central part of the sample in the mixing cup. Transfer it to a drying can for water content determination.

  For soils with a very high liquid limit, such as smectite clay, the specimen should preferably be more than 20 g to give an accurate determination of the water content.

- Replenish the mixing cup with excess soil and then remould the soil and repeat the determination.

- Repeat the determination by using the second sample. If the two determinations do not give almost the same cone penetrations, further determinations should be made.

- The water content is evaluated.

"Multi-point" determination

The determinations are performed as described above for at least three different cone penetrations, using the remoulded sample. The cone penetrations should be above 7 mm and below 10 mm and in at least three tests the penetrations should be within the interval 7 to 14.9 mm. Determination of the water content of one of the extracted specimens is sufficient for each determination. The water content is determined and plotted against the cone penetration in the same manner as for the Casagrande method.

Evaluation

"One-point" determination

- The water content of the two part-samples is evaluated and the fall-cone liquid limit w_L obtained by use of Equation (8-15) and Table 8-2. The average value is rounded off to the closest whole number.

  If the difference between the two values exceeds 2% units when the average value is less than 40, or if the difference exceeds 5% units when the average value is higher than 40, an additional test should be made.

  The results are reported in the same manner as for the Casagrande method (Figure 8-9).

"Multi-point" determination

The respective water contents are determined and the values plotted against the corresponding cone penetration. The fall-cone liquid limit w_L is obtained as the water content at 10 mm cone penetration. The value is rounded off to the closest whole number.

8.4.3 Reliability

The following sources of error may yield inaccurate values:

- Oxidation and drying of the sample by storing it too long. This applies especially to quick clays, sulphide clays and smectite clays.
- Admixture of air bubbles when remoulding the sample, or insufficient remoulding.
- Errors in determining the water content due to i.a. incomplete drying.
- Deviations from the prescribed dimensions of cups, grooving tool and from the prescribed weight of the various tool components used for evaluating the percussion and fall-cone liquid limits. They can give errors on the order of ± 5%. Thus, for smectite clays the accuracy may be as low as ± 25% units. To this comes the effect of drying and oxidation, which may be equally important.
- For silt soils the percussion method gives uncertain values due to the fact that the surface part of the sample is enriched with water during the percussion and, as a consequence, flow occurs in the water-enriched part of the sample. Furthermore, the fall-cone method gives relatively uncertain values for silt soils due to dilatancy.
- In silty soils the cone continues to sink after the initial indentation.

8.4.4 Comparison between the percussion liquid limit and the fall-cone liquid limit

Comparative tests performed by the Swedish Geotechnical Institute have shown that the percussion and fall-cone liquid limits coincide, on the whole, when $w_L \sim 40\%$. At higher values, the percussion liquid limit is generally higher than the fall-cone liquid limit, while at lower values, the opposite is the case. For silt, the percussion liquid limit is generally considerably lower than the fall-cone liquid limit whereas for organic soils it is considerably higher. For smectite-rich clays the fall-cone liquid appears to be up to 20% lower than the percussion liquid limit.

8.5 Plastic limit

8.5.1 General

Internationally, it is common practice to roll out the sample on a glass plate to reach the required state of the clay, i.e. 3 mm diameter threads that are just about to fall apart and form crumbles. In Sweden, a water-absorbing (unglazed) paper is normally used, because it has a rougher surface than glass and facilitates rolling. Furthermore, the operation is quicker because the paper absorbs water. For silty soils, unglazed paper is, however, less suitable as the water content of the sample decreases too rapidly.

8.5.2 Determination of the plastic limit

As a rule, determination of the plastic limit is made in conjunction with determining the liquid limit.

Equipment

- Mixing cup. The same type of cup as used when determining the liquid limit.
- Spatula with a blade about 70 mm long and about 20 mm wide.
- Unglazed paper or, in the case of silt, glazed paper.
- A dummy rod with 3 mm diameter.
- Drying cans equipped with lids. Volume about 25 cm^3.
- Balance with 0.01 g accuracy, preferably an electronic precision balance.
- Drying oven with thermostatic control. Temperature 105°C.

Performance

For determination of the plastic limit, 20–40 g specimens are needed. For silt and illitic clay, 20 g are usually sufficient, while for smectite clay 40 g are suitable.

If the sample has a sticky consistency, the water content should be reduced so that the sample becomes stiffer before rolling is started.

- Divide the sample into four approximately equal parts.
- Roll each of the specimens by hand to a thread, approximately 3 mm thick, on the unglazed paper (Figure 8-13) placed on a plane and hard base. In the case of silt use glazed paper.

  The rolling should be carried out with even motions of the hand, backwards and forwards, in such a way that the thread gets an even thickness. Furthermore, the pressure should be adjusted so as to successively reduce the thickness of the thread while keeping the cross section circular.
- Knead the sample together and roll it again and repeat this procedure until the thread breaks into several crumbles along its full length.
- Collect the crumbled sample, place it in a drying can and put the lid on.
- Handle the remaining part-samples in the same way. Place the two first treated part-samples in one can and the other two part-samples in a second one.
- Determine the water content of the two samples.

Evaluation

- The water content of each of the two samples is determined and the mean value calculated yielding the plastic limit w_P. Round off to the closest whole number.

  If the difference between the two values exceeds 2% units when the average value is lower than 40, additional determinations should be made. This is also required if the difference exceeds 5% units and the average figure is higher than 40. The results are suitably given by filling in the same form as used for the liquid limit (Figure 8-9).

8.5.3 Reliability

The following possible sources of error may yield inaccurate results:

- Oxidation or drying. This applies especially to quick clays and sulphide clays.
- Insufficient kneading of the specimen. When rolling the specimen, the water content is reduced more in the shallow parts of the thread than in its central part and kneading is required to make it homogeneous.
- Errors when determining the water content.

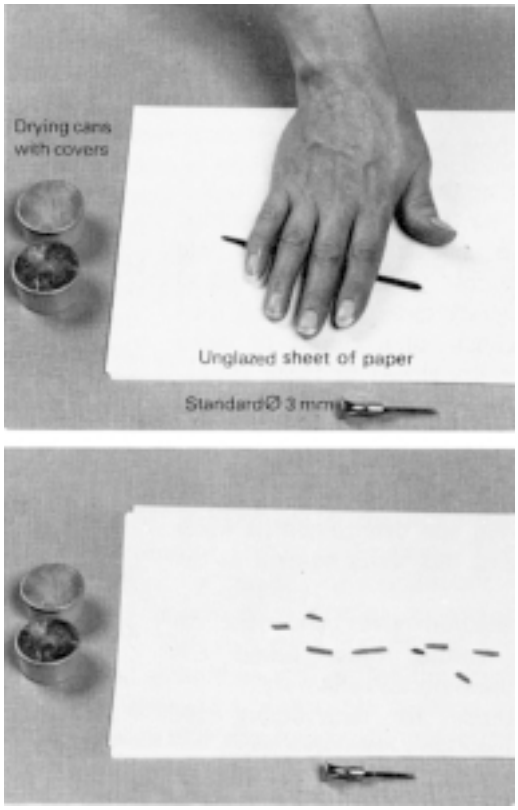

Figure 8-13. *Determination of the plastic limit. Upper: Rolling of sample. Lower: Required final state. Glazed sheets of paper may also be used.*

8.6 Shrinkage limit

8.6.1 Method principles

The Wintermayer method

Wintermayer et al introduced a method for determining the shrinkage limit that has been adopted as standard method by ASTM /6/. The determination is made on remoulded samples. To carry out the test, a so-called shrinkage dish of porcelain or other suitable material as well as a cylindrical glass cup with a cover consisting of a plane glass plate equipped with three metal prongs are required (Figure 8-14).

The moisture content of the remoulded sample is adjusted so that the sample becomes semi-liquid and it is then applied on the shrinkage dish, which should be coated with a film of grease. The sample is left to dry, first at room temperature and then in an oven, and is weighed before and after the drying. The volume of the dried sample is obtained by pressing it down into mercury in the glass cup by means of the glass plate and measuring the volume of the mercury that is thereby displaced.

The shrinkage limit w_S is calculated by means of Equation (8-7) or (8-8):

$$w_S = \frac{m - m_s - (V - V_d) \cdot \rho_w}{m_s} \cdot 100 \tag{8-7}$$

$$w_S = w - \frac{V - V_d}{m_s} \cdot \rho_w \cdot 100 \tag{8-8}$$

where:

m = mass of wet sample
m_s = mass of dry sample
V = volume of wet sample = volume of shrinkage dish
V_d = volume of dry sample
ρ_w = density of water = 1000 kg/m^3
w = water content of wet sample

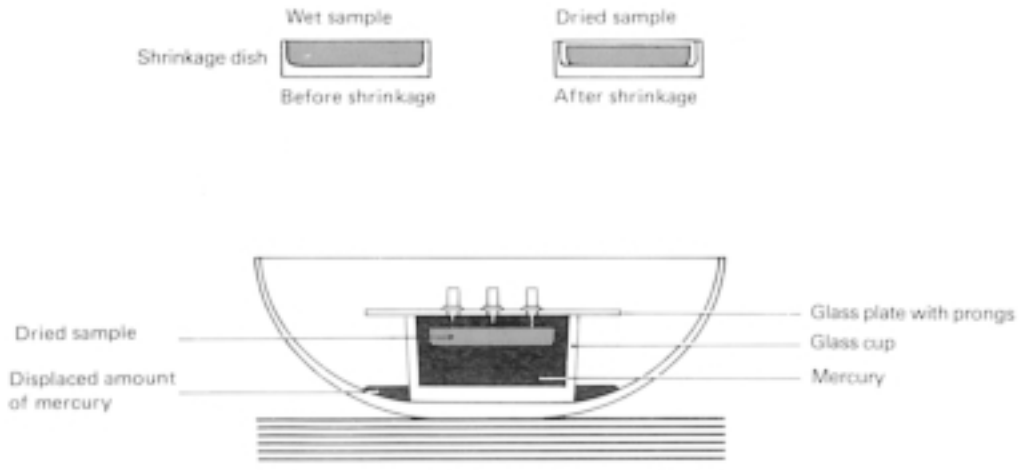

Figure 8-14. *Determination of the shrinkage limit according to ASTM method.*

The Lambe method

This method implies that one starts by preparing a sample with a plastic consistency and a round, flat shape /12/. The sample is dried and the volume determined in the way described above. In addition, the density of the minerals is determined by means of a pycnometer.

The shrinkage limit is derived by use of Equation (8-9):

$$w_s = \frac{\left(V_d - \frac{m_s}{\rho_s}\right) \cdot \rho_w}{m_s} \cdot 100 \qquad (8\text{-}9)$$

where:

ρ_s = density of the solid particles

The SGI method

A technique of general use was worked out by the Swedish Geotechnical Institute in the sixties. It makes use of the buoyancy of the sample when immersing it in paraffin oil. The volume of the wet sample is obtained by weighing it first in air, then in the oil, which is not soluble in water. The dried sample is coated with a thin layer of tap grease and then weighed in air and in distilled water.

The SGI method for the determination of the volume of the sample can also be applied for determining the void ratio or degree of saturation of fine-grained soils. The volume can be determined with great accuracy, even of specimens with an irregular shape. The method is described in detail here.

Equipment

- An electronic precision balance with 0.01 g accuracy, equipped with a hook for hanging samples.
- Sample holder of wire net with a loop by which it can be hung on the balance hook.
- Glass beaker containing ligroin or other oil that is insoluble in water.
- Glass beaker with distilled water.
- Evaporation disc.
- Tap grease (not silicon grease).
- Drying oven with thermostatic control. Temperature 105°C.

For determining the density of the ligroin, a hydrometer or a sinking body, which can be hung in the balance, is also required

Preparation of specimen

The determination of the shrinkage limit can be made on undisturbed as well as remoulded samples. They should have a diameter not larger than 50 mm and their height should be 20–40 mm.

Remoulded samples are suitably given the form of a sphere with a diameter of approximately 30 mm.

Performance

- Determine the density of the oil.
- Hang the sample holder in the balance and weigh the holder, first in air and then in oil.
- Place the soil sample in the holder and weigh sample + holder, first in air and then in oil.
- Weigh the evaporation dish and then place the soil sample in the dish. To prevent the sample from adhering to the dish, its base should be coated with a thin layer of grease.
- Let the sample dry at room temperature until it becomes lighter in color and then continue the drying in an oven for about a day.
- Weigh the evaporation disc with the dry sample.
- Coat the sample with a thin layer of tap grease.

It is important that the grease is applied evenly so that it covers the surface of the sample completely. Special attention should be paid to the covering of cavities and edges with grease.

- Weigh the sample holder in distilled water.
- Place the sample in the sample holder and weigh sample + holder, first in air and then in distilled water.

Evaluation

The volume of the wet sample is evaluated by means of Equation (8-10):

$$V = \frac{m - m'}{\rho_l} \tag{8-10}$$

where

V = volume of wet sample
m = mass of wet sample
m' = apparent mass of wet sample submerged in oil
ρ_l = density of oil (7600-7800 kg/m^3)

The volume of the dry sample is evaluated by means of Equation (8-11):

$$V_d = \frac{m_l - m_l'}{\rho_w} - \frac{m_l - m_s}{\rho_f} \tag{8-11}$$

where:

V_d = volume of dry sample
m_l = mass of dry sample + tap grease
m'_l = apparent mass of dry sample + tap grease submerged in distilled water
ρ_w = density of distilled water (1000 kg/m^3)
ρ_f = density of tap grease (900 kg/m^3)

The shrinkage limit w_S is calculated by means of Equation (8-12):

$$w_S = \left[\frac{m - m_s}{m_s} . \frac{(V - V_d) \cdot \rho_w}{m_s} \right] \cdot 100 \tag{8-12}$$

8.6.2 Reliability

Errors in the shrinkage limit values may be caused by the fact that shrinkage cracks have appeared in the sample in connection with the drying and by the fact that the layer of grease does not entirely cover the surface of the dried sample, which allows water to penetrate into the sample when weighing it in water.

8.7 References

/1/ **Atterberg A, 1911.** Lerornas förhållande till vatten, deras plasticitetsgrader och plasticitetsgränser (Relation of Clays to Water, their Degrees of Plasticity and Plastic Limits). Documents and Journal of the Royal Swedish Academy of Agriculture and Forestry, No. 2, p. 133–139, Stockholm.

/2/ **Atterberg A, 1916.** Konsistensläran – en ny fysikalisk lära (Consistency Science). The Swedish Journal of Chemistry, Vol. 28, p. 29–37, Stockholm.

/3/ **Casagrande A, 1932.** Research on the Atterberg Limits of Soils. U.S. Bureau of Public Roads, Vol. 13, No. 8, p. 121–130, 136.

/4/ **Wintermayer A M, Willis E A, Thoreen R C, 1931.** Procedures for Testing Soils for the Determination of the Subgrade Soil Constants. U.S. Bureau of Public Roads. Vol. 12, No. 8.

/5/ **Casagrande A, 1958.** Notes on the Design of the Liquid Limit Device. Harvard Soil Mechanics Series No. 57, Cambridge, Massachusetts.

/6/ **American Society for Testing Materials (ASTM), 1958, 1964.** Procedures for Testing Soils, Philadelphia.

/7/ **Public Roads, 1954.** Vol. 28, No. 3, p. 50–54 ("A Comparison of Rapid Methods for the Determination of Liquid Limits of Soils", by F.K. Olmstead & C.M. Johnston)

/8/ **Waterways Experiment Station (WES), 1949.** Correlation of Soil Properties with Geologic Information. Report No. 1. Simplification of the Liquid Limit Test Procedure, Vicksburg, Mississippi.

/9/ **Washington State Highway Dept, 1950.** Materials Laboratory Rep. No. 83. ("A Rapid Method of Determining the Liquid Limit of Soils", by J.H. Cooper & K.A. Johnson)

/10/ **Karlsson R, 1961.** Suggested Improvements in the Liquid Limit Test, with Reference to Flow Properties of Remoulded Clays. Proc. 5. International Conference of Soil Mech. a. Found. Engng. Vol. 1, p. 171–184, Paris.

/11/ **Hansbo S, 1957.** A New Approach to the Determination of the Shear Strength of Clay by the Fall-Cone Test. The National Swedish Geotechnical Institute. Proceedings, No. 14, Stockholm.

/12/ **Lambe T W, 1960.** Soil Testing for Engineers. Chap. III. p. 22–28, John Wiley & Sons, Inc., London.

9 Transport properties

This chapter deals with the migration of water by flow and ion migration by diffusion and with gas movement in buffers and backfills. Focus is on the meaning and determination of the hydraulic conductivity and of the ion diffusivity, expressed as the coefficients of apparent and effective diffusion. These parameters determine the rate and capacity of water transport through buffers and backfill as well as the transport of radionuclides.

9.1 General

From the viewpoint of design and performance assessment of repositories for radioactive waste one is primarily interested in the transport of corrodants and toxic elements in buffers and backfills which makes the following properties important:

- Hydraulic conductivity
- Gas conductivity
- Ion diffusivity rate and sorption capacity

Thermal conductivity is also an essential property; it is dealt with in the subsequent Chapter 10 on Thermal Properties.

9.2 Hydraulic conductivity

9.2.1 Definition of hydraulic conductivity, *K* [m/s]

Darcy's law is applied for the evaluation of ordinary percolation tests and for calculating flow through soils:

$$v = \frac{q}{A} = K \cdot i \qquad (9\text{-}1)$$

where

v = average flow rate [m/s]
q = amount of percolated fluid per time unit [m^3/s]
A = cross section area [m^2]
K = hydraulic conductivity [m/s]
i = hydraulic gradient, i.e. the pressure drop over the length of the percolated sample [m/m]

The *hydraulic conductivity K* is related to the (intrinsic) permeability *k* according to Equation (9-2):

$$k = \frac{K\mu}{\rho g};\ K = \frac{k \cdot \rho \cdot g}{\mu} \qquad (9\text{-}2)$$

where:

μ = dynamic viscosity [kg/m,s]
ρ = fluid density [kg/m^3]
g = acceleration of gravity [m/s^2]

Another common expression in groundwater hydraulics is the *transmissivity*, which means the rate at which water is transmitted through a unit width of geological material under a unit hydraulic gradient. It is defined as in Equation (9-3) and is expressed in m^2/s:

$$T = Kb \qquad (9\text{-}3)$$

where b = thickness of the sample or layer.

9.2.2 Microstructural implications

A major factor that influences the rate of water flow through soils is the size of the voids. The smaller the particles, the smaller the voids and the stronger the flow resistance. This is manifested by Figure 9-1, which refers to ordinary natural soils with no or very little content of smectite minerals.

Since the clay component of buffers and backfills is of primary concern, we will focus on the general relationship between the microstructural constitution and the hydraulic conductivity. It is clear that the common features of aggregation of clay-sized particles and the typical spectrum of void size in both natural and artificially prepared clayey soils imply non-uniform transport rates across a section of the soil.

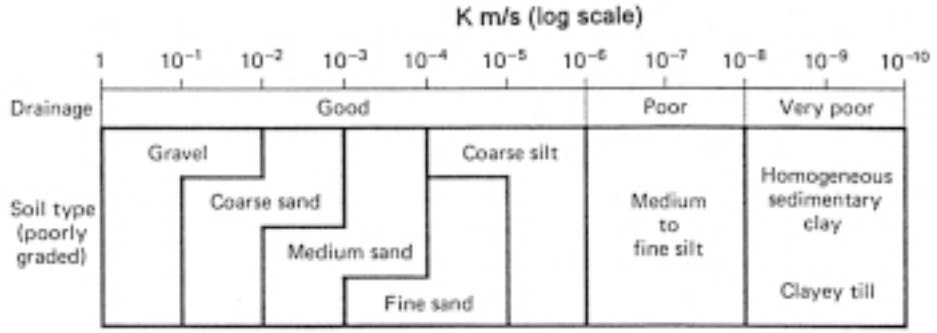

Figure 9-1. *Typical values of the hydraulic conductivity of ordinary soil types /1/.*

One way of quantifying this is to use transmission electron micrographs (TEM) for evaluating the void size expressed in terms of their largest diameter a_p and the fraction of the total area T that is made up by the void area P (Figure 9-2), /2/.

The extreme thinness of the ultramicrotone-cut sections (200–500 Å) means that they can be interpreted as two-dimensional sections. Voids smaller than a few hundred Å may hence remain unrevealed in the micrographs, which is of no significance. Typical median a_p-values for clays with a bulk density in saturated state ranging between

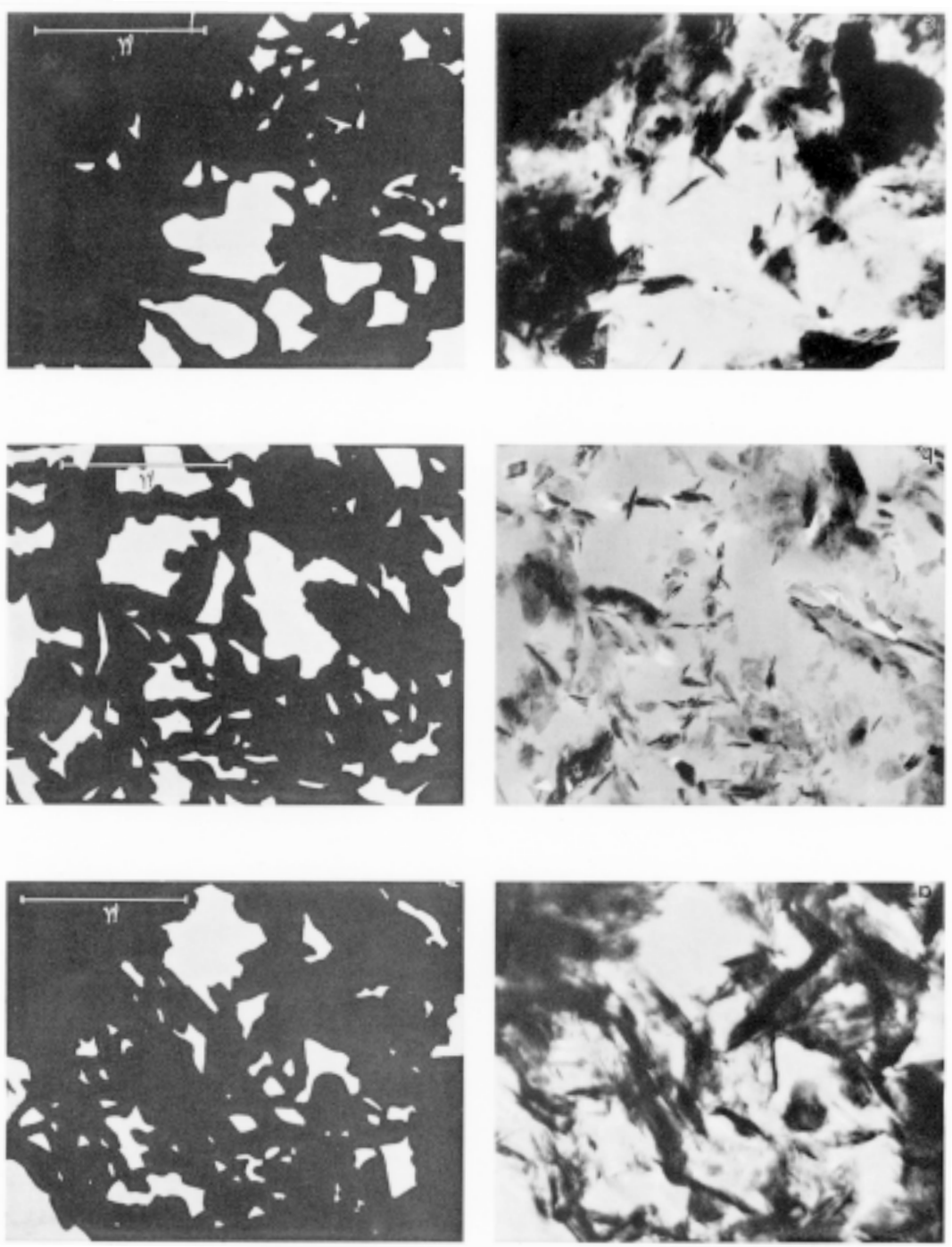

Figure 9-2. *TEM pictures and generalized two-dimensional sections of soft illitic clay for evaluation of the "two-dimensional porosity" and the void size /2/.*

1500 and 2200 kg/m^3 is 0.11–0.30 μm and *P/T* = 1.5–70% /2,3,4/. The latter parameter is rather well correlated with measured hydraulic conductivity as shown by Figure 9-3. One also finds that the stronger aggregation ("coagulation") and associated larger voids in marine clays than in fresh-water clays of similar density is manifested by higher *P/T* of the former (Figure 9-4). Brackish-water clays are intermediate in this respect. The same influence of the electrolyte content is also observed for smectite clays. The conductivity plotted in Figure 9-3 was simply evaluated as the ratio of the amount of percolated water per time unit at a known pressure gradient and defined cross section area, i.e. by considering what fraction *P* of the total cross section *T* that is really permeated.

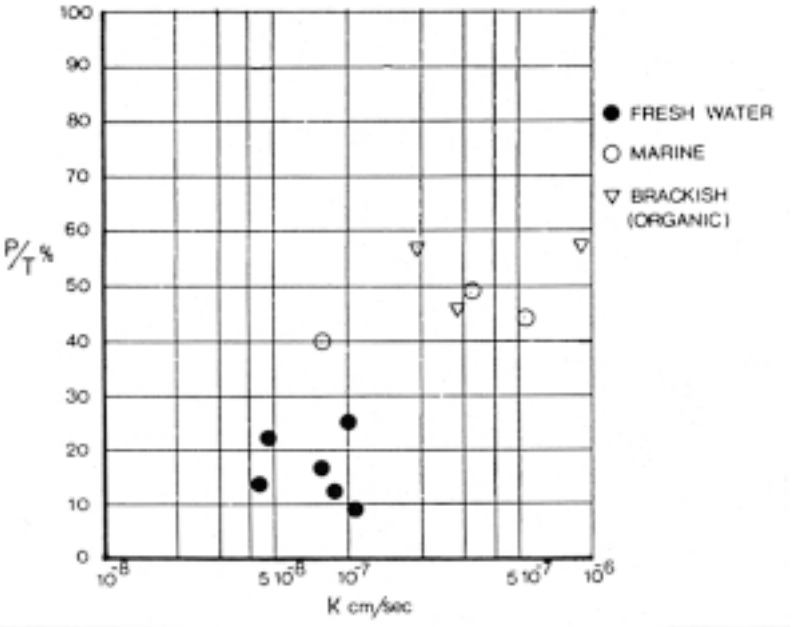

Figure 9-3. *P/T versus hydraulic conductivity of natural illitic clays /3/.*

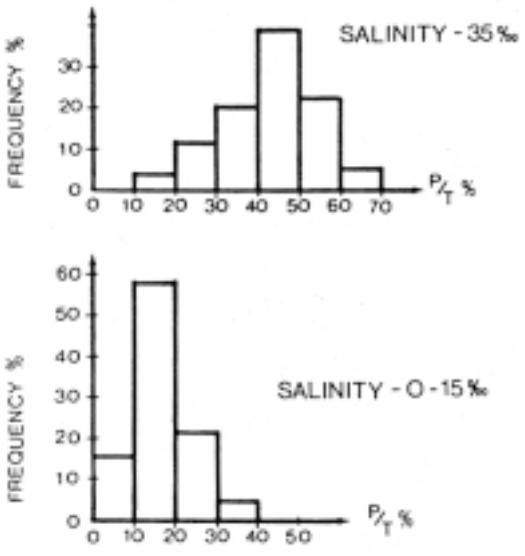

Figure 9-4. *P/T for different salinity of illitic clays /4/.*

In practice, the uniformity and rate of the percolation vary strongly according to the microstructural pattern and both frictional resistance and tortuosity combine to yield almost stagnant porewater in large parts of the clay matrix and local flow paths in which the flow rate is very high. This is particularly obvious in smectite-rich buffers, for which microstructural flow models have been proposed for illustrating the importance of density and porewater chemistry. They suggest a stochastic character of the microstructural constitution in the fashion illustrated by Figure 9-5, i.e. with impermeable granules and a permeability of the clay gels in the voids that is controlled by their density.

This, and later developed more advanced models, include evolution of the microstructure from the initial stage of powder compression, via hydration to the permeation stage, in which altered porewater chemistry can change the microstructural constitution and thereby the hydraulic conductivity. The models will be described in detail in Part 3 of this Handbook. Here, we will only show that they can explain and quantitatively describe the detailed performance of smectite clays /6/.

The compacted clay material consists of powder grains in close contact with air-filled voids between, and hydration of the clay takes place by capillary suction and adsorption of water molecules in the interlamellar space and on external surfaces of the stacks of lamellae. Penetration of water into the strongly hydrophilic powder grains causes exfoliation of their shallow parts, which disintegrate and reorganize to form soft gels in the open voids. The gels are consolidated by the expanding dense grains but complete homogeneity is not obtained. Hence, the voids between the expanded grains will be filled with clay gels with a density that is low in the largest voids and high in the smallest voids (Figure 9-5). The gel-filled voids combine to form continuous channels that are responsible for the bulk hydraulic conductivity.

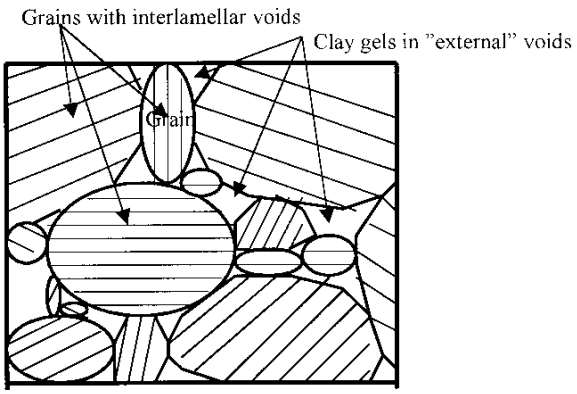

Figure 9-5. *Schematic picture of compacted sample of grains of smectite clay for preparing buffer material. The internal oriented structure of the grains, inherited from the natural clay beds where the clay was extracted, is at random except for very high uniaxial compression. After hydration the voids become filled with clay gels emanating from the expanded and deformed grains. The gel density varies depending on the void size.*

The flow rates through a cross section of buffer clay can be derived from the GMM model /5/ and such calculations show that the flow is not uniformly distributed and that the flow rate varies much as demonstrated by Figure 9-6.

Digitalization of transmission electron micrographs of ultrathin sections of suitably prepared, water saturated clay specimens verifies that the microstructure is heterogeneous as illustrated by Figure 9-7.

A practical way of quantifying microstructural heterogeneity is defined in Figure 9-8, where *a* represents the clay matrix (I in Figure 9-7), and *b* the soft gel and open space in the channels (IV in Figure 9-7).

F_2 and F_3 can be evaluated from digitalized TEM micrographs with different degrees of greyness representing different densities. Depending on the scale, *a* or *b* may dominate.

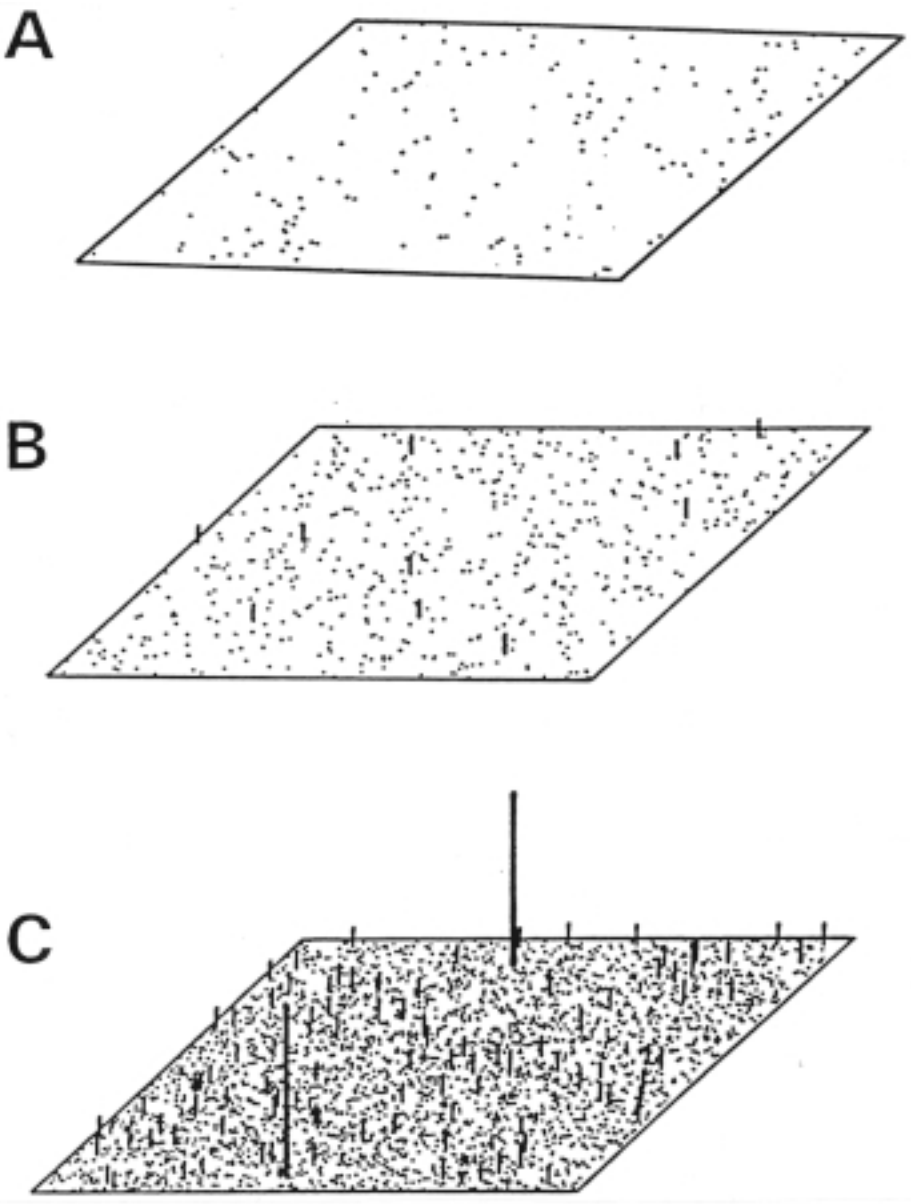

Figure 9-6. *Flow rates. Dots: In 1–5 μm gel-filled voids, Short bars: In 5–20 μm voids, Long bars: in 20–50 μm voids, (250 x 250 μm element), /5/.*

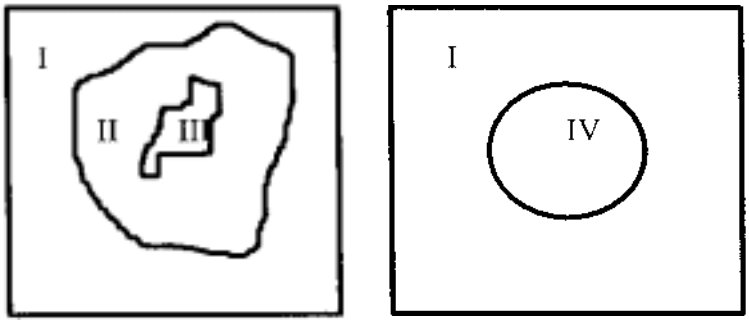

Figure 9-7. *Schematic micrographs. Left: Typical picture of ultrathin section with varying density in soft matrix region (I to III). Right: normalized picture with defined channel cross section and density of the clay gel in the channel (IV) and of the clay matrix (I).*

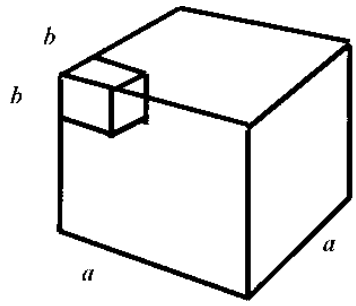

In 2D: $F_2=b^2/a^2$ $\quad b=a(F_2)^{1/2}$

In 3D: $F_3=b^3/a^3$ $\quad F_3=F_2(F_2)^{1/2}=(F_2)^{3/2}$ $\quad \rho_{av}=\rho_b F_3+\rho_a(1-F_3)$

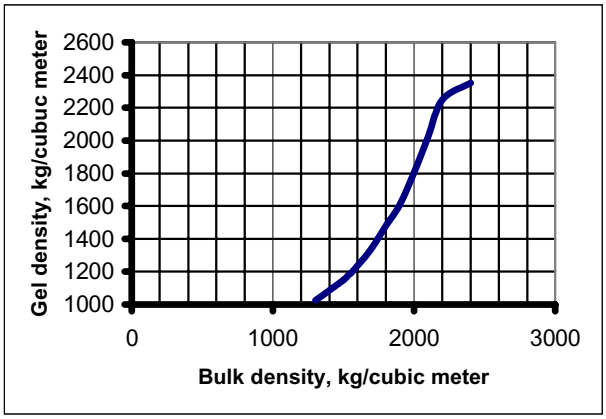

Figure 9-8. *Microstructural parameters is the average bulk density ρ_{av} of the clay and the average density of components a (impermeable clay matrix) i.e. ρ_a, and b (soft gel fillings and open space), i.e. ρ_b. The diagram shows the average gel density versus average bulk density for smectite-rich Na bentonite.*

Calculation of the bulk hydraulic conductivity of the heterogeneous clay can be made by applying basic flow theory, taking a permeated clay section to consist of a system of elements with different hydraulic conductivity. Using relevant *F*-parameter values one gets theoretical hydraulic conductivities that agree well with experimental data as illustrated by Table 9-1.

Table 9-1. Microstructural data and conductivities for MX-80 in Na form, percolation with distilled water /6/.

Bulk density, kg/m³	F_2	Gel density, kg/m³	Gel conductivity, kg/m³	Theor. bulk conductivity m/s	Experim. bulk conductivity m/s
2130	0.17	2000	7E-14	E-14	2E-14
1850	0.24	1650	2E-12	4E-12	3E-12
1570	0.80	1200	E-10	8E-11	8E-11

In practice, almost all water flow takes place within three-dimensional networks of gel-filled channels with stochastic properties (Figure 9-9). The channels, which represent the zone termed IV in Figure 9-7, are characterised by their lengths, widths, apertures and transmissivities. The clay matrix is assumed to be porous but impermeable. The basis of the development of the present model is the code 3Dchan /7/.

Calculation of the bulk hydraulic conductivity can be made by assuming that a certain number (commonly 6) of channels intersect at each node of the orthogonal network and that each channel in the network consists of a bundle of *N* capillaries with circular cross section.

The code generates a certain number of channels for a given volume, and using the Hagen-Poiseuille law the flow rate through the channel network is calculated for given boundary conditions assuming a pressure difference on the opposite sides of the cubic grid and no flow across the other four sides. This model version also yields reasonable agreement with experimental data and serves to illustrate that the true flow path system can be understood as a 3-dimensional networks of gel-filled channels.

As to the influence of porewater electrolytes, the interlamellar spacing is not or very little affected by the cationic strength as demonstrated by X-ray diffraction analysis (XRD) tests on montmorillonite soaked with water that has a salinity of approximately that of the oceans. At much higher electrolyte concentrations, for example if montmorillonite clay is contacted with brines, the interlamellar spacing may be reduced due to dehydration /5/.

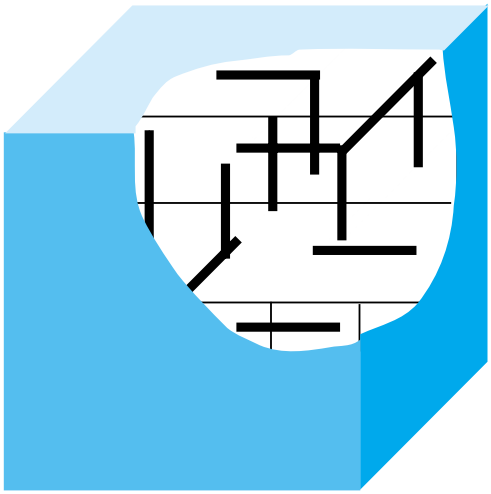

Figure 9-9. *Schematic view of the 3D model concept. Network mapped as a cubic grid with channels intersecting at a node in the grid /7/.*

9.2.3 Influence of hydraulic gradient and prewater chemistry

Very careful measurement of the hydraulic conductivity tends to show deviations from Darcy's law (Figure 9-10). Thus, at very low hydraulic gradients there is practically no flow, a phenomenon that may be due to thixotropic stiffening of water films in and adjacent to clay aggregates and coagulation of clay gels when no gradients prevail, and to breakdown and softening of the films and the gels when shearing caused by the fluid flow takes place /8/.

Experiments have shown that a water pressure of several hundred kPa applied to initially incompletely water saturated, dense smectite clay will only fill major channels with water and that this process only reaches a few centimeters into the clay /9/. After a few minutes no more water enters the clay in this quick fashion because expansion of the clay matrix surrounding the water-filled voids closes the channels and because particle aggregates released by the inflowing water become transported to constrictions of the channels where they accumulate and cause a drop in hydraulic conductivity. Such experiments demonstrate how comprehensive and quick microstructural changes can be.

High flow rates can cause erosion of water saturated and unsaturated clay (Figure 9-11), a critical rate being E-3 m/s for tearing off and transporting 0.5 μm particles, E-4 m/s for 1 μm particles, E-5 m/s for 10 μm particle aggregates, and E-7 for aggregates larger than 50 μm, as evaluated from physical models and experiments /9/. FEM calculations have shown that the flow rate in large channels in the clay matrix is on the order of 2E-6 m/s for a hydraulic gradient of 100, which is a common value in laboratory

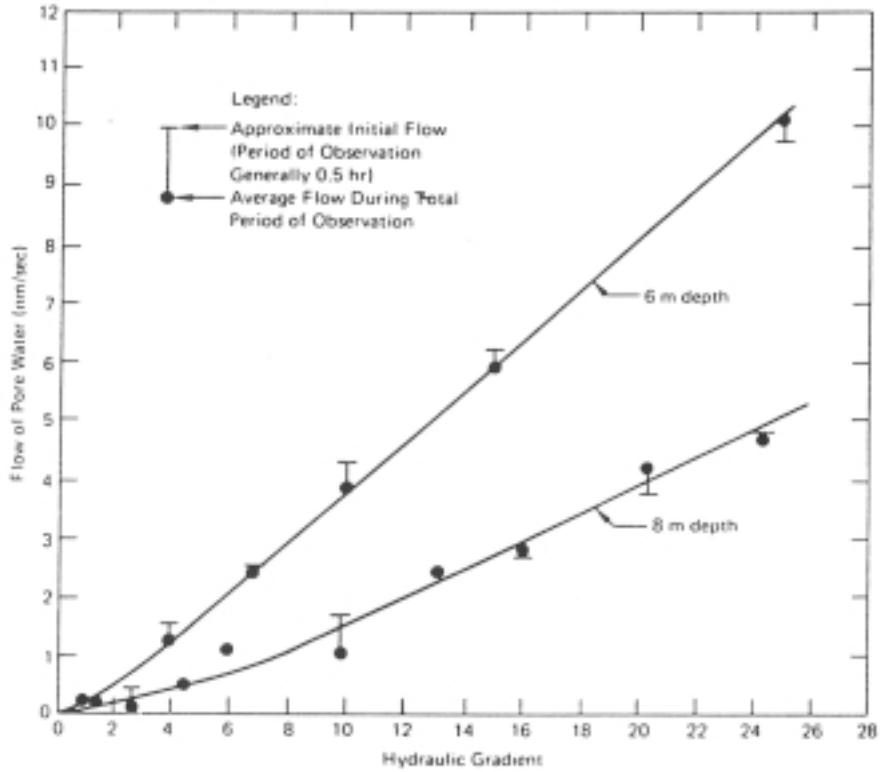

Figure 9-10. *Dependence of flow velocity on hydraulic gradient. Undisturbed soft illitic clay from Skå Edeby, Sweden /8/.*

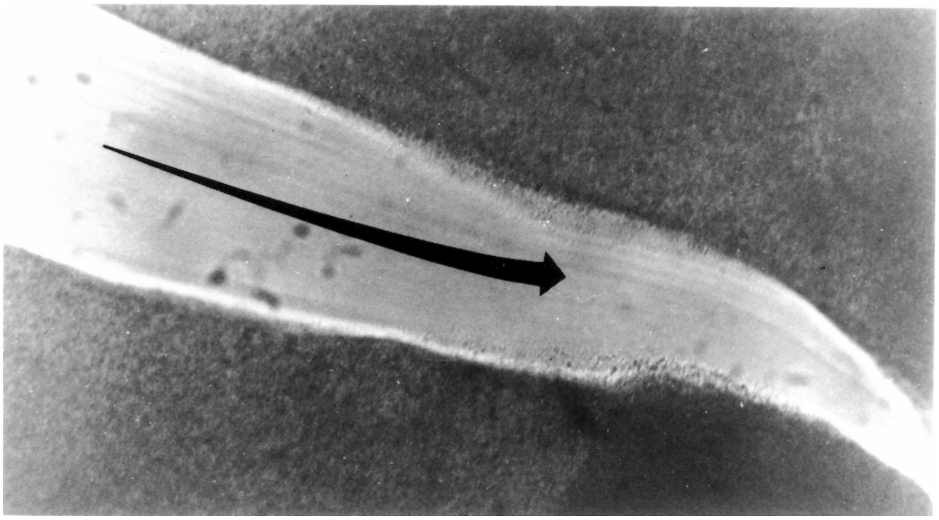

Figure 9-11. *Piping in the form of a hydraulic wedge penetrating into soft clay matrix. 20–50 μm smectite aggregates are moved by the flow (E-4 m/s) /10/.*

experiments. Hence, disruption of soft clay gels and migration of small particle aggregates may well take place at laboratory testing as well as in early hydration stages of buffers and backfills in a repository. This is verified by Figure 9-12, which shows the change in conductivity at reversed percolation of MX-80 clay with 3.5% $CaCl_2$ solution even at a moderate hydraulic gradient. The change can be interpreted as an initial increase in conductivity in conjunction with piping and erosion and a subsequent drop in conductivity because of accumulation of transported particles at channel constrictions where clogging takes place.

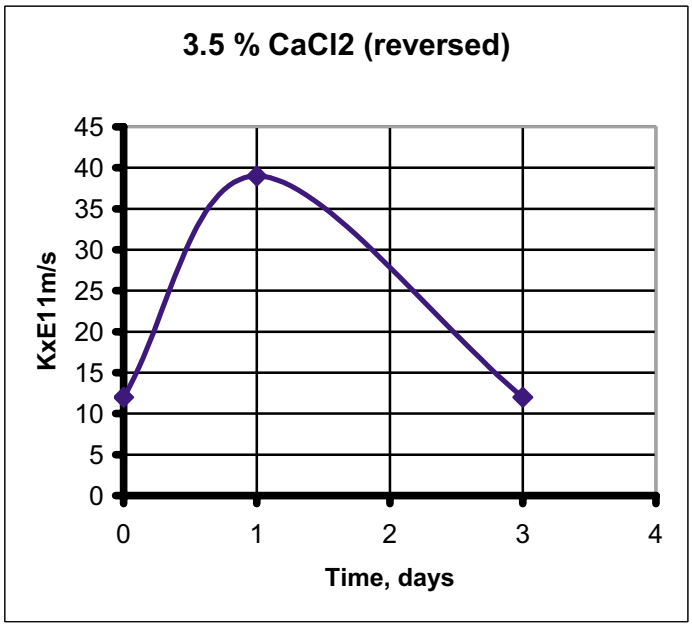

Figure 9-12. *Change in hydraulic conductivity after reversing the flow direction at percolation with 3.5% $CaCl_2$ solution of smectitic clay with a density of 1800 kg/m^3 under a hydraulic gradient of 30.*

The conceptual structural model of clay formed by compacting smectite-rich, dry grains with subsequent hydration implies that the clay does not become homogeneous but contains interconnected voids filled with clay gels of lower density than the rest of the clay matrix. Taking micrograph-derived structural parameter data as a basis and applying flow theory for heterogeneous media the calculated bulk hydraulic conductivity is about the same as the experimental. It is determined by the volume fraction and continuity of permeable parts of the microstructure, i.e. soft and medium-dense clay gels. For soft clays, especially for Ca-bentonite, the model exaggerates the conductivity, a plausible explanation being poor microstructural stability, which causes erosion, transport and accumulation of particles yielding clogging of voids and reduction in conductivity. The presence of soft parts explains why water under relatively high pressure can penetrate to a few centimeters depth in partly water saturated clay and why gas makes its way through channel-like paths in saturated clay.

Gas penetrates clay where it can displace porewater most easily, which is where it hits voids containing soft clay gels. It passes through them and proceeds through the dense matrix like in Figure 9-11. The gas pressure required to make the gas penetrate the dense matrix is on the order of the swelling pressure.

A very important phenomenon is the microstructural rearrangement caused by percolation of fluids that change the original porewater chemistry (Table 9-2). Thus, if calcium chloride solution is percolated through a Na smectite, coagulation will take place parallel to the percolation by which the conductivity is successively increased /5,10/.

A special case of practical importance in repository design is the fact that heating of buffers affects the microstructure and thereby the hydraulic conductivity. The porewater pressure is strongly increased on heating and the granules of the not fully homogenized bentonite clay become exposed to thermally induced stresses and undergo some disintegration by which the clay becomes more homogeneous. A temperature cycle to a moderate maximum temperature under fully water saturated conditions therefore tends to yield a net average reduction of the hydraulic conductivity after cooling as indicated by Figure 9-13. The increased conductivity recorded for the temperature rise from 20 to 130°C is caused by the reduced viscosity of the porewater /5/.

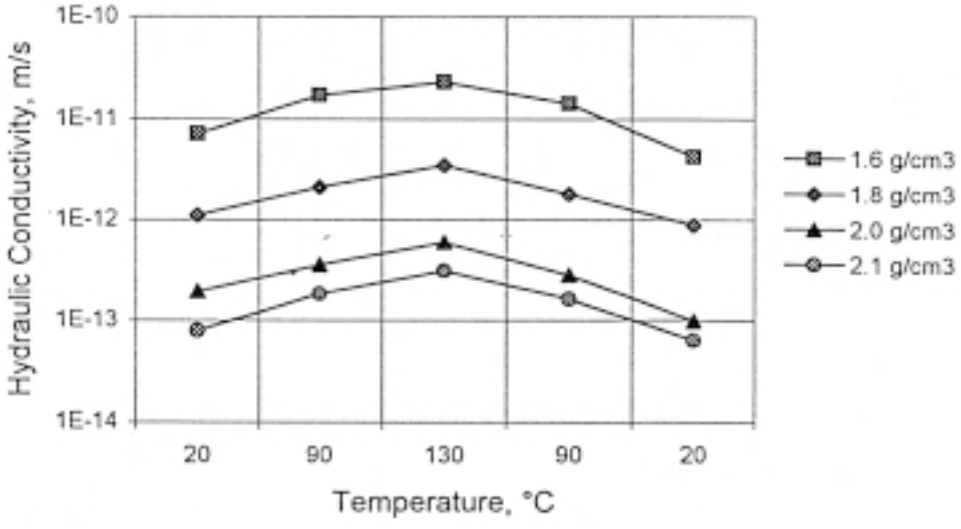

Figure 9-13. *Example of change in hydraulic conductivity by heating of Na bentonite clay saturated with distilled water /5/. The rise at heating is because of the reduced viscosity and the drop of the conductivity after cooling to a lower value than the original is because of improved microstructural homogeneity.*

Table 9-2. Hydraulic conductivity of bentonite grout /10/.

Density ρ kg/m³	Percolate	Hydraulic conductivity m/s
1080		
Na state	Distilled water	3E-9
	Ca-rich, brackish water	5E-7
	Seawater diluted by 50%	5E-7
1120		
Na-state	Distilled water	3E-9
	Ca-rich, brackish water	5E-7
	Seawater diluted by 50%	E-8
1330		
Ca-state	Na-rich, brackish water	3E-8
	Ca-rich, brackish water	5E-8

9.2.4 Influence of the mineral content

The degree of isolation of canisters in a repository depends primarily on the hydraulic conductivity of the buffer clay, which is strongly dependent on the mineral composition. The large fraction of interlamellar, immobile water in smectites yields a much lower hydraulic conductivity than of soils with other minerals at any bulk conductivity. Thus, clays with hydrous mica ("illite") and kandites (kaolinite, dickite) as major minerals are about 100 to 100 000 times more conductive than smectite in montmorillonite form (M) at one and the same void ratio. Till (moraine) with no clay minerals is much more permeable than clayey soil even at very high densities. A fact is that smectite clay gels of very low density are remarkably tight, which, in combination with their thixotropic behaviour, make them useful as grouts for sealing rock fractures.

The data in Table 9-2 were obtained from laboratory tests with bentonite with a smectite content of 80–90% and even lower values are obtained for clays with pure smectite. Correspondingly, lower contents of smectite increases the conductivity, which is the case for backfills prepared by mixing clay and ballast material. This matter will be discussed in detail in Part 2 of this Handbook.

9.3 Gas conductivity

9.3.1 General mechanisms

Gas under pressure makes its way through clays in two fashions: by diffusion of dissolved gas and by penetration in gaseous form. Diffusive transport is very slow and since the solubility of gases of interest in repository design and performance assessment is low, penetration in gaseus form is the mode of transportation that one needs to consider. It takes place in the form of finger-like penetration at a critical pressure (p_c) that is akin to that of capillary tubes although the process is much more complex in clays. Still, one can get an approximate picture of p_c by comparing the clay void system with quartz capillaries (Table 9-3).

Table 9-3. Theoretical critical pressures (p_{ct}) of the GMM reference clays A, B and C, and actually measured critical pressures (p_{cm}), /5/.

Clay	Bulk dry density kg/m³	Critical pressures, MPa p_{ct}	p_{cm} (aver)
A	1800	15–30	20
B	1350	3–6	2
C	900	3–5	0.1

In practice, gas makes its way by displacing water and soft clay gels from the largest "external" voids that remain after homogenization of the clay. At high clay densities the pressure must be sufficient to overcome the contact pressure of adjacent stacks of flakes. This would imply that the required pressure to get gas through is on the same order of magnitude as the swelling pressure (Chapter 11). This is often but not always the case.

9.4 Ion diffusivity

9.4.1 Mechanisms and basic relationships

Diffusion of ions through clayey soils is affected by several physical and chemical processes, such as ion exchange, physical and chemical adsorption, filtration, and precipitation. A common way to describe the diffusion process for ions migrating through compacted clay /11,12,13/, is to use the apparent diffusivity D_a expressed as a function of the distribution coefficient (K_d) as expressed by Equation (9-4):

$$D_a = \frac{D_p \cdot n}{n + K_d \rho_d} = \frac{D_e}{n + K_d \rho_d} \tag{9-4}$$

where:

D_a = apparent diffusivity (m² /s)
D_e = effective diffusivity (m²/s)
D_p = diffusivity in pores (pore diffusivity) (m² /s)
D_s = surface diffusivity (m² /s)
n = porosity
ρ_d = dry density (kg/m³)
K_d = distribution coefficient (m³/kg)

The fact that the apparent diffusivity can be higher for certain cations is explained by the different sorption ability of different species. It is assumed that diffusion takes place not only in the void system of the soil, but also in the form of surface diffusion. Fick's second law, Equation (9-5), gives the general expression for the concentration profile at position x and time t:

$$\frac{\partial C}{\partial t} = D \frac{\partial^2 C}{\partial x^2} \tag{9-5}$$

where:

D = diffusion coefficient
C = concentration of dissolved element

Because of the cation adsorption characteristics of clay, cations can migrate through both large pores and very narrow voids, including the interlamellar space of smectite clay, while anions are excluded from the micropores by Donnan potential and migrate only by pore diffusion through macropores. Probably, diffusion of cations in water is more or less hindered in very small voids because of the strong adsorption capacity of the exposed minerals. Thus, surface diffusion is assumed to dominate in these voids /6,13,/.

Assuming that the concentration of ions in solution is so low that the linear adsorption isotherm can be applied ($C_s = K_d\rho_d C$), Equation (9-5) can be written as:

$$\frac{\partial C}{\partial t} = \frac{D_e n + K_d \rho_d D_s}{n + K_d \rho_d} \frac{\partial^2 C}{\partial x^2} \tag{9-6}$$

$$D_a = \frac{D_e n + K_d \rho_d D_s}{n + K_d \rho_d} \tag{9-7}$$

where:

C_s = concentration of species in the film adsorbed on the mineral surfaces (kg/m^3)
D_s = surface diffusivity (m^2/s)
D_a = apparent diffusivity (m^2/s)

The true fashion in which cations migrate through smectitic clay is not fully understood and only a simplified description is given here.

For anion diffusion, the distribution coefficient is negligible ($K_d\rho_d \approx 0$) because of the dominant cation adsorption characteristics of the clay.

Furthermore, the pore diffusivity (D_p) is affected by various soil properties such that one has /6,14/:

$$D_p = (\tau)^2 \alpha D_w = f D_w \tag{9-8}$$

$$f = (\tau)^2 \alpha \tag{9-9}$$

where:

τ = tortuosity factor
α = viscosity factor
D_w = intrinsic diffusivity (m^2/s)
f = impedance factor

The intrinsic diffusivity represents the motion of an ion in an infinite solution and is given by the Nernst-Haskess equation /15/. Since, for cations, the value of the factor $K_d\rho_d$ is commonly much higher than the porosity, one can put the diffusion equation for cations in the following form:

$$D_a = \frac{D_e n}{K_d \rho_d} + D_s = \frac{f D_w n}{K_d \rho_d} + D_s \tag{9-10}$$

9.4.2 Dependence of soil density

Figure 9-14 shows a typical set of relationships between ion diffusivity and dry density. The apparent diffusivity of chlorine is highest, while the effective cation diffusivity, expressed as the product of the pore diffusivity and true porosity, is smallest. The apparent diffusivity of cations drops with increasing density, which can be explained by the increase in the fraction of immobile cations on the clay surfaces when the water content drops /6,14,16/. It has been stated that improved linking of the double-layers of adjacent particles would yield an *increase* in diffusivity, but this appears to be of insignificant importance.

The effect of density is greater when the cation has a lower valency and a larger radius, which means that Cs, which is monovalent and larger than the divalent Sr, responds most strongly to the increase in density. Table 9-4 gives characteristic parameter data for Cs-137 /14/.

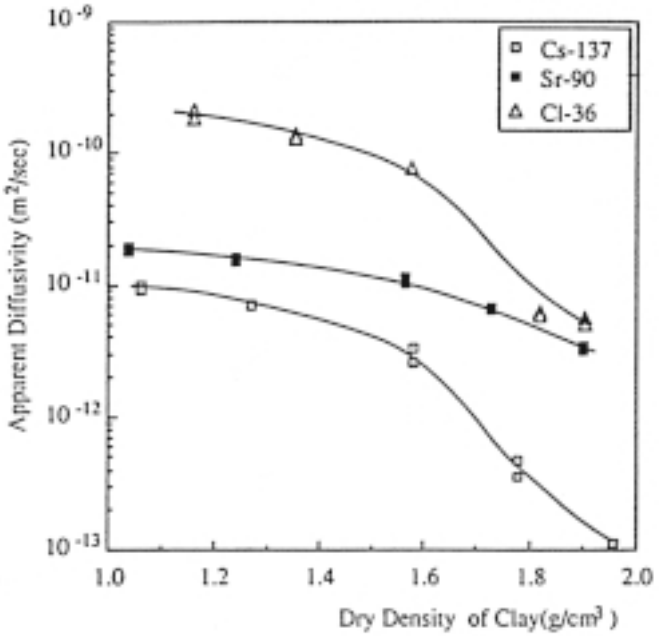

Figure 9-14. *Diffusivity of radionuclide ions with increasing dry density of clay /14/.*

Table 9-4. Diffusion parameters for Cs-137[1] /14/.

ρ, kg/m³	D_a, m²/s	D_e, m²/s
1060	E-11	9.8E-12
1270	7.2E-12	7.1E-12
1580	3.2E-12	3.2E-12
1780	4.7E-13	4.7E-13
1960	1.1E-13	1.1E-13

[1] K_d = 0.66 m³/kg

An increasing number of scientists tend to claim that surface diffusion of cations dominates over pore diffusion, while anion diffusion is generelly believed to take place only as pore diffusion. The matter is not fully cleared out and is further treated in Part 2 of this Handbook and in conjunction with modeling also in Part 3.

9.4.3 Unsaturated conditions

Hydraulic conductivity

Flow through unsaturated soil is transient and very complex and cannot even be defined if percolation is associated with microstructural changes, which is usually the case. Simple empirical expressions of unsaturated flow have been derived as the Darcy coefficient corrected with respect to the degree of water saturation as will be discussed in Part 3 of this Handbook.

Ion diffusivity

The idea that surface diffusion may be a major process in clays with high electrostatic potential like smectites would suggest that diffusion of cations is significant even at low water contents but not in air-dry clay. This can be illustrated by recording the electrical conductivity, which is a measure of the surface diffusivity for material with low matrix conductivity, like tuff and most silicates (Figure 9-15).

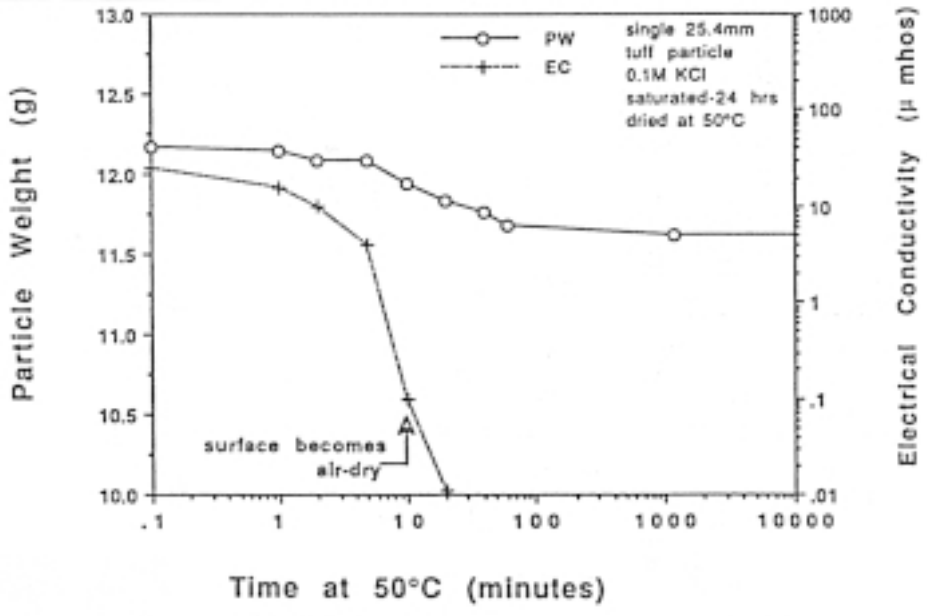

Figure 9-15. *Effect of desaturation on conductivity and, hence, surface diffusivity in porous media /17/. PW is a measure of the water content of the tuff particle, while EC is the electric conductivity.*

9.5 Gas diffusivity

Pressurized gas diffuses in dissolved form through soil if the gas pressure is low enough compared to the fluid pressure. In gas percolation experiments, the fluid pressure must therefore be sufficiently high to prevent gas from forming bubbles, which may block pores. The diffusion coefficient of dissolved nitrogen (N_2) gas in water is about 1.9 x 10^{-9} m^2/s at room temperature, while that of hydrogen (H_2) is about 4.5 x 10^{-9} m^2/s.

9.6 Experimental

9.6.1 Hydraulic conductivity

General

For design and performance assessment of buffers and backfills in repositories one is primarily interested in getting representative data on the hydraulic conductivity from laboratory experiments, for which the following criteria should be fulfilled:

- Steady state conditions must prevail.
- The flow rate must be sufficiently low to yield laminary flow and not cause piping and erosion.
- The pressure at the high-pressure end must not cause compression, i.e. consolidation of the entire sample.
- Both the inflow and the outflow must be recorded and be the same.
- Backpressure should be applied for giving complete water saturation.
- Constant temperature conditions must prevail.

The first criterion means that a sufficiently long time must pass before readings are taken. The second and third criteria are very important in testing smectite-rich clays since high pressures are commonly required to get measurable quantities of fluid through in reasonable time periods. The fourth criterion is important because recording of the flow at both ends of the sample reveals possible leakage in the tubing system. The fifth criterion is important since testing with pressure at one end may create undefined pore pressure conditions at the outflow end. The sixth condition is important when measuring flow through dense smectite clays both because the equipment, i.e. tubings, pressure gauges etc, are temperature sensitive and because the viscosity of the water is strongly affected by heat.

Technique

Measurement of the hydraulic conductivity of buffers and backfills is performed by use of permeameters – usually swelling pressure oedometers – in which the samples are prepared and exposed to fluid pressure at both ends for assuring complete saturation with the desired fluid before the hydraulic conductivity is determined. (Figure 9-16). For this purpose, the pressure at one end is increased stepwise and the amount of percolated fluid measured by using flow meters or burettes. The diameter of the permeameter should be at least 10 times the maximum grain diameter.

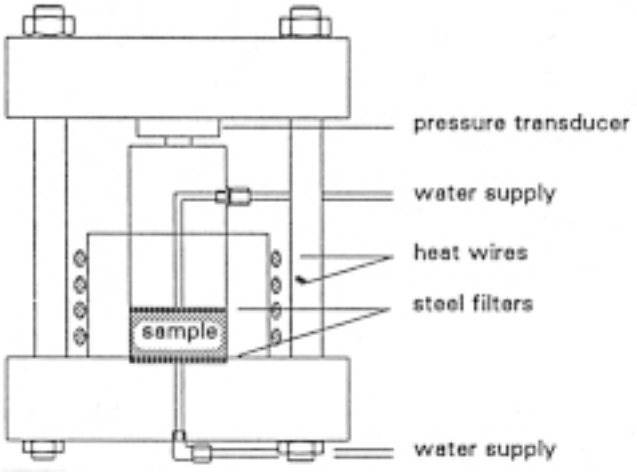

Figure 9-16. *Hydraulic conductivity can be determined by use of the swelling pressure oedometer /5/. The diameter of the sample is commonly 20–50 mm.*

The risk of leakage along the contact between sample and sample holder is not negligible and various methods have been used for avoiding it. One way is to use filters that are smaller than the base area of the sample. The triaxial apparatus (cf Chapter 11) can also be used for conductivity measurements using samples prepared and saturated in oedometers and encased in a rubber membrane. However, since the cell pressure must exceed the applied water pressure compressible samples will undergo consolidation.

For investigation of scale-dependence, larger permeameters have to be used. Figure 9-17 illustrates a "megapermeameter" used for investigating backfills consisting of mixed bentonite and ballast material with a maximum grain size of about 20 μm. The preparation of soil mixtures and application and compaction of them in the permeameter must be made in a fashion that is relevant to the construction procedure on site. It is very important to arrange sealings along the wall and the soil to avoid leakage. Also, the strain of the device must be kept at an absolute minimum in order to maintain constant density and continuous contact with the filters. This requires a rigid beam arrangement for maintaining constant volume of the sample.

Sample preparation

The preparation of clay materials as buffers and backfills depends on what form the material will have in the repository. For buffers in the form of precompacted blocks, one can either trim small samples from the large blocks prepared on an industrial scale or compact clay powder directly in the oedometer.

Composition and preparation issues are dealt with in Part 2 of this Handbook.

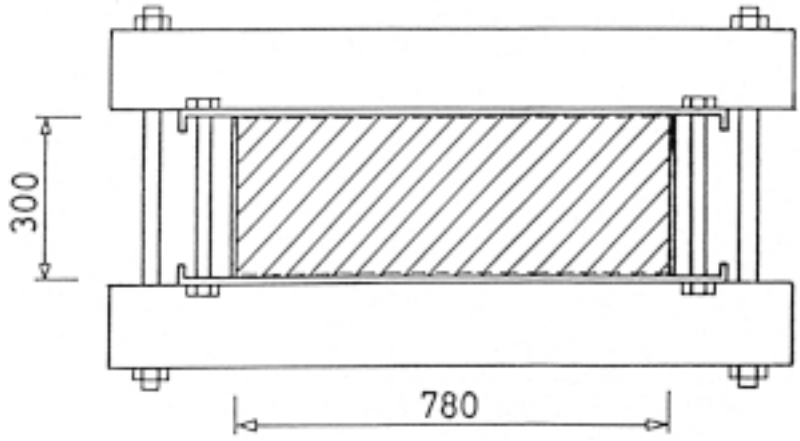

Figure 9-17. *Megapermeameter. The soil confined by filters (broken lines) at the basal surfaces, is shown hatched in the figure (dimensions in mm) /18/. The sample was produced by layer-wise application and compaction.*

Equipment

- Swelling pressure oedometer of the types shown in Figures 9-16, 9-17.
- Soil in desired form, usually air-dry.
- Pressure vessels for producing fluid pressure on the inflow side and backpressure at the outflow end.
- Fluid of desired composition.
- Flow meter (GDS equipment or direct reading of meniscus in burettes).

Performance

- The soil is applied layer-wise in the permeameter and compacted to the intended dry density and the permeameter is then tightly closed.
- The flow meter is applied in the tubing system and tested for making sure that no leaks exist.
- For determining the conductivity at complete water saturation, fluid pressures of equal magnitude are first applied at both ends until this stage has been reached, which requires a very long time for thick samples (for dense smectite clay about 1 week for a 2 cm sample, 8 weeks for a 4 cm sample, and a year for an 8 cm sample etc). This can be assured by measuring the water uptake and comparing it with the theoretically required quantity of water using the basic relationships in Chapter 1. A hydraulic gradient is then applied across the sample for determining the conductivity.
- Recordings of the flow are taken by the flow meters at regular intervals or by computer acquisition technique.

Evaluation

The hydraulic conductivity K in m/s is evaluated from the expression:

$$K = \frac{q/A}{(p_1 - p_2)/L} \tag{9-11}$$

where:

q = recorded flow (m^3/s)
A = cross section area of the sample (m^2)
p_1 = fluid pressure at the inflow end (meter water head)
p_2 = fluid pressure at the outflow end (meter water head)
L = sample height (m)

Normally, the evaluated hydraulic conductivity is not constant because of particle migration and delayed microstructural reorganization. A typical evolution of the hydraulic conductivity is therefore of the type shown in Figure 9-18. If heating of the odeometer (Figure 9-19) is made for determining the influence of increased temperature on the conductivity it is important to let any heat-induced change in porewater pressure, which depends on the thermal expansion of both the clay and the oedometer, dissipate before evaluation is made.

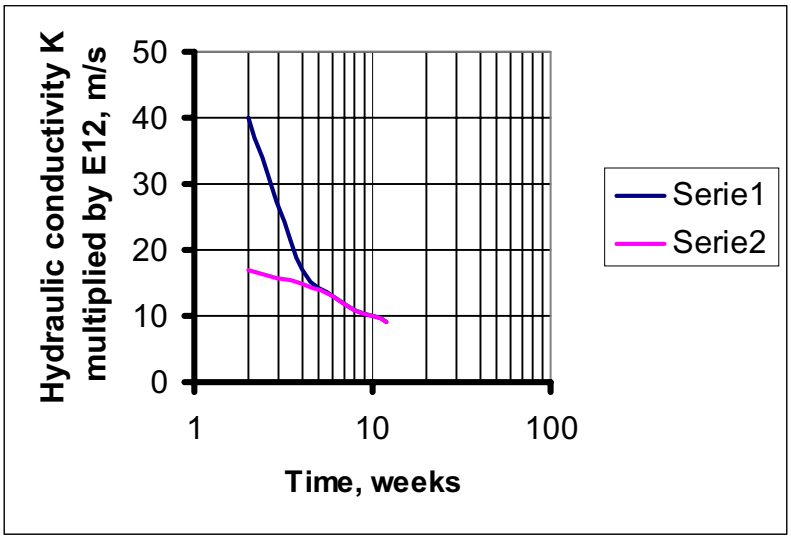

Figure 9-18. *Example of time-dependent change in hydraulic conductivity of smectite-rich clay due to microstructural rearrangement ("maturation"). Upper curve represents strongly (> 100 MPa) compacted smectite clay granules, thickness 2 cm. Lower curve represents compacted (~100 MPa) smectite clay granules, thickness 2 cm.*

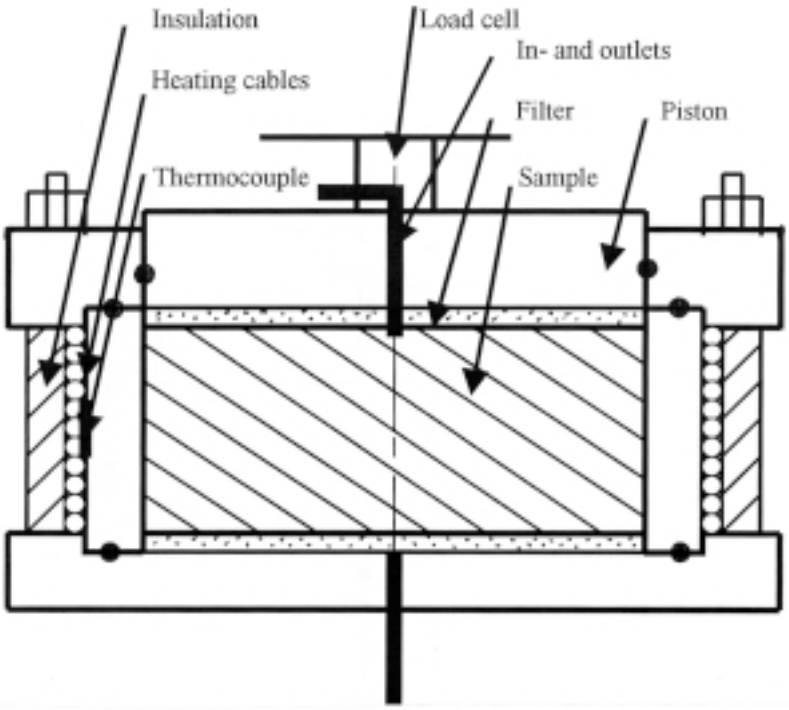

Figure 9-19. *Schematic picture of oedometer for evaluation of the influence of temperature on the hydraulic conductivity of clay. The load cell is for measuring the pressure change. Black circles are O-ring seals.*

9.6.2 Gas conductivity

Technique

Measurement of the gas conductivity can be made in the same fashion as for the hydraulic conductivity. The much more complex transport mechanisms, like dissolution and diffusion and transient return to gaseous form at the low pressure end, make the evaluation difficult. Most gas permeation tests are focused on determining the so-called critical gas pressure, which is sometimes called the capillary pressure. It can be determined by use of the equipment with which the hydraulic conductivity is determined. A major problem is to avoid leakage along the sample periphery, which makes the triaxial apparatus unsuitable for buffer material testing.

The type of gas used for the tests must not react with the soil component, which means that CO_2- and O_2-containing air is not suitable. Nitrogen or helium are suitable while hydrogen gives difficulties with respect to leakage and explosion risks.

Equipment

The most important part of the test equipment is the system employed for maintaining constant gas pressure and recording of gas flow. Figure 9-20 illustrates an equipment used for recording the critical gas pressure and gas conductivity of small samples of buffer clay with high or low density and of clay-poor backfills of high density /18/.

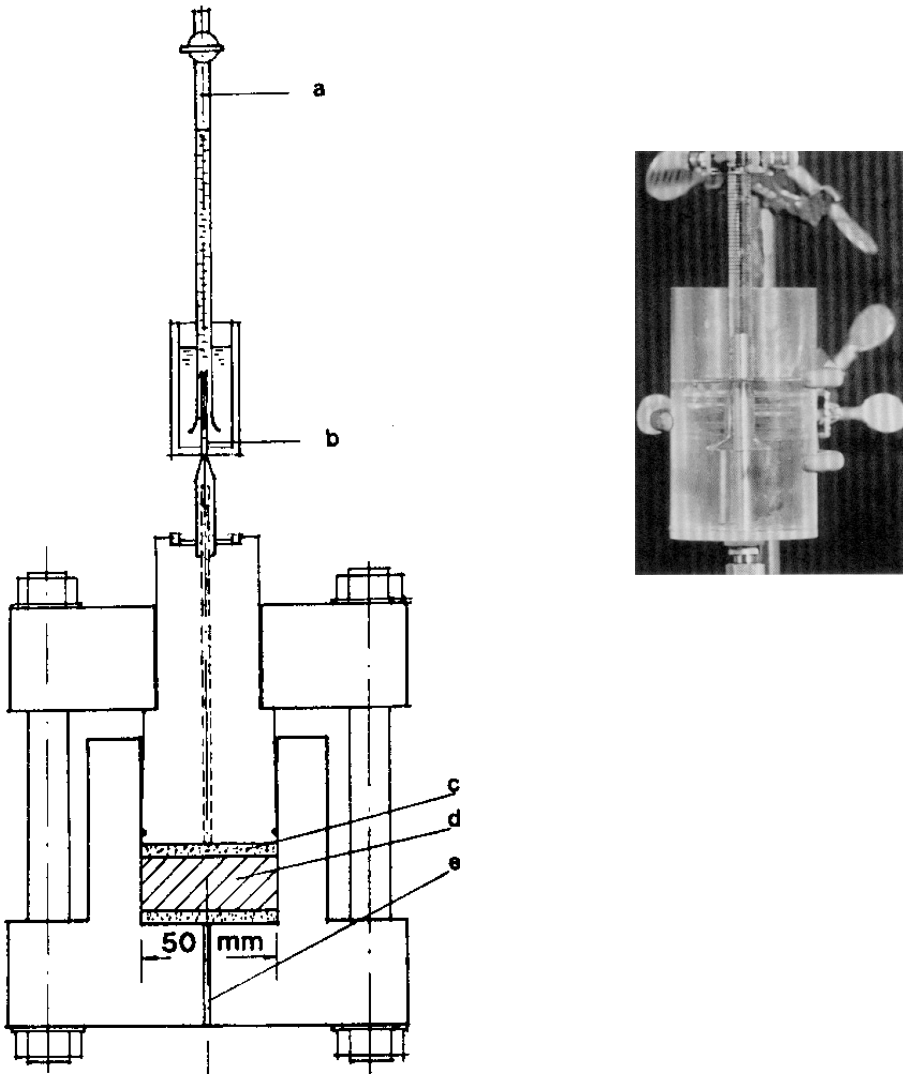

Figure 9-20. *Equipment for measuring critical gas pressure and gas conductivity. a) Burette for gas collection, b) Syringe, c) Filter, d) clay sample, e) Gas inlet. Small picture shows gas being pressed up displacing water in the burette /18/.*

Performance

- The soil is applied and fluid-saturated as in the determination of the hydraulic conductivity. The filter at the inflow end is preferably drained so that its voids are filled with gas at the test start.
- The gas pressure is increased in steps while maintaining the water pressure. The induced outflow of water and inflow of gas are recorded.

A typical result of a gas pressure test in one step is shown in Figure 9-21, /19/. The gas pressure was increased until breakthrough took place and the gas pressure ("excess") was recorded as was also the gas flow rate out of the specimen. If the gas pressure had been maintained high the gas flow would have remained high. It depends on the flow resistance of the gas sampling system in laboratory tests and of the geological surrounding in a repository.

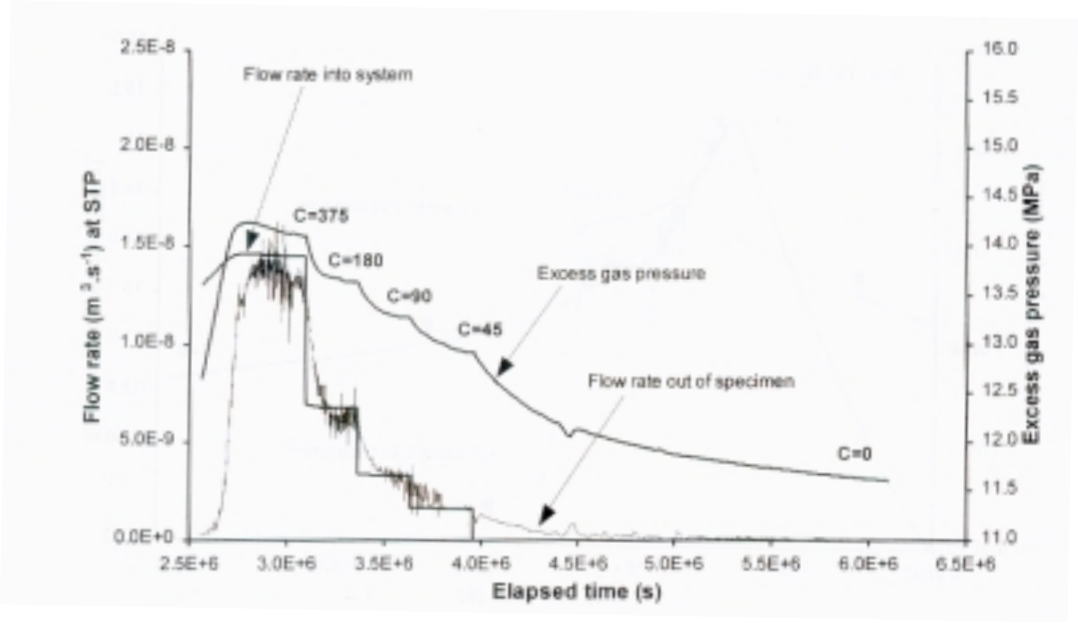

Figure 9-21. *Test of gas conductivity of MX-80 bentonite with increased gas pressure to reach breakthrough (peak value about 14 MPa) and recording of flow and excess gas pressure after terminating gas inflow /19/.*

Evaluation

Sudden displacement of more than 0.1–1% of the total porewater volume implies penetration of gas through the entire sample and this represents the critical pressure. It is evaluated from the expression:

$$p_{crit} = p_b - u \tag{9-12}$$

where

p_b = gas pressure at breakthrough
u = water pressure

An example of the composition of a test arrangement for determining the critical gas pressure is shown in Figure 9-22.

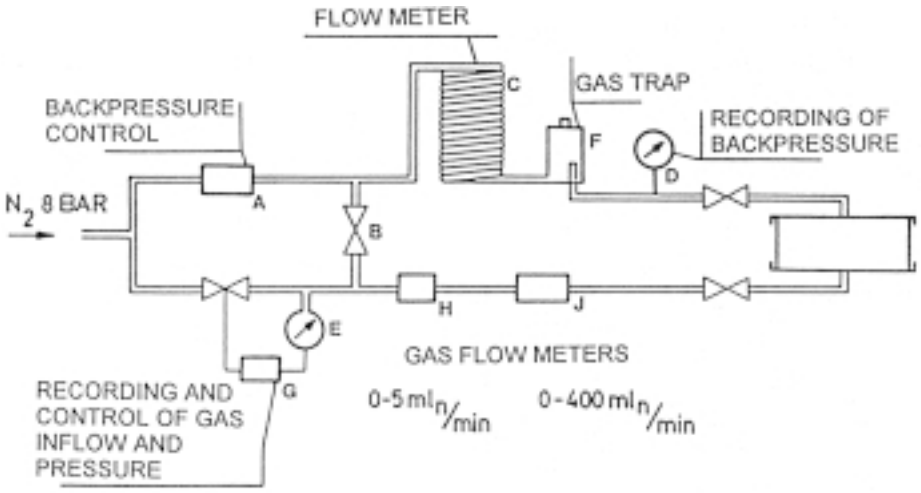

Figure 9-22. *Example of test arrangement for determining the critical gas pressure /20/.*

9.6.3 Ion diffusivity

Technique

Experimental determination of the diffusivity can be made in several ways but in practice there are two procedures that can be recommended: the non-steady (profile) method and the steady-state (through-diffusion) method /21/.

In the non-steady state method the ion species in question is introduced at one end of the confined sample and the diffusivity evaluated from the tracer concentration distribution in the sample after a certain time by fitting the theoretical curve to the measured concentration distribution. Figure 9-23 shows the experimental arrangement and concentration distribution at different distances from the high-concentration end.

The measurement gives the apparent diffusivity, which can be evaluated from Equation (9-13):

$$\frac{C}{C_0} = erfc\frac{x}{2\sqrt{D_a t}} \qquad (9\text{-}13)$$

where:

C = the ion concentration in the sample (mol/m^3)
C_0 = the ion concentration in the sample at x = 0 (mol/m^3)
x = the distance from the surface (m)
t = experimental time (s)

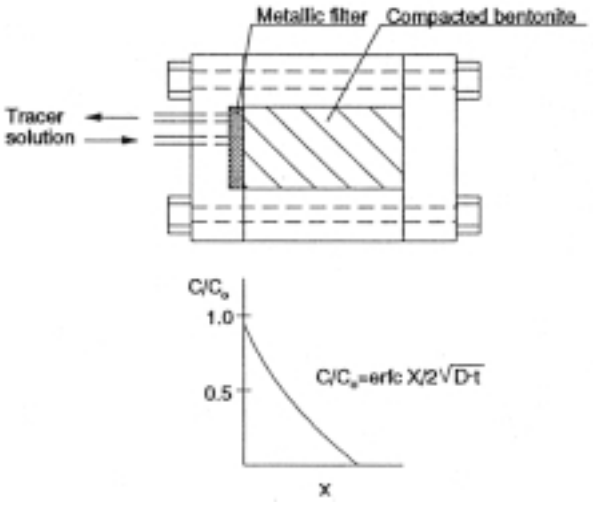

Figure 9-23. *Non-steady state diffusion experiment, where tracer is introduced keeping constant concentration at one end /13/.*

Figure 9-24 shows arrangements in which the total ion concentration remains constant throughout the experiment. At the start the ion source is confined to the center of the twin sample. At the termination of the experiment the sample is sliced and the concentration profile determined. The apparent diffusivity for the arrangement with such an "impulse" source can be evaluated from Equation (9-14):

$$\frac{C}{M} = \frac{1}{2\sqrt{\pi D_a t}} exp\left(-x^2 / 4D_a t\right) \tag{9-14}$$

where M is the total amount of tracer per interfacial area (mol/m^2).

By taking the logarithm of both sides of Equation (9-14) a linear expression is obtained, the slope of which gives the apparent diffusion coefficient.

For the "extended" source (Figure 9-24b), the distribution in the sample is obtained from Equation (9-15):

$$\frac{C}{C_0} = \frac{1}{2}\left\{ erf\ \frac{h-x}{2\sqrt{D_a t}} + erf\ \frac{h+x}{2\sqrt{D_a t}} \right\} \tag{9-15}$$

where h is the thickness of the source (m) and C_0 is the initial concentration in the source (mol/m^3).

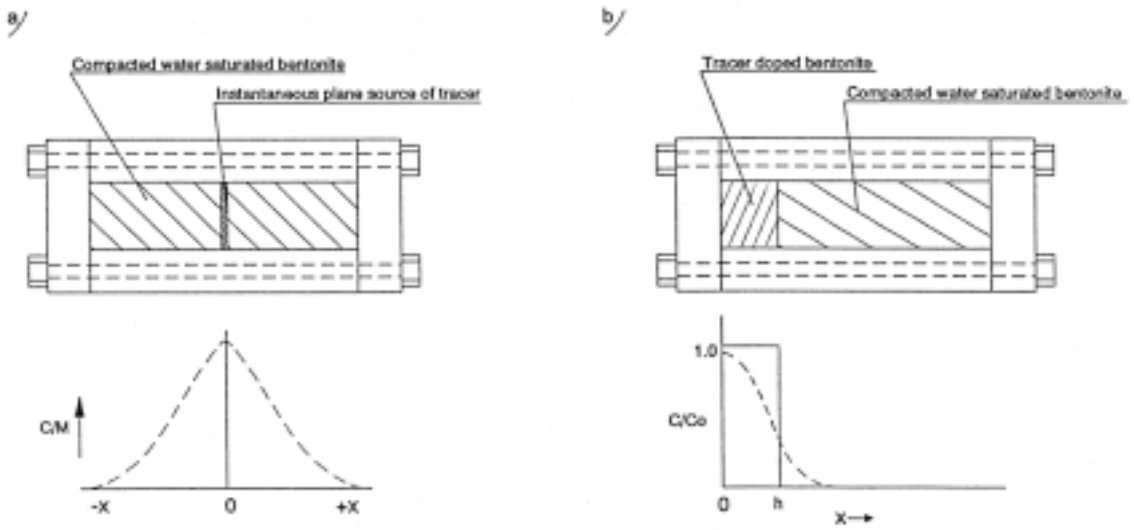

Figure 9-24. *Non-steady state diffusion experiment in which a tracer is introduced in the form of a thin "impulse" source (a) or as an "extended" source (b) /13/.*

In the steady state diffusion experiment seen in Figure 9-25, a tracer in the solution at one end of the sample is allowed to diffuse through the sample to the solution on the other side. The steady state diffusion experiment gives the effective and apparent diffusivities, which can be evaluated in various literature-reported ways /21/:

$$D_e = \frac{Ql}{A\left(C_{w1} - C_{w0}\right)} \tag{9-16}$$

$$D_a = \frac{Ql}{A\left(C_1 - C_0\right)} \tag{9-17}$$

$$D_a = \frac{l^2}{6T} \tag{9-18}$$

where:

Q = the flux through the sample (mol/s)
l = the thickness of the sample (m)
A = the surface area perpendicular to the diffusion flux (m^2)
C_{w0} = the concentration of the solution on the low-concentration side mol/m^3)
C_{w1} = the concentration of the solution on the high-concentration side (mol/m^3)
C_0 = the concentration in the porous medium on the low-concentrationside (mol/m^3)
C_1 = the concentration in the porous medium on the high-concentration side (mol/m^3)
T = the time lag, the point where the asymptote of the break-through curve intercepts the time axis (s)

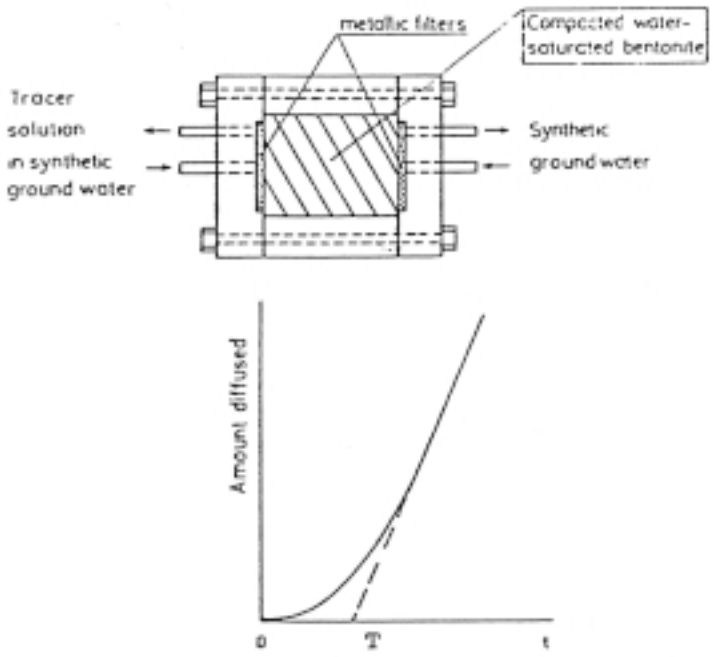

Figure 9-25. *Arrangement of a through-diffusion test /13/.*

The basic expressions for ion diffusion here imply that there is no chemical reaction between the diffusing elements and the soil components. The risk of such interaction is particularly obvious if the experiments are made in the common form of contacting the sample with solutions that contain dissolved carbon dioxide, i.e. without de-airing them.

The most common way of performing diffusion tests is to use arrangements of the sort shown in Figure 9-26 and to evaluate the diffusivity in terms of the apparent diffusion coefficient D_a by fitting the recorded curve of ion concentration across the sample length to a set of calculated curves for a number of diffusion coefficients.

Equipment

- Diffusion cell (commonly teflon).
- Soil sample.
- Vessels with solutions of desired concentrations to be connected to the ends of the sample.
- Pumps with tubings connecting the vessels and the cell for maintaining circulation of the solutions through the filters.
- Pipettes for sampling of solutions.
- Cutting device, i.e. lath or guided fine saw for cutting a few mm thick sections of the sample.
- Instrument for chemical analysis (cf Chapters 3 and 5) or for recording radiation produced by radioactive species.
- pH-meter.

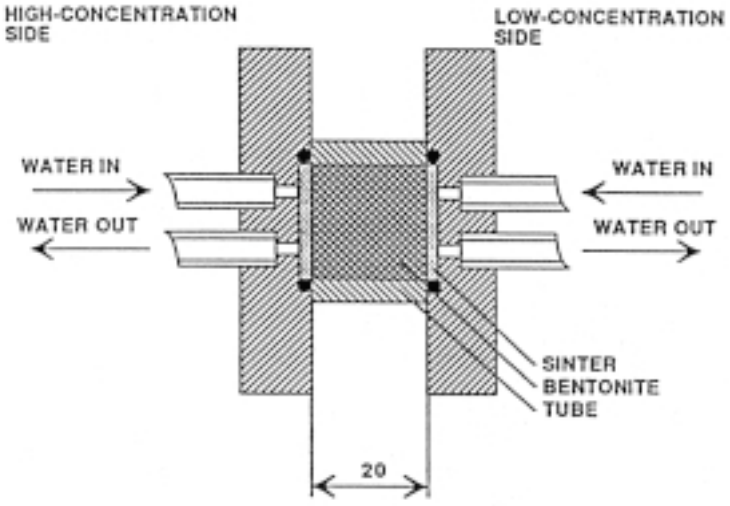

Figure 9-26. *Test equipment used for recording the concentration profile in clay sample.The concentration at both ends are maintained constant by circulationg the respective solutions /13/. The thickness of the sample is given in mm.*

Performance

- The soil sample is prepared in the same way as the sample used for hydraulic testing, using a porewater that has been equilibrated with the sample.
- Porewater solution is prepared by adding the diffusing species, preferably in chloride form, to get water with the same composition as the initial porewater.

  Parallel tests are conducted and they are terminated at various times for sectioning and analyzing the concentration. Samples from the solutions are taken for checking the composition and pH.
- The sections cut from the sample are analyzed with respect to the concentration of the diffusing element.

Evaluation

The concentration C expressed as the ratio of C/C_0, where C_0 represents the high-concentration end, is plotted as a function X from this end (Figure 9-27). The diffusion coefficient is evaluated from the mathematical form of the diffusion profile by curve fitting technique. Figure 9-28 illustrates the general shape of the concentration distribution profile.

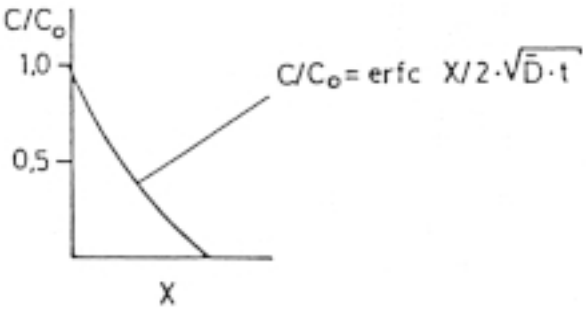

Figure 9-27. *Plotted ratio of C/C_0 versus x.*

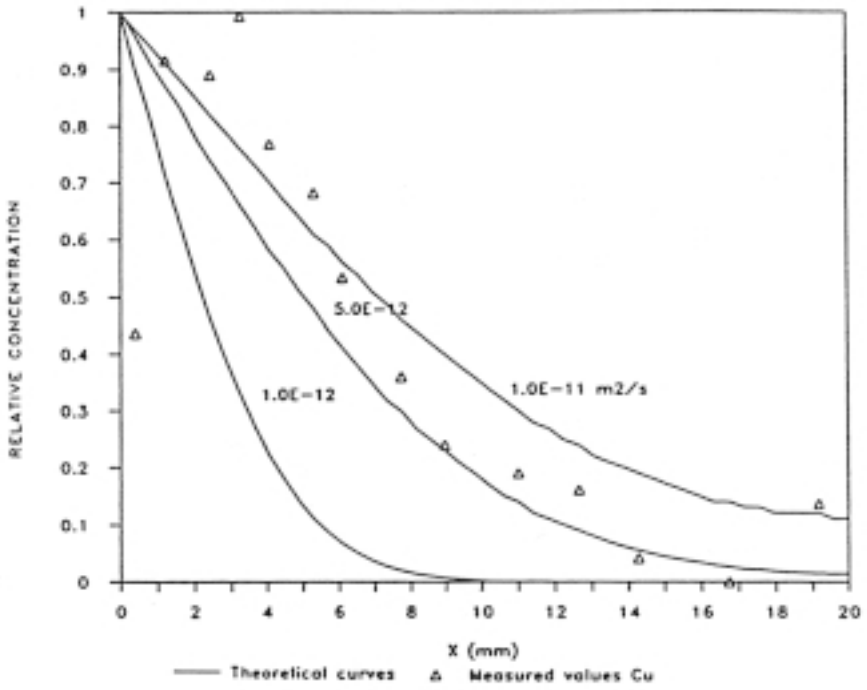

Figure 9-28. *Example of recorded concentration profile of copper in ionic form in bentonite and three theoretical curves indicating that D_a is around 10^{-11} m^2/s /21/.*

9.7 References

/1/ **Anderson D M, Pusch R, Penner E, 1978.** Physical and thermal properties of frozen ground. In: Geotechnical Engineering for Cold Regions. Eds: O B Andersland, D M Anderson. McGraw-Hill Book Company.

/2/ **Pusch R, 1967.** A technique for investigation of clay microstructure. J. Microscopie, Vol. 6, 1967 (pp. 963–986).

/3/ **Pusch R, 1973.** Influence of salinity and organic matter on the formation of clay microstructure. Proc. Int. Symp. Soil Structure, Gothenburg, 1973, Swedish Geotechnical Society, Stockholm.

/4/ **Pusch R, 1971.** Microstructural features of pre-Quaternary clays. Acta LUniversitatis Stockholmiensis, Stockholm Contributions in Geology, Vol. XXIV:1, Stockholm.

/5/ **Pusch R, Karnland O, Hökmark H, 1990.** GMM – a general microstructural model for qualitative and quantitative studies of smectite clays. SKB TR-90-43, Svensk Kärnbränslehantering AB.

/6/ **Pusch R, Muurinen A, Lehikoinen J, Bors J, Eriksen T, 1999.** Microstructural and chemical parameters of bentonite as determinants of waste isolation efficiency. Final Report, Contract F14W-CT95-0012. European Commission, Brussels.

/7/ **Pusch R, Moreno L, Neretnieks I, 2001.** Microstructural modelling of transport in smectite clay buffer. Proc. Int. Symp. on suction, swelling, permeability and structure of clays, Shizoka 2001. A. A. Balkema.

/8/ **Hansbo S, 1973.** Influence of mobile particles in soft clay on permeability. Proc. Int. Symposium of Soil Structure, Gothenburg, Swedish Geotechnical Society.

/9/ **Pusch R, Weston R, 2002.** Microstructural stability controls the hydraulic conductivity of smectitic buffer clay. Proc. Int. Workshop on Clay Microstructure and its Importance to Soil Behaviour, Lund, 2002 (In print).

/10/ **Pusch R et al, 1991.** Final Report on the Rock Sealing Project – Sealing properties and longevity of smectitic clay grouts. Stripa Project Technical Report 91-30, Svensk Kärnbränslehantering AB.

/11/ **Neretnieks I, 1985.** Diffusivities of some dissolved constituents in compacted bentonite. Nucl. Techn., Vol. 41, 1985 (pp. 458–470).

/12/ **Pusch R, Eriksen T, Jacobsson A, 1982.** Ion/water migration phenomena in dense bentonite. In: Scientific Basis for Nuclear Waste Management. Ed.: W. Lutze. Elsevier Publ. Co., New York, 1982 (pp. 649–658).

/13/ **Muurinen A, Rantannen J, Hiltunen P P, 1985.** Diffusion mechanisms of strontium, cesium and cobalt in compacted bentonite. Mat. Res. Soc. Symp., Vol. 50, 1985 (pp. 617–624).

/14/ **Kim H-T, Suk T-W, Park S-H, Lee C-S, 1991.** Diffusivities for ions through compacted Na-bentonite with varying dry density. Waste Management, Vol. 13, 1991 (pp. 303–308).

/15/ **Sherwood T K, Pigford R L, Wilke C R, 1975.** Mass transfer, MacGraw Hill, New York.

/16/ **Shainberg I, Kemper W D, 1966**. Hydration status of adsorbed cations. Soil Sci. Soc. Amer. Proc., Vol. 30, 1966 (pp. 707–713).

/17/ **Conca J L, Apted M, Arthur R, 1993.** Aqueous diffusion in repository and backfill environments. Mat. Res. Soc. Symp. Proc., Vol. 294.

/18/ **Pusch R, Ranhagen L, Nilsson K, 1985.** Gas migration through MX-80 bentonite. Technical Report 85-36. NAGRA, Wettingen, Switzerland.

/19/ **Horseman S T, Harrington J F, Sellin P, 1999.** Gas migration in clay barriers. Eng. Geol., Vol.54 (pp. 139–149).

/20/ **Pusch R, 1985.** Buffertar av bentonitbaserade material i siloförvaret. SKB Arbetsrapport 85-08. Svensk Kärnbränslehantering AB.

/21/ **Muurinen A, 1994.** Diffusion of anions and cations in compacted sodium bentonite. D. Thesis, University of Helsinki.

10 Thermal properties

This chapter deals with heat transport through buffer clay. Such transport has an impact on the temperature conditions in the buffer clay, which affect its physical state and chemical stability. Focus is on the physical background and on evaluation of the heat conductivity from laboratory measurements.

10.1 Introduction

One of the required properties of canister-embedding buffer materials in repositories is to dissipate heat that is produced in connection with the radioactive decay. The thermal properties of these materials need to be such that the temperature of the canister and of the buffer itself does not exceed a certain limit since the long-term performance of both is strongly dependent on the temperature. We will deal both with unsaturated and saturated clay of bentonite type with and without adding quartz sand, which is commonly considered as a suitable additive, both from chemical and heat conductivity points of view.

The thermal parameters are usually expressed by the parameters thermal conductivity and heat capacity as defined below /1/:

Heat (thermal) conductivity λ, *W/m,K.*

Referring to Figure 10-1 it is defined as:

$$\lambda = \frac{q}{A(T_2 - T_1)l} \tag{10-1}$$

where

q = heat flow
A = cross section area of element
$(T_2–T_1)$ = temperature difference
l = length of element

For bentonite the following empirical relationship has been derived /2/:

$$\lambda = 0.56 + 0.60\,\rho + 0.4\,\rho^3 w / (w + 1) \tag{10-2}$$

where:

w = water content
ρ = bulk density

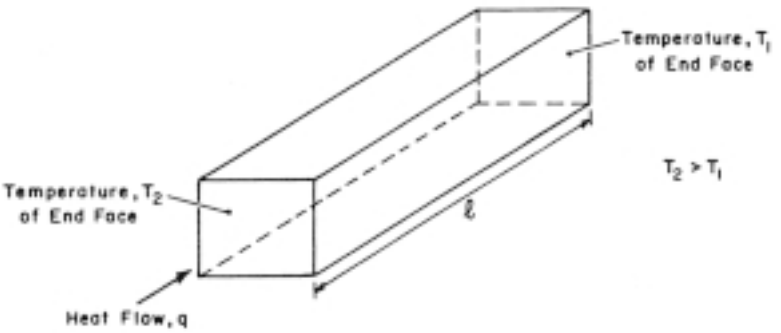

Figure 10-1. *Heat flow through a prismatic element of soil.*

Another empirical rule for bentonite is the following /3/:

$$\lambda = \lambda_0 + K_e\left(\lambda_1 - \lambda_0\right) \tag{10-3}$$

in which:

$$\lambda_0 = 0.034 \cdot n^{-2.1}$$

$$\lambda_1 = 0.56^{n} \cdot 2^{(1-n)}$$

$$K_e = 1 + \log S_r$$

where:

λ_0 = thermal conductivity at S_r = 0
λ_1 = thermal conductivity at S_r = 100%
K_e = factor representing the influence of the degree of saturation S_r
n = porosity

Both expressions for λ are functions of the degree of water saturation, which is explained by the strong influence of pore gas on the heat transport capacity. This will be discussed later in the chapter.

Heat capacity $C = \rho c$ (10-4)

where:

ρ = density
c = specific heat

This quantity is important under transient conditions. It is the energy required to raise the temperature of a unit volume by 1°C. If the volume fractions of the solid, water and air components present in unit soil volume are x_s, x_w and x_a respectively, then:

$$C = x_s C_s + x_w C_w + x_a C_a \tag{10-5}$$

where C_s, C_w and C_a are the respective heat capacities per unit volume of the solids, water and air.

The volumetric heat capacity C_u is given by /1/:

$$C_u = \frac{\rho_d}{\rho_w}\left(0.18 + 1.0\frac{w}{100}\right)C_w \qquad (10\text{-}6)$$

where:

ρ_d = dry unit weight of the soil
w = its water (or ice) content
ρ_w = unit weight of water
C_w = heat capacity of water

The thermal conductivity and volumetric heat capacity of soils with a known moisture content is given in Figure 10-2.

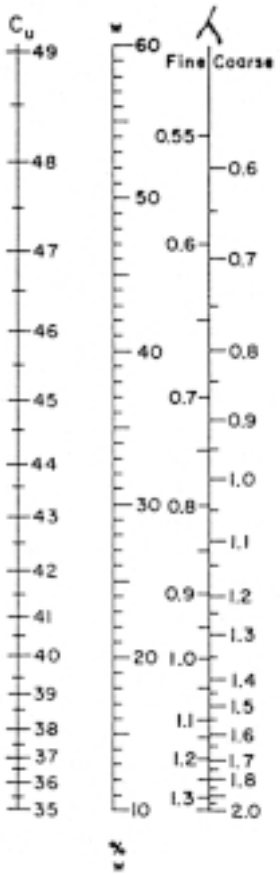

Figure 10-2. *Thermal properties and water content for saturated soils /1/.*

10.2 Mechanisms in heat transfer

10.2.1 General

In repository design one is primarily concerned with the thermal conductivity of buffer materials. An important fact that makes experimental determination of this quantity difficult is that the boundary conditions are hard to maintain uniform and constant in the laboratory and that thermal flow in unsaturated soil is associated with redistribution of the moisture content. The flow of heat by conduction is the predominant mechanism while convection and radiation have a relatively small or negligible effect /1/. The temperature levels and the soil composition including the structure, affect the heat transfer. Water phase changes in soils and their associated energies may have a significant effect on the heat transfer process. Hence, in unsaturated soils moisture may migrate by a process of evaporation followed by vapor diffusion and subsequent condensation in colder parts, thus leading to heat transfer.

In many situations the transfer of moisture and heat occurs simultaneously and unseparably. In theoretical studies of heat transfer the soil has been assumed to be homogeneous and all processes of heat transfer to take place uniformly throughout the porous medium, but in reality vapor transfer or air convection occur only in the air-filled pore space and liquid movement only in the water-filled pore space, while evaporation or condensation are associated with the water/air interfaces.

10.2.2 Heat conduction

Heat conduction occurs in all soil constituents, i.e. in the soil solids, the water (liquid, vapor or ice) and the pore gas /1/ and takes place by collision between the molecules. In water energy transfer by breaking and making hydrogen bonds in water also appears to contribute to conduction. The behaviour of liquid water lies between that of gases, with their random molecular motion, and that of crystals.

The ratio of the thermal conductivity and the heat capacity is termed the thermal diffusivity α:

$$\alpha = \lambda / C \qquad (10\text{-}7)$$

Typical data of the thermal parameters are the ones given in Table 10-1.

Quartz has the highest thermal conductivity and air the lowest, their ratio being about 350:1. The volumetric proportions of the various soil components therefore strongly influence the effective thermal conductivity of the soil.

Table 10-1. Thermal properties of soil constituents at 20°C and 1 atm pressure /1/.

Material	Density ρ (kg/m^3)	Specific heat C (Ws/kg, K)	Thermal conductivity λ (W/m,K)	Thermal diffusivity α (10^{-7} m^2/s)
Quartz	2650	733	8.4	43
Many soil minerals*	2650	733	2.9	15
Soil organic matter*	1300	1927	0.25	1.0
Water	1000	4190	0.6	1.42
Air	12	1048	0.026	0.21

* Approximate average values

10.2.3 Influence of soil structure

The solid particles in soils may be composed of one or more minerals, such as quartz or montmorillonite. Water can occur as vapor in the unfilled part of the pores or as ordinary water in the liquid phase. The soil structure is important because it implies a certain arrangement of the particles, and a certain orientation with respect to the direction of the heat flow. Finer clay particles are usually aggregated into larger secondary units of different shapes and sizes /4/. Pores exist both between the primary particles and in the larger secondary aggregates. The number and nature of the contacts between the soil particles and their interaction with water are important because most of the heat transfer occurs across these contact points or areas, particularly in the case of dry or nearly dry soils. If the solid grains are cemented together, e.g. by a clay matrix or crystalline or amorphous precipitates, the thermal conductivity is much improved.

Various changes in soil structure, and therefore in density or porosity, may occur in buffer materials. Thus, drying of smectitic clay buffer embedding hot canisters leads to shrinkage and fissuring, while water uptake leads to swelling. Other effects are coagulation of soft clay particle networks caused by cation exchange from Na to Ca or by an increase in electrolyte content.

The porosity of a soil has a strong influence on its thermal conductivity. An increase in the porosity means a decrease in dry density and more space between the solid particles. In the case of dry soils this implies more air and hence a lower thermal conductivity.

For any water content the most effective heat transfer is obtained when there are many direct particle contacts, which is the case when the space between larger grains is filled with smaller, contacting grains and the space between these is in turn filled with even smaller, contacting particles. This corresponds to soils with Fuller-type gradation (Figure 10-3), which is valuable also because it provides high density and thereby low

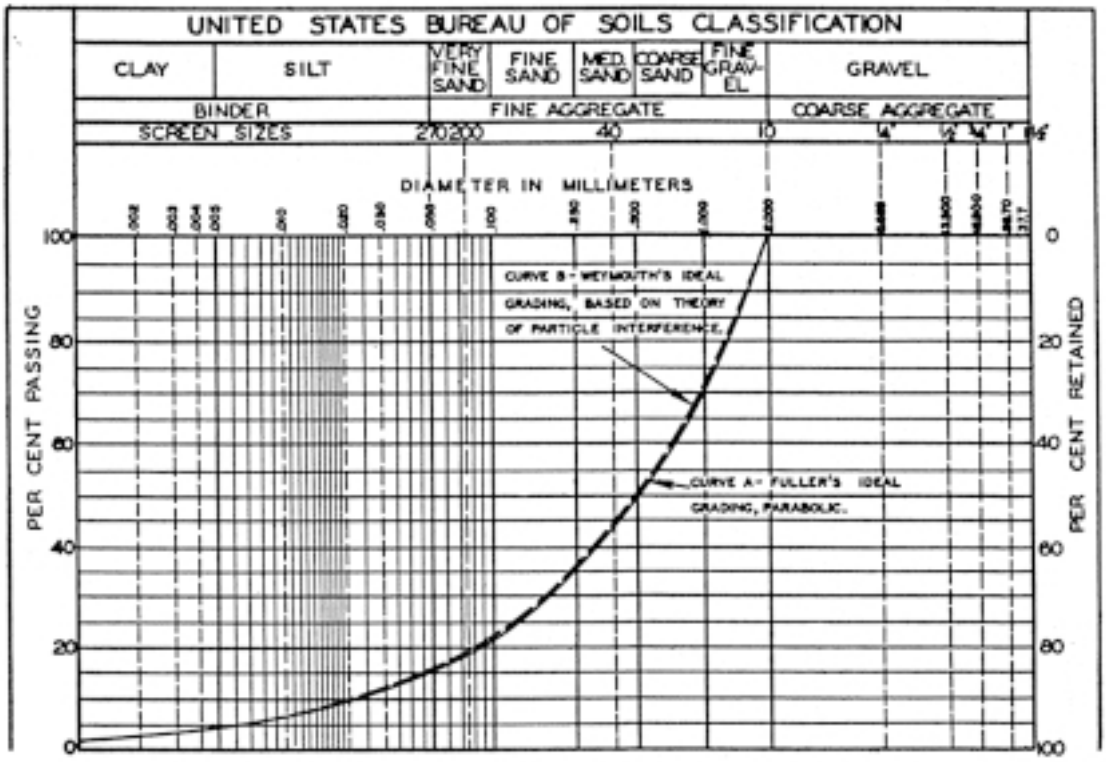

Figure 10-3. *The classical diagram of United States Bureau of Soils Classification showing Fuller-type grain size distribution. Another principle for maximum particle interference, "Weymouth's ideal grading", is shown in the diagram, both being almost entirely coincident.*

hydraulic conductivity and low compressibility. Also, the grain pressure ("effective pressure") is an important factor; classical Hertz theory of contacts explains why an increased grain pressure yields more effective heat transfer /1/.

Figure 10-4 illustrates the influence of density on the thermal conductivity of sandy soil at constant water content. Figure 10-5 illustrates the thermal conductivity of illitic clay as a function of the dry density.

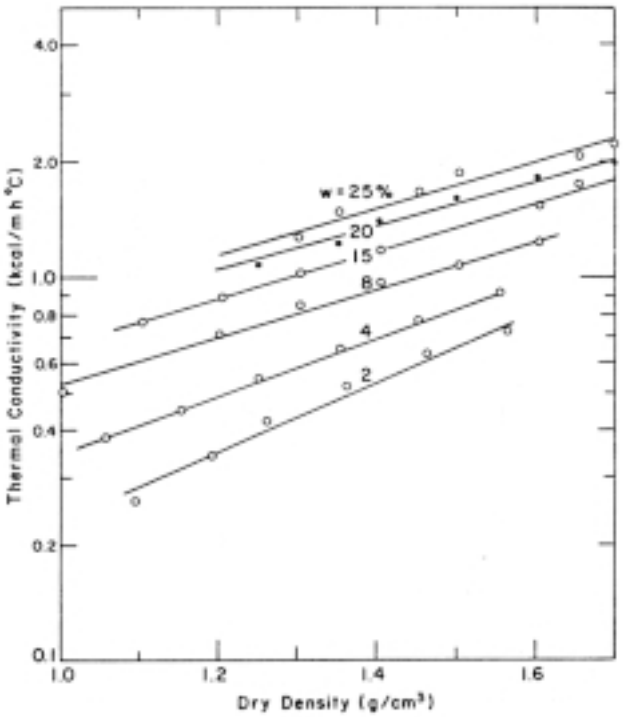

Figure 10-4. *Thermal conductivity of sandy soil vs. dry density at different water contents /3/.*

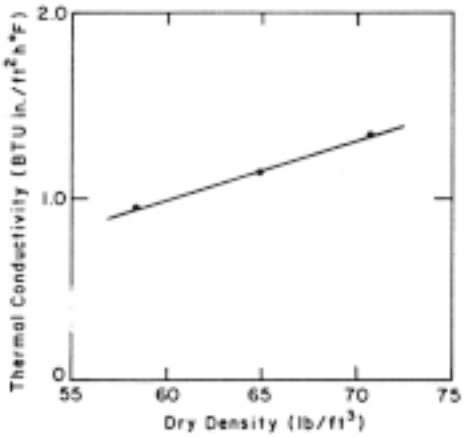

Figure 10-5. *Thermal conductivity of air-dry illitic Leda clay as a function of dry density /3/.*

10.3 Experimental

10.3.1 General

The so-called probe method, which implies that a heat pulse is triggered in the soil sample, is recommended for routine testing /5/. A pin-shaped probe with a length that is much larger than the diameter is inserted in the center of the sample and heated at constant power (Figure 10-6). The temperature is recorded by a thermocouple in the center of the probe and plotted as a function of time. If the length/diameter ratio is high enough, the axial heat conduction can be neglected and the central section modelled as a one-dimensional axial symmetric system.

The temperature increase in the probe can be calculated according to Equation (10-8) if the probe is taken as a line source:

$$\Delta T = \frac{-q}{4\pi\lambda} \cdot E_i\left(-\frac{r^2}{4\kappa t}\right) \tag{10-8}$$

and

$$E_i(-x) = \int_x^\infty \frac{1}{z} e^{-z} dz \tag{10-9}$$

where:

ΔT = temperature increase
k = heat flow per meter length
λ = thermal conductivity
r = radius
κ = thermal diffusivity
t = time from start heating

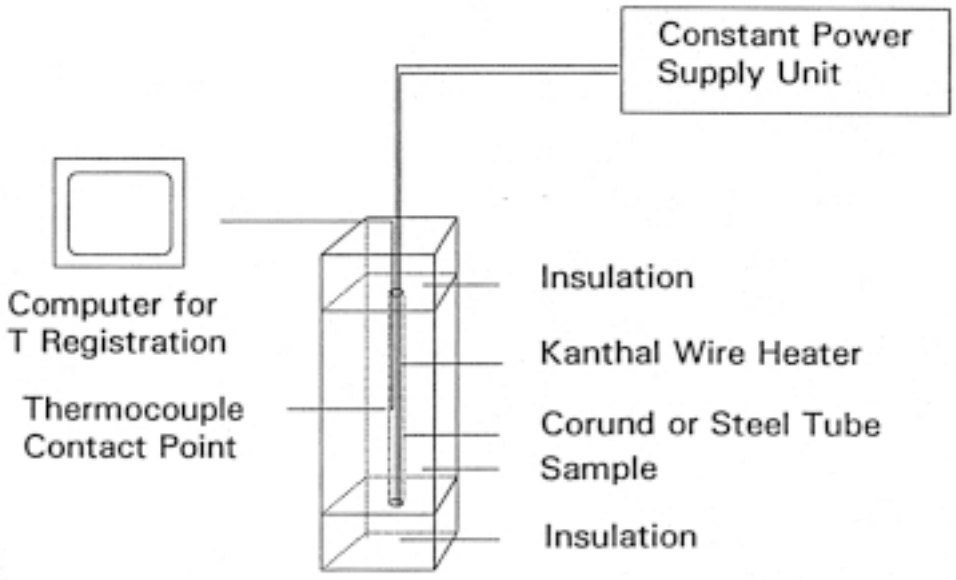

Figure 10-6. *Measurement system for determination of thermal conductivity /5/.*

The termal diffusivity κ is defined according to Equation (10-10):

$$\kappa = \frac{\lambda}{\rho C_p} \tag{10-10}$$

where:

ρ = bulk density
C_p = heat capacity

Equation (10-8) can be approximated to Equation (10-11) for long recording times and a small probe radius:

$$T_{t2} - T_{t1} = \frac{q}{4\pi\lambda} ln \frac{t_2}{t_1} \tag{10-11}$$

where T_{t1} and T_{t2} are the temperature values at time t_1 and t_2, respectively.

Application of the technique adapted to the testing of bentonite samples requires that the probe has penetrated the entire sample and that the ends of the sample be insulated in order to minimize axial heat flow.

10.3.2 Equipment

The following components are used (cf Figure 10-6).

- Supply of constant power.
- Thermal probe of thin-walled steel tube with electrically insulated Kanthal wires (placed in tubes of heat-resistant plastic that does not give off gas).
- Thermocouple inserted in the central part of the probe.
- Temperature recording unit (data logger).

10.3.3 Performance

Buffer material samples should be prepared by use of a triaxial apparatus or prepared from several oedometer samples. The diameter should be about 50 mm and the height around 80 mm. The samples are inserted in a well-fitting cylindrical plastic tube for testing.

The measuring probe is installed in a drilled hole in the sample. The hole should have the same diameter as the probe so that the probe and the sample are in close contact along the entire surface. In order to improve the contact and minimize the contact resistance the probe should be coated with silicon grease before installation. A suitable power is 1 W.

10.3.4 Evaluation

The heat conductivity λ can be calculated using Equation (10-12), which is a transformation of Equation (10-11).

$$\lambda = \frac{q}{4\pi\Delta T} 1n \frac{t_2}{t_1} \qquad (10\text{-}12)$$

where

ΔT = temperature increase of the probe in the time interval t_1 to t_2.

The proper time interval for evaluation can be determined if the temperature is plotted as a function of time in a semi-logarithmic diagram. According to Equation (10-11), this relation should be a straight line, deviation from this shape being caused by boundary effects. Such effects appear for short testing times, i.e. when the properties of the probe and the contact resistance dominate the behaviour, and after long test periods when the heating front has reached the outer boundary. Figure 10-7 shows an example of a test plotted in this way. It was made on a sample of Na-bentonite with the void ratio e=1.5 and the degree of saturation S_r = 98%. The applied power was 1 W and the length of the probe 8 cm. The diagram shows that the temperature curve *T vs. log t* is approximately a straight line between about 50 s and 500 s. If the thermal conductivity is graphically evaluated with the best fitted line for these time values, the result will be λ = 1.08 W/m,K.

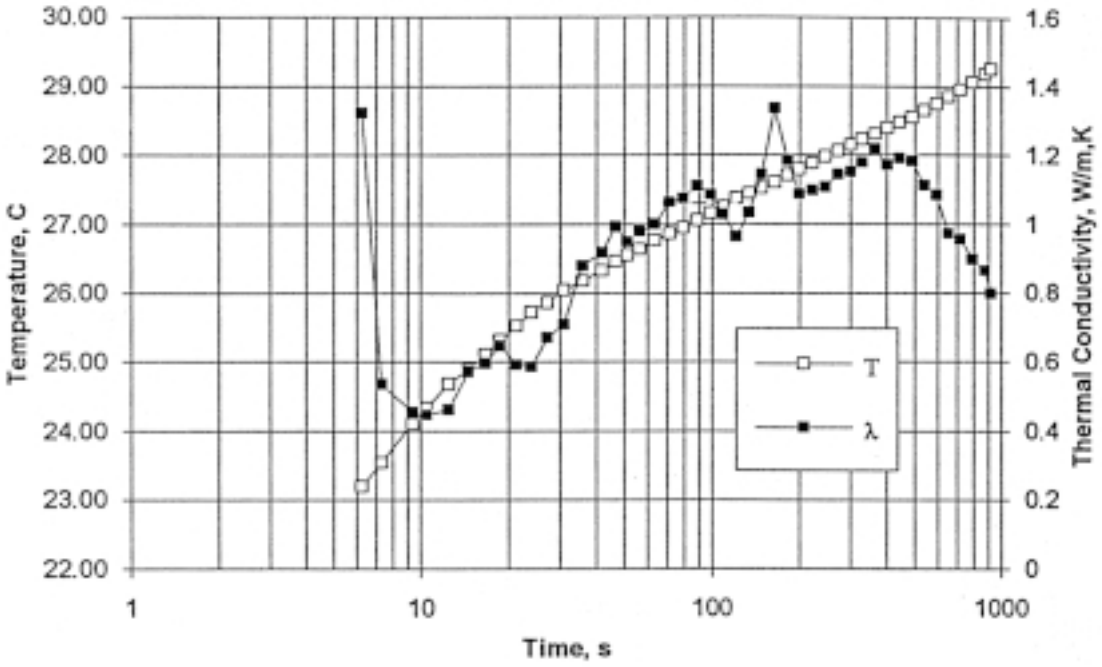

Figure 10-7. *Thermal conductivity λ evaluated from average time and temperature values in short time intervals /5/.*

10.3.5 Accuracy

Experience shows that the described heat pulse technique yields heat conductivities with an accuracy of ± 10%.

It is believed that the thermal conductivity is accurately evaluated by the graphical technique, which thus yields an average value. The calculated values are very helpful for estimating the accuracy of the measurements and for selecting the most appropriate time interval for evaluating the heat conductivity.

10.4 References

/1/ **Farouki OT, 1986.** Thermal properties of soils. Trans. Tech. Publication.

/2/ **Kahr G, Müller-Von Moos M, 1982.** Wärmeleitfähigkeit von Bentonit MX80 und von Montigel nach der Heizdrahtmethode. Nagra Technischer Bericht 82-06.

/3/ **Knutsson S, 1983.** On the thermal conductivity and thermal diffusivity of highly compacted bentonite. SKB TR 83-72, Svensk Kärnbränslehantering AB.

/4/ **Pusch R, 1970.** Clay microstructure. Document D:8. Nat. Swed. Build. Res. Council, Stockholm.

/5/ **Börgesson L, Fredrikson A, Johannesson L-E, 1994.** Heat conductivity of buffer materials. SKB TR-94-29, SKB, Stockholm.

11 Rheology

This chapter deals with the stress/strain/time relationships for saturated and unsaturated buffer clays and backfills. Focus is on basic soil mechanical parameters and moduli for defining and evaluating shear strength, compression, expansion and shear deformation. Data from testings are given and discussed with respect to their relevance to smectitic soils. The major features of a general material model for describing the rheological behaviour of smectite clay are outlined. This model and its use is treated in greater detail in Part 3 of this Handbook.

11.1 General

While in ordinary soil mechanics the impact of very long time can often be left out, it is of profound importance in repository design and performance assessment and several aspects on the rheology of buffers and backfills will be given in this chapter. For all soils one has to recognize that the stress/strain behaviour is different for undrained and drained conditions, i.e. when water is allowed to be taken up or expelled depending on the pressure and boundary conditions. Also, it is largely different for soils that are completely water-saturated and for soils which have a degree of water saturation that is below about 90%.

The most important rheological properties of completely water saturated buffer materials are the following ones:

- Stress-strain behaviour at isotropic compression (compression properties)
- Stress-strain behaviour at isotropic expansion (swelling properties)
- Stress-strain behaviour at shearing (shear strain properties)
- Shear strength
- Creep properties (change in strain with time at constant stress)

In common geotechnical literature the behaviour is not altogether described by this logic but in the form of the following properties:

- Compressibility
- Shear strain
- Shear strength
- Swelling
- Swelling pressure

For ordinary non-swelling soils the rheological behaviour is controlled by the Terzaghi effective stress. A very important question is hence whether the effective stress concept is also valid for smectite-rich buffer materials and this will be discussed in the present chapter.

11.2 The effective stress concept

11.2.1 General

The effective stress concept is the basis of all sorts of stress-related expressions for ordinary soils in soil mechanics. It states that the effective stress, defined according to Equation (11-1) controls the rheological behaviour:

$$\sigma' = \sigma - u \qquad (11\text{-}1)$$

where:

σ' = effective stress
σ = total stress
u = porewater pressure

Equation (11-1) has been proven to be valid for a variety of different inorganic soils from sand to illitic clay as well as for organic soils ranging from peat to mud. However, the complex microstructure of clayey soils and rather unknown consistency and physical properties of the interlamellar water makes the applicability less obvious for smectitic clays /2/.

The total stress is defined as by Equation (11-2):

$$\sigma = \frac{N}{A} = p\frac{A_s}{A} + u\frac{A - A_s}{A} \qquad (11\text{-}2)$$

where:

N = the total force on one side of a cube of soil
A = the total area of one side of the cube
A_s = the accumulated horizontal area of the particle contacts in a cross section
p = the (particle) contact pressure
u = the pore water pressure.

Figure 11-1 shows a cross section through a sample. The contact pressure p is very high due to the very small contact area A_s. pA_s is the total force over the area A that is transmitted through the cross section by the particle network and this force, divided by the total area, i.e. $p\frac{A_s}{A}$, is the so-called effective stress σ_c' in the sample (index c stands for contact). The remaining area of the cross section intersects water.

If $\frac{A_s}{A} = b$ the equation is written as:

$$\sigma = \sigma_c' + u(1-b) \qquad (11\text{-}3)$$

The effective stress theory is valid if A_s is very small compared to the total area and thus $b \approx 0$, which applies to ordinary soils.

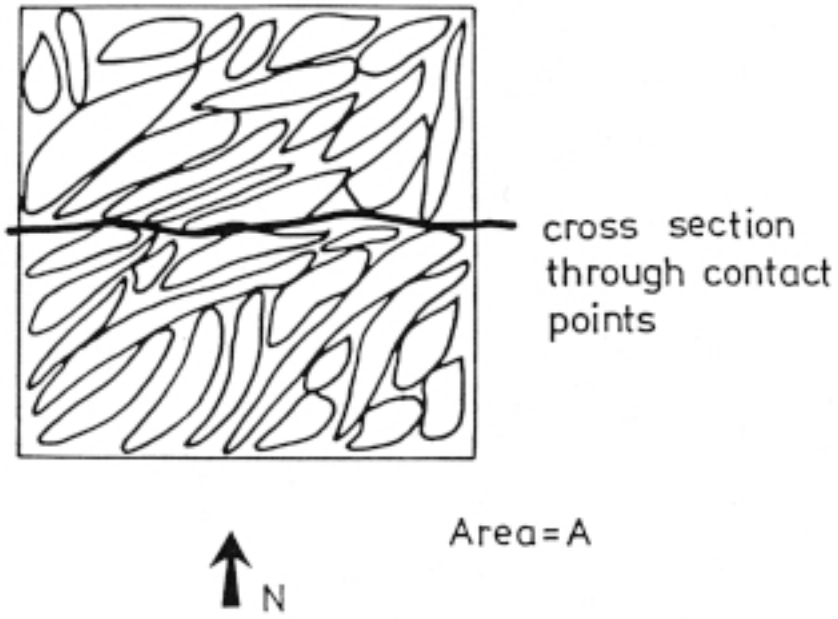

Figure 11-1. *Detail of a soil structure illustrating Equation (11-2).*

11.2.2 Relevance of the effective stress concept for smectitic clays

For smectitic clay the question is not whether the contact area A_s is small or not since there are probably no direct mineral/mineral contacts. The question is rather what the state is of the water within and between the lamellar stacks and how the stresses are transferred. The particles in Figure 11-1 may represent such stacks rather than solid particles and it can be imagined that normal and shear stresses are transferred by electro-chemical forces and interlamellar water lattices as well as by electrical double-layers at the points of interaction of adjacent stacks of lamellae /1/.

For such a system Equation (11-3) can be replaced by Equation (11-4):

$$\sigma = \frac{F_r - F_a}{A} + u(1-b) \qquad (11\text{-}4)$$

where:

F_r = the sum of the vertical repulsive forces over a cross section according to Figure 11-1
F_a = the sum of the vertical attractive forces over a cross section according to Figure 11-1

For this system $\frac{F_r - F_a}{A}$ controls the behaviour. Thus, the stress acting in the structure over the cross section area A can be considered as an effective stress σ_e' (where index e stands for "electro" although other forces are involved as well) by which Equation (11-4) turns into Equation (11-5):

$$\sigma = \sigma_e' + u \qquad (11\text{-}5)$$

For commercial bentonite the content of non-smectitic minerals is 20–90% depending on the quality. The presence of "accessory" minerals means, especially at high densities, that there is also a considerable amount of mineral/mineral contacts and the resulting stress is therefore probably a combination of Equations (11-2) and (11-4) as implied by Equations (11-6) and (11-7):

$$\sigma = \frac{N}{A} = p\frac{A_s}{A} + \frac{F_r - F_a}{A} + u\frac{A - A_s}{A} \tag{11-6}$$

$$\sigma = \sigma_c' + \sigma_e' + u(1-b) \tag{11-7}$$

As an average, the effective stress is thus the sum of the "contact" and the repulsive interlamellar and electrical double-layer pressures:

$$\sigma' = \sigma_c' + \sigma_e' \tag{11-8}$$

In practice one can refrain from distinguishing between these stress components and use the effective stress concept as a measure of particle interaction. This practical rule seems to apply sufficiently well in practice /2,3/.

11.3 Basic relationships

11.3.1 Definitions

The rheological behaviour of any soil can be described by use of partly elastic recoverable and partly plastic, unrecoverable stress/strain relations /2/. In a simplified form the stress/strain relationship can be expressed as tangent and secant moduli (Figure 11-2). The firstmentioned is commonly applied and will be used in this document.

Two basic types of stress/strain moduli are in use; the compression modulus *K* and the shear modulus *G*. The first represents changes in volume and the second changes in shape.

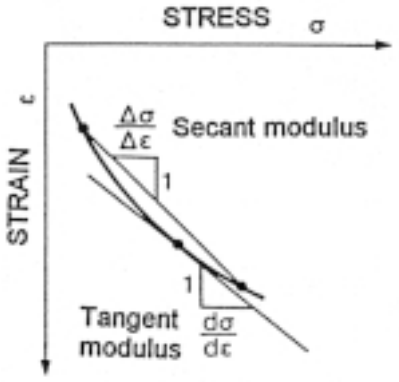

Figure 11-2. *Secant and tangent moduli /3/.*

Compression modulus K

Compression is expressed by use of K as defined by Equation (11-9):

$$K = \frac{d\sigma'}{d\varepsilon_v} = \frac{d\sigma'}{d\varepsilon_1 + d\varepsilon_2 + d\varepsilon_3} \tag{11-9}$$

where:

σ' = effective stress
ε_v = volumetric strain
ε_1, ε_2, ε_3 = linear strain

K can be determined by isotropic, drained triaxial tests.

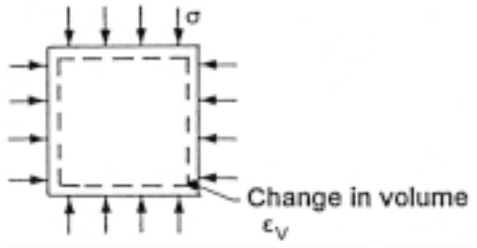

Figure 11-3. *Isotropic compression.*

Shear stress modulus G

Simple shear yields:

$$G = \frac{d\tau}{d\gamma} \tag{11-10}$$

and can be determined by undrained shear tests.

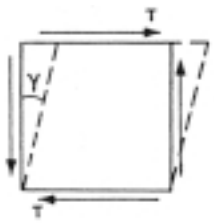

Figure 11-4. *Simple shear.*

For linear elastic materials one can derive relationships between these basic moduli and Poisson's ratio v as well as other moduli /4/:

$$E = \frac{3G}{1 + G/3K} \tag{11-11}$$

$$v = \frac{1 - 2G/3K}{2 + 2G/3K} \tag{11-12}$$

The modulus of elasticity E can be determined by uniaxial compression tests and the G modulus can then be evaluated from E and K.

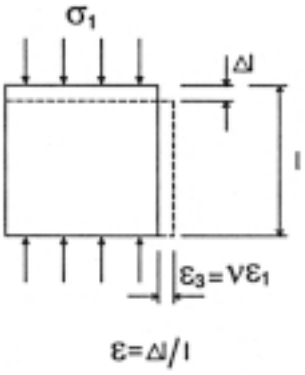

Figure 11-5. *Uniaxial unconfined compression.*

E can also be derived from undrained triaxial tests and is expressed in terms of the tangent modulus /5/:

$$E = \frac{d\left(\sigma_1' - \sigma_3'\right)}{d\varepsilon} = \frac{d\left(\sigma_1 - \sigma_3\right)}{d\varepsilon} \tag{11-13}$$

where:

σ_1 = major principal stress
σ_3 = minor principal stress (cell pressure)

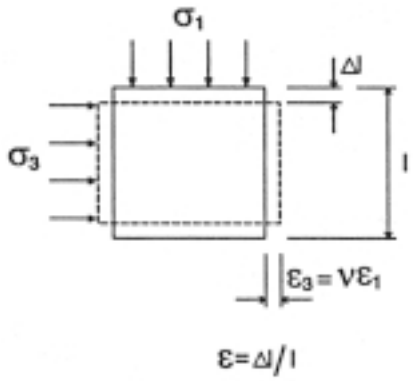

Figure 11-6. *Pure shear.*

A further possibility to estimate E is to apply the empirical relationship:

$$E = N \cdot \tau_{fu} \tag{11-14}$$

where

N = coefficient ranging from 150–400; 250 being a recommended mean for ordinary clay materials
τ_{fu} = undrained shear strength

Oedometer modulus M

Oedometer compression gives:

$$M = \frac{d\sigma'}{d\varepsilon} \tag{11-15}$$

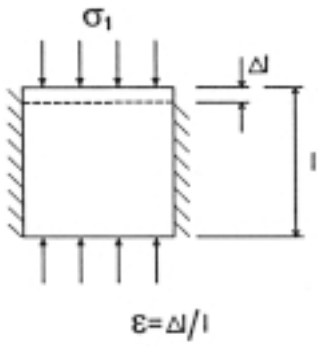

Figure 11-7. *Uniaxial confined compression (oedometer testing).*

M can be derived from K and G:

$$M = K + 4G/3 \tag{11-16}$$

and is determined by performing oedometer tests.

Plotted oedometer and shear strain curves are hardly ever straight lines on any scale and M and G usually obey the following general expression where D stands for any deformation modulus (Figure 11-8), /4/:

$$D = A\sigma_j \left(\frac{\sigma'}{\sigma_j} \right)^B \tag{11-17}$$

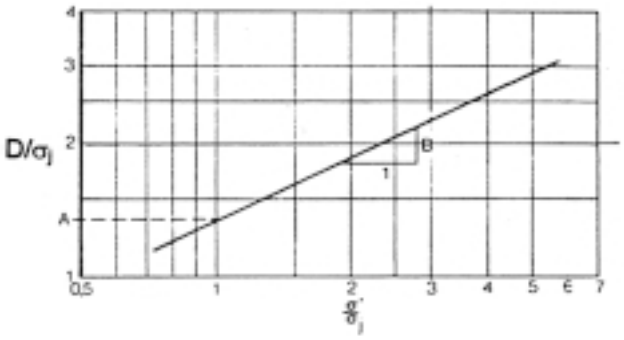

Figure 11-8. *D (A or B) evaluated from a stress/strain curve /4/.*

11.3.2 Compression properties

General

In its most simple form, the compressibility of soils is expressed in terms of the compression index C_c or the index ε_2, which can be evaluated from oedometer tests (Figure 11-9). One finds for linearly scaled void ratio and log-scaled pressure /3/:

$$C_c = \frac{\Delta e}{\Delta\left(log\,\sigma'\right)} \tag{11-18}$$

and if the load is doubled:

$$C_c = \varepsilon_2 \left(1 + e_o\right) \Big/ log\,2 \tag{11-19}$$

where e_0 = void ratio before load increase ($\Delta\sigma'$ or σ' in Figure 11-9).

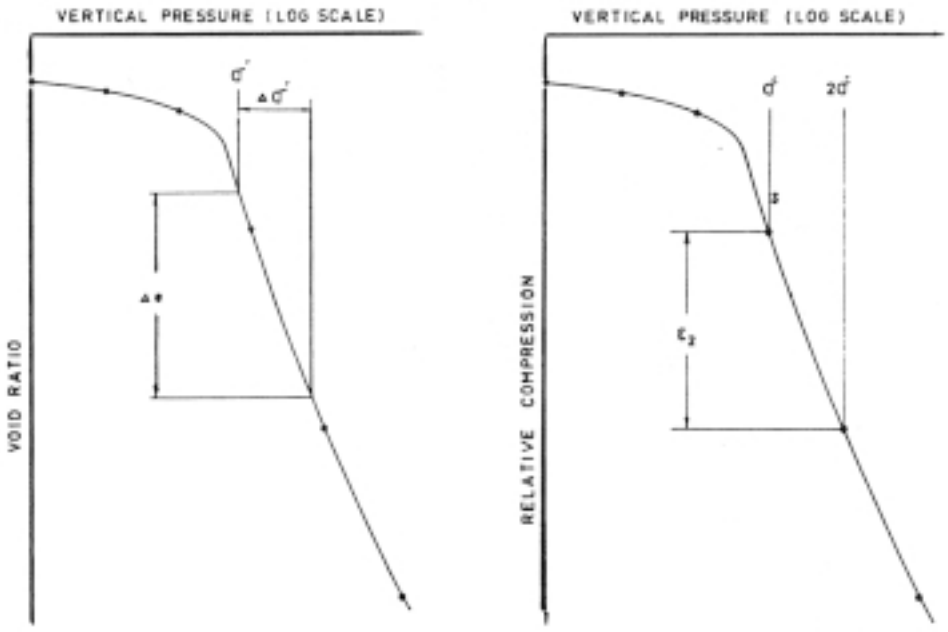

Figure 11-9. *Evaluation of the compression index C_c (left) and the index ε_2 (right) /6/.*

The fact that the compression curve is usually not a straight line has led to derivation of more general expressions of the type represented by Equation (11-16), /4,5,6/. For M, expressed as tangent modulus $M = d\sigma'/d\varepsilon$, one has:

$$M = m\sigma_j \left(\frac{\sigma'}{\sigma_j} \right)^{(1-\beta)} \qquad (11\text{-}20)$$

where:

M = oedometer modulus
m = modulus number
β = stress exponent
σ' = effective compressive stress
σ_j = reference stress, commonly 100 kPa

In Germany a similar expression $E_s = v \cdot \sigma^w$ is often used, with v interpreted for σ' = 100 kPa /4,5/.

Depending on the stress exponent, M can be an increasing or decreasing function as illustrated by Figure 11-10 for frictional soils.

Integration of the expression $d\varepsilon = \frac{d\sigma'}{M}$ yields the compression ε:

$$\varepsilon = \frac{1}{m\beta} \left(\frac{\sigma'}{\sigma_j} \right)^{\beta} + C \qquad \text{for } \beta \neq 0 \qquad (11\text{-}21)$$

$$\varepsilon = \frac{1}{m} ln \left(\frac{\sigma'}{\sigma_j} \right) + C \qquad \text{for } \beta = 0 \qquad (11\text{-}22)$$

These expressions can be used for calculation of the settlement of foundations on soils /6/. They have been applied in a number of cases for prediction of the movement of heavy, waste-containing cells – like the 16000 ton SFR silo at Forsmark in Sweden for disposal of low- and intermediate-level radwaste. It was constructed on compacted soil consisting of a mixture of 10% Na bentonite and suitably graded glacial silt/sand/gravel /7/.

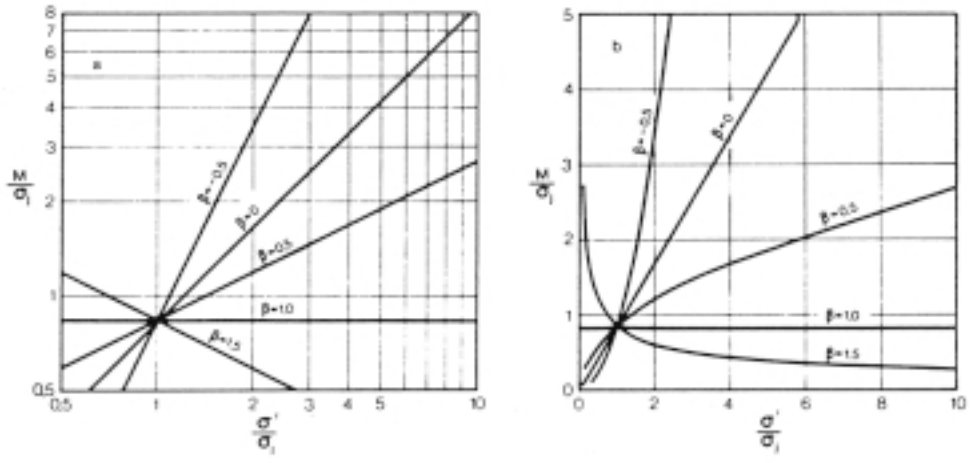

Figure 11-10. *Stress dependence of the oedometer modulus. Left: log/log form. Right: linear scales /5/.*

m and β are evaluated from oedometer tests in the fashion shown in Figure 11-11. Typical data are given in the diagram in Figure 11-12.

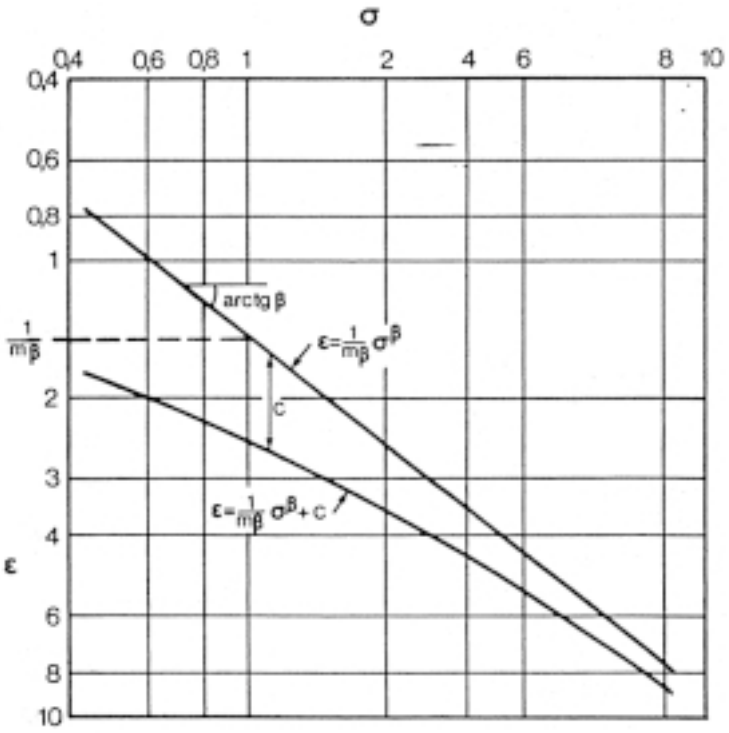

Figure 11-11. *Oedometer compression curve plotted in log/log diagram. The primary curve is the lower one, which is transformed to the upper one by finding a value Δε=C for which a straight line is obtained. Once this has been made, 1/mβ is directly obtained for σ' = 1 bar = 100 kPa. β is evaluated from the inclination of the line, which then yields the m-value /5/.*

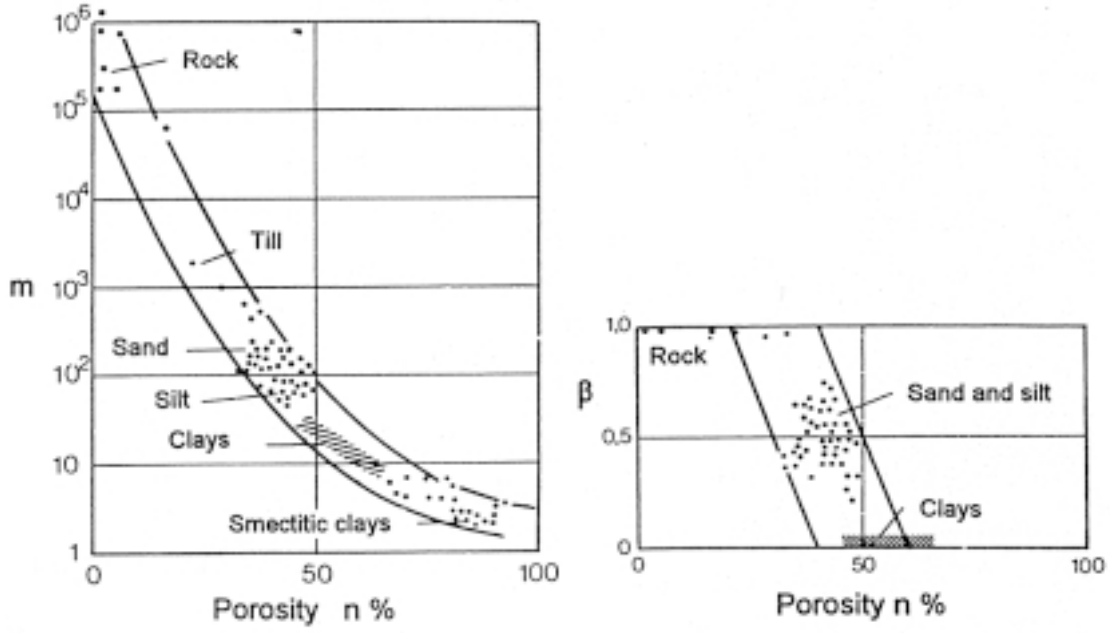

Figure 11-12. *Typical m- and β-values for various soil materials. Rock represents crushed rock /5/.*

Time dependence

Compression always proceeds as a function of time because the porewater overpressure in saturated soil has to be expelled, and because shear-induced rearrangement of the particle network is a visco/elasto/plastic process. The compression associated with porewater expulsion is called "primary consolidation", and strain after dissipation of the porewater overpressure is called "secondary consolidation". The diffusion-like process of primary consolidation is expressed in ordinary soil mechanics by use of the consolidation coefficient, c_v, which is evaluated from recording of the compression as a function of time. Conventionally, stepwise loading is made but the compression is sometimes also performed with constant rate of strain (CRS) and recording of the porewater pressure. This yields diagrams of the type shown in Figure 11-13 /8/.

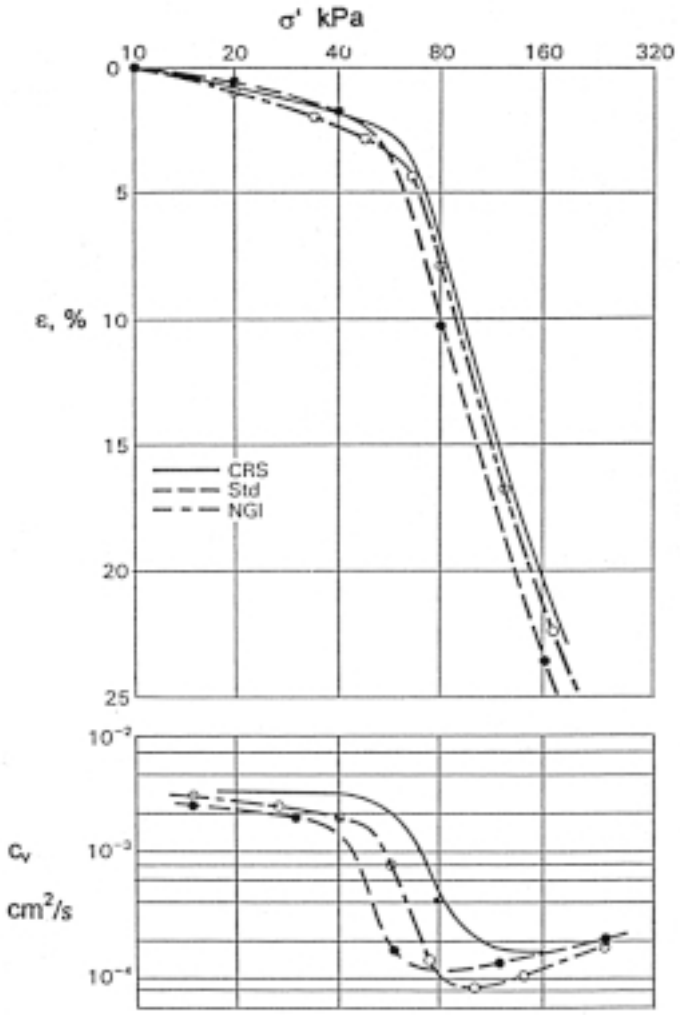

Figure 11-13. *Examples of consolidation tests using different equipments and techniques. Upper: Compression curves. Lower: The corresponding c_v-values /6/. CRS = Constant rate of strain. Std = Stepwise loading, Swedish standard. NGI = Stepwise loading, Norwegian standard.*

The time-dependence of the compression (consolidation) is obtained from the two parameters c_v and T_v, which are related according to Equation (11-23). For each load increment at stepwise loading T_v is evaluated as:

$$T_v = \frac{compression\ after\ time\ t}{total\ compression\ after\ completed\ \ primary\ consolidation}$$

T_v is related to c_v and sample thickness d according to Equation (11-23):

$$c_v = \frac{T_v d^2}{t} \qquad (11\text{-}23)$$

where:

c_v = consolidation coefficient
t = time after onset of consolidation
d = half thickness of the soil sample or the soil layer (for two-sided drainage)

Compression of clay-rich soils continues after the dissipation of the load-generated porewater overpressure, yielding "secondary consolidation", which is represented by α_s in Figure 11-14.

Secondary consolidation can be expressed by use of the coefficients α_s and C_α in the following fashions, using logarithmic time scales:

$$\alpha_s = d\varepsilon / d(\log t) \qquad (11\text{-}24)$$

$$C_\alpha = de / d(\log t) \qquad (11\text{-}25)$$

where:

ε = compressive strain
e = void ratio

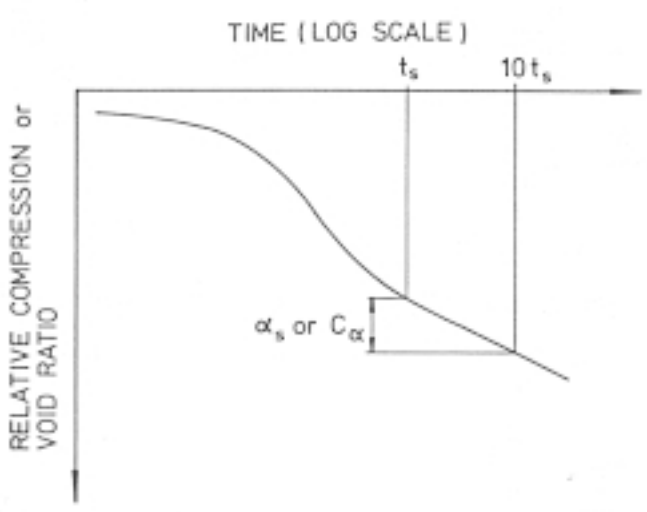

Figure 11-14. *Compression as a function of time with definition of secondary consolidation expressed in terms of the coefficients α_s and C_α /8/.*

11.3.3 Shear strain

General

Shear strain can be evaluated from direct shear tests and from triaxial tests (Figure 11-15). The stress conditions in a triaxially loaded sample are defined by the effective average normal stress $p' = \frac{\sigma_1' + 2\sigma_3'}{2}$ and the deviator stress, $q = \sigma_1' - \sigma_3'$, which are changed by altering the major principal total stress σ_1 keeping the cell pressure σ_3, i.e. the minor principal total stress, constant such that stress paths of the type shown in Figure 11-15 are followed until failure is reached. The stress state in a sample exposed to simple shear (Figure 11-4) is also well defined but this is not so for the direct shear that represents the practical application of this loading case as will be shown later in this chapter.

The axial strain $\Delta l/l$ and the volumetric strain $\Delta V/V$ are measures of the shear strain /9/. Typical recordings are shown in Figure 11-16, which represent illitic clay from Cigar Lake in Canada. It is believed to be the residue of an initially smectite-rich clay.

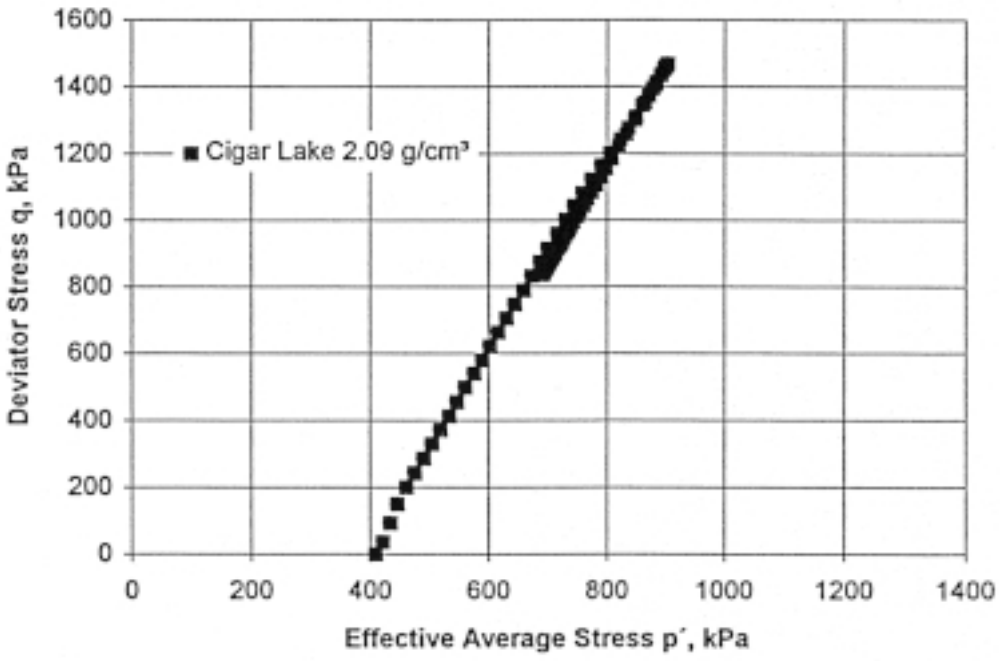

Figure 11-15. *Example of stress path in ordinary triaxial tests performed under drained conditions /9/. Illitic clay with a density of 2090 kg/m³ at saturation.*

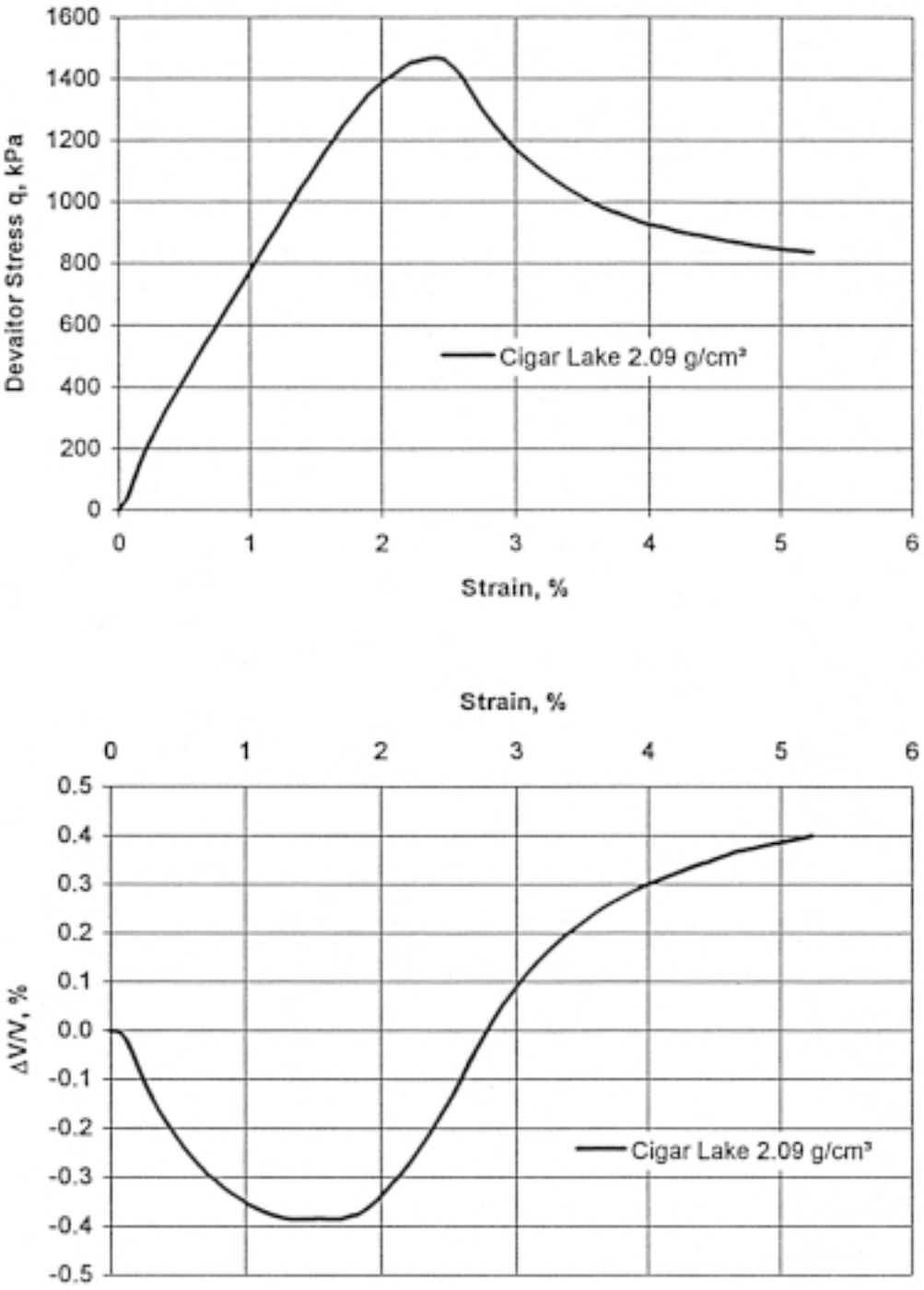

Figure 11-16. *Example of recorded axial strain of illitic clay with a density of 2090 kg/m³ at saturation as a function of the deviator stress. Upper: Axial strain versus deviator stress. Lower: Axial strain strain versus volumetric strain /9/.*

Creep

Secondary consolidation, which primarily results from creep strain on the microstructural scale, is particularly important for clays with a high water content (cf Figure 11-17), and this is also the case for shear strain. Smectite-rich buffers and backfills are apt to deform rather much with time when exposed to a deviator stress even at low water content i.a. because of weak contacts of adjacent stacks of flakes /1/.

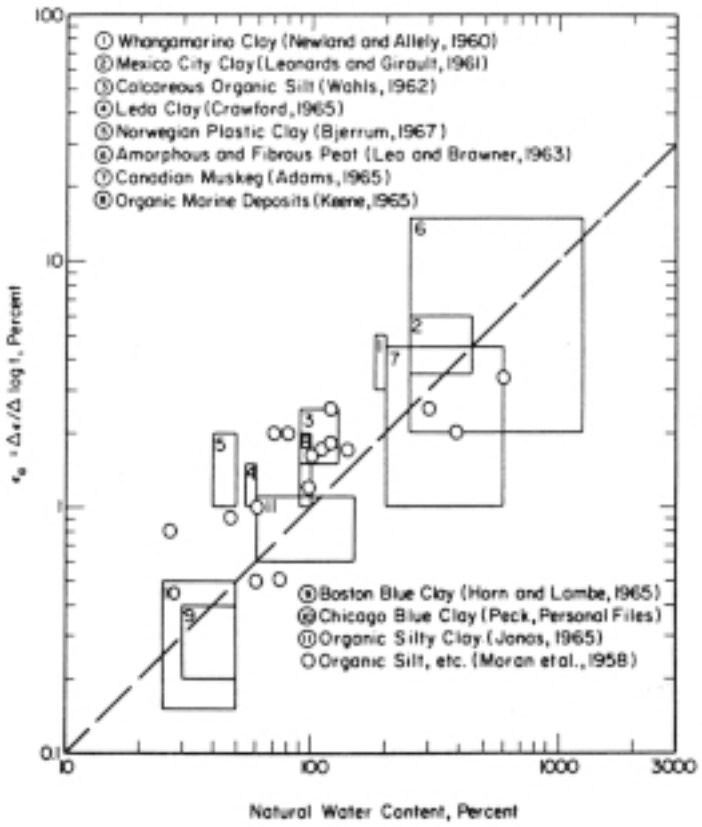

Figure 11-17. *Coefficient of secondary consolidation as a function of the water content /6/.*

Shear-induced creep can best be explained by applying rate process theory and relevant microstructural models, yielding creep laws of various forms /9,10,11/. Theoretically, log-time performance would be expected but in a short term perspective (months to years) other creep laws yield curves that agree better with recorded ones.

An empirical model of general applicability has been proposed by Singh and Mitchell /10/ and it has the following form:

$$\dot{\gamma} = \frac{d\gamma}{dt} = Ae^{\alpha\tau} \cdot t^{-n} \qquad (11\text{-}26)$$

where:

A, α and n = constants

τ = shear stress
$\dot{\gamma}$ = rate of shear strain
t = time

This expression can be normalized and related to a reference time t_r:

$$\dot{\gamma}_0 = Ae^{\alpha\tau_0} \cdot t_r^{-n} \qquad (11\text{-}27)$$

This expression, which is largely empirical, shows that the strain rate is not proportional to the shear stress and time after loading.

If the shear stress is replaced by the degree of mobilization of the shear strength (τ/τ_f) one has /8,9/:

$$\dot{\gamma} = \dot{\gamma}_0 \cdot e^{\alpha\tau/\tau_f} \cdot e^{-\alpha\tau_0/\tau_f} \cdot \left[\frac{t}{t_r}\right]^{-n} \qquad (11\text{-}28)$$

where τ_f = shear strength

Equation (11-28) can be put in the following form:

$$\log\dot{\gamma} = \log\dot{\gamma}_0 - \alpha\frac{\tau_0}{\tau_f} + \alpha\frac{\tau}{\tau_f} - n\left(\log t - \log t_r\right) \qquad (11\text{-}29)$$

which shows that *log/log* plotting of the strain rate $\dot{\gamma}$ and the time after onset of creep t gives a practically straight line.

For normalizing data from creep tests, t_r and τ_0/τ_f should be given standard values:

t_r = 10^4 s
τ_0/τ_f = 0.5

Figure 11-18 shows a typical plotting of the creep of smectite-rich clay. The n-factor is given by the inclination of the straight line in *log/log* diagrams. For this particular clay $n \sim 1$, i.e. the creep is of purely log time type after about 10^4 s.

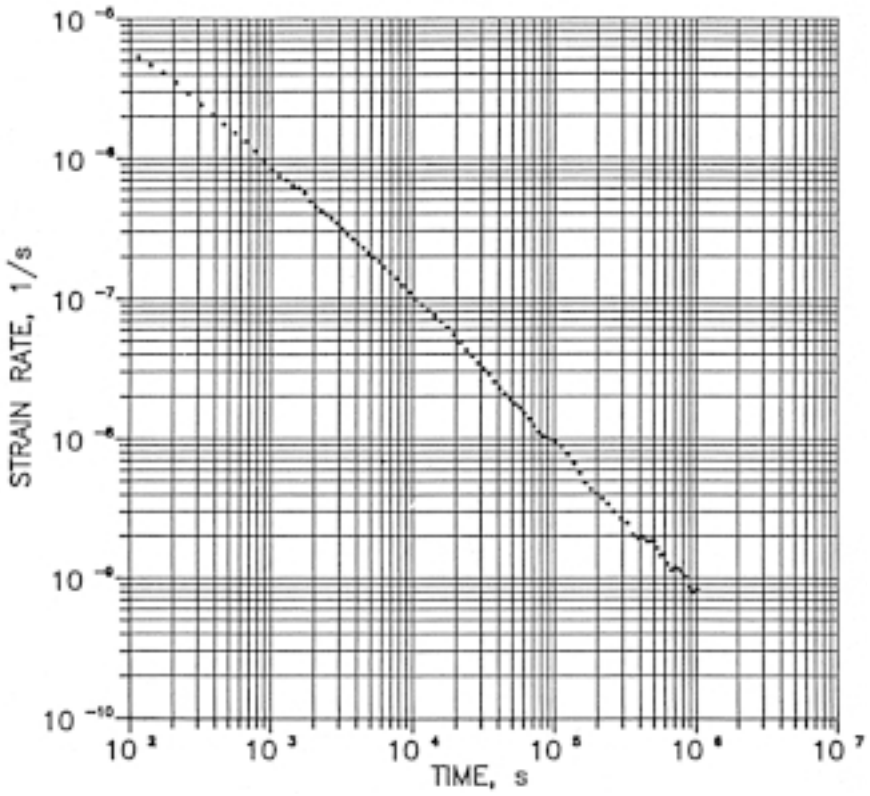

Figure 11-18. *Typical creep curve of Na bentonite showing almost perfect log time behaviour [n = 1 in Equation (11-28)], /9/.*

11.3.4 Shear strength

The ability of soils to resist shear stresses is a major requirement for most geotechnical applications. Both quick shearing under undrained conditions, and slow shearing under drained conditions, are relevant to the performance of buffer materials. The first-mentioned maximum shear stress is called the *undrained shear strength* and the latter *drained shear strength*.

Undrained shear strength

The undrained shear strength can be determined with the following methods:

1. Laboratory vane boring (for very soft clays)
2. Quick direct shear tests
3. Quick unconfined uniaxial compression tests
4. Undrained triaxial tests

Cone testing, which is a very common method for soft illitic clay has not been extensively for smectite rich clays and further calibration is needed.

The *vane borer* is a metal cross that is pressed down into the clay and rotated at a constant rate until failure takes place in the form of shearing along a cylindrical slip plane (Figure 11-19). At failure, the turning torque is equal to the torsional resistance and simple geometry yields the expression:

$$\tau_f = \frac{T}{\pi d^2 \left(h/2 + d/6\right)} \tag{11-30}$$

where:

T = torque
d = vane diameter
h = vane height

The *unconfined compressive strength* C_0 is (approximately) equal to two times the undrained shear strength as evaluated from Mohr's concept (Figure 11-20). Hence, for practical purposes one can take:

$$t_f = \frac{C_0}{2} \tag{11-31}$$

Like for the other quick-shear tests the stress conditions are only known in terms of total stresses. The effective stresses at failure are unknown.

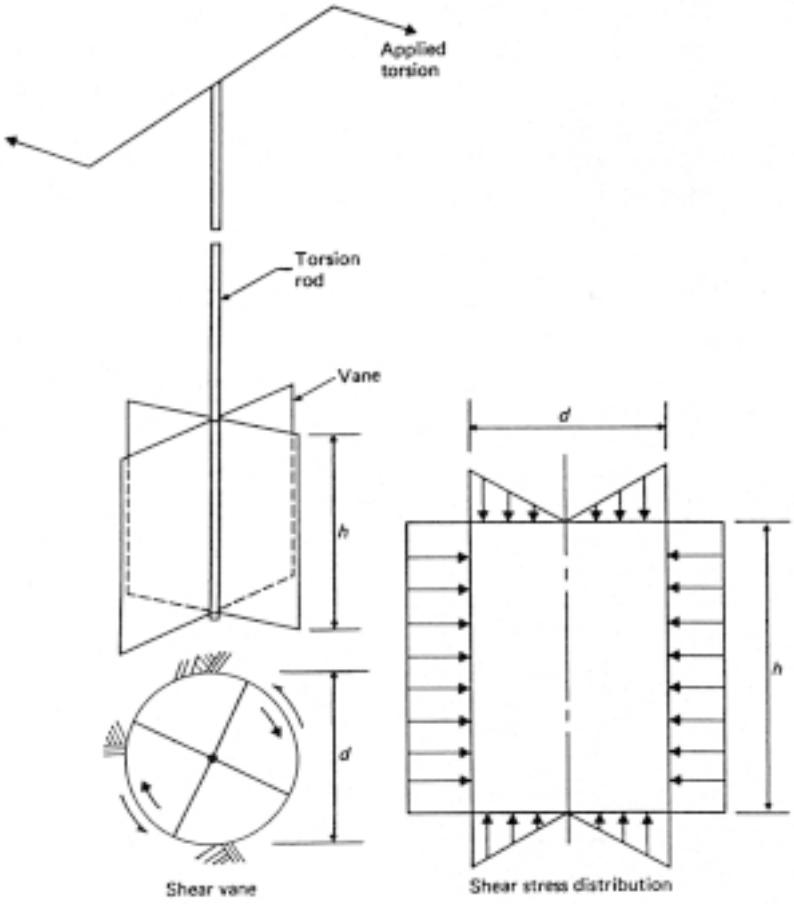

Figure 11-19. *Vane boring. The torsion rod is turned until the vane slips.*

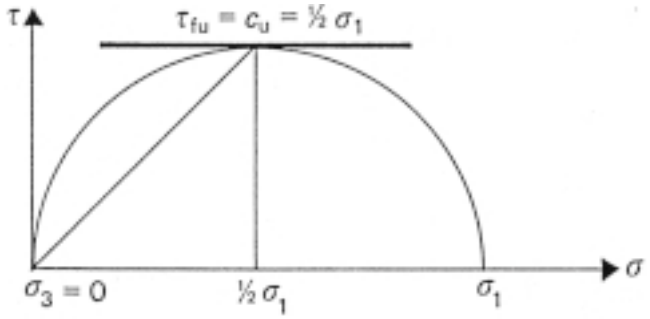

Figure 11-20. *Mohr's circle at unconfined compression implying that the minor principal stress is zero.*

Drained shear strength

The drained shear strength referring to any effective normal stress, can be determined by direct shear tests or triaxial tests /10/. The latter give more accurate results and are to be preferred since the principal stresses are known and controlled, and their orientations maintained constant throughout the test. Such a test is conducted as described in Section 11.2.3, i.e. by increasing the deviator stress until failure takes place. Two or three tests performed at different cell pressures (σ_3' or σ_3) yield the failure curve from which the parameters c' and ϕ' applying Mohr/Coulomb's relationship according to Equation (11-32) are evaluated (Figure 11-21):

$$t_f = c + \sigma' \tan \phi \qquad (11\text{-}32)$$

where

c = cohesion (zero for friction soils)
ϕ = angle of internal friction

11.3.5 Swelling

Quantification of the swelling potential of expansive clays can be made by reducing the pressure in oedometer tests and recording the expansion when equilibrium conditions have been reached (Figure 11-22). The swelling potential is expressed in terms of the swelling index α_s.

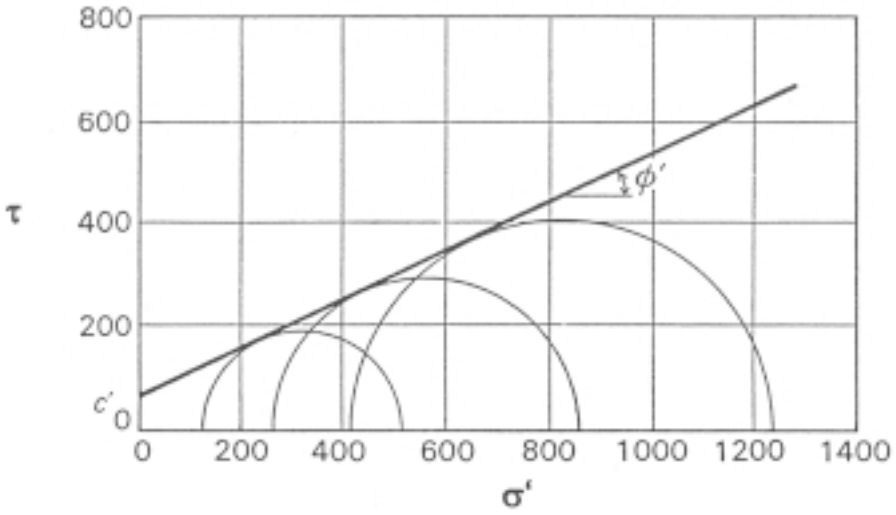

Figure 11-21. *Failure curves of bentonite from which the cohesion (intercept) c' and the angle of internal friction φ' can be evaluated.*

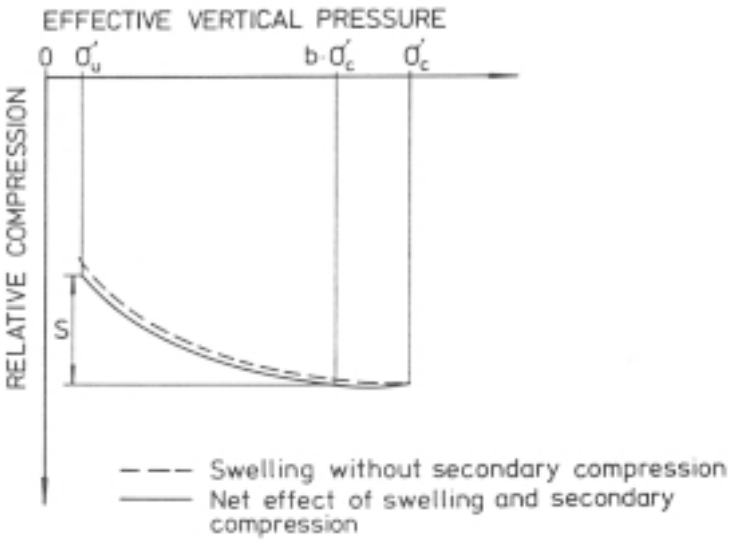

Figure 11-22. *Expansion on unloading of compressed clay /8/.*

The swelling index α_s is evaluated from Equation (11-33), /8/:

$$S = \alpha_s \, ln \frac{b\sigma'_c}{\sigma'_u} \tag{11-33}$$

where:

S = expansive strain (ratio of actual expansion and total sample height)
b = load factor; usually 0.8
σ_c' = preconsolidation pressure, or swelling pressure before expansion
σ_u' = pressure after expansion

11.3.6 Swelling pressure

The swelling pressure of expansive clays has several components:

- stored elastic energy of compressed particles and deformed particle network
- osmotic pressure between electrical double layers at contacting stacks of flakes
- hydration potential of the interlamellar space

The first- and lastmentioned components dominate at high bulk densities, while the second one controls the swelling pressure at low densities. Figures 11-23, 11-24 and 11-25 illustrate how they operate. The main difference between the smectites with sodium and calcium (e.g. multivalent cations) is that Na-clays expand to maximum 3 interlamellar hydrate layers, while the thicker stacks of flakes in Ca clays do not hold more than 2 hydrate layers. This results in less expandability and much lower swelling pressures at lower densities of the latter clays /1/.

The theoretical basis for prdicting and explaining the swelling potential of smetites is further discussed in Part 2 of this Handbook.

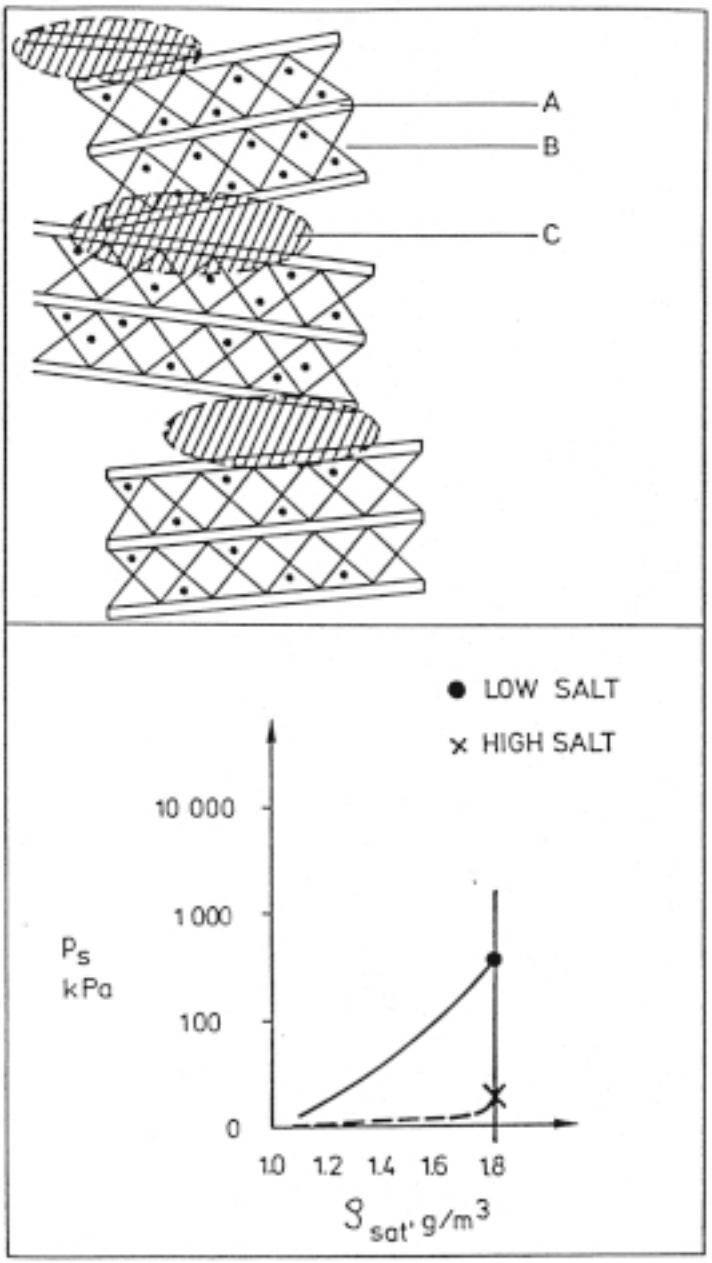

Figure 11-23. *Schematic picture of stack assemblage in Na montmorillonite and influence of ion strength on the swelling pressure at low densities. A) montmorillonite flake, B) interlamellar space, C) stack contact with interacting electrical double-layers and "disjoining" water /1/.*

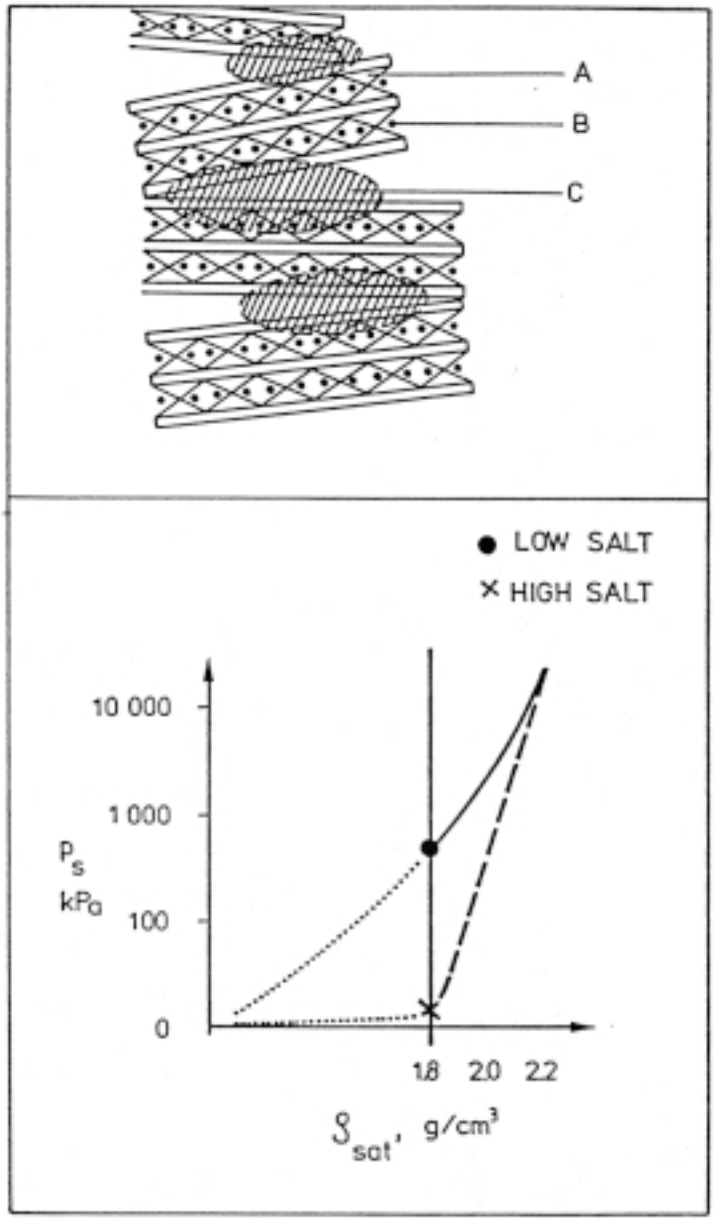

Figure 11-24. *Same as Figure 11-23 at high densities /1/.*

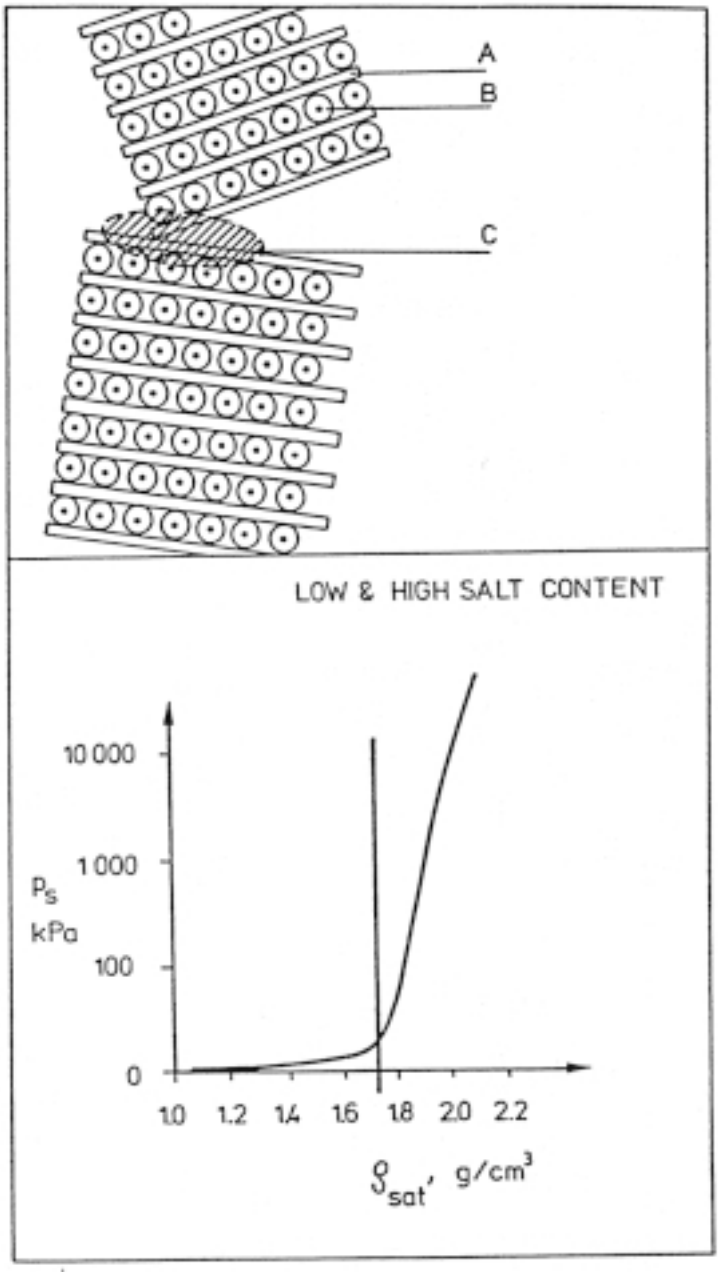

Figure 11-25. *Schematic picture of stack assemblage in Ca montmorillonite and influence of density and salinity on the swelling pressure. A, B, C are the same symbols as in Figure 11.23 /1/.*

11.4 General material model

While a number of problems in ordinary soil mechanics and also in repository design and performance assessment can be treated and solved by applying the simple, individual models for compression, shearing etc, coupled processes including expansion and thermal processes require general material models. They will be treated in detail in Part 3, but we will summarize the basic features of a general model for smectitic soils that turns out to be valuable in calculation of more advanced cases. Two models have been derived. The first one, which will be described in this chapter, has been improved to yield a model that includes a curved failure envelope and plastic behaviour at consolidation.

Properties modeled

The components and the material model can be grouped as follows /2/.

- Drucker-Prager Plasticity behaviour
- Porous Elasticitic behaviour
- Pore and Particle properties behaviour
- Thermal and thermomechanical behaviour
- Initial conditions

Drucker-Prager Plasticity, extended version

The simple Mohr/Coulomb-failure criterion is not sufficiently accurate for many purposes and an extended version of the Drucker-Prager Plasticity model may therefore haveto be applied. It implies that the influence of the intermediate principle stress can be taken into account and that dilation can also be simulated /2/.

The parameters used in the model are illustrated in Figure 11-26, which shows that the stress dependence is caused by the "friction angle" β in the σ_j-p plane and that the parameter d illustrates the "cohesion". Introducing plastic flow $d\varepsilon^{pl}$, the flow direction is perpendicular to the yield surface angle, which means that $\psi=\beta$. In order to decrease the resulting dilation it is necessary to assume non-associated flow by putting $\psi<\beta$. When the stress path enters the plastic region ds^{pl}, the yield surface is moved upwards until it reaches the failure surface.

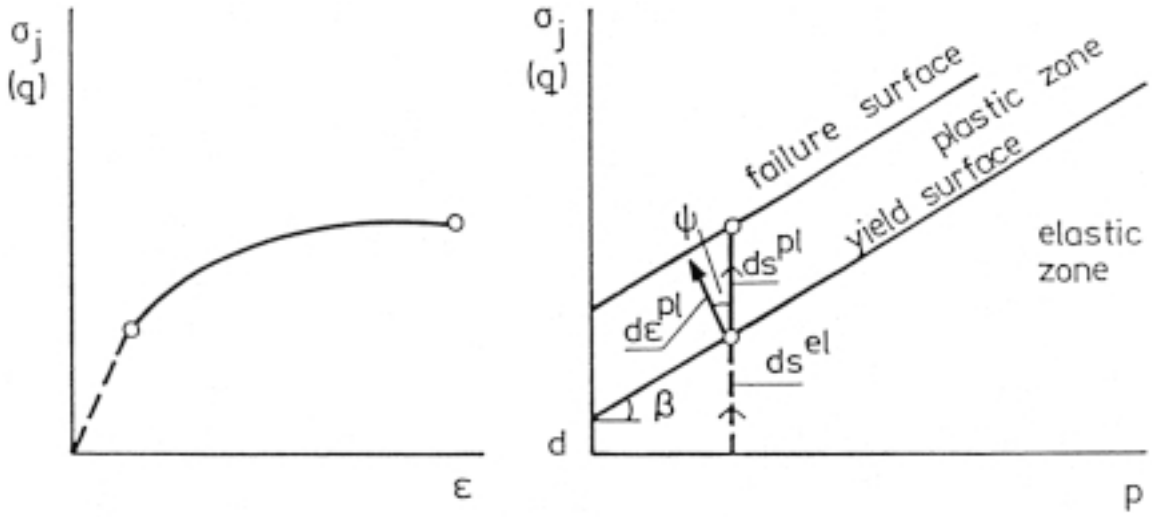

Figure 11-26. *Basis for Drucker-Prager plasticity model /2/. σ_j (q) represents the shear stress, p the normal stress, and ε the axial strain of the clay element.*

The model also includes a constant *K*, which controls the dependence of the yield surface on the intermediate principle stress. This surface is defined so that *K* is the ratio of the yield stress in triaxial tension and the yield stress in triaxial compression. The parameters needed for the extended Drucker-Prager model are thus β, *d*, *K*, ψ and the yield function *f*. Typical values for bentonite at high density of those parameters are:

β = 20°
d = 100 kPa
ψ = 2°
K = 0.9

The yield function, i.e. the relationship between σ_j and ε_y, is given in the form of discrete data in Table 11-1.

In Table 11-1, σ_j represents the Mises stresses and ε_y the plastic strain for a stress path that corresponds to uniaxial compression, i.e. when there is no confining pressure. Linear interpolation can be made using these data.

Table 11-1. Yield function /2/.

σ_j (kPa)	ε_y
113	0
138	0.005
163	0.02
188	0.04
213	0.1

Porous Elasticity

The stress/void ratio relation can be expressed by use of the model of "porous elasticity", in which the volumetric behaviour is defined according to Equation (11-34), /2/:

$$\frac{\kappa}{1+e_0} ln\left(p_0 / p\right) = j^{el} - 1 \qquad (11\text{-}34)$$

where:

e_0 = initial void ratio
p_0 = initial average stress
κ = the inclination of the e-log p relation
j^{el} = the elastic volume ratio

The key parameters κ, is the logarithmic bulk modulus for which a typical value is 0.21 /2/.

Pore and particle properties

The water density ρ_w and the bulk compression modulus K_w of the pore water as well as the bulk compression modulus of the solid particles K_s can be taken as:

ρ_w = 1000 kg/m^3
K_w = 2.1 · 10^6 kPa
K_s = 2.1 · 10^8 kPa

The flow of water through the model clay is expressed by using Darcy's law with the hydraulic conductivity K being a function of the void ratio e as given by Table 11-2. Interpolation between the values can be made.

Table 11-2. Derived K-data vs the void ratio of the model clay /2/.

e	*K* (m/s)
0.45	1.0 · 10^{-14}
0.70	6.0 · 10^{-14}
1.00	3.0 · 10^{-13}

11.5 Experimental

11.5.1 General

The procedures in performing oedometer and triaxial tests on smectitic clay require experience and insight in the behaviour of low-permeable soils. The major problem in most laboratory tests is the very low hydraulic conductivity, which means that expulsion of porewater on loading and uptake and homogenization on unloading normally take very long time, i.e. many months or even years. Great effort must be made to avoid leakage in tubes and even very moderate changes in room temperature in order to get accurate values.

11.5.2 Compressibility and swelling

For ordinary non-smectitic soils one can use standard oedometers but the high pressures normally involved in testing smectite-rich soils requires very rigid oedometers of which the swelling pressure oedometer shown by Figure 9-15 in Chapter 9 is suitable. It can be used for preparation of highly compacted smectite buffers and for determining the hydraulic and gas conductivities as well as the swelling index and pressure.

Equipment

- Swelling pressure oedometer with load cell and transducers for recording of the axial force and strain.
- Soil material and percolates (fluids). For artificially prepared soils like buffers and backfills the required granular size distribution is used. Fluids should be distilled water and 3.5% $CaCl_2$ solution representing "extreme" conditions.
- Several, at least three, separate tests should be made with different dry densities for determining the swelling pressure and expandability at complete fluid saturation. Alternatively one can use only sample and let it expand to different desired densities after recording of the swelling pressure.

Performance

The piston of the oedometer is fixed and the initially unsaturated sample allowed to hydrate while measuring the swelling pressure by use of the load cell. For compression tests the strain, total pressure and porewater pressure are measured for each load step until the porewater overpressure has dissipated.

Evaluation

The *swelling pressure* p_s, which is also the (quasi) effective pressure, is derived from the force F given by the load cell:

$$p_s = \frac{F}{A} - u \qquad (11\text{-}35)$$

where:

A = cross section area
u = backpressure (water)

The *compression index* C_c, expressed as Equation (11-18) is obtained by plotting the void ratio e versus the effective pressure $\sigma' = p_s$ and calculating the change in void ratio Δe caused by the compression that is generated by the pressure increase.

The *oedometer modulus* M is obtained by applying Equation (11-20). Plotting of the compressive strain ε is made as a function of effective stress σ' as in Figure 11-11, and m and β evaluated as shown in this figure. M is obtained by inserting σ_j = 100 kPa.

The *swelling index* α_s is obtained by applying Equation (11-33). Plotting is made as in Figure 11-22 and the strain $\varepsilon = S$ evaluated. The swelling index, obtained from tests in which the sample is allowed to expand, is calculated by putting b = 0.8 in the formula and inserting the actual ratio $\frac{\sigma_c'}{\sigma_u'}$, where $\sigma'_c = p_s$ for the initial, higher density and $\sigma'_u = p_s$ for the final, lower density.

11.5.3 Shear strain, creep

Triaxial testing – equipment

- Triaxial apparatus (Figure 11-27) equipped with load cell and transducers for recording of strains and porewater pressure. Flow meters or burettes are used for recording the amount of expelled or absorbed water.
- Samples of buffer material are preferably prepared by compression and fluid saturation of the clay powder in oedometers. A suitable diameter is 2.5–5 cm of the 1–2 cm high samples. Such disc-shaped samples are placed on top of each other to yield a height/diameter ratio about 2 for triaxial cell testing.
- For drained tests, the samples are equipped with peripheral paper drains extending over their entire length to the basal filters. The rubber membrane confines the sample with its drains and is tightly connected to the end plates.

Triaxial testing – performance

The most simple way of triaxial testing is to increase the deviator stress q stepwise while recording the axial strain and the porewater pressure as a function of time. Other stress paths, represented by keeping the effective normal stress constant when the deviator stress is increased, are also common.

Triaxial testing – evaluation

The deviator stress $q = \sigma_1 - \sigma_3$ is calculated by using the recorded axial force and the cell pressure, and the normal pressure $p = \frac{2\sigma_1 + \sigma_3}{2}$ is obtained in the same way although the backpressure u must be subtracted from p in order to express it as effective pressure:

$$p' = p - u \qquad (11\text{-}36)$$

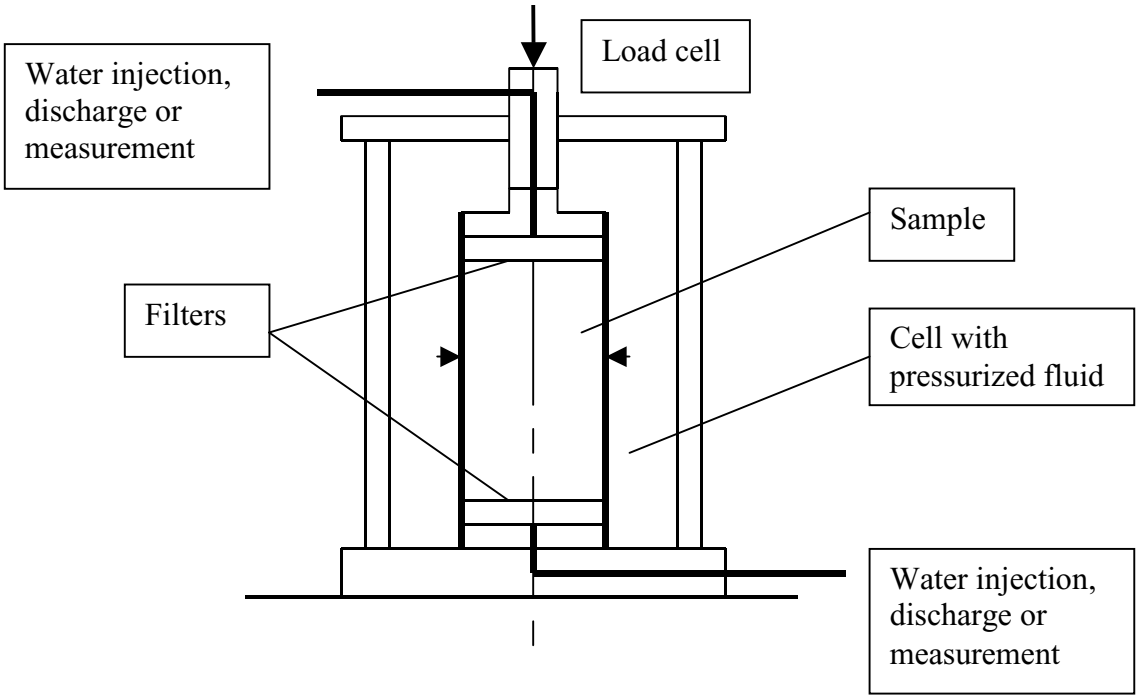

Figure 11-27. *Triaxial apparatus.*

The axial strain ε is evaluated by applying the expression:

$$\varepsilon = \frac{\Delta l}{l} \tag{11-37}$$

where:

Δl = axial shortening
l = initial sample height

For creep testing the axial and volumetric strain (in drained tests) is recorded and plotted as a function of time as in Figure 11-18. α and n are evaluated by applying Equation (11-30) for $t = 10^4$s after onset of the creep.

Simple (direct) shear – equipment

- The direct shearing, which in its most simple form is performed by use of a shear box consisting of two rigid halves moved mutually as indicated in Figure 11-28. The apparatus can be equipped with a load cell and transducers for recording of shear and normal strain and porewater pressure. Flow meters or burettes are used for recording the amount of expelled or absorbed water.
- Samples of buffer material can be prepared directly in the shear box like in an ordinary oedometer. A suitable diameter is 3–5 cm of the 1–2 cm high samples.

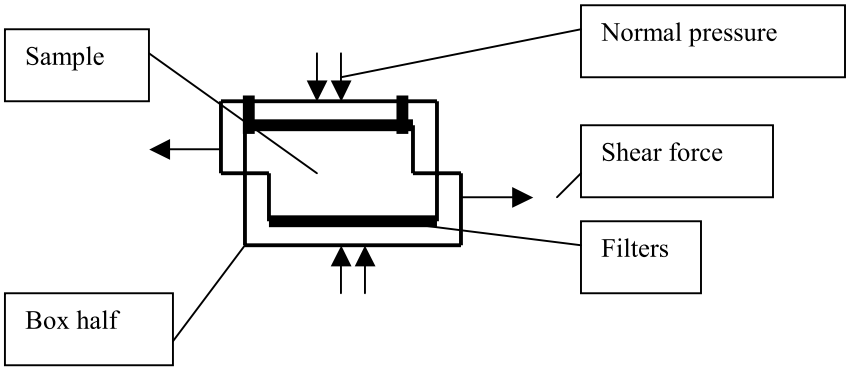

Figure 11-28. *Schematic picture of shear box. The total normal pressure is transferred via a piston and it can be kept constant with recording the pore pressure or, alternatively, the sample can be drained through the filters by which the effective stress is known.*

Direct shear testing – performance

The test is performed by consolidating the sample under the desired effective normal stress. Shearing is then made either by stepwise loading with recording of strain or by shearing at constant rate with recording of the shear force and porewater pressure. The firstmentioned procedure can be applied for determination of typical creep data as described in Chapter 12.

Direct shear testing – evaluation

Figure 11-29 shows the outcome of a FEM calculation in 2D of the orientation and ratio of the principal stresses assuming the clay to behave as an elasto/plastic material /12/. The stress contours in the sample at a shear strain of less than about 1% imply that the central part of a clay sample remains elastic while plastization occurs at the edges and this condition is suitable for measuring the creep rate in the elastic range. The height of the non-plasticized part is approximately one third of its diameter. For stresses lower than about 2/3 of the shear strength and for smaller shear strain of the total sample (Δ/D where Δ is the displacement of the box halves and D the sample diameter) than 1%, the average shear stress can be taken as the ratio F/A, where F is the shear force and A the total cross section area.

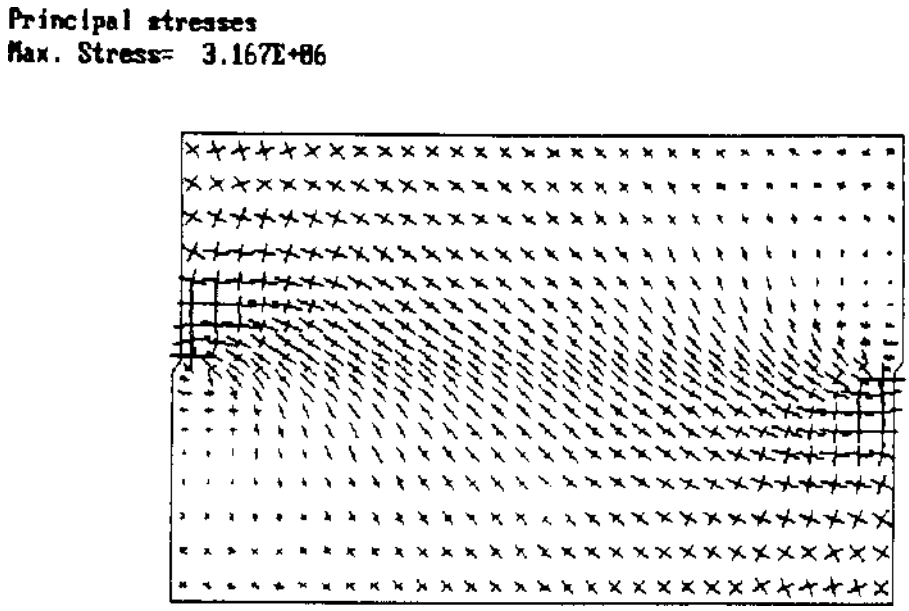

Figure 11-29. *Orientation and ratio of the principal stresses for 1% shear strain /12/. The deviator stress, i.e. the difference between the principal stresses, is small except in the central part of the sheared sample, especially in the potential shear plane at failure.*

11.5.4 Undrained shear strength

Equipment

- The triaxial and direct shear equipments can be used with the drainage closed and porewater pressure measured. The vane bore (laboratory or field versions) can also be used with torque facility for constant rotating speed (Figure 11-19). The blade dimensions are d = 10–50 mm depending on the density of the soil. The height/diameter ratio should be 2.
- Loading frame for uniaxial compression tests, preferably the same as for triaxial tests.

Performance and evaluation – triaxial test and unconfined compression test

The sample is tested as for drained conditions with recording of the porewater pressure. In the triaxial cell pressures are first applied to yield consolidation under drained conditions and the axial stress is then increased stepwise until failure occurs while keeping the sample undrained /8/. In the unconfined compression test no cell pressure is applied. The load steps in both tests are taken small enough to reach significant strain reduction before the next load is applied, usually corresponding to about 1/5 to 1/10 of the failure load. Commonly, the test is made applying a constant rate of strain, normally 0.1% per minute, and recording the force by use of the load cell. Maximum force yields the unconfined compressive strength.

Performance and evaluation – direct shear test

The test is performed as under drained conditions, i.e. first consolidated under drained conditions and then sheared under undrained conditions while measuring the porewater pressure. The strength is preferably determined by applying a constant rate of strain, normally 0.1% per minute, and recording the force by use of the load cell. Maximum force yields the unconfined compressive strength.

Performance and evaluation – vane bore

The vane bore is rotated at a speed of 1 radian/minute and the torque recorded. The maximum torque represents the undrained shear strength, which is evaluated from Equation (11-30).

11.5.5 Drained shear strength

Equipment and performance

The test can be made by use of the triaxial apparatus and the direct shear apparatus.

Evaluation

The evaluation of the shear strength is made in the same fashion as in tests performed for evaluating the undrained shear strength but with drainage allowed throughout the test.

Irrespective of the stress path, failure is obtained when a critically high shear stress $\tau_f = \frac{\sigma_1 - \sigma_2}{2}$ has been reached for any average effective pressure $p' = \frac{\left(\sigma_1' + 2\sigma_3'\right)}{2}$.
Failure takes place when the shear stress has reached a maximum value. The corresponding τ_f is plotted versus the applied σ'-values, which yields a relationship of the type shown in Figure 11-21.

For triaxial tests one can make the plottings as shown in Figure 11-26, which is adapted to the general material model described in Section 11.3. $q = q_f$ value is plotted versus the applied p'-value, and the performance of two or more tests yields failure curves of the type shown in Figure 11-30. If plotted in simple linear diagram form, the Mohr/ Coulomb parameters c' and ϕ' are obtained.

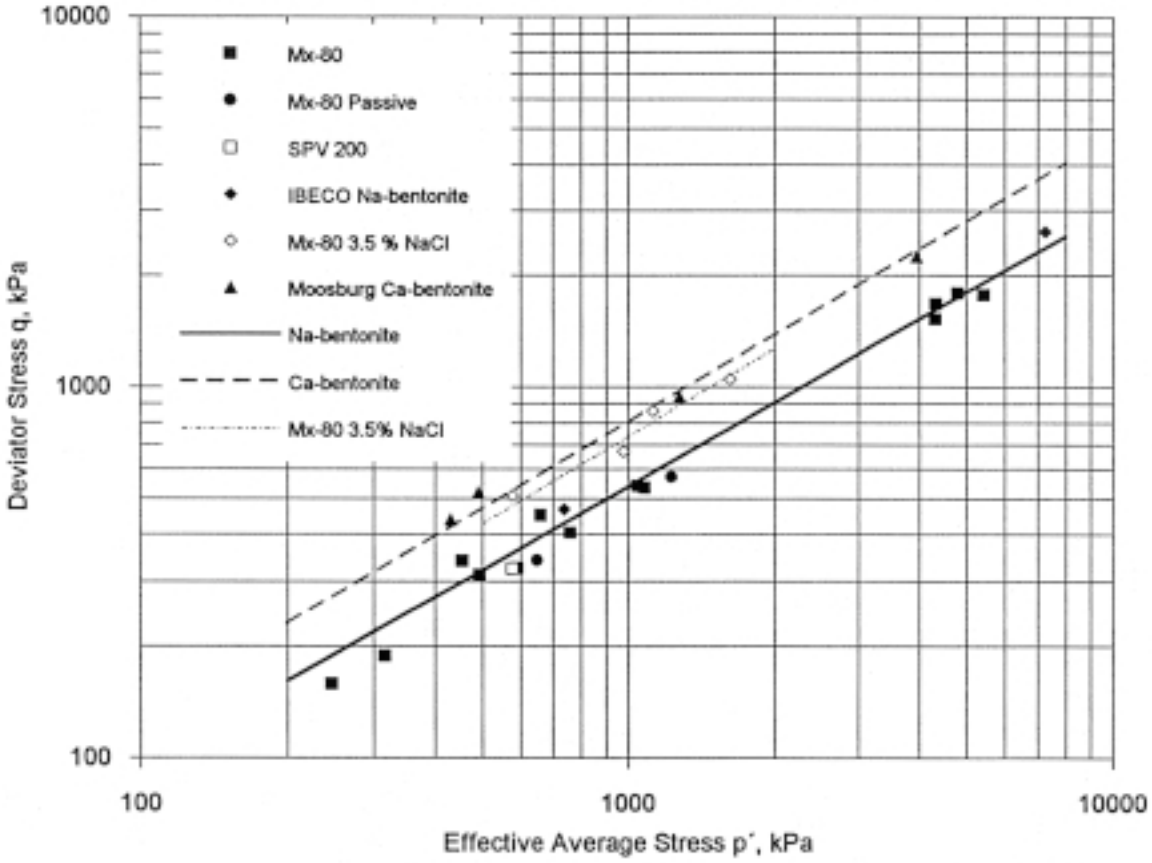

Figure 11-30. *Example of evaluation of the Mohr/Coulomb parameters c' and ϕ' from triaxial tests.*

11.6 References

/1/ **Pusch R, Karnland O, Hökmark H, 1990.** GMM – A general microstructural model for qualitative and quantitative studies of smectite clays. SKB TR-90-43, Svensk Kärnbränslehantering AB.

/2/ **Börgesson L, 1990.** Interim report on the laboratory and theoretical work in modeling the drained and undrained behavior of buffer materials. SKB TR-90-45, Svensk Kärnbränslehantering AB.

/3/ **Graham J, Oswell J M, Gray M N, 1992.** The effective stress concept in saturated sand-clay buffer. Canadian Geotechnical Journal, 29: 1033–1043.

/4/ **Odhe J, 1951**. GrundbaUmechanik, Bd III, Hütte, Berlin.

/5/ **Andreasson L, 1972.** Kompressibilitet hos Friktionsjord. D. Thesis, Chalmers University of Technology, Gothenburg.

/6/ **Janbu N, 1967.** Settlement calculation based on the tangent modulus concept. I: guest lectures at Moscow University. Geoteknikk Medd. 2, Norwegian Institute of Technology, Trondheim.

/7/ **Pusch R, 1994.** Waste Disposal in Rock, Developments in Geotechnical Engineering, 76. Elsevier Publ. Co ISBN:0-444-89449-7.

/8/ **Larsson R, 1986.** Consolidation of soft soils. Report No. 29, Swedish Geotechnical Institute, Linköping, Sweden.

/9/ **Börgesson L, Hökmark H, Karnland O, 1988.** Rheological properties of sodium smectite clay. SKB TR-88-30, Svensk Kärnbränslehantering AB.

/10/ **Pusch R, Feltham P, 1980.** A stochastic model of the creep of soils. Géotechnique, Vol. 30, No. 4, (pp. 497–506).

/11/ **Singh A, Mitchell J K, 1968.** General stress-strain-time functions for soils. Amer. Soc. Civ. Engrs. Proc., Vol. 94, No. SM 1.

/12/ **Pusch R, Börgesson L, Erlström M, 1987.** Alteration of isolating properties of dense smectite clay as exemplified by seven pre-Quaternary clays. SKB TR-87-29, Svensk Kärnbränslehantering AB.

12 Routine methods for quality assurance of large quantities of buffer clay and ballast

This chapter describes a test scheme for quick but accurate quality checking of buffers and backfills. It can be required for application by manufacturers of buffer and backfill materials and used by buyers and licensing authorities for acceptance of material delivered to a repository construction site. Adequate laboratory resources are required.

12.1 General

The selection of suitable components for preparation of buffers and backfills requires very careful and comprehensive laboratory investigations using standard procedures. At the stage when decision has to been taken concerning the choice of soil materials simple routine methods are required for checking the quality of the large quantities that will be delivered to the construction site. Such methods, which may well represent different levels of accuracy for different purposes, must comprise techniques for very quick determination of important properties, like the content of smectite in material intended for preparation of buffers. This implies that the methods should indicate if the material data are on the right order of magnitude, rather than giving exact information on the properties.

12.2 Criteria

The basis of the definition of quality criteria is of course performance analyses and safety assessment, which specify the required, minimum isolation potential of the various buffers and backfills, primarily in terms of hydraulic and gas conductivity, diffusivity, and rheological behaviour. They are all functions of the granulometric and mineralogical compositions and of the density. Examples of typical material data are given in Part 2 of this Handbook.

The material properties to be checked when accepting delivery of components for large-scale preparation of buffers, backfills, plugs and grouts are virtually the same, although the quality criteria may differ depending on the intended use. A most important thing is that the clay must perform sufficiently well for long periods of time and this means that certain smectite types cannot be accepted. One such species is beidellite. Also, the content of certain accessory minerals or minerals in the ballast with which the clay is mixed for preparing backfills must be limited. Species of this sort are sulphides, sulphates and potassium-bearing minerals. The grain size is also important: the granules of bentonite for preparation of compacted blocks must be suitable and not too small, while clays intended for grouting must not contain accessory minerals with a size that exceeds about 2 μm. For clay-poor backfills, the size of the granules must be selected so that they effectively fill the space between coarser grains.

The SFR project, i.e. the construction of an underground repository for low- and intermediate radioactive waste at Forsmark in Sweden, serves as an example of how criteria can be defined and material properties checked before accepting shippings.

Two sorts of clay-based materials were used for the SFR, i.e. a coarse-granulated Na bentonite that was used to fill the space between a large silo containing radioactive waste and the surrounding rock, and a granulated Na bentonite that was mixed with ballast material and compacted on site for providing a low-compressible bottom bed with low hydraulic conductivity for the silo (Figure 12-1), /1/.

For the more than 6000 ton slot fill the following criteria were set:

1. The size distribution of the granules – checked for each 50 ton delivery – must be within a certain range for obtaining a suitable density (Figure 12-2).
2. The water content of the bentonite granulate must not exceed 18% for the reason that only material with lower water content had been tested and found acceptable in full scale experiments, and for cost reasons.

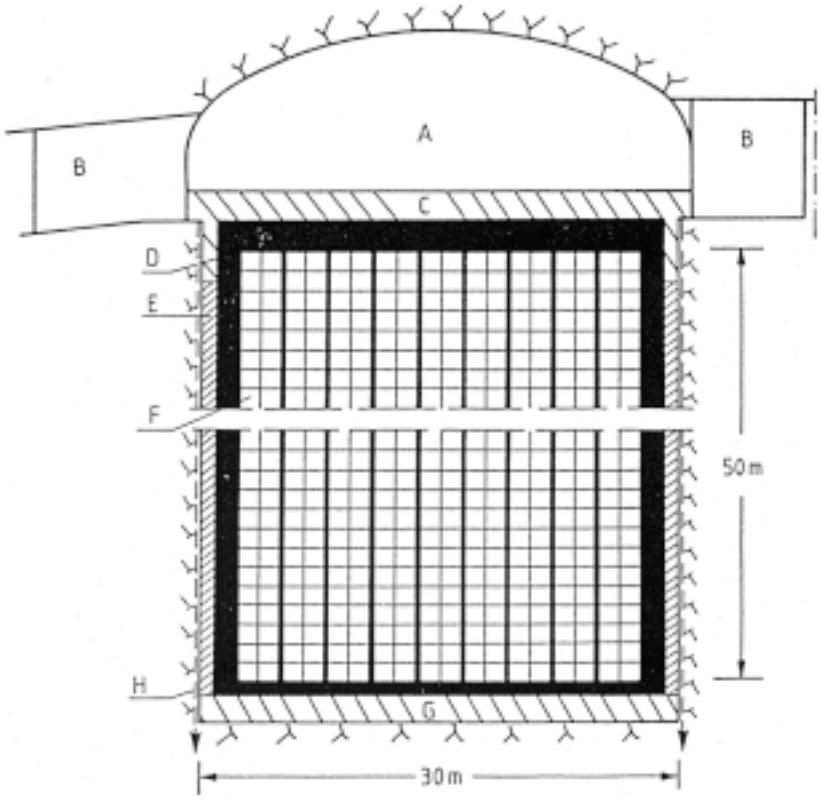

Figure 12-1. *Schematic cross section of the silo cavern. A) Cement-stabilized sand-fill, B) Concrete plugs, C) Bentonite/sand top bed, D) concrete silo, E) Bentonite backfill, F) Waste packs, G) Bentonite/sand bottom bed, H) Drains connected to tunnel system.*

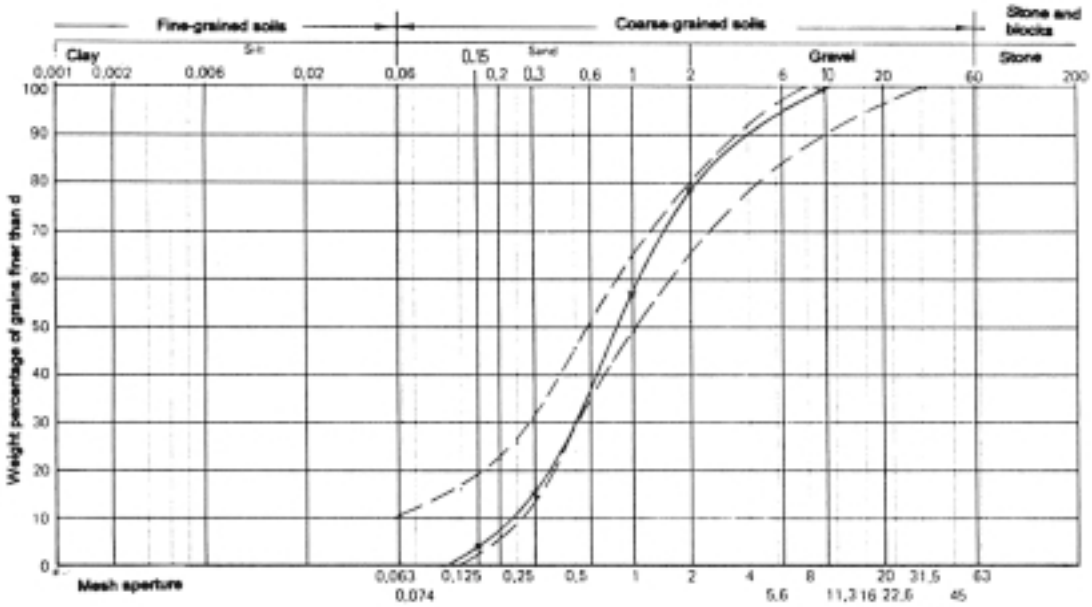

Figure 12-2. *Size diagram of bentonite grains (granules). The solid line represents a dry-sieve curve within the acceptable range between the two dashed curves.*

3. The smectite should be montmorillonite and it must represent at least 60% of the total mineral mass of the bentonite. X-ray diffraction analysis (XRD) must be used for checking that the smectite is montmorillonite in each 500 ton shipment before delivery. The percentage of smectite must be checked for each 50 ton delivery by determining the liquid limit (Casagrande). It must not be lower than $w_L \leq 325\%$.
4. The mineral density checked for each 500 ton shipment must be within the range of 2600–2750 kg/m^3.
5. pH checked for each 500 ton shipment. It must be within the range 8.5–10.5.
6. The sulphur content, expressed in terms of the content of soluble SO_4 checked for each 500 ton shipment, must not exceed 0.3% SO_4^{2-}.

For the bottom bed the criteria for the bentonite were the same as for the slot fill, except that the size distribution of the granules, checked for each 10 tons, should be such that more than 92% passed the 0.074 mm sieve.

For the ballast material it was required that the total content of micas, carbonates and sulphide minerals should be less than 1%. The content of K-bearing feldspars should be less than 10% of the total mineral mass.

For comparison, the limits for acceptance of the reference buffer material (RBM) used by AECL in the site URL were as specified in Table 12-1 /2/. This material is defined as a 50/50 mixture of clay and graded sand. Routine quality control tests were those specified in Table 12-2.

Table 12-1. Limits for acceptance of RBM and its components /2/.

Test	Raw Clay	Raw Sands	Graded Sand	Buffer
Consistency Limits				
W_L (% moisture)	> 200	N/A	N/A	> 100
W_P (% moisture)	< 50	N/A	N/A	< 20
I_P (W_L–W_P)	> 150	N/A	N/A	> 80
Particle Size Analysis				
% clay	> 60	N/A	0	> 30
% silt	< 40	< 1	< 6	< 20
% sand	< 1	–	94–100	50 ± 5
Moisture Content				
(% of dry weight)	0–10	< 1	< 1	17–19

N/A = Not Applicable

Table 12-2. Routine quality control tests required for buffer production /2/.

Test	Raw Clay	Raw Sands	Graded Sand	Buffer
Atterberg Limits	Y	N	N	N
Sieve Analysis	N	Y	Y	Y
Moisture Content	Y	Y	N	Y

Y = Yes

N = No

12.3 Routine characterization scheme

12.3.1 General

In addition to the required testing of granulometry and mineralogy, a general clay characterization scheme should comprise also simple physical tests. Firstly, because the physical properties are the ones that give direct information on whether the material behaves as required according to the performance criteria and safety assessment, and secondly because so much experience has been gathered respecting these properties that one can easily see whether the material behaves acceptably.

12.3.2 Scheme for characterization

Granulometric composition

Purpose

The grain size distribution gives a good picture of the content of clay minerals since they appear almost entirely in the clay fraction (minus 2 μm). The compaction properties of the material can be estimated by the character of the entire grain size curve, from which one can conclude if the material is suitable for backfilling purposes.

Techniques

Sieving, and sedimentation tests using the hydrometer or the Atterberg pipette techniques are recommended (SI standards). Automatic techniques, like the Coulter counter method, are applicable but calibration by use of one of the afore-mentioned techniques is required.

Chemical composition

Purpose

The chemical composition determines the relationship between silica, aluminum, magnesium and iron, and knowing the amounts of these elements one can identify the dominant smectite type: i.e. montmorillonite, beidellite, saponite, or nontronite. It also provides a basis for identifying accessory minerals of importance, like calcite and sulphides.

Techniques

Spectroscopic (IPC) analyses applying dissolution in $LiBO_2$ melt should be made as standard tests, while EDX tests, using transmission or scanning electron microscopy, are recommended for special purposes. Tests of material with all granular sizes, i.e. including the clay fraction (minus 2 μm) must be made.

Element analyses are made with respect to the presence of SiO_2, Al_2O_3, Fe_2O_3, MgO, CaO, K_2O, Na_2O, S and LOI, the latter representing the ignition loss (LOI). All data are given in weight percent units (examples of tests of a number of commercial clays are given in Part 2 of this Handbook.

A typical set of element data for montmorillonite corrected with respect to the LOI is that in Table 12-3:

Table 12-3. Typical chemical composition of montmorillonite-rich clay expressed in oxide form.

SiO_2	Al_2O_3	Fe_2O_3	MgO	CaO	K_2O	Na_2O	S
65	20	6	5	1.8	1.8	0.3	0.1

Mineralogical composition

Purpose

The main purpose is to determine the content and type of smectite minerals as well as the nature and amount of accessory minerals of importance, of which K-feldspars, calcite and other carbonates, as well as sulphate and sulphide minerals are of particular interest.

Techniques

XRD, and determination of the cation exchange capacity (CEC) and the Atterberg consistency limits are made for standard characterization. Transmission electron microscopy (TEM) of microstructurally intact soil in combination with element analysis (EDX) are used for checking purposes. Optical microscopy can be useful for identification of accessory minerals and for determining the size and shape of clay particles.

XRD

Several charts for XRD-identification of clay minerals are in use, a simple but sufficiently accurate one being Tank's scheme /3,4/. It can be applied to samples prepared both of bulk material (finer than 74 μm) and of the clay fraction. Sedimented specimens are prepared, and heating to 250 and 600°C as well as glycol treatment are applied.

Major characteristics when applying CuK_α radiation (Ni filter) are:

- *Kaolinite*
  Regular basal sequence of peaks of 7.1, 3.57 and 2.39 Å. Crystalline character lost on heating to 600°C.
- *Chlorite*
  First- and third-order reflections are 14.0 and 4.7 Å, respectively. Only partial dehydration takes place at 600°C. Strong solubility in warm dilute hydrochloric acid.
- *Hydrous mica (illite)*
  Sequence of basal reflections at 10, 5 and 3.3 Å; (020) reflection at d=4.5 Å.
- *Smectites*
  Basal (001) peaks at about 12 to 15 Å in air-dry condition. 15–17 Å peaks on glycol treatment indicates Ca and Na as the respective major cation. Heating to 250°C yields collapse to 10 Å basal spacing.

  Beidellite is distinguished from montmorillonite by not expanding to more than 14.1 Å on exposing Na-saturated clay to 100% relative humidity environment. On such treatment, montmorillonite gives a basal spacing of more than 16 Å.
- *Mixed-layer minerals*
  Identification of large (001) spacing and regular series of sharp, higher order reflections indicate regularly interstratified minerals. Non-integral series of basal plane reflections indicate randomly interstratified minerals. Altered peak shape and intensity by cation saturation indicates segregated minerals; if layers expand on glycol treatment and collapse on heating the material is termed smectite.

- *K-feldspars*
  The following peaks are characteristic:

d-value (Å)	Intensity (100 max)
4.23	60
3.31–3.29	100
3.26–3.23	40–100
2.99	50
4.21–4.04	60–70 (K/Na)

- *Calcite*
  The only easily identified reflection is the very strong characteristic peak for the d-distance 3.035 Å.

- *Iron sulphide (pyrite)*
  The peaks in Table 12-4 are characteristic:

Table 12-4. Iron sulphide XRD fingerprints.

d-value (Å)	Intensity (100 max)
2.423	65
2.709	85
1.633	100

While this sort of interpretation of XRD spectra primarily serves to give a qualitative picture of the mineral assemblage, a rough semi-quantitative evaluation can be made by using certain peak height ratios. The uncertainty is considerable, however, and for routine testing other measures of the mineral composition, like determination of the consistency limits, are preferred.

Cation Exchange Capacity

The cation exchange capacity (CEC) should be determined only for the clay fraction. Chapman's method for determination of the total cation exchange capacity and of the amounts of adsorbed cations is recommended because of its relative simplicity. This technique involves exchange to NH_4^+ by repeated washing with ammonium acetate solution. The supernatants are saved for analysis of the initially adsorbed cations.

Washing with isopropyl alcohol to remove excess NH_4^+ ions is made and NaCl solution finally used for transfer to Na saturated conditions. The supernatant is analyzed with respect to NH_4^+ for evaluation of the total CEC.

Typical CEC-values, expressed in terms of meq/100 g are those given in Table 12-5. The technique is described earlier in Part 1 of the Handbook and also in Part 2.

Naturally, soils composed of two or several major clay minerals can give any CEC value in the range of about 10 to 100, which demonstrates that additional techniques must be applied to make identification possible.

Table 12-5. CEC-values of common minerals.

Material	CEC, meq/100 g
Zeolites	300–100
Vermiculite	150–100
Montmorillonite	150–80
Chlorite	47–4
Hydrous mica	40–10
Kaolinite	15–3
Feldspar, quartz	1

Atterberg Consistency Limits

The hydration capacity of minerals is manifested by the three consistency limits: w_L – *the liquid limit*, w_P – *the plastic limit*, *and* w_S – *the shrinkage limit*. For estimation of the smectite content the liquid limit serves as a valuable indication. The w_L-data in Table 12-6 can be taken to be representative. The technique is described earlier in Part 1 of the Handbook.

It is obvious from the fact that there is a considerable difference in w_L of sodium- and calcium saturated clay that variations in clay content (minus 2 μm fraction) makes estimation of the smectite content very uncertain. Hence, w_L data should only be used for this purpose if the clay fraction has been separated and tested, and if the type of adsorbed cation has been determined by XRD analysis.

Transmission Electron Microscopy, TEM

TEM of dispersed clay material sedimented on the common types of very thin organic films can be performed for making a rough estimate of the relative amounts of kaolinite, hydrous mica and smectite based on the diagnostic morphology of these clay minerals /5/. Applying TEM to suitably embedded clay, the general fabric can be identified and cementing agents revealed, and element analyses (EDX) performed. This trchnique, which is described earlier in this Handbook, is very helpful in derivation of the genesis of the soil. Embedment is suitably made by stepwise saturation with ethylene alcohol and plastic monomers and polymerization at 60°C.

Scanning Electron Microscopy, SEM

SEM of samples that are mechanically fractured after air-drying, freeze-drying or critical point drying and coated with carbon (or gold if element analyses are not going to be made) serves to illustrate the general microstructure with less tedious preparation than what TEM requires. The resolution power (50–100 Å) is considerably lower than in TEM analyses but acceptable for many routine studies. EDX element analyses (spot or area) can readily be made.

Table 12-6. Characteristic liquid limit data for montmorillonite.

Clay	w_L, %
Na montmorillonite (60–95%)	250–600
Ca montmorillonite (60–95%)	80–120

Optical Microscopy

Dispersed or undisturbed material embedded in acrylate plastic and ground to 30 μm thickness of the specimen is investigated in polarized light for identification of accessory minerals (cf Figure 12-3).

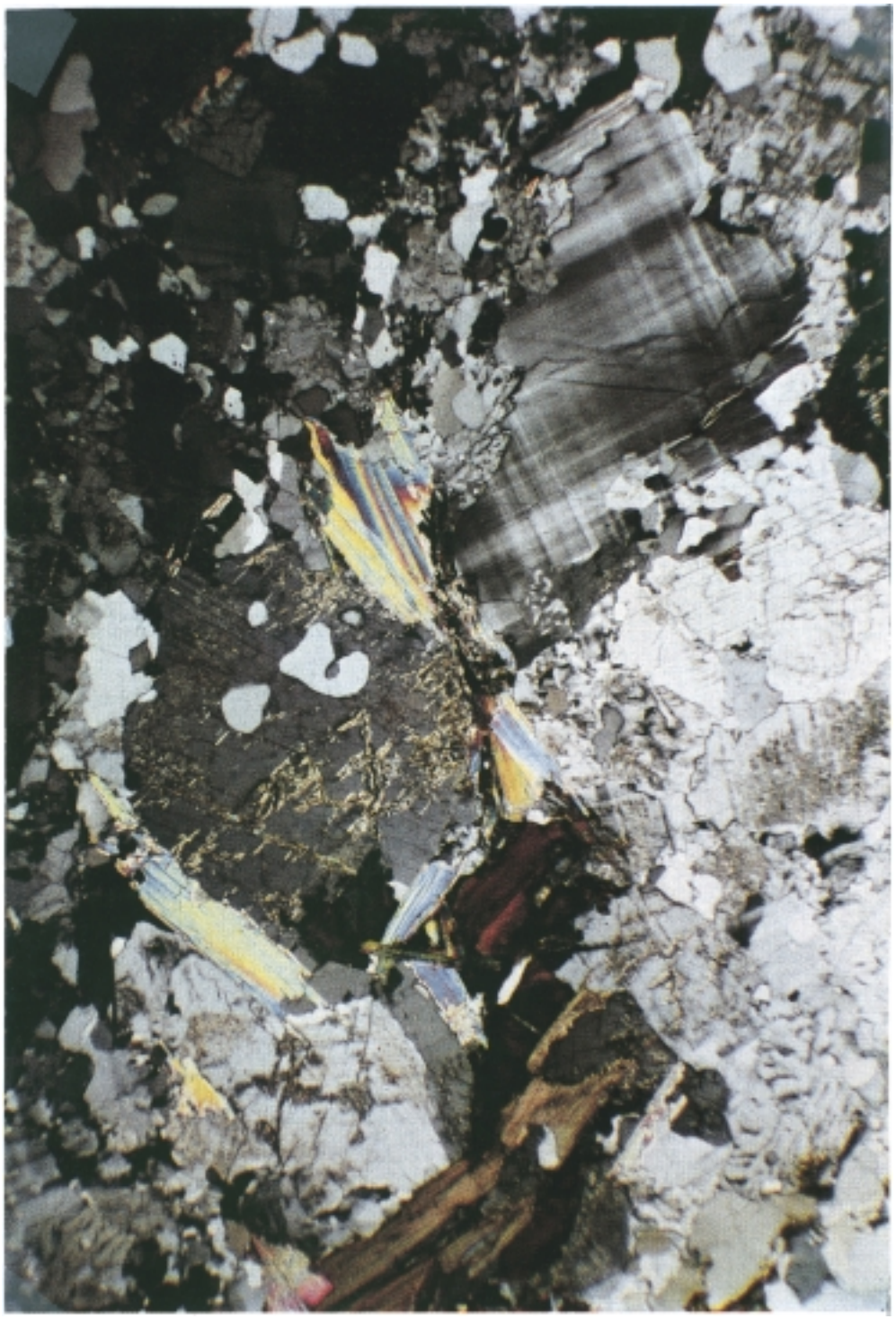

Figure 12-3. *Crystal assembly of feldspar (checkered), mica (deformed) and quartz (mostly grey). Magnification 50 x.*

Additional

A very detailed determination of the amounts of accessory minerals can be made by utilizing differences in specific gravity of the minerals. Thus, heavy minerals of particular interest, such as sulphides, can be determined by separation in liquids with different, suitable densities, using centrifuges. Such techniques are very tedious and not of practical use except for checking the homogeneity of smectitic buffers to which small amounts of graphite (ρ_{sat} = 2090–2230 kg/m^3) have been added.

Physical properties

Purpose

The hydraulic conductivity and swelling pressure as functions of the bulk density are very helpful in estimating the content of smectite minerals, and they give a direct measure of the usefulness of the material for buffer and backfill purposes. The heat conductivity and capacity are important as well and need to be tested for characterization of candidate materials. It is hardly necessary to determine these properties in routine testing, however.

Techniques

Hydraulic conductivity and swelling tests, as well as rheological tests should be made by using water saturated material. Thermal properties may be of interest also at lower degrees of saturation but the testing procedure is very complicated and the evaluation difficult, and it is therefore recommended that they be determined using saturated material.

A standard preparation procedure must be applied in order to get reproducibility and for all the tests the following method is proposed:

1. Drying at 60°C for 3 days of 500 g samples.
2. Careful crushing and sieving to yield a maximum grain size of 1 mm.
3. Application of the air-dry material in a swelling pressure oedometer or in a shear box to the dry densities 1100, and 1600 kg/m^3, with subsequent saturation with distilled water. At least for smectite-poor materials a backpressure has to be applied for water saturation. The height of the sample should be about 20 mm both for testing the hydraulic and swelling properties and for the creep behaviour.
4. Homogenization for one week under confined conditions before the testing is started.

The equipments and procedures for determining the hydraulic conductivity and swelling pressure are described earlier in this part of the Handbook.

Hydraulic conductivity

The hydraulic conductivity is determined by percolating the water saturated clay sample with distilled water and preferably also with 3.5% $CaCl_2$ solution. The percolation should be conducted at constant room temperature for at least one week at a water pressure that must not exceed 50% of the swelling pressure in order to avoid consolidation. A backpressure of 10–20% of the swelling pressure is suitable. Parallel tests at 90°C can be helpful for characterizing the behaviour of the clay at higher temperature but they are not necessary in routine testing.

Swelling pressure

The signals from the pressure transducer are recorded in the course of the water saturation for the conductivity testing, by which the successive build-up of the swelling pressure is visualized. It is usually fully developed in less than one week. A typical graph of tests with different densities is shown in Figure 12-4.

A simple checking of the swelling potential of the soil sample is made by reducing the normal load by 15 to 50%. A very small expansion indicates reduced expandability, which can be due to a low smectite content, or to cementation. A quick check can also be made by simply letting a given amount of air-dry clay hydrate and expand in distilled water or a weak NaCl solution as described in Part 2 of this Handbook.

Creep Testing

All rheological tests must be made under specified stress conditions in order to yield parameter data that can be used in stress/strain calculations. Thus, triaxial tests or simple shear tests are suitably used but they are impractical for quick checking of whether the soil material is cemented or not. The shear box is better suited for such tests although the stress situation is too complex to allow for very accurate evaluation of other strength parameters (cf Chapter 11 in Part 1 of this Handbook).

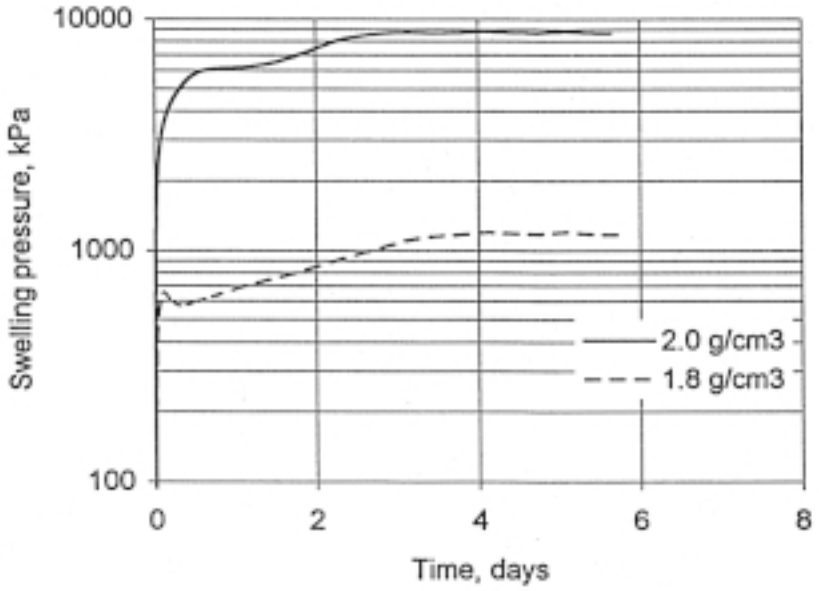

Figure 12-4. *Typical build-up of swelling pressure in the course of water saturation of a smectite-rich sample prepared from air-dry bentonite powder. (1.0 g/cm^3 is 2000 kg/m^3, after Clay Technology AB).*

The shear box has a diameter of down to 20 mm and can be used both for artificially prepared samples as described in the preceding text, and for carefully trimmed undisturbed clay samples. The theoretical background of the stress/strain relationships used for evaluating the standard parameters A, B and t_o of the creep Equations (12-1) and (12-2) that can usually be applied, is given in /6/:

$$\gamma = B\ln\left(t + t_o\right) + A \qquad (12\text{-}1)$$

$$\gamma = B\left(t + t_o\right)^{-1} \qquad (12\text{-}2)$$

where:

γ = angular shear strain (radians per second)
t_o = constant, seconds (cf Figure 12-5)

The parameter B is a measure of the deformability. High values indicate a low shear modulus, and low ones a high stiffness. A low B-value associated with a low or negative t_o-value indicates cementation, which is also usually manifested by jerky creep.

Typical data of different types of smectite material prepared from air-dry powder are given in Table 12-7.

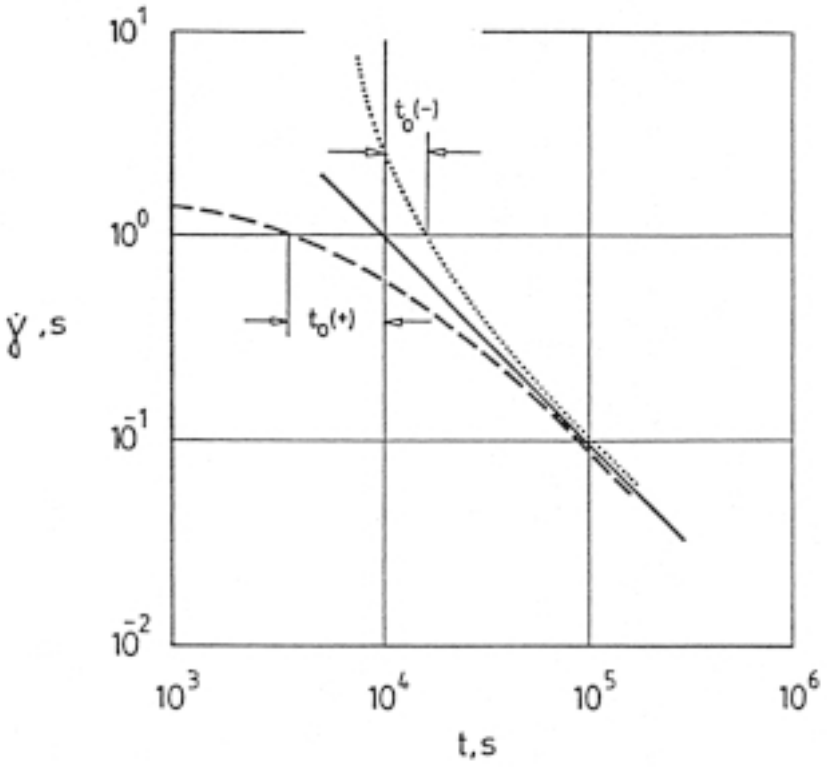

Figure 12-5. *Creep curves showing how t_o is determined.*

Table 12-7. Creep parameter values for smectite-rich clay /6/.

Material	Dry density kg/m³	A	B	t_o x 10^{-4} s
Na-smectite	1750	–20	5	2 000
Ca-smectite	1650	–20	4	1 600
Ca-smectite (cemented)	1800	116	6	–150

Thermal properties

The heat conductivity of water-saturated samples is relatively easily measured by use of a rod-shaped heat sond that is inserted in the sample, the technique being applied as a standard at several laboratories (see Chapter 10 in this part of the Handbook).

The principle is that the sond is heated, yielding a transient heat flow, and that its surface temperature, which is directly related to the heat conductivity of the surrounding soil sample, is measured for about 30 minutes. The conductivity is evaluated from plottings of temperature versus log time, with the energy input and geometry of the sond as known parameters. determination of the thermal properties testing is recommended if it is known that considerable variations occur in a candidate buffer or backfill material.

12.4 References

/1/ **Pusch R, 1994.** Waste Disposal in Rock. Elsevier Publ. Co.

/2/ **Dixon D, Horatio D S J, Kohle C L, 1992.** Preparation and quality control of materials used in the reference buffer material. Atom Energy of Canada Ltd., Technical Report TR-575, COG-92-133, Fuel Waste Technology Branch, Whiteshell Laboratories, Pinawa, Manitoba.

/3/ **Pusch R, 1971.** Microstructural features of pre-Quarternary clays. Acta Universitatis Stockholmiensis, Stockholm Contributions in Geology, Vol. XXIV:1.

/4/ **Tank R W.** Clay mineralogy of some lower Tertiary (Paleogene) sediments from Denmark. Danmarks Geologiske Undersøgelse, IV Raekke, No. 9 (pp. 9–38).

/5/ **Pusch R, 1962.** Clay particles. Handlingar Nr 40, Transactions. Nat. Swed. Build. Res. Council, Stockholm.

/6/ **Pusch R, Börgesson L, Erlström M, 1987.** Alteration of isolating properties of dense smectite clay in repository environment as examplified by seven pre-Quaternary clays. SKB TR-87-29, Svensk Kärnbränslehantering AB.

ISSN 1404-0344

CM Digitaltryck AB, Bromma, 2002